INTERNATIONAL ORGANIC ELECTRONIC MATERIAL TECHNOLOGIES CONFERENCE

oemt'16

CONGRESS BOOK

OEMT2016

2nd International Conference on

Organic Electronic Material Technologies

17-19 May 2016

Kolin Hotel-Çanakkale/TURKEY

ÇANAKKALE ONSEKİZ MART ÜNİVERSİTESİ • 1992 •

COMMITTEES

HONORARY PRESIDENT

Prof. Dr. Yücel ACER	Çanakkale Onsekiz Mart University - Rector

CONFERENCE PRESIDENT

Osman DAYAN	Çanakkale Onsekiz Mart University
Fahrettin YAKUPHANOĞLU	Firat University

ORGANIZING COMMITTEE

İsmail TARHAN	Çanakkale Onsekiz Mart University
İsmet KAYA	Çanakkale Onsekiz Mart University
Vildan BİLGİN	Çanakkale Onsekiz Mart University
Ali BİLİCİ	Çanakkale Onsekiz Mart University
Mustafa KURT	Çanakkale Onsekiz Mart University
Kıvanç SEL	Çanakkale Onsekiz Mart University
Mehmet YILDIRIM	Çanakkale Onsekiz Mart University
Ayhan ORAL	Çanakkale Onsekiz Mart University
Fatih DOĞAN	Çanakkale Onsekiz Mart University
Feyza KOLCU	Çanakkale Onsekiz Mart University
Zafer SERBETCI	Bingöl University
Dilek BAHÇECİ	Çanakkale Onsekiz Mart University
Diğdem ERDENER	Çanakkale Onsekiz Mart University
Elif KARACAN	Çanakkale Onsekiz Mart University
Melek TERCAN	Çanakkale Onsekiz Mart University
Serkan DAYAN	Erciyes University
Kevser TEMİZKAN	Çanakkale Onsekiz Mart University
Emrah SARICA	Çanakkale Onsekiz Mart University
Uğur CENGİZ	Çanakkale Onsekiz Mart University
Fatma AYDIN	Çanakkale Onsekiz Mart University
Ergün GONCA	Çanakkale Onsekiz Mart University
Ahmet ÇETİN	Bingöl University

SCIENTIFIC COMMITTEE

Bekir ÇETİNKAYA	Ege University
Nilgün KALAYCIOĞLU ÖZPOZAN	Erciyes University
Mehmet SAÇAK	Ankara University
Abdülmecit TÜRÜT	Medeniyet University
Orhan ÖZDEMİR	Yıldız Technical University
Tolga KAYA	Central Michigan University
İdris AKYÜZ	Eskişehir Osmangazi University
Grzegorz KARCZEWSKI	Polish Academy of Sciences
Ahmed A. ALGHAMDI	King Abdul-Aziz University
Attieh A. ALGHAMDI	King Abdul-Aziz University
Denis NIKA	Moldova State University
Yasemin ÇAĞLAR	Anadolu University
B.Filiz ŞENKAL	Istanbul Technical University
Mehmet KANDAZ	Sakarya University
Saliha ILICAN	Anadolu University
Gökhan SAVAROGLU	Osmangazi University

Şükrü KARATAŞ	Sutcu Imam University
Ram K. GUPTA	Pittsburg State University
Salem EL-FAIFY	Khalid University
Hakan USTA	Abdullah Gül University
Şemsettin ALTINDAL	Gazi University
Ömer MERMER	Ege Univeristy
Asmaa HENDI	King Abdul-Aziz University
Khasan S. KARIMOV	GIK. Institute
Muhammad H. SAYYAD	GIK. Institute
Faten AL-HAZMI	King Abdul-Aziz University
Savas SONMEZOGLU	Karamanoglu Mehmetbey University
Luis BANARES	Universidad Complutense de Madrid
Nadia ABDEL-AAL	Suez Canal University
Luisa TORSI	Universita Bari Aldo Moro
Nouredine SENGOUGA	Université de Biskra
Christian WENGER	IHP - Leibniz Institute
Fumihiko HIROSE	Yamagata University
W.A. FAROOQ	King Saud University
F. M. AMANULLAH	King Saud University
Ekrem KALKAN	Ataturk University
Tayyar GUNGOR	Mehmet Akif Ersoy University
Sait Eren SAN	Gebze Technical University
Serap GÜNEŞ	Yıldız Technical University
Niyazi ÖZDEMİR	Fırat University
Namık ÖZDEMİR	Ondokuz Mayıs University
Mujdat ÇAĞLAR	Anadolu University
Atif MUHAMMED	King Saud University
Farid EL-TANTAWY	Suez Canal University
Ahmad UMAR	Najran University
Ibrahim S. YAHIA	King Khalid University
Adem TATAROGLU	Gazi University
Marco SCHIAVON	Universidade Federal de Sao Joao del-Rei
Elias STATHATOS	Tecnological-Educational Institute of Patras
Giorgio SBERVEGLIERI	C.N.R. - National Institute of Optics
Witold Daniel DOBROWOLSKI	Polish Academicy of Sciences
Jingkun XU	Technology Normal University
Abdel Salam Hamdy MAKHLOUF	University of Texas Rio Grande Valley
Luisa TORSI	University of Bari
Wojtek WLODARSKI	RMIT University
José M. KENNY	University of Perugia
Tülay BAL DEMİRCİ	İstanbul University
Harun BAYRAKDAR	Çanakkale Onsekiz Mart University
Ruhan BENLİKAYA	Balıkesir University
Rafet KILINÇARSLAN	Pamukkale University
Mehmet KARAKUŞ	Pamukkale University
Emin KARAPINAR	Pamukkale University
Wolfgang ENSINGER	Technische Universität Darmstadt

Welcome Massage

Organic Electronic Material Technologies (OEMT) congress is an annual international scientific congress. OEMT2016 will be held at the Kolin Hotel in Çanakkale. OEMT2016 received contributions from a large variety of research fields associated with organic electronics including renewable energy applications, environment protection, catalysis, nanomaterials, conducting materials, thin films, semiconductors, shape memory materials etc.

Our goal was to create a platform that introduces the newest results on internationally recognized experts to local students and colleagues. Now, OEMT2016 is honored by the presence of over 100 colleagues from various countries. Three inviting speakers, 40 oral presentations, and 168 posters are in the program.

Thus, we hope that getting first-hand access to so many new results, establishing new connections and enjoying the Çanakkale, Turkey ambiance will make you feel that your resources were spent well in OEMT2016.

Our warmest thanks go to all invited speakers, authors, and contributors of OEMT 2016 for accepting our invitation, visiting Çanakkale and using OEMT2016 as a medium for communicating your research results.

We hope that you will enjoy the conference and look forward to meeting you again in one of the forthcoming OEMT events.

Assoc.Prof.Dr.Osman DAYAN
Conference President

Sponsors


ANT TEKNİK


TERRA


B
R
K


bilim
BİLİM LABORATUAR CİHAZLARI SAN. LTD. ŞTİ.


Tekno-TIP
Tekno-TIP Analitik Sistemler Ltd. Şti.


INTERLAB
LABORATUAR ÜRÜNLERİ SAN. ve TİC. A.Ş

INVITED SPEAKERS

FROM ORGANIC- TO BIO-ORGANIC DEVICES FOR SUSTAINABLE OPTOELECTRONICS AND SOLAR ENERGY CONVERSION

Niyazi Serdar Sariciftci
Linz Institute for Organic Solar Cells (LIOS) at the
Johannes Kepler University of Linz, A-4040 Linz Austria
www.lios.at

Organic light emitting diodes (OLEDs), organic photovoltaic cells (OPVs) and organic field effect transistors (OFETs) are device elements for a future organic optoelectronics. Maturing from the academic research into the industrial development, such devices are entering the markets. Pure organic nanostructures and organic/inorganic hybrid nanostructures are comparatively studied for devices. This talk gives an overview of materials' aspect and devices.

In order to account for a sustainable future, the application of biodegradable and biocompatible systems for organic optoelectronics is needed. The use of cheap electronic devices in a large scale will introduce a "consumable electronics" into the market of "consumer electronics". As such the contribution of electronic devices to urban waste is already increasing rapidly today. Therefore environmentally friendly materials are important to use. This is a next great challenge to material science in organic electronics. New developments of bio-inspired and/or bio-origin, bio-compatible materials are interesting. Such materials can also be used to interface the biological and biomedical research with the organic electronics field.

OPTOELECTRONIC PROPERTIES OF DONOR–ACCEPTOR TYPE CONJUGATED POLYMERS

Ali Cirpan[1,2,3,4]

[1] *Department of Chemistry, Middle East Technical University, 06800 Ankara, Turkey*

[2] *Department of Polymer Science and Technology, Middle East Technical University, 06800 Ankara, Turkey*

[3] *Department of Micro and Nanotechnology, Middle East Technical University, 06800 Ankara, Turkey*

[4] *The Center for Solar Energy Research and Application (GUNAM), Middle East Technical University, 06800 Ankara, Turkey*

E-mail :acirpan@metu.edu.tr

The interest in using organic semiconductor thin films in electronic and optoelectronic applications has grown rapidly due to many technological advantages intrinsic to these unconventional semiconductors, such as low material cost, ease of processing, and compatibility with flexible substrates. Many organic-based devices, including organic light-emitting devices, photovoltaic cells, and electrochromic devices have been demonstrated over the last two decades, with OLEDs now available in commercial display products. Low band gap donor-acceptor type quinoxaline-based three random copolymers were synthesized. The effect of varying substituent groups on quinoxaline groups on the performance of bulk-heterojunction polymer solar cells was investigated. Electrochemical and optical studies indicate that these copolymers are promising materials for both electrochromic and polymer solar cells applications. CoP2 and CoP3 were found as excellent candidates for NIR electrochromic devices owing to their 60% and 94% optical contrast values respectively in NIR region with <1 s switching times. Photovoltaic properties of copolymers were performed by conventional device structure. The organic solar cell devices based on copolymer: PC71BM (1:1, w/w) exhibited the best power conversion efficiency of 2.13% with an open circuit voltage of 0.53 V, a short circuit current of 8.07 mA/cm^2, and a FF of 50%.

CATALYTIC ARYLATION REACTIONS IN VIEW OF GREEN CHEMISTRY

Bekir Çetinkaya
Ege University, Chemistry Department, 35100 Bornova-Izmir

In the late 1970s, Heeger, MacDiarmid and Shirakawa discovered that the electrical conductivity of a certain form of polyacetylene increased by a factor of ten million when it was doped with iodine.[1] Subsequent developments have produced diverse applications for the technology: conductive plastics are used in anti-static materials, filters for blocking the radiation produced by computer screens, and electronic windows that can switch light transmission on and off. Semiconducting polymers have also been incorporated into light-emitting diodes, solar cells and displays. Conducting polymers have evoked much interest among researchers because of their reasonably good conductivity, stability, ease of preparation, affordability and redox properties compared to other organic compounds.

Variations of the side chains on the backbone of a material provide opportunities to tailor the molecular assembly and electronic properties. The placement of side chains relative to one another can greatly influence the bulk properties of the material. Therefore, the synthetic methods (Scheme 1) for monomers are an important issue. In this presentation the arylation reactions will be discussed in view of the green chemistry.

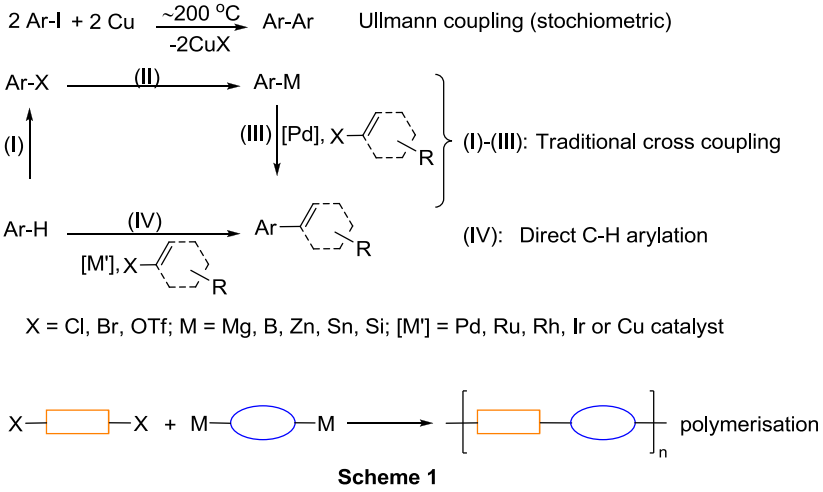

Scheme 1

The first arylation reaction is the Ullmann reaction which requires stochiometric copper under very harsh conditions. Whereas Pd or Ni catalyzed reactions (steps I-III) are selective and take place under mild conditions. On the other hand, direct C-H arylations (step IV) avoids intermediate steps and are preferable from point of green chemistry principles.[2] Difunctional substrates result in polymeric materials.

References

1. Shirakawa, Hideki; Louis, Edwin J.; MacDiarmid, Alan G.; Chiang, Chwan K.; Heeger, Alan J. ("Synthesis of electrically conducting organic polymers: Halogen derivatives of polyacetylene, (CH) x". *J. Chem. Soc. Chem. Commun.*,**1977**, (16), 578-581.
2. Anastas, P. T.; Warner, J. C. *Green Chemistry: Theory and Practice*, Oxford University Press: New York, **1998.**

ORAL PRESENTATIONS

MODELING AND DESIGN OF A SWEAT SENSING DEVICE USING CALORIMETRIC HEAT AND CAPACITIVE RELATIVE HUMIDITY SENSORS

C.T. Ho[1], A.T. Iftekhar[1], Y. Yao, S. Campo, and T. Kaya[1]

[1]*School of Engineering and Technology, Central Michigan University, Mt. Pleasant, 48859, USA*

E-mail: kaya2t@cmich.edu

Studying sweat and its contents can reveal important information regarding human physiology. Particularly, sweat conductivity is a good indication for hydration status. However, sweat rate changes the concentration. Therefore, knowing the sweat rate would help assess the sweat conductivity better. Here, calorimetric flow meter was discussed for measuring sweat flow rate thanks to its ability to detect low liquid flow rates (1µl/min ± 0.1µl) and its small form factor. Additionally, initial flow rate sensing is utilized with humidity sensors and they measure the relative humidity in the channel before sweat enters the sweat channel. A numerical model for the sweat flow rate sensor has been developed. The main goal of this paper was to optimize device dimensions for the sweat flow rate sensor such as the distance between the heater and the upstream and downstream temperature sensors and the height of the channel. This paper also presents finite element analysis simulation results of the device using COMSOL Multiphysics. Our results showed that the sensitivity is a strong function of the position of the heater and sensors along with the dimension of the channel. Moreover, MATLAB and COMSOL simulation also showed that channel length is also a function of the thermal boundary layer of the channel which is basically the height of the channel.

GRAPHENE/SILVER NANOWIRES HYBRID ELECTRODES FOR POLYMER-BASED ORGANIC SOLAR CELLS

Y. Altin[1], M.Tas[1,2], İ. Borazan[3,4], S. Gungor[1], A. Demir[3,4] and A. Bedeloglu*[1]

[1]*Department of Fiber and Polymer Engineering, Bursa Technical University, Bursa, Turkey*

[2]*Textile Engineering Department, Cukurova University, Adana, Turkey*

[3]*Faculty of Textile Technologies and Design, Istanbul Technical University, Istanbul, Turkey*

[4] *TEMAG Laboratory, Istanbul Technical University, Istanbul, Turkey*

E-mail : ayse.bedeloglu@btu.edu.tr

The use of silver nanowires in organic solar cells attracted great attention in recent years since they can be produced via cost-effective and easier techniques compared to ITO which is the common transparent electrode. Especially, to achieve the flexible applications, silver nanowires are more suitable contrary to ITO showing poor mechanical performance. Different synthesis methods including polyol method, chemical reduction method, microemulsion techniques, photoinduced reduction, uv-initiated photoreduction, electrochemical synthetic method and template-directed methods are used to obtain silver nanowires in different dimensions. Silver nanowires can be coated on the substrates using different solution-based techniques such as dip coating, spin coating, printing, spraying, air-brushing and etc. In this study, by using modified polyol-mediated process hybrid graphene/silver nanowire structure was obtained and used as a transparent electrode in polymer-based organic solar cell. A mixture of P3HT:PCBM was employed as photoactive layer of the solar cell. Characterizations were performed by measuring optical, photoelectrical and morphological properties of obtained devices.

This study was supported by Turkish Scientific and Technical Research Council, TUBITAK, Project No: 113M950.

A WHİTE-LIGHT BIASED EXTERNAL QUANTUM EFFICIENCY SYSTEM FOR SOLAR CELL APPLICATIONS

Fahrettin Yakuphanoglu
Physics Department, Faculty of Science, Firat University, Elazig, TURKEY
Nanoscience and Nanotechnology Laboratory, Firat University, Elazig, TURKEY

Here, we manufactured a white light biased external quantum efficiency (EQE) system to measure the recombination parameter (αEQE*) as a function of wavelength and white-light intensity in organic solar cells, dye sensitized solar cells or quantum dots solar cells [1]. The photocurrent density-wavelength and intensity measurements are shown in Fig.1. The schematic diagram of white-light biased external quantum efficiency measurement is shown in Fig.2. In organic photovoltaic devices, generated charge carrier is governed by bimolecular recombination. This causes the low fill factor compared with inorganic solar cells. The recombination parameter can be determined from short circuit current dependence of illumination intensity. In literature, it is seen that the method is not enough to determine recombination parameter. Thus, we offered a new apparatus to measure recombination parameter as a function of wavelength.

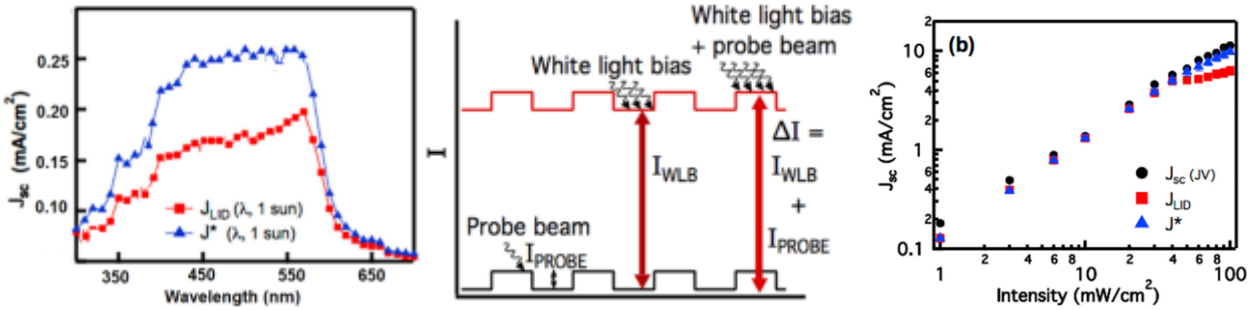

Fig.1. Obtained results from the system

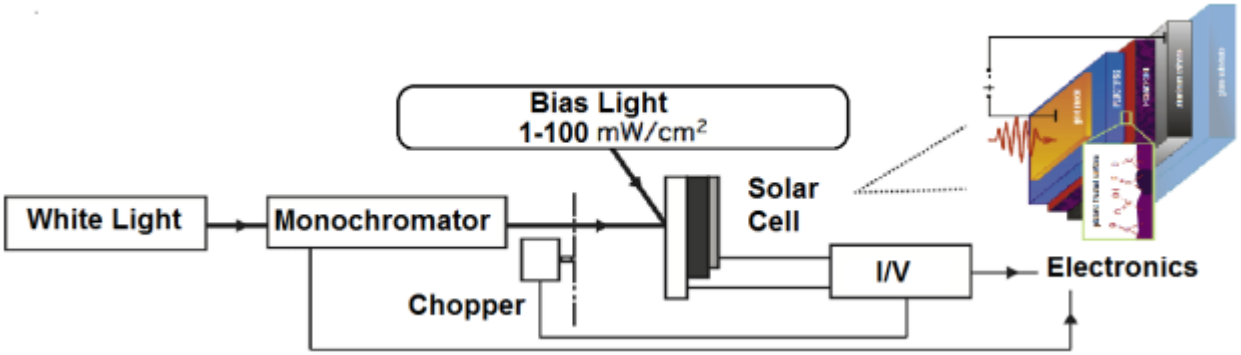

Fig.2. Schematic diagram of the system

Keywords: Organic Solar Cells, External quantum efficiency

[1] Sarah R. Cowan, Jian Wang, Juan Yi, Yun-Ju Lee, Dana C. Olson, and Julia W. P. Hsu, JOURNAL OF APPLIED PHYSICS 113, 154504 (2013)

ANALYZING THE InGaN LED STRUCTURES FOR WHITE LED APPLICATION

İ.KARS DURUKAN[1], O.Sarıarslan[2], M.K.Öztürk[2,3], S.Özçelik[2,3],and E.Özbay[4]

[1]Life Sciences Research and Application Center, Gazi University, Ankara, Turkey
[2]Department of Physics, Faculty of Sciences, Gazi University, Ankara, Turkey
[3]Photonics Research Center, Gazi University, Ankara, Turkey
[4]Department of Physics, Bilkent University, Bilkent, Ankara
E-mail :ilknurdurukan@gazi.edu.tr

DETERMINING ELECTRICAL AND DIELECTRIC PROPERTIES DEPENDENCE ON VARIOUS FREQUENCIES OF Al/ZnS-PVA/p-Si (MPS) STRUCTURES

Nalan Baraz[1], İbrahim Yücedağ[2], Yashar Azizian-Kalandaragh[3,4], Şemsettin Altındal[5]

[1]Department of Electric and Energy, Gölyaka Vocational High School, Düzce University, 81800, Düzce, Turkey

[2]Department of Computer Engineering, Technology Faculty, Düzce University, 81620, Düzce, Turkey

[3]Department of Physics, University of Mohaghegh Ardabili, P.O. Box 179, Ardabil, Iran

[4]Department of Engineering Sciences, Sabalan University of Advanced Technologies, Namin, Ardabil, Iran

[5]Department of Physics, Faculty of Sciences, Gazi University, Ankara, Turkey

Email: nalanbaraz@gmail.com

We have studied electrical and dielectric parameters of the Al//ZnS-PVA/p-Si structures using admittance measurements. For this aim, capacitance/conductance-voltage-frequency (*C/G-V-f)* measurements were performed at various frequencies (10 kHz-1 MHz) and voltages (±4V) by 50 mV steps at 300K. The series resistance (R_s) of this structure was decreases with increasing frequency. The effects of R_s and interfacial layer on the *C-V and G/-V* characteristics are found remarkable at low frequencies. In addition, the main dielectric parameters such as the dielectric constants (ε' and ε''), loss tangent ($tan\delta$), electric modules (M' and M''), and ac electrical conductivity (σ_{ac}) values were obtained using *C* and *G/* data and they are found to a strong functions of frequency and applied bias voltage. Experimental results confirmed that the ε', ε'', and $tan\delta$ increase with increasing frequency, while The M' and σ_{ac} decrease with increasing frequency. Moreover, the ε', ε'', $tan\delta$, and σ_{ac} increase with applied bias voltage, while The M' decreases with increasing applied bias voltage. The M'' values have peaks which are peak shift to the right with increasing bias voltage and it disappears at high frequencies. Experimental results confirmed that the R_s and interfacial layer of the MPS structure are more important parameters that strongly influence both the electric and dielectric properties.

ELECTRODEPOSITED NITROGEN DOPED ZnO RODS: STRUCTURAL, MORPHOLOGICAL AND ELECTRICAL PROPERTIES

P. Bilgic Ozden[1], Y. Caglar[2], S. Ilican[2], M. Caglar[2]

[1]Graduate School of Sciences, Anadolu University, Eskisehir, Turkey

[2]Physics Department, Anadolu University, Eskisehir, Turkey

E-mail: pbilgic@anadolu.edu.tr

Zinc oxide (ZnO) rods have been successfully deposited and doped by various elements by many researchers. Among these dopants, nitrogen (N) has been reported for many times to produce p-type ZnO. Due to the radius of N is approximately equal to the substituted element in the structure (which is oxygen in this case), N does not disturb the lattice as other dopants do. Furthermore, N is considered as the most promising p-type doping element for ZnO.

In this study, N doped ZnO films (ZnO:N) were deposited onto indium tin oxide (ITO) substrates using electrochemical deposition technique. The ZnO:N films were electrodeposited in a solution consist of hexamethylenetetramine (HMTA, $C_6H_{12}N_4$, ≥ 99.5 %), zinc nitrate hexahydrate ($Zn(NO_3)_2.6H_2O$, ≥ 99.0 %) as precursors and ammonium nitrate ($N_2H_4O_3$, ≥ 99.999 %) as doping agent. Doping ratios were 1-10%. The solution temperature was kept at 90 °C, applied voltage was -1.0 V, deposition time was 90 min. and molarity of the solution was 0.01 M. Electrode positions were carried out in a conventional three electrode cell with ITO as working electrode, Ag/AgCl as reference electrode and a platin wire as counter electrode.

The crystal structure, morphology and electrical properties of the films were investigated via X-ray diffraction (XRD), Scanning Electron Microscopy (SEM) and Hall Effect Measurement techniques, respectively. XRD measurements were used to determine whether there is a lattice distortion because of the doping process. SEM was used to investigate the surface morphology. Hall effect measurements were used to determine the conductivity type, carrier concentration and carrier mobility of the films.

Acknowledgements: This work was supported by Anadolu University Commission of Scientific Research Projects under Grant No. 1207F118, 1305F082 and 1501F031

WETTABILITY PERFORMANCES OF POLYMERIC ELECTROCHROMIC SURFACES: FROM HYDROPHILICITY TO OLEOPHOBİCİTY

M. Yıldırım[1]

[1]*Department of Materials Science & Engineering, Faculty of Engineering, Canakkale Onsekiz Mart University, Canakkale, Turkey*

E-mail:mehmetyildirim@comu.edu.tr

Polymeric electrochromic materials have been significant candidates of electrochromic devices (ECDs) in a few decades. They can be used in smart windows, flexible displays, EC mirrors etc. [1]. Recently, some investigations about wettability performances of polymeric electrochromic surfaces have been carried out [2]. These surfaces could be contaminated by water or oil base pollutants. Their wettability properties simultaneously characterize the durability under humid conditions. In this study, wettability performances of common polymeric EC surfaces (Polycarbazol (PCarb), PEDOT etc.) and their some substituted forms have been investigated.

Electropolymerizations of EDOT, Carbazole and pyrrole monomers were carried out by bulk electrolysis method using two different electrolysis potentials (1.2 and 2.5 V) and possible defect formation is investigated spectroscopically. Higher potential gains higher roughness to surface and effects the wettability. Then, perfluorohexyl substituted pyrrole polymer (PFHP) was synthesized by chemical methods and dip-coated on PEDOT sublayer to obtain EC bilayer surfaces with high roughness. Also, polyethylene main chain with carbazole and perfluoroalkyl moieties (p(VCarb-co-PFA)) was synthesized by chemical radicalic copolymerization and then, electropolymerized onto PEDOT coated ITO/glass by unsubstituted carbazole side groups. EC characteristics were obtained by spectroelectrochemical characterization. Wettability properties were characterized by static contact angle measurements.

PEDOT is hydrophilic and becomes superhydrophilic over particular conditions. PCarb hydrophobic but its water contact angle (WCA) reaches up to just 120˚. However, perfluoroalkyl substituted polymeric electrochromics have higher contact angles. PEDOT/PFHP bilayer surfaces become superhydrophobic (WCA>170˚), but superoleophilic (oil contact angle-OCA~0˚). On the other hand, electropolymerization of p(VCarb-co-PFA) onto PEDOT/ITO forms superhydrophobic (WCA>170˚) and superolephobic (OCA~165˚) polymeric bilayer surface having EC properties.

Common polymeric ECs have low WCA and could be contaminated under humid conditions. Structural modifications like perfluoroalkyl substitutions particularly increased their WCA and OCA and significantly increased their durability as exposed to contaminants.

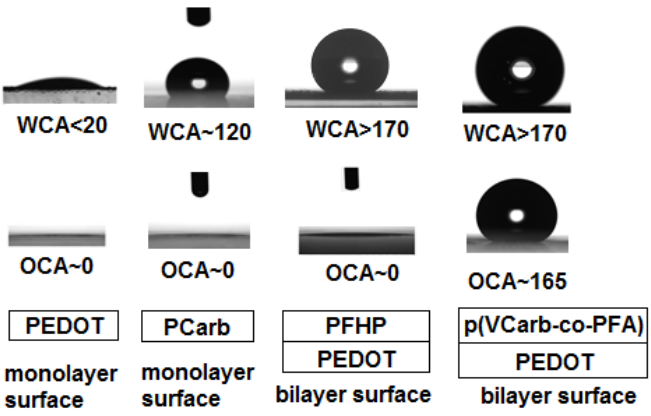

[1] P. Camurlu and N. Karagoren, React. Funct. Polym. 73, 847 (2013).

[2] H. F. Zhu, J. Hou, R. Qiu, J. Zhao and J. K. Xu, J. Appl. Polym. Sci. 131 (2014).

DEPOSITION OF PROTECTIVE DIAMOND-LIKE CARBON FILMS ONTO THE INNER WALLS OF ALUMINIUM TUBES

Sevda Ayata[1] and Wolfgang Ensinger[2]

[1]Chemistry Department, Faculty of Science, Dokuz Eylul University, Izmir, Turkey
[2]Department of Materials Science, Darmstadt University of Technology, Darmstadt, Germany
E-mail : sevda.ayata@deu.edu.tr

Often, the performance of a tube in use is not satisfactory, because the tube material fails. Deposition of a protective film may improve the situation. Although physical vapour deposition of a film inside a tube is difficult, as the tube aperture is small compared to its length, there are possibilities for coating when special techniques are used. Apart from plasma techniques, ion beam sputtering can be used. A sputter target is moved through the tube. An ion beam is directed into the tube along its taxis. The ions impinge onto the sputter target, and the sputtered atoms are deposited onto the tube walls. When this technique is used, tube and beam need to be carefully aligned. Even if so, often the coating is inhomogeneous in thickness in the circumference. Another problem is fluctuations in the ion beam density which causes a variation of the sputtering rate along the tube, leading to axial inhomogeneities.

In this contribution, a second generation set-up for coating tubes by ion beam sputtering is described. For an improved homogeneity in the circumference, the tube is rotated. Fluctuations of the ion beam density are balanced by measuring the ion current on the sputtering target and adapting the speed of the sputtering target, when it travels through the tube, by a feed-back system. Thus, the deposition rate can be controlled along the tube axis.

The system was tested by measuring the film thickness along both the circumference and along the axis of the tube. As a model system, aluminum tubes were coated with carbon films. The film thickness was determined by Photo Electron Spectroscopy. The results show that a uniform film with only a few percent of variation in film thickness can be deposited.

Carbon films on aluminum may act for corrosion protection. In order to test the quality of the films, electrochemical corrosion measurements in aqueous environment were performed. They show that the films are dense and well adhering and are suitable for protecting aluminum tubes against pitting corrosion.

POLYMER-BASED ION-CONDUCTING NANOPORES FOR ELECTROCHEMICAL SENSING OF BIOMOLECULES - THE INAPO PROJECT -

W. Ensinger[1], G. Thiel[2], Ivana Duznovic[1], Saima Nasir[1], Mubarak Ali[1]

Technische Universität Darmstadt, Darmstadt, Germany

[1]Department of Materials Science, Materials Analysis

[2]Department of Biology, Membrane Biophysics

E-mail : ensinger@ma.tu-darmstadt.de

Living cells communicate and exchange small molecules and ions with their surroundings via nanopores in their membranes. Among these, ion conducting nanopores, based on membrane transport proteins, are of particular interest. Channel proteins can be engineered in such a way that they alter their ionic conductance in the presence of certain molecules to be analyzed. With this approach, highly sensitive biomolecular sensors can be realized. The major drawback of such natural nanopores is that they are embedded in a fragile and unstable lipid bilayer. Thus, they are not suitable for technical applications. In order to get rid of such restrictions, various routes have been tried for fabricating nanopores in solid-state materials with the ability to mimic functions of biological nanopores, being more robust than the latter while keeping their sensoric sensitivity and selectivity as much as possible. The approach, used for the present studies, is the so-called ion track etching technique. Here, polymer foils are through-irradiated with a beam of highly energetic ions in a particle accelerator. The ion damage track is chemically etched into a nanopore. The nanopore walls are functionalized by an appropriate coupling chemistry with a biorecognition unit, i.e. a molecule which specifically reacts with another molecule, in a key-lock principle. In an electrochemical two-compartment cell, the polymer foil acts as separation membrane. The electrolyte current flowing through the naopore is measured as a function of the applied potential. In the presence of specific analyte molecules, which selectively bioconjugate with the biorecognition unit insider the nanopore, these ionic currents are changed. Thus, a highly sensitive nanosensor for biomolecules is available. The preparation and working principle of this type of nanosensor is described. As example, results on the sensing of proteins and carbohydrates are shown [1, 2].

The goal of project *iNAPO* is the combination of biological protein-based and synthetic polymer-based nanopores and their implementation into a micro-device in order to create a new type of sensing device for analytical applications, e.g. for environmental or medical applications, such as water analysis and diagnostics.

[1] M. Ali, S. Nasir, P. Ramirez, J. Cervera, S. Mafe, W. Ensinger, J. Phys. Chem. C117, 18234 (2013)

[2] M. Ali, S. Nasir, W. Ensinger, Chem. Comm. 51, 3454 (2015)

PIEZOELECTRICITY AS SMART MATERIALS

B. Akgenc[1], C. Tasseven[2] and T. Cagin[3]

[1]*Department of Physics, Kirklareli University, Kayali Campus, Kirklareli, Turkey*

[2]*Department of Physics, Yildiz Technical University, Esenler, Istanbul, Turkey*

[3]*Department of Materials Science and Engineering, Texas A&M University, College Station,Texas,USA*

berna.akgenc@klu.edu.tr

Piezoelectric materials are called as smart materials which are outstanding technological interest for industrial and commercial applications such as actuators, sensors, capacitors and energy harvesting devices. Piezoelectric materials show a form of electromechanical coupling, that is, the polarization of the material change in response to an applied strain or vice versa.

The piezoelectric constants of ABO_3 type perovskite structure are computed by first principle calculations. Both direct and converse piezoelectric constants are constructed in terms of electronic “clamped-ion” and nuclear “ion-relaxed” contributions. This study deals with the elastic and piezoelectric properties of ABO_3 type perovskite structures and its alloy forms that are considered tetragonal at zero hydrostatic pressure. The role of alloying on piezoelectricity is found to be dramatic this leading to gaint piezoelectric response. The aim of this work is new, previously unknown and designing high performance ABO_3 type perovskite structures.

THE EFFECT OF PRESSURE ON STRUCTURAL, ELECTRONIC, ELASTIC, VIBRATION AND OPTICAL PROPERTIES OF LiScC COMPOUND

İ.Ö. Alp[1] and Y.Ö. Çiftci[2]
[1,2]*Gazi University, Department Of Physics, Ankara, TURKEY*
E-mail: iremoner@gazi.edu.tr

The pressure dependence of the electronic, elastic, vibration and optical properties for LiScC half-Heusler compound in cubic MgAgAs-type structure was systematically performed using the density functional theory within plane-wave pseudopotential method (PAW) and the generalized gradient approximation of Perdew, Burke and Ernzerhof (GGA-PBE) [1] for the exchange-correlation potential. The computed lattice parameters are in reasonable accord with available experimental data. Using the elastic constants and related parameters, the crystal rigidity and mechanical stability were discussed. The calculated electronic band structures revealed that LiScC have an indirect gap in Γ-X Brillouin zone. We also presented phonon dispersion relation and density of phonon states. It is found that the substituted structure is stable for this compound between 0 and 50 GPa pressure. The optical properties were also predicted. To the best of our knowledge, most of the studied properties such as elastic, optical properties and especially phonon dispersion curves were reported for the first time.

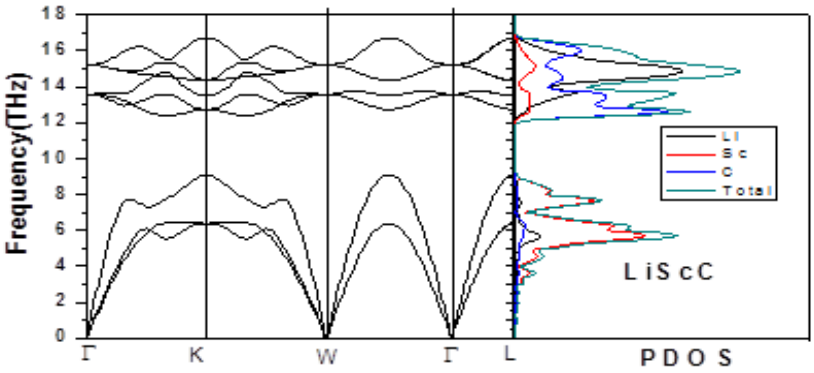

Figure 1. The phonon dispersion curves and partial density of states for LiScC

[1] J.P. Perdew, K. Burke, and M. Ernzerhof, Generalized Gradient Approximation Made Simple, Phys. Rev. Lett. 77, 3865 (1996).

FABRİCATİON OF RUTHENİUM DYE AND IONİC CONDUCTOR FOR SOLİD-STATE DYE-SENSİTİZED SOLAR CELLS (ssDSSCs)

S. Dayan, N. Kalaycıoğlu Özpozan
Department of Chemistry, Faculty of Science, Kayseri, Erciyes University, Turkey
E-mail: serkandayan_@hotmail.com

Dye-sensitized solar cells (DSSCs), which have emerged as one of the most promising photovoltaic devices, have been studied extensively due to their respectable power conversion efficiency, facile fabrication processes, and potential low cost. The typical DSSC is, in its original form, composed of dye sensitized nano-crystalline TiO_2 film as the working electrode, a Pt-coated conductive glass as the counter electrode, and the redox couple I^-/I^{3-} in a volatile organic solvent as the electrolyte. Although power conversion efficiency over 12% has been achieved for DSSCs with a volatile organic liquid electrolyte, DSSCs containing liquid electrolyte are limited for outdoor applications in view of the need for robust encapsulation of the volatile organic liquid [1]. For this reason, considerable efforts have been made to replace the liquid electrolyte with solid-state electrolytes, such as p-type inorganic semiconductors (CuI, CuSCN, etc.), organic hole-transporting materials and ionic conductors [2-3].

Herein, novel *N*-coordinate ruthenium complexes bearing sulfonamide and carboxylic acid groups and ionic conductors have been successfully designed and synthesized. The structural elucidations of the materials were characterized by different methods such as FT-IR, H-NMR, C-NMR, Elemental Analysis and UV-vis. The synthesized ruthenium complexes were tested as dye in dye-sensitized solar cell (DSSC). In addition, solid state DSSC with iodide salts as the single-component solid-state electrolyte has achieved a light-to-electricity power conversion efficiency of 1.57% under illumination of simulated solar light (100 mW cm^{-2}). This finding also helps to simplify the components in the solar cell device and hence reduce the total cost.

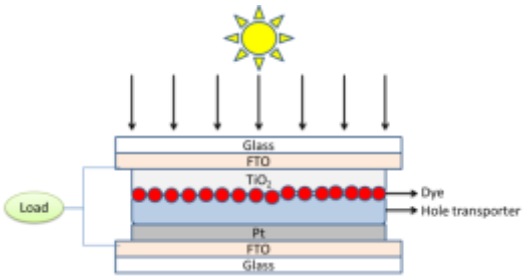

Figure-1 DSSC with a Single-Component Solid State Electrolyte

Acknowledgments
We acknowledge the financial support granted by Erciyes University (ERUBAP), (FDK-2015-6013).

[1] B. C. O'Regan and M. Grätzel, A low-cost, high-efficiency solar cell based on dye-sensitized colloidal TiO_2 films Nature 353, 737 (1991).
[2] Q. B. Meng, K. Takahashi, X. T. Zhang, I. Sutanto, T. N. Rao, O. Sato, A. Fujishima, Fabrication of an Efficient Solid-State Dye-Sensitized Solar Cell, Langmuir 19, 3572 (2003).
[3] H. Wang, J. Li, F. Gong, G. Zhou, and Z. Wang Ionic Conductor with High Conductivity as Single-Component Electrolyte for Efficient Solid-State Dye-Sensitized Solar Cells J. Am. Chem. Soc. 135, 12627 (2013).

EFFICIENCY DEPENDENCY OF MDMO-PPV BASED POLYMER SOLAR CELLS ON SURFACE MORPHOLOGY AND MOLECULAR WEIGHT

Abuzer Yaman[1], S. E. San[2], A. Kösemen[2,3] and Y. Yerli[2,4]

[1]*Department of Electronic and Automation, Van Vocational School, Yuzuncu Yil University, 65080 Van, Turkey*
[2] *Organic Electronics Research Group, Department of Physics, Gebze Institute of Technology, 41400 Gebze/Kocaeli, Turkey*
[3] *Department of Physics, Faculty of Arts and Science, Muş Alparslan University, 49100 Muş, Turkey*
[4]*Department of Physics, Faculty of Arts and Science, Yildiz Technical University, Davutpaşa/İstanbul, Turkey*

E-mail : yaman@yyu.edu.tr

In the scope of this study, polymer solar cells were fabricated by using poly[2-methoxy,5-(30,70-dimethyl-octyloxy)]-p-phenylene vinylene (MDMO-PPV) with three different molecular weight (A:25000, B:85000, C:450000). Their efficiencies were investigated and the highest efficiency was obtained in organic solar cells, which were prepared with batch of B polymer. On the other hand, the least efficiency values were detected by group A polymer. Studied Solar Cells are solution processable and prepared by Spin Coating. Obtained Efficiencies and AFM profiles of prepared solar cells were compared. When AFM images of three groups of MDMO-PPV polymers were examined, it was seen that surfaces of high efficiency B batch solar cells were smoother than those of A and C groups and the cells of lowest efficiency (batch A cells) had been showing the worst roughness values in compared to the others. Obtained results constitute an optimization basis for Organic Solar Cell applications, where MDMO-PPV based materials can propose an alternative perspective. We are also planning to improve the current efficiencies by doping tailored nanoparticles such as C_{60} to our optimized results.

ANALYSIS OF TEMPERATURE EFFECT ON THE MECHANICAL BEHAVIOR OF NANOCATILEVER

M.Tahmasebipour [1] and R. Ahmadi [2]

[1]*Faculty of New Sciences and Technologies, University of Tehran, Tehran, Iran*
[2]*Department of Mechanical Engineering, Islamic Azad University, Parand branch, Parand, Tehran, Iran*

E-mail :tahmasebipour@ut.ac.ir

Increasing development of nanoscience and nanotechnology has led to widespread applications of nanoelectromechanical systems (NEMS) in various fields. Some NEMSs are actually nanocantilever-based devices used in the form of nano-accelerometers, nanosensors (for gases and chemicals), displays, deformable mirrors (DM), RF switches, nanoelectromechanical relays, and nanoresonators. Two modes of operations are used in nanocantilever applications: the static mode and the dynamic mode. In the static mode, nanocantilever deflection occurs as a result of a change in mass or application of a static load. By determining the extent of such bending through conventional ways, the amount of the corresponding mass change or the exerted static load can be obtained. This mode is used for highly sensitive sensing and switching applications. In the dynamic mode, the nanocantilever is vibrated at its resonant frequencies. Changing the mass of the nanocantilever or applying force to its surface would introduce a shift in its resonant frequency. By measuring this resonant frequency shift, we can determine the corresponding change in mass or the applied force. This mode is generally used in sensing applications. Understanding the thermo-mechanical behavior of nanocantilevers can open up new avenues for better implementation of their already diverse and broad range of applications. In this study effect of temperature on the mechanical behavior of gold nanocatilever has been analyzed using the molecular dynamics (MD) method.

FIELD EFFECT TRANSISTOR PERFORMANCE OF FULLERENE PENDANT STYRENE COPOLYMER

Engin Başaran[1], Büşra Şennik[2], Fatih Mehmet Coşkun[1], Mustafa Coşkun[1], Faruk Yilmaz[2]
[1]*Department of Engineering Physics, Istanbul Medeniyet University, 34720 Istanbul, Turkey*
[2]*Department of Chemistry, Gebze Technical University, Kocaeli 41400, Turkey*
E-mail: engin.basaran@medeniyet.edu.tr

In this study we report characterization and field effect transistor properties of a styrene copolymer, P(S-*co*-CMS-C_{60}) polystyrene block containing C_{60} pendant groups. Recently Şennik et al [1] reported the synthesis and gas sensing properties of Styrene Copolymer containing Fullerene (C_{60}) Pendant Moieties (P(S-*co*-CMS-C_{60})). In this study, P(S-*co*-CMS-C_{60}) was employed in organic field effect transistors (OFETs) as a semiconducting material and various commercial materials as insulators. Transport properties of P(S-*co*-CMS-C_{60}) and transfer characteristics of P(S-*co*-CMS-C_{60}) based OFET devices were investigated.

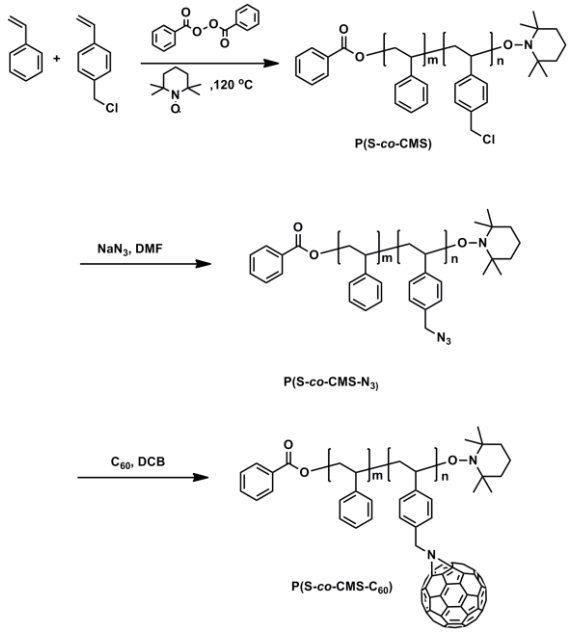

Scheme 1. General Reaction Scheme for the Synthesis of Styrene Copolymer Containing Fullerene Side Groups

[1] Erdem Şennik, Büşra Şennik, Onur Alev, Necmettin Kılınç, Faruk Yılmaz, Zafer Ziya Öztürk, α-Thiophene End-Capped Styrene Copolymer Containing Fullerene Pendant Moieties: Synthesis, Characterization, and Gas Sensing Properties, Journal Of Applied Polymer Science, pp.43641-43651, 2016.

GRAPHENE FİBER: A MACROSCALE APPROACH

E. Özçakır[1], B. Ballı[1,2], V. Eskizeybek[1] and M. Toparlı[2]
[1]*Department of Materials Science and Engineering, Faculty of Engineering, Çanakkale, Turkey*
[2]*Metallurgical and Materials Engineering Department, Dokuz Eylul University, İzmir, Turkey*
E-mail :veskizeybek@comu.edu.tr

THE GROWTH OF CuInTe TERNARY THIN FILMS BY ELECTRODEPOSITION IN AQUEOUS SOLUTIONS AT ROOM TEMPERATURE

A. Peksoz, S.K.Akay
Department of Physics, Faculty of Sciences and Arts, Bursa, Turkey
E-mail :kakay@uludag.edu.tr

CuInTe ternary thin films were grown on ITO substrates by electrochemical deposition in aqueous solutions at 25 ^{o}C for five different cathodic potentials. The deposition bath consisted of 10 mM $CuCl_2$, $InCl_3$, Na_2TeO_3 and H_2SO_4. The pH of the electrolyte was adjusted to 2.0 in addition of HCl. The deposition process was performed using chronoampermetry technique for 5 min. The film deposition potentials were selected as -1.6, -1.3, -1.0, -0.7 and -0.4 V. The band gap energy of the film produced at -1.0 V was found to be nearly 1.56 eV from UV measurements. It was found that the band gap energy of the CuInTe film varies with deposition voltage. It was also observed from SEM and EDX studies that the elemental composition of the films sensitively changes depending on the applied cathodic potential. Hall-effect measurements showed that the produced CuInTe ternary thin films have p-type semiconductor behavior.

ORGANIC PHOTODETECTORS FOR SOLAR TRACKING SYSTEM APPLICATIONS

Niyazi ÖZDEMİR

Faculty of Technology, University of Fırat, Metallurgy and Material Engineering Department, Elazığ, Turkey

Organic semiconductors have been extensively investigated due to their various electronic and optoelectronic applications. In present study, we fabricated a region-regular poly(3-hexylthiophene-2,5-diyl) polymer based photodetector to obtain a high photoresponsivity. The photodetector was prepared on p-type silicon substrate by sol gel spin coating method. The photoconduction mechanism of organic polymer photodetector was analyzed by the reserve photocurrent dependence of the illumination intensity. It is evaluated that the prepared photodetector can be used as a photosensor for solar tracking systems.

Keywords: Photosensor, Photodetectors, Organic semiconductor

ELECTRICAL CHARACTERIZATION OF GEM FOIL (PMDA-ODA)

Y. Kalkan

[1]*Department of Physics, Faculty of Science, Muş, Turkey*

E-mail :yalcinkalkan@gmail.com

EFFECT OF INORGANIC SALT ON PROPERTIES OF ELECTRODEPOSITED PANI THIN FILM FOR ELECTROCHROMIC DEVICES

Y.E. Fırat, A. Peksoz
Department of Physics, Faculty of Sciences and Arts, Bursa, Turkey
E-mail :yunusef@uludag.edu.tr

THE ROUGHNESS EFFECT ON DYNAMIC OLEOFOBIC ORGANIC/INORGANIC HYBRID SURFACE

U. Cengiz, Ö. Mutlu

Department of Chemical Engineering, Faculty of Engineering, Canakkale Onsekiz Mart University, Canakkale, TURKEY

E-mail :ucengiz@comu.edu.tr

Self cleaning surface were obtained not only super-repellent surface but also dynamic liquid surface. Both of the surface was shown the self cleaning properties due the low tilting angle (TA) value below 5-8^{o} or contact angle hysteresis value that was defined the differences advancing and receding contact angle. The principles of super repellent surfaces is that firstly a solid surface having low surface free energy must be formed and secondly the roughness of these surfaces must be high to accommodate the air pockets within them. Higher and robustness surface roughness is necessary especially the oil repellency. However, increase in the surface roughness resulted in decrease in the mechanical and chemical stability. Thus, the dynamically oleofobic surface is more important application area due to the both of the higher mechanical and chemical stability and surface cleaning properties [1]. In this study, dynamically oleophobic surfaces were obtained by using the $FAS_{17}(CF_3(CF_2)_7–CH_2CH_2Si(OMe)_3)$ and TMOS/TMMS in an isopropanol(IPA)/hydrochloric acid(HCl) solution for 4h at room temperature by solgel method. The molar ratio of the solution was as follows: Si-OR/IPA/H_2O/HCl=1:6.3:1:1.8×10^{-4}. The surface roughness of the hybrid films on dynamic oleophobic surfaces were carefully studied and it was found that, increase in the surface roughness resulted in increase in the TA value of oil drops. In addition, the $R_{Si/C}$ ratio and surface tension of liquid effect on dynamically oleofobicity was also investigated and it is found that, increasing the surface tension from 21.6 to 35.8 resulted in increased the tilt angle from 4 to 25^{o} of probe liquid as given in Figure-1.

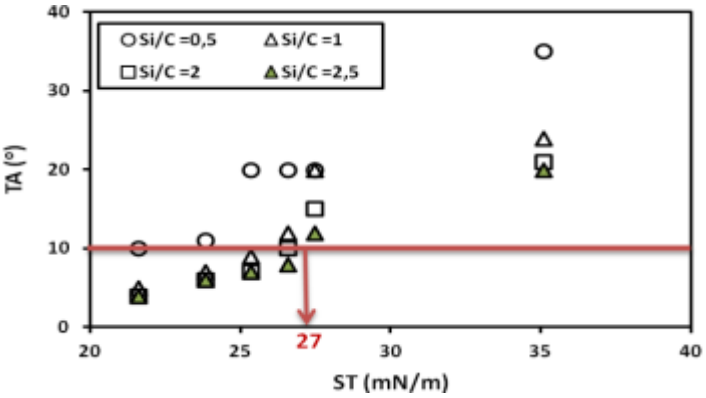

Figure-1. The deviation of the TA angle values change with the surface tension of oils on FAS17-TMOS.

This study was financially supported by the Scientific and Technological Research Council of Turkey (TUBITAK,Project-114M475).

[1] J. Park, C. Urata, B. Masheder, D.F. Cheng and A. Hozumi, Long Perfluoroalkyl Chains Are Not Required For Dynamically Oleophobic Surfaces, Green Chemistry, 15, 100 (2013).

FABRICATION OF POROUS NiTi ALLOY IMPLANTS BY SHS

N. Özdemir, F. Sarsılmaz, İ. Kırık, O. Yiğit

Fırat University, Technology Faculty, Metallurgy and Materials Engineering Department, 23190, Elazığ, Turkey

In this study, TiNi porous alloys were prepared as artificial bone by Self-propagation High-temperature Synthesis (SHS) in order to develop new biomaterials. The mixture of titanium and nickel powder with 50.5 at.% Ni and 49.5 at.% Ti were blended for 12h and hot pressed in the different pressures (60, 80 and 100 MPa) . Then compacted samples were ignited at the various preheating temperatures (200, 250 and 300oC) under argon gas atmosphere. The effects of compaction pressure and preheating temperature on the characteristics and compressive properties of the samples were investigated. Microstructure, phase compositions, and mechanical properties were studied by optical microscope, scanning electron microscope (SEM), X-ray diffraction (XRD), energy-dispersive spectrometer (EDS), and compression test, respectively. The obtained results indicate that the compaction pressure and preheating temperature greatly affect porosity, and compressive strength of porous NiTi porous alloys. The general porosity of the synthesized porous sample is in the range of 54–67% and the pores in the samples are mostly open with an open porosity ratio of 80–95%.

SYNTHESIS AND ELECTROCHEMICAL STUDY OF M-Pd@C CORE/SHELL NANOMATERIALS FOR NON-ENZYMATIC HYDROGEN PEROXIDE SENSOR

H. Çelik Kazıcı[1*], F. Salman[1], and H. Demir Kıvrak[1]

1 Chemical Engineering Department, Yüzüncü Yıl University, Van, Turkey

E-mail : hilalkazici@yyu.edu.tr

Rapid and accurate determination of hydrogen peroxide (H_2O_2) is of practical importance in various fields such as food, clinical and environmental analyses. Recently, it is of great interest to develop an enzyme-less electrochemical sensor with high sensitivity, fast response time, and long-term stability. In particular, electrochemically active nanomaterials consisting of metals have been extensively studied for non-enzymatic electrochemical sensors [1–2].

In this study, bimetallic core-shell nanocatalyst is synthesized in order to increase the catalytic activity of Pd using Ni metal. Therefore Pd:Ni (9:1, 7:3, 5:5) atomic ratios were fixed for M-Pd@C catalyst and employed for non-enzymatic hydrogen peroxide (H_2O_2) sensing activity. The structure and morphology of these catalysts were examined via X-ray diffraction (XRD), transmission electron microscope (TEM). H_2O_2 measurements was performed in the 0.5-80 mM concentration range for the Pd@Ni (9:1, 7:3, 5:5) catalysts and was observed to increase with increasing concentration of hydrogen peroxide reduction peak current. Best current was obtained at 50 mM H_2O_2 concentration for all catalysts. CV results demonstrated that M-Pd@C catalyst exhibited excellent electrocatalytic activity to the reduction of H_2O_2. As a result, Pd@Ni (7:3) have the highest sensitivity between the core catalysts on the other hand Ni@Pd (5:5) have the highest sensitivity among shell catalyst. 10 mM hydrogen peroxide responses of these two catalysts were compared to determine which combination is best and is given in Figure 1. As shown in Fig. 1 of Nickel (Ni) in the core and palladium (Pd) to be included in the shell being obtained a higher sensitivity to hydrogen peroxide.

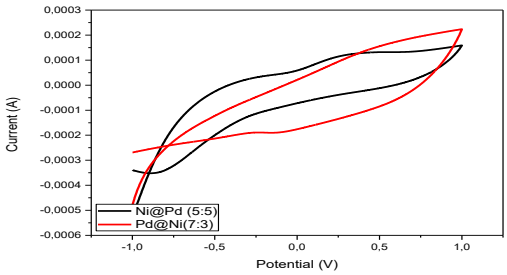

Fig. 1. Cyclic voltammograms of a comparison of hydrogen peroxide response of catalysts Pd@Ni core and Ni@Pd core

[1] S. Park, T. D. Chung, H.C. Kim, Anal. Chem. 75, No.3046 (2003).

[2] Y. Li, Y.Y. Song, C. Yang, X.H. Xia, Electrochem. Com. 9, No. 981 (2007).

STUDIES ON ELECTROCHEMICALLY SYNTHESIZED POLYPYRROLE (PPy) THIN FILMS FOR CONDUCTING POLYMERS APPLICATION

A. A. Kaya[1], Y. E. Firat[1], A. Peksoz[1], N. Kucuk[1] and I. Kucuk[1]
[1]*Department of Physics, Faculty of Art and Science, Bursa, Gorukle, Turkey*
E-mail :aslitay@uludag.edu.tr

SYNTHESIS OF NOVEL TWISTED CARBAZOLE DERIVATIVES WITH 1,3,5-BENZENE CORE: HOST MATERIAL FOR PHOTODIODEs

K. Görgün[1]

[1] *Eskişehir Osmangazi University, Department of Chemistry, Faculty of Art and Science, Eskişehir, Turkey*

E-mail: kgorgun@ogu.edu.tr

Carbazole derivatives are widely used as optical, electroactive materials for their excellent electron donating and host materials because of their high triplet energy and good hole-transporting properties. In the literature had shown that the incorporation of the strong electron-withdrawing fluorinated substituents into hole transporting material, which may contribute to tuning the electronic properties and altering charge transport properties. In particular, electron-withdrawing groups, such as –CN, -F and -CF_3, in direct conjunction with the electron-donor N atoms of the well-known as hole transport material carbazole derivatives. Therefore, electron-withdrawing groups fluorinated substituents, lower the HOMO levels and the hole mobility and tune the molecular properties, such as solubility or stability.

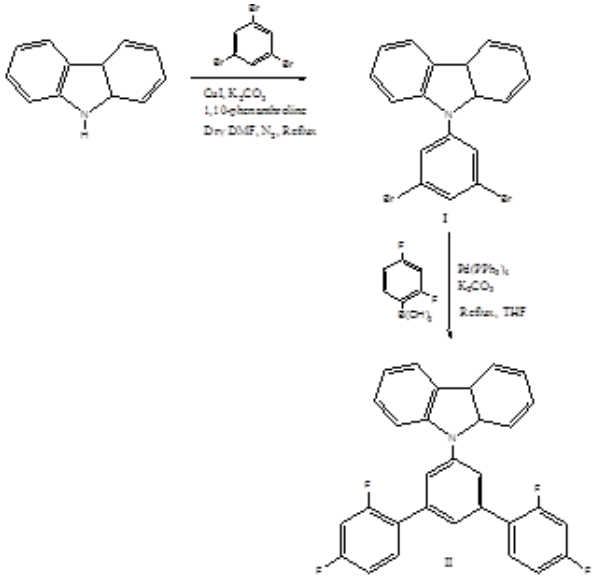

Scheme 1: Synthetic route to the compound II

Considering the information given in the literature the Ullman and Suzuki-Miyaura coupling reaction were carried out using carbazole, 1,3,5 tribromo benzene and aryl boronic acid (Scheme 1). Synthesized novel carbazole derivatives are characterized by elemental analysis, IR, MS, XRD, 1H NMR and 13C NMR and photophysical and thermal properties were investigated.

Acknowledgements: This work was supported by Anadolu University Commission of Scientific Research Project under Grant No. 1505F310.

TEMPERATURE DEPENDENT ELECTRICAL CHARACTERISTICS AN ORGANIC BASED HETEROJUNCTION DEVICE

M. Soylu[1], F.Yakuphanoglu[2]

[1]*Department of Physics, Faculty of Arts and Sciences, Bingol University, Bingol, Turkey*

[2]*Department of Physics, Faculty of Sciences, Firat University, Elazig, Turkey*

[1]E-mail: soylum74@yahoo.com

An organic/inorganic heterojunction diode having ZnPc on p-Si substrate was fabricated. ZnPc/p-Si heterojunction structure shows rectifying behavior. It has been seen that diode parameters are significantly different than those of conventional Al/p-Si metal–semiconductor contacts. The ZnPc/p-Si heterostructure exhibits a non-ideal I–V behavior with the ideality factor greater than unity that can be ascribed to the interfacial layer, interface states and series resistance. The current-voltage characteristics at low forward voltages show the ohmic behavior, limiting extraction of holes from p-Si over the ZnPc/p-Si heterojunction. Temperature dependent charge transport mechanism appears to be space charge limited conduction (SCLC) mechanism, taking into account the presence of an exponential trap distribution with total concentration of traps. The series resistance is found to be temperature-dependent.

Phthalocyanines (Pcs) have been intensively studied as photosensitizers and semiconductors [1-5]. Phthalocyanines have been attracted attention in device applications. Zinc phthalocyanine (ZnPc) is a p type semiconductor. Pcs act as a photosensitizing substance for cancer treatment in photodynamic therapy. Pc dye sensitizers have a large absorption coefficient in the red/near-IR (Q-band) and the UV/blue (Soret-band) light regions [6].The characteristics of heterojunction are strongly affected by energy level alignment and charge transport. ZnPc may act as an electron blocking layer for hole extraction despite of relatively low LUMO level. Fig. 1 shows the current-voltage (I–V) measured in wide temperature range. Conduction mechanisms that are accounted for the organic/inorganic devices are analyzed from the I–V characteristics.

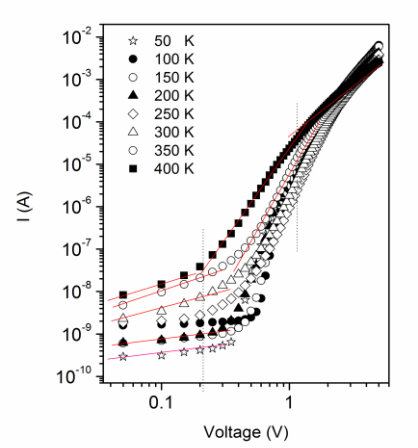

Figure-1: the curves of log (I) vs. log (V) at positive bias.

The operating conduction mechanism is marked by ohmic conduction at low forward voltages. Whereas the plots of log(I)-log(V) exhibit a power law dependence of the form $I \alpha V^{3-5}$ at higher bias.

[1] M. Calvete, G.Y. Yang, M. Hanack, Synthetic Metals 141, 231 (2004).

[2] V.N. Nemykin, E.A. Lukyanets, Arkivoc 1, 136 (2010).

[3] D. Wohrle, G. Schnurpfeil, S.G. Makarov, A. Kazarin, O.N. Suvorova, Macroheterocycles 5, 191 (2012).

[4] J.W. Ryan, E. Anaya-Plaza, A. de la Escosura, T. Torres, E. Palomares, Chem Commun 48, 6094 (2012).

[5] N. Masilela, T. Nyokongi, Synthetic Metals 162, 1839 (2012).

[6] W. Shi, B. Peng, L. Lin, R. Li, J. Zhang, Tianyou Peng, Materials Chemistry and Physics 163, 348 (2015).

DEVELOPMENT OF A NEW MICROBIAL BIOSENSOR BASED ON CONDUCTIVE POLYMER / MULTIWALLED CARBON NANOTUBE AND ITS APPLICATION TO PARACETAMOL DETERMINATION

E. Bayram[1], E. Akyilmaz[1]

[1]*Department of Biochemistry, Faculty of Science, City, State, Country*

E-mail :byrmezgi@gmail.com

TENSILE TEST OF BIOCOMPATIBLE GELATIN BASED FILMS WITH GLUCOSE AND SODIUM CHLORIDE

İ. Ulusaraç[1], N. Koyuncu[1], B. Demirbay[2] and F.G. Acar[1*]

[1]*Department of Physics Engineering, Faculty of Science and Letters, İstanbul Technical University, 34469 Maslak, İstanbul, Turkey*

[2]*Physics Engineering Program, Institute of Science and Technology, İstanbul Technical University, 34469 Maslak, İstanbul, Turkey*

[*] E-mail:acarg@itu.edu.tr

In recent days, biocompatible materials make a progress in the fields of material science since the use of those materials has great benefits for the health systems of mankind. For example, the process of cell transfer can be implemented by the use of biocompatible gelatin in the presence of methacrylamide under UV for the damaged biological tissues [1]. The term that is mentioned above, biocompatibility, specifically considers the compatibility of the biomaterials on biological systems. The durability and strength of produced biomaterials is very significant as mechanical property of materials is one of the essential parameters of being biocompatible. Therefore, the major purpose of this work is to investigate the mechanical properties of biocompatible films from gelatin with other additive materials that are sodium chloride (NaCl) and glucose.

In order to prepare films, the additive glucose and NaCl which have various concentrations, were mixed with gelatin solutions. In the preparation of solutions, NaCl and glucose solutions with percentages of 1%, 2%, 3%, 4%, 5%; and 2% of pure gelatin solution were used at the room temperature. The mixtures were constituted through using 80% of pure gelatin and 20% of additive solutions. As a result of this process, gelatin-glucose and gelatin-NaCl solutions were obtained at different concentrations. In 2-3 days, films were acquired by the vaporization of water compounds. Two types of films which are solvable in distilled water, were obtained depending on which material is used. From those films, lamel-sized samples were obtained which then those samples were used in tensile strength test. During the tests of samples, medium was at room temperature. After all experimental process, the results were evaluated. It is understood that elasticity modulus and mechanical properties of the specimens were varied depending on which content and concentration is used.

To sum up, elasticity modulus, maximum strength, type of films and mechanical characteristics of all specimens were investigated mathematically. The experimental data and the possible application fields of those biocompatible films will be given with the details.

[1] Rose, James B. et al., Gelatin-based materials in ocular tissue engineering, Materials, 7,3106-3135 (2014)

DIELECTRIC PROPERTIES OF SEGMENTED POLYURETHANES GRAFTED ONTO PEMA-co-PHEMA

P.Demir
Department of Chemical Technology, EOSB Maden Higher Vocational School, Elazığ, Turkey
E-mail :pdemir@firat.edu.tr

Polyurethane (PU) elastomers have a significant electric field stress [1]. Also they have remarkable properties such as abrassion resistance, high mechanical strength[2]. The PU elastomers studied here are grafted onto poly(ethylmethacrylate)-co-poly(2-hydroxyethylmethacrylate),(PEMA-co-PHEMA) and these elastomers have block copolymers of soft and hard segments. In this study, the hard segments (HS) are composed of 4,4'-methylene bis (phenyl diisocyanate) (MDI) and ethyleneglycol (EG), whereas poly(ε-caprolactone) is employed as soft segments (SS). The structure of graft PU presented Fig.1.

Dielectric properties of all polymers were measured. For this purpose, the all polymers were ground with an agate mortar and pestle, and the final fine powders were pressed at four tons of pressure into disk-shaped samples with a thickness ranging from 0.87 mm to 1.98 mm and a diameter of 12 mm. The capacitance measurements were carried out at room temperature with a QuadTech 7600 precision LRC meter impedance analyzer over the frequency range 100 Hz– 2 kHz [3]. The dielectric features against the frequency of segmented polyurethanes at room temperature were examined. Real and imaginary parts of the dielectric permittivity and the real and imaginary parts of dielectric modulus versus temperature for the all polymers at 1 kHz and 0.5 kHz were examined.

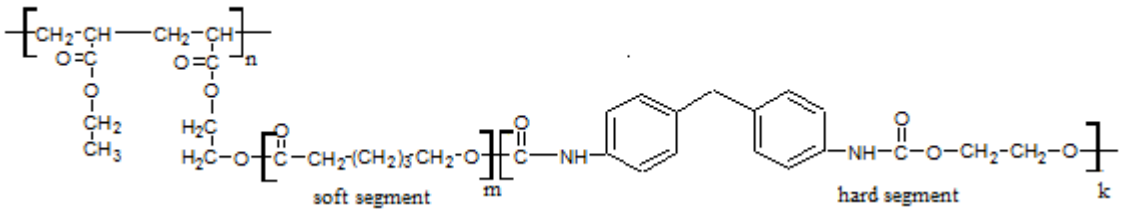

Figure 1. structure of graft PU.

[1] Guiffard B, Seveyrat L, Sebald G, Guyomar D. Enhanced electric field induced strain in non percolative carbon nanopower/polyurethane composites. J Phys D Appl Phys;14:3053-7(2006).

[2] Guelcher SA, Gallagher KM, Didier JE, Klinedinst DB, Doctor JS, Goldstein AS, et al. Synthesis of biocompatible segmented polyurethanes from aliphatic diisocyanates and diurea diol chain extenders. Acta Biomater;4:471-84 (2005).

[3] Coşkun M, Seven P, Synthesis, characterization and investigation of dielectric properties of two-armed graft copolymers prepared with methyl methacrylate and styrene onto PVC using atom transfer radical polymerization. Reactive & Functional Polymers;71: 395–401(2011).

THERMOELECTRIC PROPERTIES OF PHTHALOCYANINE-BASED COVALENT ORGANIC FRAMEWORKS: A FIRST-PRINCIPLES STUDY

F. Aksakal[1], Y. Chumakov[2], and A. Dimoglo[3]

[1]*Department of Chemistry, Faculty of Science, Kocaeli, Turkey*

[2]*Department of Physics, Faculty of Science, Kocaeli, Turkey*

[3]*Department of Environmental Engineering, Faculty of Engineering, Kocaeli, Turkey*

fatmaaksakal@gtu.edu.tr

THE ELECTRICAL CHARACTERIZATION OF PLASMA DEPOSITED PHOSPHORUS DOPED N-TYPE HYDROGENATED AMORPHOUS SILICON CARBIDE THIN FILMS

K.Sel, B. Alçınkaya,

Department of Physics, Faculty of Arts and Sciences, Çanakkale, Turkey

E-mail :kivanc@comu.edu.tr

Phosphorus doped n-type hydrogenated amorphous silicon carbide (a-SiC_x:H) thin films were deposited by radio-frequency (13.56 Mhz) plasma enhanced chemical vapor deposition (PECVD) system by using silane, ethylene and phosphine gases. The carbon content of the four set of deposited films were modified to four different values by adjusting the gas flow rates of the source gases, silane and ethylene, whereas the flow rate of phosphine was fixed for all of them. The elemental compositions (x) of these films, which were analyzed by X-ray photoelectron spectroscopy, were determined as x=0, 0.19, 0.46, 0.62, respectively. The thicknesses of the films were investigated by UVVIS transmission spectroscopy. The electrical conductivities of the films were calculated from the Ohmic region of the current-voltage curves obtained by temperature dependent current-voltage measurements, each of which was performed under constant temperature. The room temperature conductivities of the films were determined and it is observed that the conductivity of the silicon rich film, which was around $2.5x10^{-3}$ $S.cm^{-1}$, is about 10^8 $S.cm^{-1}$ times higher than that of the carbon rich film, respectively. Finally, the electrical activation energies were determined by fitting the conductivity values in the Arrhenius plot as a function of the standard transport model. The activation energy of the silicon rich film was about 0.25 eV. The activation energies increased as x increases and reached around 0.70 eV for carbon rich film.

OPTOELECTRONIC PROPERTIES OF FLUORESCEIN CONTAINING POLY(2,5-DITHIENYLPYRROLE) DERIVATIVES

Pınar Çamurlu, Neşe Güven

[1]*Akdeniz University, Department of Chemistry, 07058, Antalya, Turkey*

E-mail :pcamurlu@akdeniz.edu.tr

In this study, a new fluorescein containing 2,5-dithienylpyrrole derivative (SNS- Fluores) was synthesized through a click reaction. The monomer was subjected to electrochemical homopolymerization (PSNS-Fluores) and the homopolymer thoroughly characterized for its electrochromic properties via spectroelectrochemistry, kinetic, coloration efficiency studies and colorimetry measurements. Spectroelectrochemical analysis of neutral homopolymer revealed electronic $\pi-\pi^*$ transitions at 341 and 445 nm, indicating dual band structure of PSNS-Fluores which is not common for poly(2,5-dithienylpyrrole) derivatives [1-3]. The homopolymer had an electronic band gap of 2.39 eV with a yellow to a greenish yellow color transition in 3.85 s. Additionally, the copolymerization of SNS-Fluores and EDOT was successfully achieved electrochemically in $LiClO_4$/ACN by direct anodic oxidation of the monomer mixture. Copolymer, on the other hand, revealed an enhanced color pallet ranging from brown, orange, yellow, light green to olive green with a switching time of 1.49 s.

We are grateful to TUBITAK (Project No: 110T640) for the support of this study.

[1] G. G. Abashev, A. Y. Bushueva and E. V. Shklyaeva, N-substituted 2,5-di(2-thienyl)pyrroles: application, production, properties, and electrochemical polymerization (review), Chem. Heterocycl. Compd. 47, 130 (2011).

[2] P. Camurlu and N. Karagoren, Clikable, versatile poly(2,5-dithienylpyrrole) derivatives, React. Funct. Polym. 73, 847 (2013).

[3] N. Guven and P. Camurlu, Electrosyntheses of Antracene Clicked Poly(thienylpyrrole)s and Investigation of Their Electrochromic Properties, Polymer 73, 122 (2015).

THEROTICAL STUDIES OF ELECTRONIC PROPERTIES OF POLYPRROLE (Ppy) OLIGOMER

Y. Kaya[1], A. A. Kaya[2]

[1]*Department of Chemistry, Faculty of Art and Science, Bursa, Gorukle, Turkey*

[2] *Department of Physics, Faculty of Art and Science, Bursa, Gorukle, Turkey*

E-mail :ykaya@uludag.edu.tr

MAGNETIC FEATURED HORSERADISH PEROXIDASE-Cu2+ HYBRID NANOFLOWERS (MhNFs) FOR ENZYMATIC ELIMINATION OF PHENOL

N.Özdemir[1], I. Ocsoy[2,3], C. Altınkaynak[2,3], and S. Tavlasoğlu[1]

[1]*Department of Chemistry, Faculty of Science, Erciyes, University, Kayseri, Turkey*

[2] *Department of Analytical Chemistry, Faculty of Pharmacy, Erciyes University, Kayseri, Turkey*

[3] *Nanotechnology Research Center, Erciyes University, Kayseri, Turkey*

E-mail :ozdemirn@erciyes.edu.tr

Enzymes have been immobilized in/on various supports, such as inorganic or organic materials. In general, immobilized enzymes show improved stability, making them efficient, reusable and economical. However, increased catalytic activity is generally limited due to mass transfer limitations between the enzyme and substrate and conformational changes in the enzyme. Recently, Zare and co-workers reported an elegant approach for the synthesis of immobilized enzymes in the form of hybrid (organic-inorganic) nanoflower with highly enhanced catalytic activity and stability [1].

In this study, magnetic featured horseradish peroxidase-Cu^{2+} hybrid nanoflowers (mhNFs) were prepared and some characteristics of them were determined. And these prepared mhNFs were also used for phenol elimination. As it known, phenolic compounds are among the most ubiquitous pollutants and they are widely known to be toxic and difficult to degrade [2].

The synthesis of hNFs was accomplished using a described method before [2- 4] and magnetic featured was gained. The structure of the synthesized mhNFs was confirmed by FT-IR, XRD, and EDX. The catalytic activity of synthesized mhNFs was evaluated, and phenol elimination was studied using these mhNFs. The activities of mhNFs were higher than free and hNFs under all conditions. 100% phenol elimination was accomplished after 2 hours incubation using mhNFs. Optimum pH was found pH 7 for phenol elimination.

This work was supported by a grant from the Scientific and Technological Research Council of Turkey (TUBİTAK) (Project no: 115Z092).

[1] J. Ge, J. Lei and R.N. Zare, Nature Nanotechnology, 7, 428-432 (2012).

[2] J. L. Gomez, A. B´odalo, E. Gomez, A. M. Hidalgo, M. Gomez, M. D. Murcia, Chemical Engineering Journal, 127, 47–57 (2007).

[3] B. Somtürk, M. Hancer, I. Ocsoy, N. Özdemir, Dalton Transactions, 44(31), 13845-13852 (2015).

[4] C. Altınkaynak, İ. Yılmaz, Z. Köksal, H. Özdemir, I. Ocsoy, N. Özdemir, International Journal of Biological Macromolecules, 84, 402-409 (2016).

THE INFLUENCE OF ANNEALING MEDIUM ON NiO FILMS DEPOSITED BY HOMEMADE SPIN COATER

T.Taşköprü[1,2] and E. Turan[1]

[1,2]Department of Physics, Anadolu University, Eskisehir 26470, Turkey

[2]Department of Physics, Çankırı Karatekin University, Çankırı 18100, Turkey

E-mail :tasturan@gmail.com

Nickel oxide (NiO) is one of the versatile oxide materials and has drawn much attention due to its excellent chemical stability as well as optical, electrical and magnetic properties. NiO films have immense potential in a number of applications such as electrochromic devices, solar thermal absorber, supercapacitors, solar cells, lithium-ion batteries and gas sensors. NiO is one of few stable metal oxides exhibiting p-type semiconducting behavior and gas sensing capabilities [1,2].

NiO films were produced on glass substrates and FTO coated glass substrates by sol-gel spin coating technique. The effect of the annealing atmosphere on the structural, morphology and electrochemical properties of the films was investigated. The deposited samples were annealed at 500 °C for 2 h in air, oxygen, nitrogen and argon atmospheres. The XRD studies revealed that the samples had nickel oxide cubic structure. The annealing of the samples in inert atmospheres leads to Ni phase formation in the structure. FESEM images showed that the heat treatments in inert atmosphere boost the larger clusters and crystallite size varying in the range 21- 39 nm. It is found that the NiO films annealed under air and oxygen atmospheres exhibit high transmittance whereas a decrease is seen in the transmittance for the other samples.Transmission of the films decreased from 85 to 20% as a function of annealing atmospheres. The electrochemical behavior of the films was studied by means of cyclic voltammetry in 0.3 M KOH solution. Cyclic voltammograms showed that anodic peak shift takes place for the films annealed in argon and nitrogen with respect to those annealed in air and oxygen atmospheres.

[1] M. R. Al-Bahrani, et al. NiO-NF/MWCNT nanocomposite catalyst as a counter electrode for high performance dye-sensitized solar cells. Appl Surf Sci. 331, 333 (2015).

[2] P. C. Chou, et al. Hydrogen sensing performance of a nickel oxide (NiO) thin film-based device. Int J Hydrogen Energy. 40, 729 (2015).

COPOLYMERIZATION OF BENZYL METHACRYLATE AND A METHACRYLATE BEARING CHALCONE SIDE GROUPS: SYNTHESIS, CHARACTERIZATION AND DIELECTRIC BEHAVIORS

Taner ÇELİK, M. Fatih Coşkun

E-mail: tanercelik76@gmail.com

Firat University, Faculty of Science, Department of Chemistry, 23119, Elazig/Turkey

In this study, firstly (2E)-1-(1-benzofuran-2yl)-3-(4-hydroxyphenyl)propen-1-one **(1)** was synthesized from the reaction of 1-(1-benzofuran-2-yl)ethanone with 4-hydroxybenzaldehyde. Secondly 4-[(1E)-3-(1-benzofuran-2-yl)-3-oxoprop-1-en-1-yl]phenyl chloroacetate **(2)** was synthesized from the reaction of compound **(1)** and chloroacetyl chloride. The monomer was prepared by the reaction of compound **(2)** and sodium methacrylate. The copolymerization of compound **(2)** and benzyl methacrylate was performed by the free radical polymerization method.

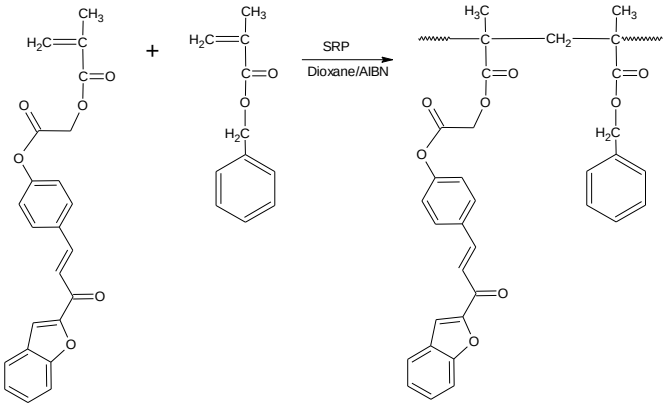

The structure characterizations of these polymers were defined by FT-IR, ^{1}H and ^{13}C- NMR techniques. The thermal behaviors of homo and copolymers were investigated by DSC and TGA measurements. The results were compared with each other.

The dielectric measurements (dielectric constant, dielectric loss factor and conductivity) of the graft copolymers were carried out by means of an impedance analyzer as a function of the frequency from 100 Hz to 2000 Hz.

Keywords: Chalcone , Dielectric Properties, Conductivity

References

[1] R, Balaji., S. Nanjundan. Synthesis and characterization of photocrosslinkable functional polymer having pendant chalcone moiety Reactive & Functional Polymers 49 (2001) 77–86.

[2] A. M. Lotonov, N. D. Gavrilova, E. Yu. Kramarenko, E. I. Alekseeva, P. Y. Popov, G. V. Stepanov, Polymer Science-Ser.B.48, 267 (2006).

[3] D. Bhadra, M.G. Masud, S. Sarkar, J. Sannigrahi, S.K. De, B.K. Chaudhuri, J. Polym. Sci. B. 50, 572 (2012).

INVESTIGATION OF LANTHANUM WITH CHITOSAN COMPOUND USING QUANTUM MECHANICAL METHODS

Aslı Öztürk Kiraz

Department of Physics, Faculty of Science&Arts, Denizli, Turkey

E-mail : aslio@pau.edu.tr

One of the most commonly used biopolymeric materials is chitosan which has features such as low-cost and abundance in nature. Chitosan is used in many different areas from controlled release of the drug to biomedical technologies and environmental applications. For these reasons, it's very importanat to know the physical properties of the chitosan, and also espicially interaction with the lanthanum.

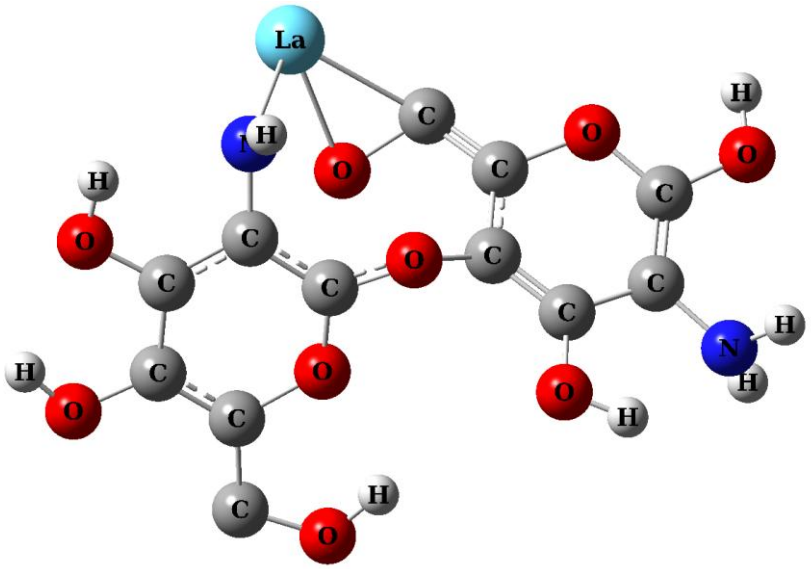

Figure1. Optimized geometry of the compound

In this study, Chitosan with Lanthanum compound investigated by Density Functional Theory (DFT) at B3LYP/CEP-121G level. The structural, electronical, optical, termodynamic parameters and also highest occupied molecular orbital (HOMO) energies, the lowest unoccupied molecular orbital (LUMO) energies, NBO analysis of the compound have been calculated by the Gaussian 09W [1] package.

[1] M.J. Frisch, et al., Gaussian 09, Revision C.01, Gaussian, Inc., Wallingford CT, 2010.

EXPERIMENTAL AND THEORETICAL STUDIES ON NOVEL SILVER COMPOUNDS

M.T. Bilkan[1]

[1]*Department of Physics, Faculty of Science, Çankırı Karatekin University, Çankırı, Turkey*

E-mail:mtbilkan@gmail.com.tr

Experimental and theoretical studies of silver containing new chemical compounds have been performed in this study. Novel complexes were synthesized by chemical synthesis methods. Three-dimensional geometric structures of the compounds obtained by single crystal XRD method were used in calculations. The optimizations of the molecular structures were carried out by using Density Functional Theory and LanL2DZ basis set. Vibrational frequencies and their intensities, HOMO-LUMO energies, thermochemical properties and atomic charges for the compounds were also computed by same level of the theory. In the experimental part of this study, mid-IR and Raman spectra of the compounds were recorded by attenuated total reflection (ATR) technique. CHNS elemental analysis and experimental far-IR spectra were employed to identify the metal-ligand binding. The theoretical and experimental results show that the ligands are coordinated to the metal center in bidentate and unidentate fashions.

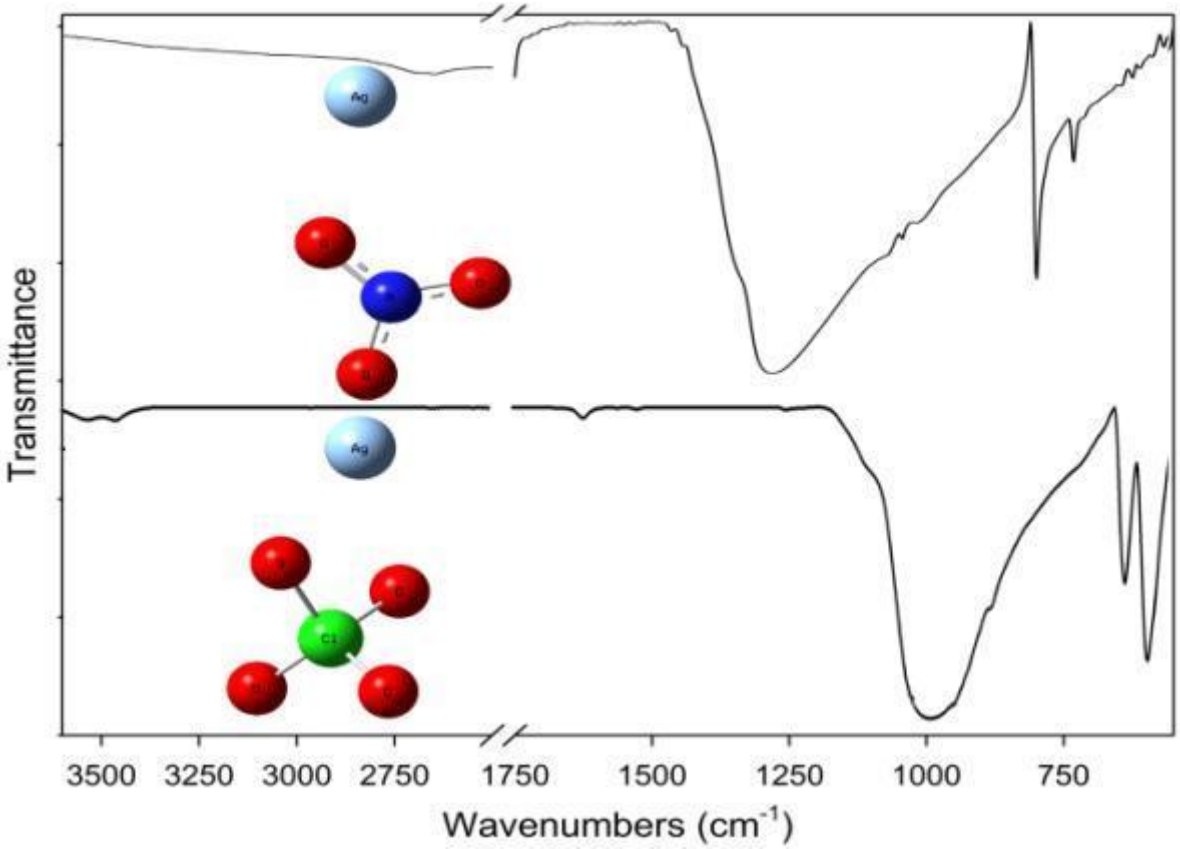

SYNTHESIS AND DSSC APPLICATIONS OF RU COMPLEXES BEARING BENZIMIDAZOLE TYPE LIGANDS

Melek Tercan[1] and Osman Dayan[1]

[1]*Department of Chemistry, Faculty of Arts and Science, Çanakkale, Turkey*

E-mail: melektercan@comu.edu.tr

Various polypyridine ligands and their Ru(II) complexes have been reported and most of these complexes reviewed important electrochemical and photovoltaic property characteristics that are useful for dye-sensitized solar cells applications [1]. It is possible to arrange photophysical properties of the complex by choice of ligands. The use of a ligand with electron-withdrawing substitution (–COOH or $–COOC_2H_5$) causes an emission at higher wavelengths because of their lower π* levels. Oppositely the ligands that have electron-donating substitutions (-CH3) will stabilize the metal center and increase the energy gap, which will increase the yield and lifetimes. Furthermore, greater stability and solubility could be achieved with ligand substitutions containing aliphatic chains while absorption shifts could be controlled by conjugated substituents [2].

In this study; new Ru complexes of benzimidazole-type ligands were synthesized and derivated by bipyridine-dicarboxylic acid and isocyanate ligands. The synthesized complexes were characterized by IR, UV-vis, ^{1}H-NMR and ^{13}C-NMR spectroscopy. Then DSSC applications were performed and current-voltage characteristics were identified.

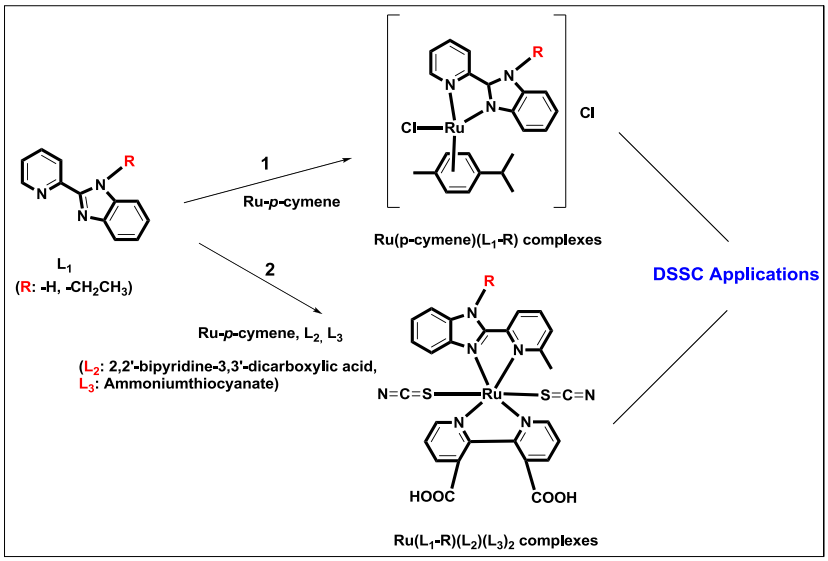

[1] M. Beley and P. C. Gros, Ruthenium polypyridine complexes bearing pyrroles and ∏-extended analogues. Synthesis, spectroelectronic, electrochemical and photovoltaic properties, Organometallics. 33, 4590 (2014).

[2] A.O. Adeloye and P.A. Ajibade, Towards the development of functionalized polypyridine ligands for Ru(II) complexes as photosensitizers in dye-sensitized solar cells (DSSCs), Molecules. 19, 12421 (2014).

NOVEL SOLUBLE ESTERIFIED METALLO, METAL-FREE, MONOMERIC, AND OLIGOMERIC PORPHYRAZINE COMPLEXES WITH EIGHT (5-THIOPENTYL 2-METHOXY-4,6-BİS (TRİFLUOROMETHYL)BENZOATE) UNITS

E. Gonca

Faculty of Engineering, Department of Chemical Engineering, Çanakkale Onsekiz Mart University, Terzioglu Campus, TR 17020 Çanakkale, Turkey

E-mail :egonca@comu.edu.tr

Metallo tetrapyrrole compounds bearing fluorine atoms are receiving a great deal of attention due to their high thermal and chemical stability, interesting electron-transporting characteristics, hydrophobicity, lipophobicity, and decreased intermolecular attractive forces in comparison to their hydrocarbon analogues [1]. It has been reported that the position and the number of pentafluorophenyl groups on the macrocycle ring has a marked effect on the stability and catalytic activity [2].

The novel soluble esterified metallo, metal-free, monomeric, and oligomeric porphyrazine complexes with up to 48 fluorine-containing substituents on the periphery were reported and also the effects of the substituents on the spectroscopic properties of the porphyrazine complexes in different solvents were reported. However, iron - porphyrazine derivatives with eight 5-thiopentyl 2-methoxy-4,6-bis(trifluoromethyl)benzoate substituents appending to the periphery positions were synthesized. Chloro [octakis (5-thiopentyl 2-methoxy-4,6-bis (trifluoromethyl)benzoate) porphyrazinato] iron (III) was prepared by the reaction of metal-free porphyrazine with iron (II) acetate and further treatment with HCl solution. The monomeric bisaxial complex $[FePz(py)_2]$ as well as the bridged complex $[FePz(pyz)]_n$ was formed as stable complexes by reacting FePzCl with pyridine or pyrazine, respectively. By using different spectroscopic methods, novel compounds have been characterized.

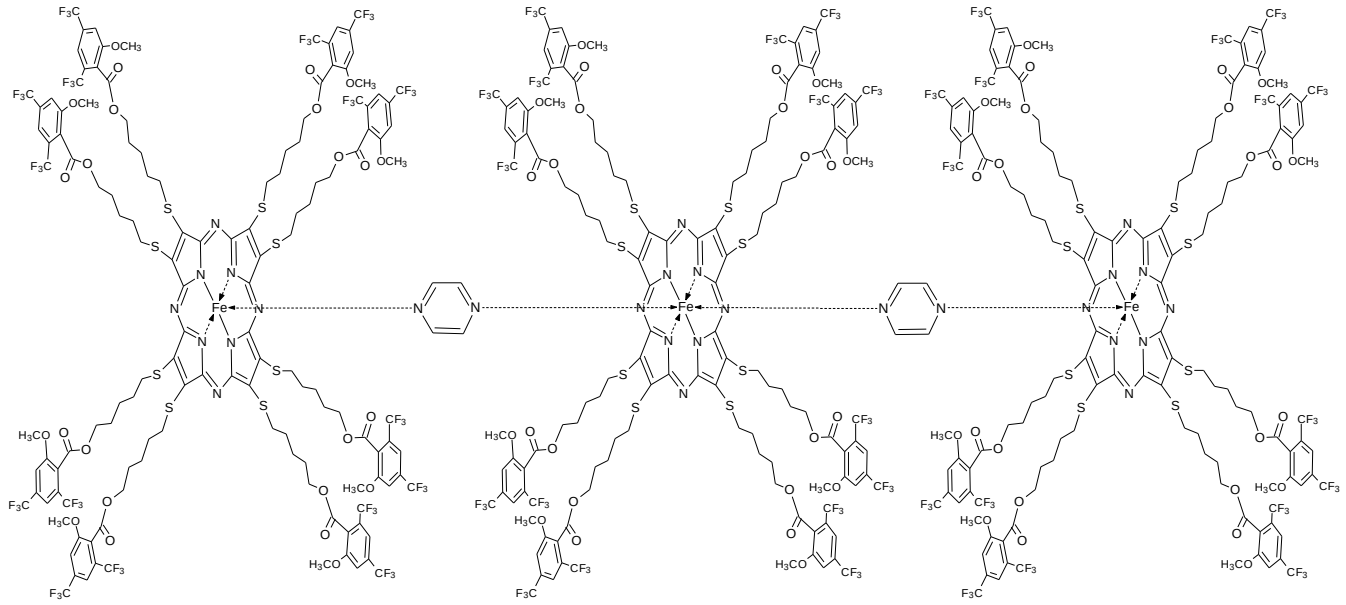

[1] E. Kol'tsov, T. Basova, P. Semyannikov and I. Iqumenov, Mater. Chem. Phys. 86, 222 (2004).

[2] J.R.L. Smith and G. Reg

inata, Org. Biomol. Chem. 1, 2543 (2003).

PREPARATION, CHARACTERIZATION AND ANTITUMOR ACTIVITY OF THIOXANTHONE DERIVATIVES

T.Paralı[1], O. Paralı[2], and M. Tulu[2]

[1]*Canakkale Onsekiz Mart University Lapseki Vocational College, Lapseki, Canakkale, Turkey*

[2]*Yıldız Technical University, Faculty of Arts and Sciences Dept. of Chemistry, Esenler, Istanbul, Turkey*

E-mail :tezcanparali@comu.edu.tr

Thioxanthones are one of the important class of synthetic compounds, with a common heterocyclic scaffold showing interesting biological and photochemical properties. Thioxanthones (TX) have been used as an example of the photophysical manifestations of vibronic coupling between nearby $n\pi^*$ and $\pi\pi^*$ excited states. Therefore TX derivatives significant photoinitiators widely used in UV curable inks for food packaging applications several representative derivatives have already proven safety to be used in humans.[1]

Thioxanthones are located extensively in diverse pharmacological activities. Over the years, TX derivatives have been synthesized comprehensively and studied grateful to their various biological activities such as antischistosomal effects, monoamine oxidase, antibiotic activity, inhibitory activity, activation of P-glycoprotein, and antitumor activities. Hycanthone was the first generation TX compound in 1980s and have been used for medicinal purposes. However, it didn't continue due to hepatotoxicity and non-proportional pharmacokinetic parameters. SR271425, the third generation of TX, was carried out clinical studies based on vigorous *in vivo* antitumor activity, the derivative of Hycanthone. Because of the potential proved by these structures, TX is still a candidate structure as an anticancer agent that warrants further lead optimization.[2]

In this study, the novel TX derivatives were synthesized and molecular characterization made by NMR, ATR, FT-IR, MALDI-TOF/MS and UV. Then, *in vitro* drug release studies of the drug delivery systems at different pHs were carried out using the dialysis membrane and the amount of emission determined by HPLC. IC_{50} and EC_{50} values will be defined with spectrophotometric measurements by interacting characterized drug release system with the cancer cell lines.

[1] A.M. Paiva, M.M. Pinto and E. Sousa, A Century of Thioxanthones: Through Synthesis and Biological Applications, Current Medicinal Chemistry, 20, 2438-2457 (2013).

[2] HSu-Shan Huang et.al., Synthesis and evaluation, of new 3-substituted-4-chloro-thioxanthone derivatives as potent anti-breast cancer agents,Arabian Journal of Chemistry, (2015).

POSTER PRESENTATIONS

Solid state and solution photophysical properties of a novel symmetric porphyrin Schiff base ligand and its metal complexes

M. Tümer, A. R. Çiftaslan, and M. Köse
Chemistry Department, K.Maras Sütcü Imam University, K.Maras, Turkey
E-mail :ahmetrasit2008@hotmail.com

For the blue light-emitting materials, such as polyfluorenes, high efficiency was achieved, but there are frequent problems with stabilities and lifetimes [1]. Many porphyrins emit quite strongly in the red region of the spectrum, owing to their rigid, highly conjugated structures. Moreover, they have quite narrow bandwidths, potentially favouring high colour purity if used in an OLED. The electronic absorption and photoluminescence spectra of the ligand, its metal complexes and the metal salts used for preparing of the complexes were investigated in the solid and solution state. The emission and excitation data of the $CuCl_2.2H_2O$ in both solid and the solution state were observed in the longest wavelength. On the other hand, the emission value of the $ZnCl_2$ salt was shown at the shortest wavelength. The emission values of the LCu_4Cl_3 and LPt_4Cl_3 complexes in the solid state are bigger than the other metal salts. The ligand and its metal complexes show the very interesting absorption spectral properties in the solid state. Metal complexes have less number Q bands in the solid state. The UV-vis spectrum of the Zn(II) complex is given in the Figure 1.

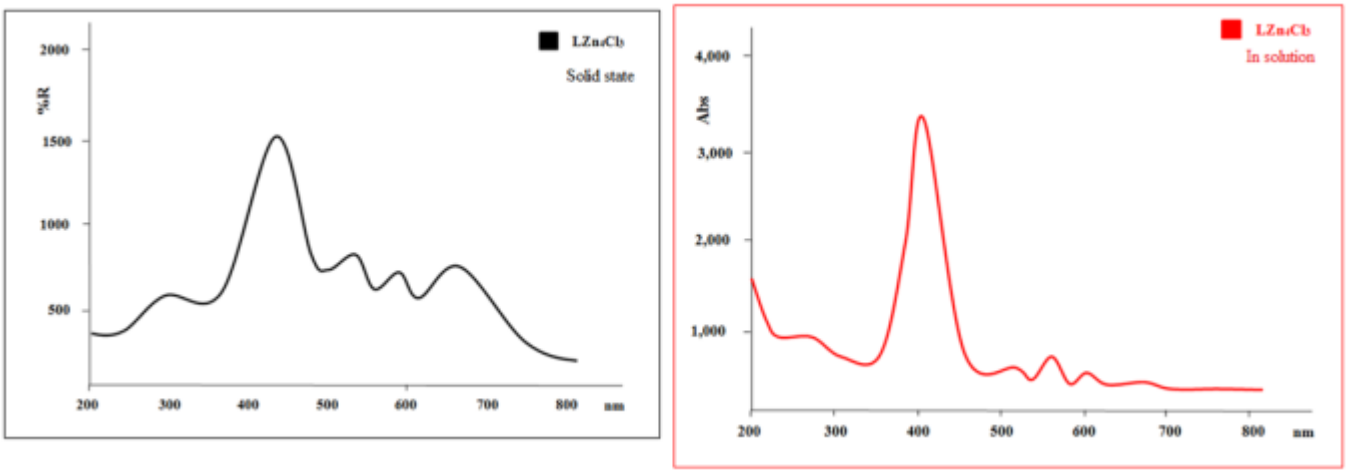

Figure 1. The UV-vis spectra of the Zn(II) complex.

[1] J. Rault-Berthelot, E. Raoult, F. Le Floch, Synthesis and anodic oxidation of a dimer EDOT-dicyanomethylenefluorene-EDOT: towards mixed polymers with very low band gap, J Electroanaly. Chem., 546, 29 (2003).

Acknowledgments
We are grateful to The Scientific & Technological Research Council of Turkey (TUBITAK) (Project number: (113Z907) for the support of this research.

Material properties of the novel asymmetric porphyrin imine ligands and their metal complexes

F. Tümer, M. Köse, and A. R. Çiftaslan

Chemistry Department, K.Maras Sütcü Imam University, K.Maras, Turkey

E-mail : ahmetrasit2008@hotmail.com

Porphyrins are one of the vital chemical units essential for a number of life processes on the earth. Many biological molecules function with prosthetic groups essentially made of these units. Porphyrins and their complexes were extensively studied and their applications in many area were done. For example, porphyrin compounds were used in the medical research, clinical disease diagnostics, and environmental monitoring [1]. We investigated the substituent effects on the electronic and photoluminescence properties of the porphyrin Schiff base ligands. In the course of the investigation of the spectroscopic properties of the compounds in the DMF, DMSO, $CHCl_3$, toluene and CH_2Cl_2 solutions, the aggregation was not shown. The electrochemical properties of the ligands and their metal complexes were investigated in DMF solution and at different scan rates. The ligands showed reversible redox potentials in the positive regions. The Raman spectra of the ligands and their metal complexes were investigated and determined the similar Raman bands of the compounds. The 1931 CIE (x,y) chromaticity coordinates of the ligands and their metal complexes were investigated and the x, y values of the complexes were found close to the very deep red color.

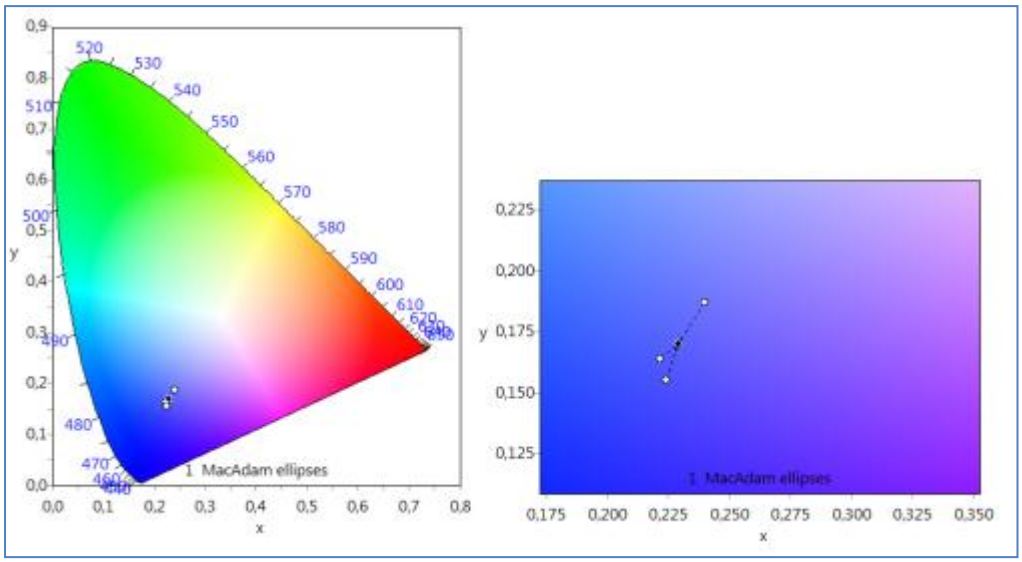

Figure. The CIE 1931 chromaticity plot for colour coordinates of the Zn(II) complex.

[1] V. Torres -Costa, R. J. Martin-Palma, Application of nanostructured porous silicon in the field of optics. A review, J. Materials Sci., 45, 2823 (2010).

Acknowledgments

We are grateful to The Scientific & Technological Research Council of Turkey (TUBITAK) (Project number: (113Z907) for the support of this research.

Synthesis and antioxidant properties of novel thiosemicarbazide derivatives

Ahmet ÇETİN

Department of Chemistry, Faculty of Science and Art, Bingol University, 12000, Bingol, Turkey

acetin74@hotmail.com.tr

Abstract- Novel derivatives of thiosemicarbazide were synthesized and evaluated for their antioxidant properties. Starting from readily available pyridine-2,5-dicarboxylic acid the title compounds were prepared. The reaction of carboxylic acid with absolute ethanol afforded the corresponding diethyl pyridine-2,5-dicarboxylate. The reaction of compound 1 with hydrazine hydrate good yielded pyridine-2,5-dicarbohydrazide. Refluxing compound 2 with alkyl/aryl isothiocyanate for 3-8 h afforded 1,4-disubstituted thiosemicarbazides in good yield (75-90%). The final compounds showed very high activity (88.16-71.34%) against 2,2-diphenyl-1-picrylhydrazyl free radical at the concentration of 25 µg/mL while the others showed lower activity.

Keywords: 1,2,4-triazoles, thiosemicarbazides, antioxidant activity, reducing power.

Introduction- Synthesis of novel thiosemicarbazide compounds is an important issue since they are key compounds used in pharmacology and already present in many medicinal preparations. The ring-closure reactions of carbohydrazide reactions afforded five-membered heterocycles bearing three heteroatoms such as 1,3,4-oxadiazoles, 1,3,4-thiadiazoles, and 1,2,4-triazoles [1]. The chemistry of 1,2,4-triazoles and their heterocyclic derivatives has gained notable attention due to their biological importance [2]. For instance, a large number of derivatives of thiosemicarbazide have been shown interesting drug candidates such as anti-inflammatory, CNS stimulants sedatives, antianxiety, antimicrobial agents [3,4] and antimycotic activity like fluconazole, intraconazole, voriconazole [5].

Besides these noteworthy biological applications, carbohydrazides are also of great utility in synthetic organic chemistry, for example, these compounds can undergo different types of reaction to yield other heterocyclic compounds in the present of various reagents, e.g., 1,2,4-triazoles, thiazolotriazoles, triazolothiadizoles, triazolothiazepines, and triazolothiadiazines. For the synthesis of the target compounds, the reaction sequences are outlined in Scheme. Dimethyl pyridine-2,5-dicarboxylate (**1**) was synthesized by the reaction of pyridine-2,5-dicarboxylic acid with absolute methanol in presence of H_2SO_4. The fusion of 2,5-bis-pyridine compound 2 with hydrazine hydrate afforded pyridine-2,5-dicarbohydrazide (**2**) in good yields. The treatment of compound **2** with isothiocyanates gave thiosemicarbazide derivatives (**3a-e**), respectively, in nearly quantitative yields. Crystallization solvents, melting points, yields%, and all spectral data of the compounds are given in experimental section.

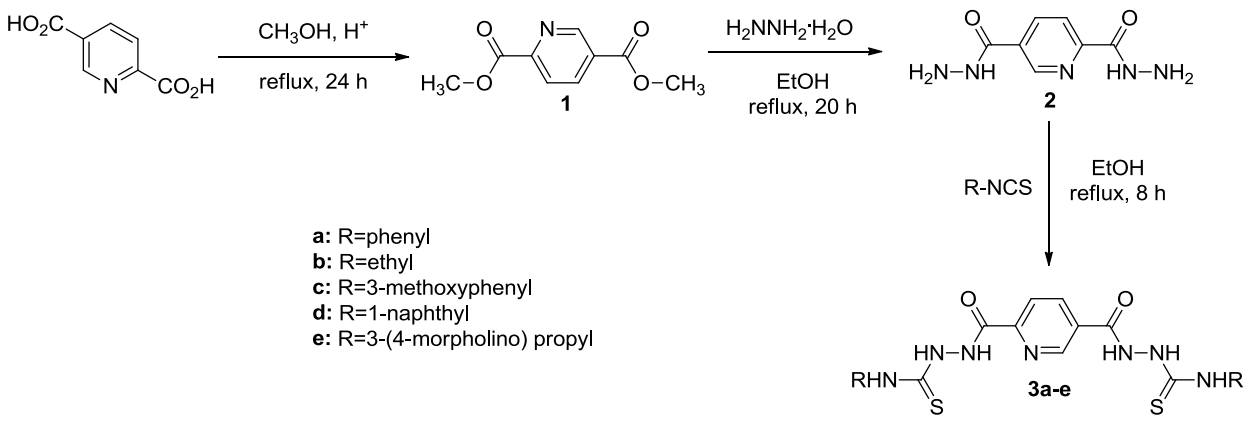

Scheme. The reaction sequences for the synthesis of the target compounds

Results and discussion- Thiosemicarbazides and their derivatives substituted with active functional groups are

exhibited analgesic, antipyretic and anti-microbial properties[6-8]. Such promising biological activities of these heterocyclic compounds provoked us to synthesize new compounds that substituted with different size functional groups such as –phenyl, -ethyl, -1-naphthyl, -3-methoxyphenyl and -3-(4-morpholino) propyl. Aim of this study was to investigate the biological activities of synthesized novel 1,2,4-triazole compounds containing different functional groups by comparing the different antioxidant activity parameters such as DPPH radical scavenging activity, ABTS cation radical scavenging activity, metal chelating activity and reducing power activity. Furthermore, the cyclization effect and the functional groups requirements of thiosemicarbazide moieties to reveal in the newly synthesized 1,2,4-triazole series.

Stable DPPH radical containing unpaired electrons shows a strong absorption at 517 nm. The amount of absorption is reduced when the stoichiometric match with an electron or a hydrogen atom the DPPH radical containing a single electron and indicate that the decrease of DPPH radical. For this purpose, we used stable DPPH radical to test free radical scavenging effectiveness of newly synthesized triazole derivatives. These compounds prepared at different concentrations (25-200 µg/mL) were added to the test medium and DPPH radical remaining in the medium was determined by measurement of absorption at 517 nm at the end of 30 min incubation period. Values of DPPH radical scavenging percent of the tested compounds are shown in Figure 1.

While the starting compounds (**1-2**), showed weakly DPPH radical scavenging activity, thiosemicarbazide series (**3a-e**) have demonstrated potent DPPH radical scavenging activity. Among the tested compounds were determined to be the activity ranking 3c > 3b > 3d > 3a > 3e > 1 > 2 at the concentration of 25 µg/mL.

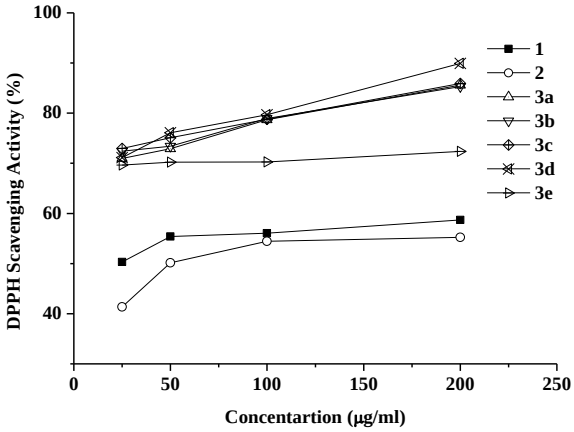

Figure 1. Percentage of DPPH scavenging of the compounds at 30 min incubation time in the range of different concentrations (25-200 µg/mL)

Reducing power capacity of the newly synthesized compounds were performed by evaluation of the degree of conversion of Fe^{3+} to Fe^{2+} form of test compounds preparing in the range of different concentrations (25-200 µg/mL). High absorbance value indicates a high reducing capacity of compounds. The newly synthesized compounds showed an increase linearly with increasing concentrations. The reducing ability of a compound can provide information about the potential antioxidant activity of this compound. The newly synthesized thiosemicarbazide compounds the containing groups of –phenyl, -ethyl, -3-methoxyphenyl (**3a, b, d**) (Figure 2).

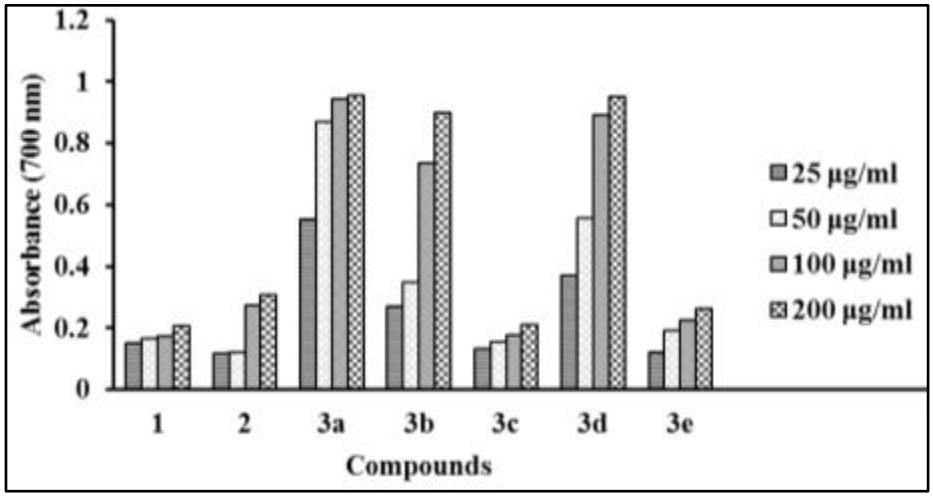

Figure 2. Reducing power capacities for compounds of starting (**1-2**), thiosemicarbazide (**3a-e**) and 1,2,4 triazole (**4a-e**) at the concentrations of 25, 50, 100 and 200 µg/mL (High absorbance value indicates a high reducing capacity of compounds)

Thiosemicarbazide compounds (**3a, b, d**) have exhibited highly reducing power according to 1,2,4-triazole compounds due to thiosemicarbazide series of compounds that could be attributed to a large number of H atoms [9].

Hydroxyl radicals occurring in biological systems are one of the most harmful of reactive oxygen species.

According to Fenton reaction ferrous ions (Fe^{2+}) are react with the hydrogen peroxide produced metabolically to form hydroxyl radicals. Free or weakly bound ferrous ions in vivo system leads to the formation of many diseases involving cell death and apoptosis events [10]. For this, there is need about antioxidant agents to quench reactive oxygen species such as hydroxyl radical, which are harmful to the body. Metal chelating activities of Newly synthesized starting compounds (**1-2**), and thiosemicarbazide compounds (**3a-e**) were tested in different concentration ranges (25-200 µg/mL). At the concentration of 200 µg/mL 1,2,4-triazole compounds (79.38-85.01 %) showed very high chelating activity than the starting compounds (17.35-34.38%) and thiosemicarbazide compounds (12.51-50.63 %) (Figure 3). These results show that cyclization of the thiosemicarbazide moieties to 1,2,4-triazole derivatives generate the active antioxidant compounds.

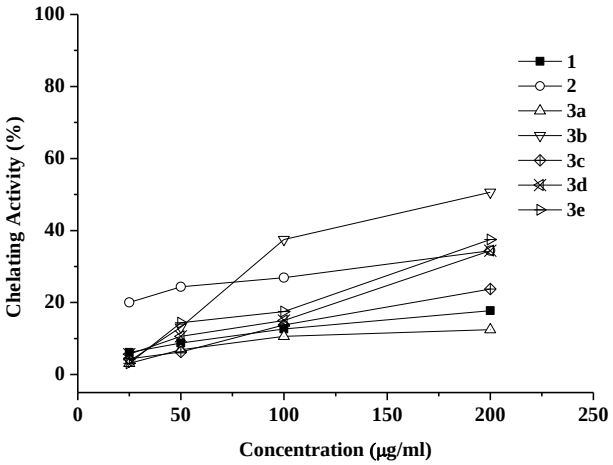

Figure 3. Ferrous ion-chelating activities for compounds of starting (**1-2**), thiosemicarbazide (**3a-e**) at the concentrations of 25, 50, 100 and 200 µg/mL.

To confirm radical scavenging activities of thiosemicarbazide (**3a-e**) compounds against ABTS cation radical were assessed. Figure 4 shows the IC_{50} values that obtained from active absorbance values at 723 nm by adding of test compounds preparing in the concentration range of 2-16 µg/mL to ABTS cation radical solution. The IC_{50} value is the

concentration of sample required to inhibit 50% of the ABTS cation radicals. Thiosemicarbazide (**3a-e**) and 1,2,4 triazole (4a-e) compounds exhibited significantly ABTS cation radical scavenging activity according to the starting compounds (**1-2**). In activity ranking of test compounds 3d> 3b> 3a> 3c> 3e> 2> 1 and low IC_{50} values indicate high ABTS cation radical scavenging activities.

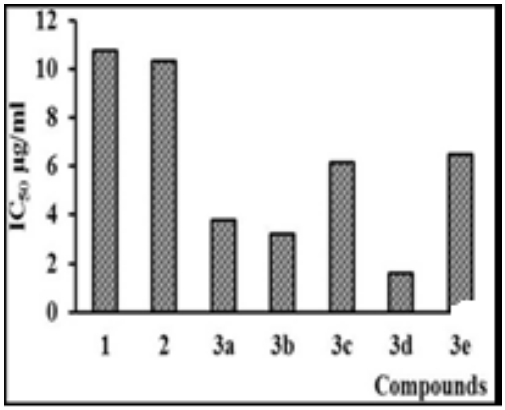

Figure 4. ABTS cation radical scavenging activities for compounds of starting (**1-2**), thiosemicarbazide (**3a-e**) and 1,2,4 triazole (**4a-e**) (IC_{50} values were calculated by fitting the data to a linear dose-response curve using the OriginPro 8.5 software packgage)

In summary, we synthesized a series of thiosemicarbazide (3a-e) derivatives and tested successfully by different antioxidant activity test parameters of their biological activities. The newly synthesized compounds that have exhibited high antioxidant activity from the starting compounds (1-2). The Compounds showed extremely high activity against both the stable DPPH radical and ABTS cation radical among of tested compounds.

Experimental- Melting points (mp) were determined on a Perkin-Elmer DSC-4000 apparatus and were uncorrected. The IR spectra were recorded with a Perkin-Elmer 100 FT-IR spectrophotometer. All ^{1}H-NMR and ^{13}C-NMR spectra were recorded on a Varian-Mercury-Plus 400/100 MHz spectrometer, in DMSO-d_6 and $CDCl_3$ with TMS as an internal standard. Elemental analyses (C, H, N) were carried out using LECO-932 CHNSO by Technical and Scientific Research Council of Turkey, TUBITAK. Starting materials was obtained from Merck or Aldrich.

Synthesis of dimethyl pyridine-2,5-dicarboxylate 1. pyridine-2,5-dicarboxylic acid (3.33 g, 0.02 mol) was refluxed with 100 mL of absolute methanol for a 24-h period using 1.80 mL of concentrated H2SO4 and 50 ml of benzol. The water was removed and excess of ethanol was distilled then 100 mL of water was added and the residual acid was neutralized to pH 6.5–7.0 with Na_2CO_3 powder. The mixture was extracted with $CHCl_3$ (2x25 mL). The sum of organic phases was dried over anhydrous Na_2SO_4, evaporated under reduced pressure, and dried in vacuum; white crystals were obtained in good yield. Yield 3.04 g, (78 %), mp 167°C. IR(cm^{-1}): 3100-3010 (Ar.CH), 2960-2857 (Al.CH), 1716 (C=O), 1597-1470 (Ar C=C). ^{1}H-NMR spectrum, δ, ppm (*J*, Hz): 3.89 (s, 3H, OCH_3-2), 3.90 (s, 3H, OCH_3-5), 8.15 (d, *J*=8.05, 1H, CH-3), 8.40 (dd, *J*=8.05, 2.20, 1H, CH-4), 9.40 (d, *J*=1.83, 1H, CH-6). ^{13}C-NMR spectrum, δ, ppm (*J*, Hz): 165.19 2, 165.15, 151.21, 150.63, 139.10, 128.86, 125.48, 53.43. Found, %: C 55.02; H 4.73; N 7.11. $C_9H_9NO_4$. Calculated, %: C 55.39; H 4.65; N 7.18.

The synthesis of pyridine-2,5-dicarbohydrazide 2. A mixture of 0.02 mol of ester and 98% hydrazine hydrate (0.06 mol) in 50 ml of ethanol was refluxed on a steam bath for 20 h. The reaction mixture was concentrated to a volume of 30 ml and allowed to cool. The solid mass which separated out on cooling was removed by filtration and washed with small amounts of ice-cold ethanol. The solid mass was dried and recrystallized from absolute ethanol and dioxane (2:1). Yield 3.55 g (91%), mp 245°C. IR(cm^{-1}): 3306-3204 (NH_2/NH), 3130-3051 (Ar.CH), 1704 (C=O), 1635 (NH), 1611 (C=N). ^{1}H-NMR spectrum, δ, ppm (*J*, Hz): 4.63 (br, 4H, 2xNH_2), 8.05 (d, *J*=8.08, 1H, CH-3), 8.32 (dd, *J*=8.12, 2.18, 1H, CH-4), 9.40 (d, *J*=1.82, 1H, CH-6), 10.10 (br, 1H, NH-2), 10.05 (br, 1H, NH-5). ^{13}C-NMR spectrum, δ, ppm (*J*, Hz): 163.55 2, 161.81 5, 151.49, 146.99, 136.28: 130.70, 121.43. Found, %: C 42.72; H 4.70; N 35.97. $C_7H_9N_5O_2$. Calculated, %: C 43.08; H 4.65; N 35.88.

General procedure for the synthesis of 2,2'-(pyridine 2,5-diyldicarbonyl) bis(N-substituted hydrazinecarbothioamide) (3a-e). 0.005 mol (0.975 g) of pyridine-2,5-dicarbohydrazide in 50 mL of absolute ethanol was heated until it dissolved. 0.01 mol appropriate substituted isothiocyanate derivatives was added and the mixture were refluxed for 8 hours. After the completion of the reaction, the crude product which precipitated on cooling was filtered, washed with diethyl ether, dried and crystallized from suitable solvents.

2**,2'-(pyridine-2,5-diyldicarbonyl) bis(N phenyl-hydrazinecarbothioamide) 3a.** Yield 2.048 g(88%), yellowish, mp 204°C, (EtOH:hexane 2:1). IR(cm^{-1}): 3671, 3363-3090 (NH), 3100-3030 (Ar.CH), 1682 (C=O), 1610 (NH), 1250 (C=S). ^{1}H-NMR spectrum, δ, ppm (*J*, Hz): 7.11-7.43 (m, 10H, Ph), 8.05 (d, J=8.08, 1H, CH-3), 8.47 (dd, *J*=8.56, 2.18, 1H, CH-4), 9.12 (s, 1H, CH-6), 9.80 (br, 2H, S=C-NH-Ph), 9.88 (br, 2H, NH-CO), 10.90 (br, 2H, N-NH-C=S). ^{13}C-NMR spectrum, δ, ppm (*J*, Hz): 181.33, 165.35, 164.77, 149.52, 148.49, 139.89, 139.17, 137.90, 131.35, 128.76, 125.61, 122.80. Found, %: C 53.80; H 4.23; N 20.92. $C_{21}H_{19}N_7O_2S_2$. Calculated, %: C 54.18; H 4.11; N 21.06.

Synthesis of 2,2'-(pyridine-2,5-diyldicarbonyl)-bis(N-ethylhydrazinecarbothioamide) 3b. Yield 1.515 g (82 %), yellowish, mp 240°C, (EtOH:hexane 2:1). IR(cm^{-1}): 3658, 3341-3150 (NH), 3180-2030 (Ar. CH), 2968-2896 (Al. CH), 1680 (C=O), 1610 (NH), 1246 (C=S). ^{1}H-NMR spectrum, δ, ppm (*J*, Hz): 1.06 (t, *J*= 7.13, 3H, $CH_2\underline{CH_3}$), 3.46 (q, *J*= 6.41, 3H, $\underline{CH_2}CH_3$), 8.19 (d, *J*=8.06, 1H, CH-3), 8.45 (dd, *J*=8.28, 2.10, 1H, CH-4), 9.11 (d, *J*=2.00, 1H, CH-6), 9.37 (br, 2H, S=C-NH-eth), 9.38 (br, 2H, NH-CO), 10.70 (br, 2H, N-NH-C=S). ^{13}C-NMR spectrum, δ, (*J*, Hz): C7b: 180.99, C7a: 180.93, C6b: 164.61, C6a: 163.99, 152.58, 148.77, 138.40, 127.83, 122.58, 38.53, 14.39, 14.43. Found, %: C 41.76; H 5.22; N 27.04. $C_{13}H_{19}N_7O_2S_2$. Calculated, %: C 42.26; H 5.18; N 26.54.

Synthesis of 2,2'-(pyridine-2,5-diyldicarbonyl) bis[N-(p-methoxyphenyl) hydrazinecarbothio amide] 3c. Yield 2.102 g (80%), yellowish, mp 193°C, (EtOH:hexane 3:1). IR(cm^{-1}): 3670, 3225-3137 (NH), 3134-3015(Ar.CH), 2962-2836 (Al.CH), 1680 (C=O), 1612 (NH) 1251 (C=S). ^{1}H-NMR spectrum, δ, ppm (*J*, Hz): 3.71 (s, 3H, O-CH3-2), 3.73 (s, 3H, O-CH3-5), 6.70-7.25 (m, 8H, Ph), 8.18 (d, *J*=8.36, 1H, CH-3), 8.47 (dd, *J*=8.06, 2.20, 1H, CH-4), 9.12 (s, 1H, CH-6), 9.81 (br, 2H, S=C-NH-Ph), 9.83 (br, 2H, NH-CO), 10.87 (br, 1H, N-NH-C=S-2).10.90 (br, 1H, N-NH-C=S-5). ^{13}C-NMR spectrum, δ, ppm (*J*, Hz): 181.10, 165.34, 164.74, 149.56, 148.51, 140.99, 140.89, 139.19, 131.36, 129.46, 123.30, 55.44. Found, %: C 53.25; H 4.28; N 19.06. $C_{23}H_{23}N_7O_4S_2$. Calculated, %: C 52.56; H 4.41; N 18.65.

Synthesis of 2,2'-(pyridine-2,5-diyldicarbonyl) bis[N-(1-naphtyl) hydrazinecarbothioamide] 3d. Yield 2.262 g (80%), white, mp 220°C, (EtOH:dioxane 3:1). IR(cm^{-1}): 3665, 3220-3130(NH), 3120-3015(Ar.CH), 1678 (C=O), 1250 (C=S). ^{1}H-NMR spectrum, δ, ppm (*J*, Hz): 7.33-8.22 (m, 14H, Nph), 8.23 (d, *J*=8.03, 1H, CH-3), 8.49(dd, *J*=8.05, 2.20, 1H, CH-4), 9.19 (s, 1H, CH-6), 9.94 (br, 2H, S=C-NH-Nph), 10.12 (br, 2H, NH-CO), 11.06 (br, 2H, N-NH-C=S). ^{13}C-NMR spectrum, δ, ppm (*J*, Hz):183.36, 183.05, 165.28, 165.09, 148.51, 146.20, 137.91, 136.32, 134.40, 131.33, Cnaftil: 132-123. Found, %: C 61.73; H 3.85; N 16.59. $C_{29}H_{23}N_7O_2S_2$. Calculated, %: C 61.57; H 4.10; N 17.33.

Synthesis of 2,2'-(pyridine-2,5-diyldicarbonyl) bis[N-4-(3-isothiocyanatopropyl) morpholino hydrazinecarbothioamide] 3e. Yield 2.214 g (78%), brown, mp 233 °C, (EtOH:dioxane 1:1). IR(cm^{-1}): 3662, 3342-3174(NH), 3120-3018(Ar.CH), 2982-2860(Ar.CH), 1679 (C=O), 1246 (C=S). ^{1}H-NMR spectrum, δ, ppm (*J*, Hz): 1.86 (m, 4H, NH-CH2-CH2-CH2-N), 2.48 (m, 4H, NH-CH2-CH2-CH2-N), 2.70 (t, *J*= 4.40, 8H, -CH2-N-CH2), 3.82 (m, 4H, NH-CH2-CH2-CH2-N), 4.10 (t, *J*= 4.40, 8H, -CH2-O-CH2), 8.41-8.43 (m, 2H, CH-3,4), 9.08 (s, 1H, CH-6), 10.02 (br, 2H, S=C-NH-CH2), 10.07 (br, 2H, NH-CO), 10.76 (br, 2H, N-NH-C=S). ^{13}C-NMR spectrum, δ, ppm (*J*, Hz):181.91, 169.05, 168.33, 151.31, 148.69, 137.79, 125.93, 122.15, 66.70, 55.43, 53.92, 43.00, 26.28. Found, %: C 48.04; H 6.80; N 22.32. $C_{23}H_{37}N_9O_4S_2$. Calculated, %: C 48.66; H 6.57; N 22.20.

DPPH free radical-scavenging activity- The samples were tested with DPPH free radical according to the method previously defined [11]. with some modifications. Shortly, 0.5 mL of synthesized compounds prepared at different concentrations (25–200 µg/mL) were taken into test tubes and stirred with 2.5 mL of 2 mM DPPH solution. The mixture was stirred thoroughly and incubated for 30 min in dark laboratory conditions. The absorbance at a wavelength of 517 nm was measured by UV spectrophotometry. To determine DPPH free radical scavenging activity (FRSA) was used in the following equation.

FRSA (%)=$[(A_0-A_1)/A_0]$x100

A_0 is the absorbance values without specimen and A_1 the absorbance in the presence of specimen. As opposed to increasing concentration of specimens decline of absorbance is an indication that destroyed DPPH radical.

Ferrous chelating capacity- The ferrous chelating capacities of samples were conducted following the method used [12]. with slight modifications. 2 mL of sample of concentration labeling between 25 and 200 µg/mL were added to 50 µL of 2 mM $FeCl_2$ and well mixed. The reaction mixture was incubated in laboratory conditions. The reaction occurred by the addition of 100 µL 5 mM ferrozine. After 10 min of incubation period, the absorbance of the solution was measured at 562 nm using a UV–visible spectrophotometer. Percentages of the chelating activity were calculated using the equation as described above was used for DPPH free radical scavenging activity.

Assay of Reducing Power- The reducing power was determined according to the method of [13]. with slight modifications various concentrations of compounds (2.5 mL) were mixed with 2.5 mL of 200 mM sodium phosphate buffer (pH 6.6) and 2.5 mL of 1% potassium ferricyanide. The mixture was incubated at 50 ºC for 20 min. After 2.5 mL of 10% trichloroacetic acid (w/v) were added, the mixture was centrifuged at 1000 rpm for 8 min. The upper layer (5 mL) was mixed with 5 mL of deionized water and 1 mL of 0.1% of ferric chloride, and the absorbance was measured spectrophotometrically at 700 nm. The assays were carried out in triplicate. It was indicated that high absorbance of the sample was good reducing power in the reaction conditions.

ABTS cation radical scavenging activity. To determine the antioxidant activity of compounds, ABTS cation radical-scavenging activity was employed in this study [14]. with slight modifications. The ABTS (2,2'-azino-bis(3-ethylbenzothiazoline-6-sulphonic acid)) cation radical cation was generated by mixing ABTS stock solution (7 mM in water) with 2.45 mM potassium persulfate. This mixture was kept at ambient temperature for 24 h until the reaction was complete and the absorbance was stable. Briefly, 1.9 mL of an ABTS cation radical were added to 0.1 mL of different concentrations of samples. After 10 min, an absorbance was read at 734 nm, and distilled water was used as a blank (each measured in triplicate). The IC_{50} is the concentration of an antioxidant that is required to quench 50% of the initial ABTS cation radicals under the experimental conditions given.

References

[1]. Fülöp, F.; Semega, E.; Dombi, C.; Bernath, G. J. Heterocyclic Chem., 27, 951, (1990).

[2]. Shaker, R. M. Arkivoc, 2006, 9, 59.

[3]. Heindel, N. D.; Reid, J. R.; J. Heterocycl. Chem., 17, 1087, (1980).

[4]. Holla, B. S.; Kalluraya, B.; Sridhar, K. R.; Drake, E.; Thomas, L. M.; Bhandary, K. K.; Levine, M. S. Eur. J. Med. Chem., 29, 301, (1994).

[5]. Haber, J. Cas. Lek. Cesk., 140, 596, (2001).

[6]. Aytac, S.; Tozkoparan, P. B.; Kaynak, F. B.; Aktay, G.; Göktaş, Ö.; Ünüvar, S. Eur. J. Med. Chem. 44, 4528, (2009).

[7]. Song, Y. T.; Connor, D. T.; Sercel, A. D.; Sorenson, R. J.; Doubleday, R.; Unangst, P. C.; Roth, B. D.; Beylin, V. G.; Gilbertsen, R. B.; Chan, K.; Schrier, D. J.; Guglietta, A.; Bornemeier, D. A.; Dyer, R. D. J. Med. Chem. 42, 1161, (1999).

[8]. Tozkoparan, B.; Kupeli, E.; Yesilada, E.; Işık, Ş.; Özalp, M.; Ertan, M. Arzneimittel Forsch. Drug Res. 55, 533, (2005).

[9]. Shimada, K.; Fujikawa, K.; Yahara, K.; Nakamura, T.; Journal of Agricultural and Food Chemistry 40, 945–948, (1992).

[10]. Kell, D. B. Archives of Toxicology, 84, 825, (2010).

[11]. Zovko Koncic D.; Kremer, K.; Karlovic, K. and Kosalec, I. Food Chem. Toxicol. 48, 2176, (2010).

[12]. Decker, E. A. and Welch, B. J. Agric. Food Chem. 38, 674, (1990).

[13]. Oyaizu, M. Jpn. J. Nutr. 44, 307, (1986).

[14]. Re, R.; Pellegrini, N.; Proteggente, A.; Pannala, A.; Yang, M.; Rice-Evans, C. Free Radic. Biol. Med., 26, 1231, (1999).

The Synthesis of Acid Derived Compounds Bearing 1,3,4-oxadiazole-2-thion Ring as Potential Antimicrobial Agents

Ahmet ÇETİN

Department of Chemistry, Faculty of Art and Science, Bingol University, 12000, Bingol-TURKEY
email; acetin74@hotmail.com

Abstract- Aromatic heterocycles are very important motifs in medicinal chemistry field. 1,3,4-oxadiazole exhibits a wide range of biological especially antifungal, activities [1]. 1,3,4-oxadiazole and their fused heterocyclic derivatives has gained notable attention due to their effective bio-synthetic importance[2-5].

In this work, various new compounds including ring 1,3,4-Oxadiazole were synthesized from the reactions of hydrazide compounds with carbon sulphur in basic medium. Acid derivatives were prepared by thiol tautomer form of 1,3,4-Oxadiazole (Scheme 1). Furthermore, structure-activity relationship was evaluated in respect to effect of different substitutions in newly synthesized 1,3,4-oxadiazole series. Then these compounds were characterized by performing of melting point, FT-IR, ^{1}H-NMR (400 MHz), and ^{13}C-NMR(100 MHz).

Keywords: 1,3,4-oxadiazole, Mannich Bases, Thiol-thione tautomerism.

Introduction-Nowadays, the synthesis of polyfunctional and heteroatom bearing cyclic compounds in which possess wide range of antimicrobial and biological activity is an important field in synthetic organic chemistry.

Plenty of infirmation can be found about the ring closure reaction of carbohydrazide compounds. In this type of reaction, three heteroatom bearing five-membered hetrocyclic compounds such as 1,3,4-oxadiazole, 1,3,4-thiodiazole, and 1,3,4-thiazole are formed [6]. Carboxylic acid hydrazides react with CS2 in ethanolic KOH to form potassium-3-arylthiocarbazide salts in good yiled. This formed salt converted to 5-aryl-2-mercapto-1,3,4-oxadiazole via ring closure reaction in the presence of pyridine or anhydrous NaOH [7, 8]. Magnetic properties of metal complexes of proper oxadiazole and thiodiazole is another investigating subject [9]. 1-acylthiosemicarbazide, 1,3,4-oxadiazle, 1,3,4-thiodiazole and 1,2,4- triazole-3-thione derivatives were detected as pain releiver and therapeutic effect on stomach diseases such as ulcer, gastritis. Furthermore, no side effect of these synthesized compunds has been detected [10].

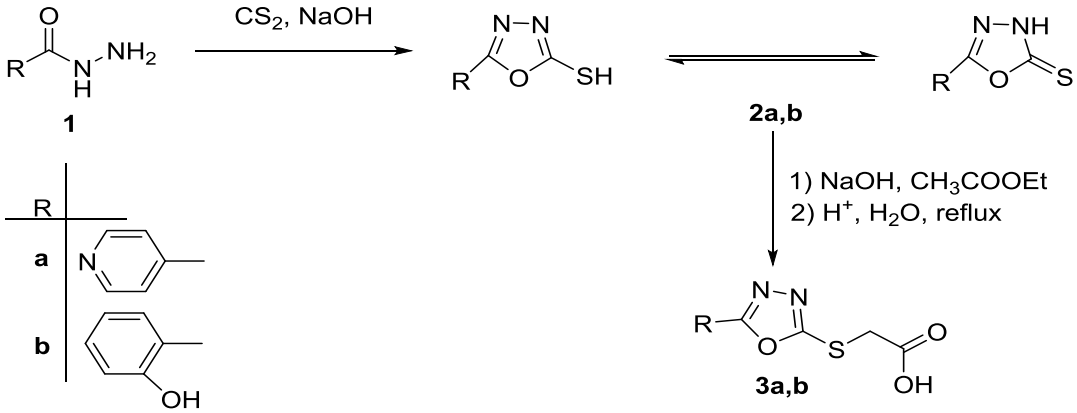

Scheme 1: Synthesized compounds

Experimental

The synthesis of 5-Pyridin-4-yl-1,3,4-oxadiazole-2-thiol (2a)

0.05 mol (6.86 g) isonicotinohydrazide was dissolved in 50 mL of ethanol, sodium hydroxide 0.05 mol, 2 g.) and carbon disülfide (0.05 mol, 3.3 mL) were added. the mixture was refluxed for 3 hours. The solvent was evaporated under reduced pressure. The residue was dissolved in water and fyltered, the fyltrate was asidified and fyltered. The precipiate was crystallized from mixture of ethanol-dioksan (5:1) Yield: %54, m.p: 279-280 ^{0}C.

The synthesis of 2-(5-Mercapto-1,3,4-oksadiazol-2-yl)phenol (2b)

7.60 g (0.05 mole) 2-hidroksibenzohydrazide was dissolved in 50 ml of ethanol, 2 g of sodium hydroxide (0.05 mole), and 3.3 ml of carbon disulfide (0.05 mole) were added. the mixture was refluxed for 3 hours. The solvent was evaporated under reduced pressure. The residue was dissolved in water and filtered, the filtrate was asidified and filtered. The precipiate was crystallized from mixture of ethanol-dioksan (5:1). 8.74 g, (90%), m.p. 207-208 ^{o}C;

The synthesis of 2-((5-Pyridin-4-yl-1,3,4-oxadiazol-2-yl-)thio)acetic acid (3a)

The 5-pyridin-4-yl-1,3,4-oxadiazolee-2-thiol (0.01 mole, 1.79 g.), (0.01 mole, 0.4 g.) NaOH in ethanol (40 mL) was refluxed for 1 h. Ethyl-bromoacetate (0.01 mol, 1.65 g) was added to this solution, and the mixture refluxed for 4 hour. After a slow cooling process, the solution was poured into ice and recrystallization was performed with a mixture of ethanol-water(4:1). Yield: %62, m.p: >375 ^{0}C.

The synthesis of 2-((5-(2-hydroxyphenyl)-1,3,4-oxadiazol-2-yl]thio)acetic acid (3b)

A solution of the 2-(5-mercapto-1,3,4-oxadiazol-2-yl)phenol, 1.94 g (0.01 mole) **2b,** and 0.40 g (0.01mole) of sodium hyroxide in 40 ml ethanol was refluxed for 1 hour. Ethyl bromoacetate (1.65 g, 0.01 mole) was added, and the resulting mixture refluxed for 4 hours. The solution was transferred to ice after cooling and the solid mass recrystallized from a mixture of ethanol-water (4:1), Yield: 1.21 g. (48%), m.p.>375 ^{o}C;

Result and discussion

FT-IR, ^{1}H-NMR and ^{13}C-NMR spectrums of compound **2a,b** and **3a,b** are listed sequentially.

5-Pyridin-4-yl-1,3,4-oxadiazole-2-thiol (2a)

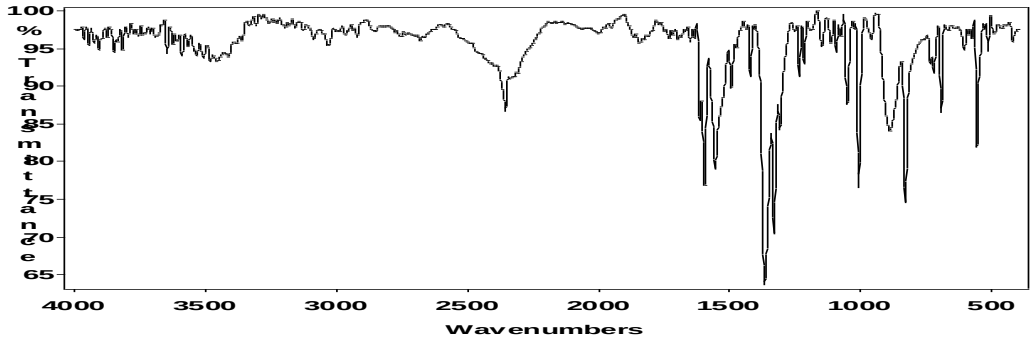

Scheme 2: FT-IR Spectrum of **2a**

FT-IR (KBr, ν_{max}/cm^{-1}): 3443-3220 (N-H), 3131-3000 (Ar.C-H), 3000-2883 (Al.C-H), 1252 (C=S), 1621 (C=N)

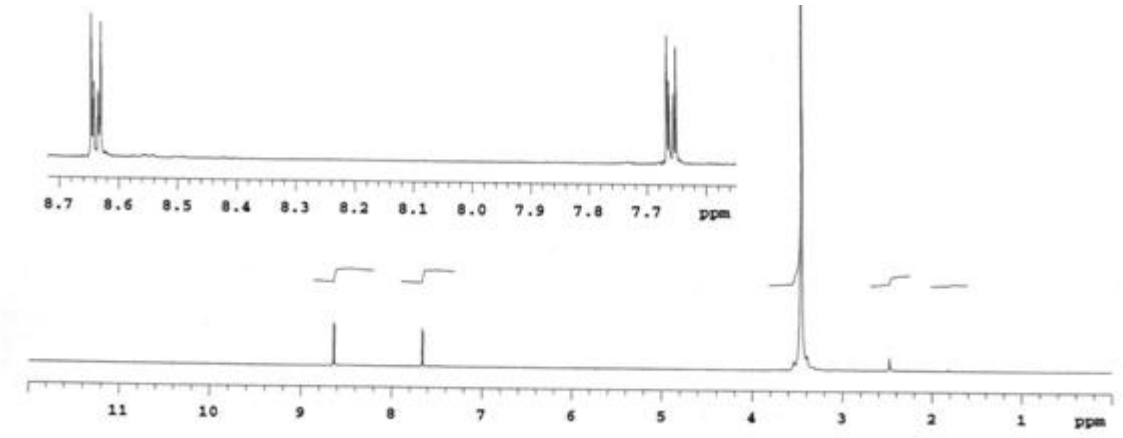

Scheme 3: ^{1}H-NMR Spectrum of **2a**

^{1}H-NMR (400 MHz, DMSO-d6, ppm) : δ 7.78 (dd, J=6.23, 1.83, 2H, Ar. C-CH), 8.78 (d, J=5.83, 2H, Ar. N-CH)

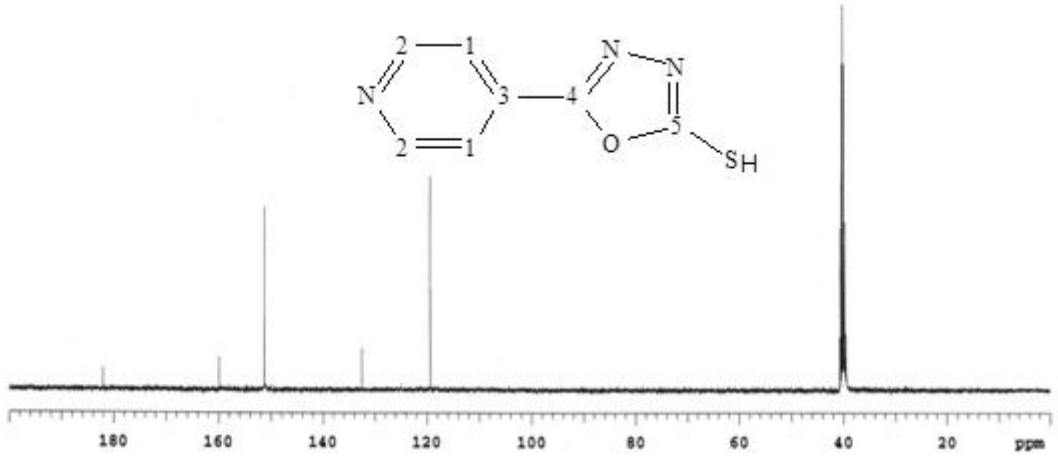

Scheme 4: ^{13}C-NMR Spectrum of **2a**

^{13}C-NMR (100 MHz, DMSO-d6, ppm) : δ C_5: 182.05, C_4: 159.88, C_2: 151.47, C_3: 132.44, C_1: 119.291.

2-(5-Mercapto-1,3,4-oksadiazol-2-yl)phenol (2b)

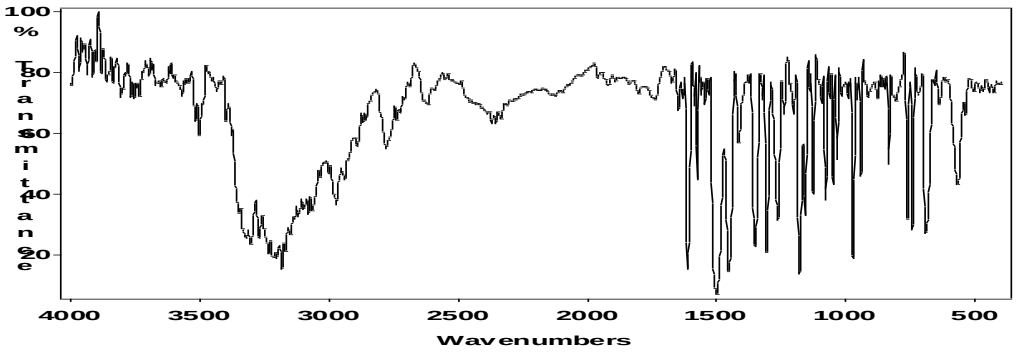

Scheme 5: FT-IR Spectrum of **2b**

FT-IR (KBr, v_{max}/cm^{-1}): 3503-3180 (O-H), 3131-2830 (C-H), 2976-2777-2554 (S-H), 1622 (C=N)

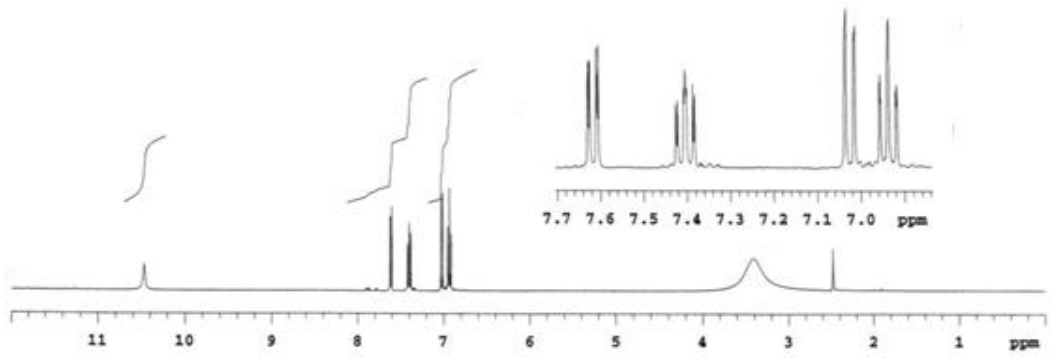

Scheme 6: ^{1}H-NMR Spectrum of **2b**

^{1}H-NMR (400 MHz, DMSO-d6, ppm) : δ 6.94 (t, J=8.43, 1H, H_3), 7.02 (d, J=8.43, 1H, H_1), 7.40 (t, J=8.80, 1H, H_2), 7.61 (d, J=8.06, 1H, H_4), 10.47 (s, 1H, OH).

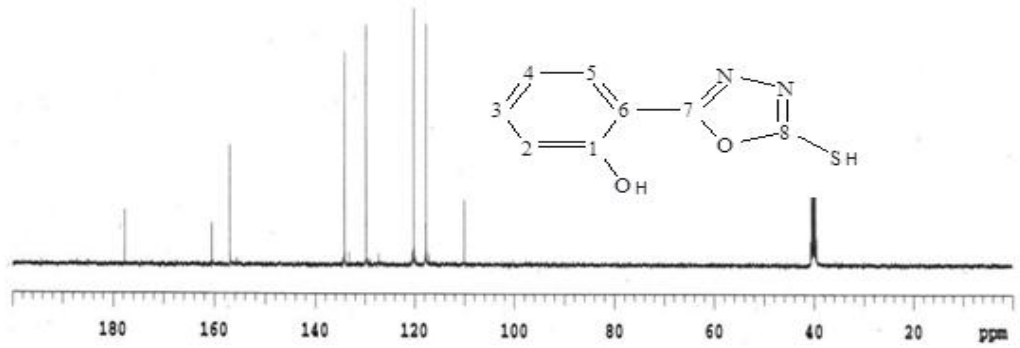

Scheme 7: ^{13}C-NMR Spectrum of **2b**

^{13}C-NMR (100 MHz, DMSO-d6, ppm) : δ C_8: 177.74, C_1: 160.52, C_7: 156.96, C_3: 134.13, , C_5: 129.73, C_4: 120.13, C_2: 117.70, C_6: 110.05.

2-((5-Pyridin-4-yl-1,3,4-oxadiazol-2-yl-)thio)acetic acid (3a)

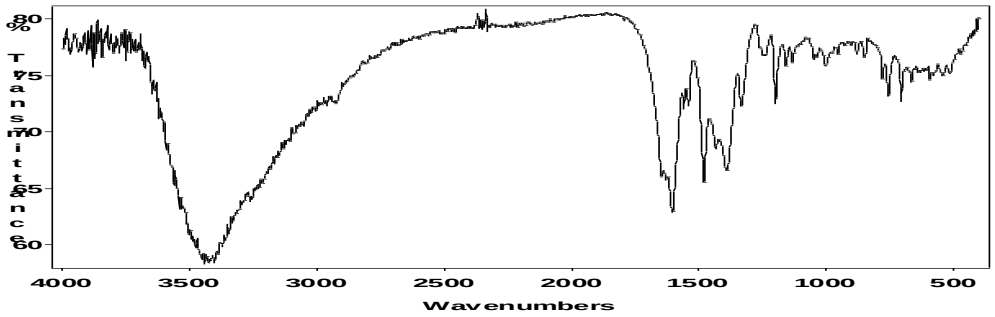

Scheme 8: FT-IR Spectrum of **3a**

FT-IR (KBr, ν_{max}/cm^{-1}): 3516-3246 (O-H), 3131-2925(Ar/AlC-H), 1740 (C=O), 1610 (C=N)

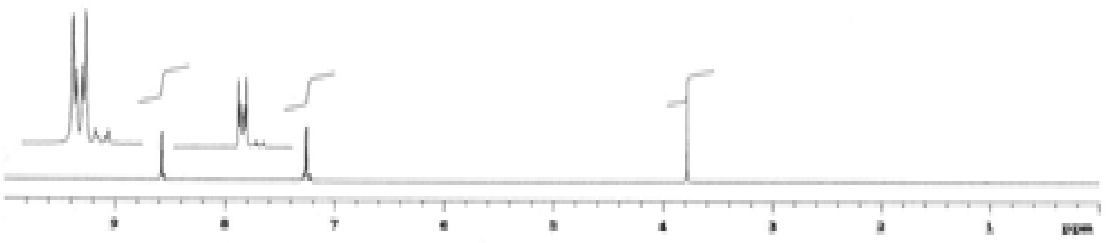

Scheme 9: ^{1}H-NMR Spectrum of **3a**

^{1}H-NMR (400 MHz, DMSO-d6, ppm) : δ 3.79 (s, 2H, S- CH_2 CO), 7.28 (dd, J=6.23, 1.83, 2H, Ar. C-CH), 8.78 (d, J=5.83, 2H, Ar. N-CH).

2-((5-(2-hydroxyphenyl)-1,3,4-oxadiazol-2-yl]thio)acetic acid (3b)

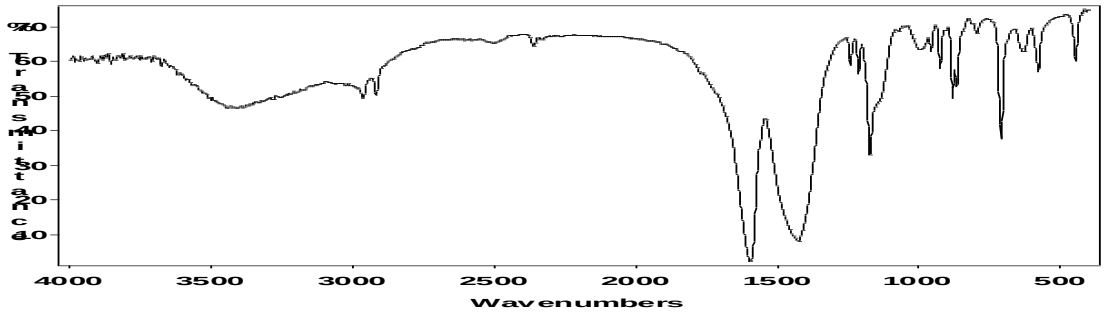

Scheme 10: FT-IR Spectrum of **3b**

FT-IR (KBr, ν_{max}/cm^{-1}): 3600-3120 (O-H), 3115-2915 (Ar/AlC-H), 1735 (C=O), 1608 (C=N)

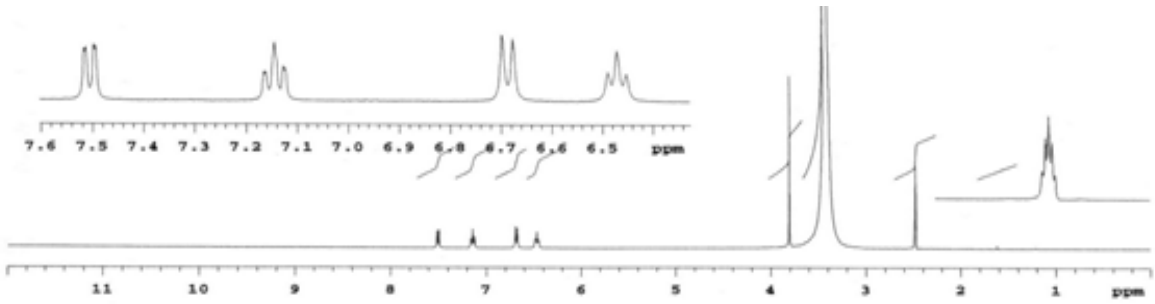

Scheme 11: ^{1}H-NMR Spectrum of **3b**

^{1}H-NMR (400 MHz, DMSO-d6, ppm) : δ 3.81 (s, 2H, S-CH_2-CO), 6.48 (t, J=7.33, 1H, H_3), 6.68 (d, J=8.43, 1H, H_1), 7.12 (t, J=8.43, 1H, H_2), 7.51 (dd, J=7.70, 1.46, 1H, H_4).

Antibacterial and antifungal activity- The compounds (**2a–b**, **3a,b**) were examined for antibacterial activity against E. Coli, S. Aureus and B. Subtilis by agar diffusion technique using ciprofloxacin as the reference (50 µg/ml), antifungal activity against A. Niger and C. Albicans by agar diffusion technique using fluconazole as reference (50 µg/ml). The results and observations are outlined in Table 1 and Table 2.

Comp.	E.Coli (Conc.)				S. Aureus(Conc.)				B. Subtilis(Conc.)			
	10 µg/ml	50 µg/ml	100 µg/ml	500 µg/ml	10 µg/ml	50 µg/ml	100 µg/ml	500 µg/ml	10 µg/ml	50 µg/ml	100 µg/ml	500 µg/ml
2a	-	+	+	++	-	+	+	++	-	-	+	++
2b	+	++	++	+++	+	++	++	+++	-	+	++	++
3a	-	+	+	++	-	+	+	+	-	+	+	++
3b	+	++	++	+++	-	+	++	++	+	+	++	+++
Cipro-floxacin	++	+++	+++	+++	+	++	+++	+++	+	++	+++	+++

Symbols: (-): < 10% inhibition, (+): 10-30% inhibition, (++): 30-60% inhibition, (+++):60-90% inhibition, Ciprofloxacin ≥ 90% inhibition

Table 1 The degree of inhibition of antibacterial activity of the synthesized compounds

Compounds	**C. Albicans (Conc.)**		**A. Niger (Conc.)**	
	50 µg/ml	100 µg/ml	50 µg/ml	100 µg/ml
2a	+	+	++	++
2b	++	++	+	++
3a	+	+	+	+
3b	+	++	++	++
Flucanazole	+++	+++	+++	+++

Symbols: (-) no inhibition, (+) weakly active, (++) moderately active, (+++) highly active

Table 2 Antifungal activity of compounds against C. Albicans, and A. Niger

References

[1] S. Kumar, G.V. Rajendraprasad, Y. Mallikarjuna, B.P. Chandrashekar, S.M. C. Kistayya, Synthesis of some novel 2-substituted-5-[isopropylthiazole] clubbed-1,2,4-triazole and 1,3,4-oxadiazoles as potential antimicrobial and antitubercular agents, *Eur. J. Med. Chem*. 45, 2063-2074 **(2010).**

[2] F. Fülöp, E. Semega, C. Dombi, G. Bernath, Synthesis of new heterocyclic compounds as potential pharmaceutical agents, *J. Heterocyclic Chem*. 27, 951 **(1990)**.

[3] M. D. Mullican, M. W.Wilson, D. T. Connor, C. R. Kostlan, D. J. Schrier, R. D. Dyner, Design of 5-(3,5-di-tert-butyl-4-hydroxyphenyl)-1,3,4-thiadiazoles, -1,3,4-oxadiazoles, and -1,2,4-triazoles as orally-active, nonulcerogenic antiinflammatory agents, *J.Med. Chem.* 36, 1090-1099 **(1993)**.

[4] R. M. Shaker, Synthesis of polyfunctionally substituted benzo[5,6]chromeno[4,3,2-de][1,6] naphthyridines and 5H-benzo[5,6]chromeno[3,4-c]pyridines, *Arkivoc*. 9, 59 **(2006)**.

[5] A. Rehman, K . Nafeesa, M.A. Abbasi, H. Kashfa, S. Rasool, I. Ahmad, S. Arshad, Synthesis, characterization and biological screening of various S-substituted derivatives of 5-(3-Nitrophenyl)-1,3,4-Oxadiazole-2-thiol, *Pak J Chem*. 3:1–8 **(2013)**.

[6] M. Koparır, A. Çetin, A. Cansız, 5-furan-2yl[1,3,4]oxadiazole-2-thiol and 5-furan-2yl-4H [1,2,4] triazole-3-thiol and their thiol-thione tautomerism, *Molecules*. 9(12), 204-212 (**2004).**

[7] J. R. Reid, N. D. Heindel, Improved synthesis of 5-substituted −4-amino-3-mercapto-4H-1,2,4-triazoles, *J. Heterocyclic Chem.* 13, 925 **(1976)**.

[8] D. Rigo, D. Couturier, Studies on pyrrolidinones. Synthesis of 5-(5-oxo-2-pyrrolidinyl)-1,3,5-oxadiazole-2-thione derivatives, *J. Heterocyclic Chem*. 22, 287 **(1985)**.

[9] F. Bentiss, M. Lagrenee, J. P. Wignacourt, E. M. Holt, Complexes of cobalt(II), nickel(II) and copper(II) with a thia ligand; 2,5-bis(2-pyridyl)-1,3,4-thiadiazole: structural identification, *Polyhedron* 21, 403-408, **(2002)**.

[10] E. Palaska, G. Şahin, P. Kelicen, N.T. Durlu, G. Altınok, *Il Farmaco*. 57, 101-107, **(2002)**.

Oxidative Polymerization of a Phenolic Monomer with Azomethine Moiety: Synthesis and Characterization

Ali BİLİCİ, Esranur YÜKSEL, İsmet KAYA

Çanakkale Onsekiz Mart University, Faculty of Sciences and Arts, Department of Chemistry, Polymer Synthesis and Analysis Lab. 17020 Çanakkale, Turkey

e-mail:alibilici@comu.edu.tr

Polyphenols are macromolecules having biological and pharmacological importance [1]. Their anti-inflammatory, antioxidant, antimutagenic, anticarcinogenic and antiviral properties have been widely investigated [1, 2]. It is known that these properties are important to preventing diseases and protecting genome stability [1, 3].

In here, the facile synthesis and characterization of a novel phenol polymer carrying azomethine moiety is presented. For this purpose, firstly, a Schiff base monomer was prepared by condensation reaction of 3, 4-di-hydroxybenzaldehyde with the 8-amino-2-naphtol and then, the monomer prepared was subject to oxidation by NaOCI in aqueous alkaline medium. The oxidation products were characterized by spectroscopic techniques: NMR, FTIR, UV-vis. Thermal stabilities of monomer and polymer were determined by means of TG analyses.

References

[1] L. Chebil, G.B., Rhouma, LC., Ghedira and M. Ghoul.Enzymatic Polymerization of Rutin and Esculin and evaluation of antioxidant capacity of Polyrutin and Polyesculin Biochemistry, Genetics and Molecular Biology ''Biotechnology'' ISBN 978-953-51-2040-7, 2015, DOI: 10.5772/60413

[2] W. Bhouri, M.B. Sghaier, S. Kilani, I. Bouhlel, M.G. Dijoux-Franca, K. Ghedira, L.C., Ghedira. Evaluation of antioxidant and antigenotoxic activity of two flavonoids from Rhamnus alaternus L. (Rhamnaceae): Kaempferol 3-*o*-[beta]-isorhamninoside and rhamnocitrin 3-*o*-[beta]-isorhamninoside, Food and Chemical Toxicology 2011;49(5) 1167-1173.

[3] B.Sghaier, M.J, Boubaker, I. Skandrani, I. Bouhlel, I. Limem, K. Ghedira, L.C., Chekir-Ghedira. Antimutagenic, antigenotoxic and antioxidant activities of phenolic-enriched extracts from Teucrium ramosissimum: Combination with their phytochemical composition. Environmental Toxicology and Pharmacology 2011;31(1) 220-232.

This work was supported by Research Fund of the Çanakkale Onsekiz Mart University. Project Number: FYL-2016-674).

Synthesis and Characterization of 2 amino-4-methyl phenol Oligomer Obtained by Enzymatic Oxidation

Ali BİLİCİ[a], Yunus ÇOĞAL[b], İsmet KAYA[a]

[a]Çanakkale Onsekiz Mart University, Faculty of Sciences and Arts, Department of Chemistry, Polymer Synthesis and Analysis Lab. 17020 Çanakkale, Turkey

[b]Republic of Turkey, Ministry of food Agriculture and Livestock, Çanakkale Food Control Laboratory Directorate, Ataturk Street Nu: 33 17100, Çanakkale, Turkey

e-mail:alibilici@comu.edu.tr

An enzyme-catalyzed polymerization has been extensively studied as a methodology for polymer synthesis [1]. It is alternative route for the preparation of functional polymers including polyphenols, polyamines, polycarbazole, polyferrocene, poly Schiff base ext. [2].

In here, Horse radish peroxidase catalyzed oxidative polymerization of a functional monomer, 2-amino-4 -methyl phenol, in dioxane/phosphate buffer mixture are reported for the first time. H_2O_2 is used as an oxidizer and the resulting oligomer are characterized by different analytical techniques including NMR, FTIR, UV-vis. UV-vis and NMR analysis results show that the oxidation product has a conjugated structure and monomer units take part into polymerization in a regio-random rank.

References

[1] L. Zhang, W. Zhao, Z. Ma, G. Nie, Y. Cui, Enzymatic polymerization of phenol catalyzed by horseradish peroxidase in aqueous micelle system, European Polymer Journal, 48 (3), 580-585, 2012.

[2] A. Bilici, İ. Kaya, D. Şenol, Side Groups Containing Fluorene Polymer Synthesized By Catalytic Oxidative Polymerization Polymers for Advanced Technologies, 22, 1953-1958, 2011.

This research has been supported by The Scientific and Technical Research Council of Turkey (TUBİTAK) (Project No: 215M074).

Enhancing Methylnaphthalenes Content in Coal Tar Naphthalene Oil Fraction Using Methylation with Methanol over Metal/Bimetal Doped Beta Zeolite Catalysts

Aysun Özen[1], Fatih Güleç[1] and Ali Karaduman[1]

[1]*Department of Chemical Engineering, Ankara University Engineering Faculty, Ankara,TÜRKİYE*

E-mail: karaduman@ankara.edu.tr

Coal Tar Naphthalene Oil Fraction (CTNOF) is a cheap mid product of iron steel industry. The composition of CTNOF provides a fertile field for chemical industry especially production of naphthalene compounds . The important naphthalene compounds such as monomethyl naphthalenes and dimethyl napththalenes especially 2-Methylnaphthalene (2-MN) and 2,6-Dimethylnaphthalene (2,6-DMN) can be produced by methylation of CTNOF. They are prominent naphthalene compounds for polyethylene naphthalate (PEN) industry. PEN is a polymer which has charactaristics that can be an alternative to PET [1-3]. However, PEN production is not very common due to uneconomical synthesis of 2,6-DMN . When compared with other developed catalysts for production of 2,6-DMN in the literature, zeolites are significant catalysts in terms of their porous structure, ion exchange capacity and high surface area [3,4]. In this study, synthesis of 2,6-DMN and 2-MN were examined by methylation of CTNOF over H-Beta, Pd/Beta, Pd-Cu/Beta, Pd-Ni/Beta and Pd-Zr/Beta zeolite catalysts. In the experiments a solution which's mass composition was 1:5:5 CTNOF:Methanol:1,2,4-Trimetilbenzene was used. The Beta zeolite was supplied from ACS material corporation (USA). Metals were doped by using wet impregnation method. The methylation reaction of CTNOF with methanol were carried out in a fixed bed reactor operating at a range of 300°C-400°C, and weight hourly space velocity (WHSV) ranging from $1h^{-1}$ to $3h^{-1}$. Gas products were condensed with a condenser in the jacket of which cold water was used. Liquid products obtained in condenser were analyzed with GC-MS which has 60 meter capillary column. The catalysts were characterized by XRF, SEM and BET, FTIR, XRD techniques. As a result, conversion of 2-MN and 2,6-DMN were increased with temperature and decreased with WHSV. Generally, ratio of 2,6-DMN/2,7-DMN was above 1.0 and 2-MN/1-MN was above 5.0. The selectivities of 2,6-DMN and 2-MN were improved with using metal loaded Beta zeolite.

Acknowledgements

We are thankful and greatfully appreciate Ankara University Scientific Research Projects (AÜ-BAP) for the support of this work. (Project No: 15B0443009)

References

[1] M.D.G. Azpiroz, C.G. Balanco, M.D.C. Banciella, The use of solvents for purifying industrial naphthalene from coal tar distilled oils, Fuel Processing Technology, 89, 111-117 (2008).

[2] W. Tang, M. Fang,, H. Wang, P. Yu, Q. Wang,, Z. Luo, Mild hydrotreatment of low temperature coal tar distillate: Product composition, Chem. Eng. Journal, 236, 529-537 (2014).

[3]L. Zhao., X. Guo, M. Liu, X. Wan, C. CJ. Song, Methylation of 2-Methylnaphthalene with Methanol over NH_4F and Pt Modified HZSM-5 Catalysts Chinese Journal of Chem. Eng. 18, 742-749 (2010)

[4] A. Niftaliyeva, F. Güleç, E. H .Şimşek, M. Güllü, A. Karaduman, Cu-Y ve La-Y zeolit katalizörleri üzerinde 2-metilnaftalinin metilasyon kinetiği, Anadolu University Journal of Science and Technology –A Applied Sciences and Engineering, 16, 167-178 (2015).

Impedance Properties of Conducting Polymers/ Basalt Composites Under Magnetic Field

A. E. Bulgurcuoğlu, S. Erdönmez, Y. Karabul, M. Kılıç, N. Y. Canli, O. İçelli, M. Okutan

Department of Physics, Yıldız Technical University, İstanbul, Turkey

e-mail: aysevrim@gmail.com

Conducting polymers are known as synthetic metals because of their optical, magnetic and electronic attributes inherent to semiconductors or metals [1]. Among the conducting polymers, polyaniline, polypyrrole and polythiophene have incomparable properties due to their good, relatively low-cost, good process ability, environmental stability, electrical and electrochemical properties, ease of synthesis and high electrical properties. Conductive polymers have been widely utilized in fuel cells, computer displays and microsurgical tools, and are now finding applications in the field of bio-analytical science and biocompatibility [1, 2].

Basalt is a very widespread volcanic rock that is dark colored and relatively rich in iron and magnesium, almost located every country in the world. Basalt is chemically rich with oxides of magnesium, calcium, sodium, potassium, silicon and iron, along with traces of alumina. The chemical content may differ based on the geographical distribution. Basalt is used for a wide variety of purposes: these rocks have been used in the refused rock industry, building tiles, construction industrial, highway engineering. Powders and fibers of basalt rocks are widely used of radiation shielding, thermal stability, heat and sound insulation [3-5].

In this work, the dielectric properties of Conductive Polymers/Basalt composites (three type conductive polymer and one type basalt rock is coded KYZ-13: Polyaniline/ KYZ-13, Polypyrrole/KYZ-13 and Polythiophene/ KYZ-13) in different concentrations (10.0, 25.0, 50.0 wt.%) have been investigated. These composites were prepared by mechanical mixing and then compression molded in a cold press at room temperature. Each one of these mixtures prepared as a pellet having 13 mm diameter, ~0.500 g weight and 1.8-2.2 mm thickness. In the frequency range of 1×10^2 - 17.5×10^6 Hz, the electrical properties of samples have been examined by a dielectric spectroscopy method under magnetic field at the room temperature. A detailed analysis of this investigation will be presented.

[1] M. Ates, A review study of (bio)sensor systems based on conducting polymers, Materials Science and Engineering C 33, 1853 (2013).

[2] R. Balint, N. J. Cassidy, S. H. Cartmell, Conductive polymers: Towards a smart biomaterial for tissue engineering" Acta Biomaterialia, 10, 2341 (2014).

[3] A. W. A. El-Shennawi, M. A. Mandour, M. M. Morsi, and S. A. M. Abdel-Hameed, Monopyroxenic Basalt-Based Glass-Ceramics, J. Am. Ceram. Soc. 82, 1181 (1999).

[4] W. A. Deer, R. A. Howie, and J. Zussman, Introduction to the Rock-Forming Minerals, Mineralogical Society, London (2013).

[5] A. Çetin, M. Okutan, O. Içelli, Z. Yalçin, S. E. San, R. Kibar, and E. Pesen, Electrical and optical properties of chalcedony and striped chalcedony, Vacuum 97, 75 (2013).

High Detectivity Organic Photodiodes

Ayşegül Dere

Physics Department, Faculty of Science, Firat University, Elazig, TURKEY

Nanoscience and Nanotechnology Laboratory, Firat University, Elazig, TURKEY

Organic photodiodes are promising electronic devices due to low cost, large area and optoelectronic applications. Photodiodes can be used in private households and industry. Combining of the organic semiconductors with metal oxide nanosemiconductors allows to fabricate solar light photodetectors. Here, we fabricate a solar light sensitive, organic photodiode with a high photoresponsivity. The photodiode under solar irradiation exhibits excellent photoresponse capabilities. The photodiode was prepared by a drop casting method using of nanostructure zinc oxide and coumarin semiconductor. The photodiode exhibited a linear photoconduction mechanism. The obtained results suggest that the fabricated diodes could be used as an optical sensor in various optoelectronic applications.

Keywords: Optical sensor materials, Organic Semiconductor, Photodiode

Interface Trap States in Organic Photodiodes

A. Dere, F. Yakuphanoglu

Physics Department, Faculty of Science, Firat University, Elazig, TURKEY

Nanoscience and Nanotechnology Laboratory, Firat University, Elazig, TURKEY

Organic semiconductors are promising materials for optical sensing and optic communication applications. Here, we show that charge trapping phenomena is controlled by the graphene oxide doing. We demonstrate that the organic photodiodes have the large photocapacitance which is be achieved at light levels 20-100 mW/cm^2 by appropriate interface engineering. The interface trap states are controlled by solar light intensity. Such device characteristics indicate that the photodiodes based interface trap states are suitable for industrial applications.

Keywords: Optical sensor materials, Organic Semiconductor, Photodiode

Capacitive behaviour of reduced azido graphene oxide electrodes decorated with metallophthalocyanine

U. Şahintürk[1], B. Keskin[2], and A. Ekerim[1]

[1] Department of Metallurgical and Materials Engineering, Faculty of Chemistry-Metallurgical, Yildiz Technical University, 34210 Istanbul, Turkey

[2]Department of Chemistry, Faculty of Arts and Sciences, Yildiz Technical University, 34210 Istanbul,

E-mail : utkans@yildiz.edu.tr

Graphene oxide (GO) is a nanomaterial which can be prepared from graphite in large amounts and processed from solution. GO is an electrically insulating material due to their disrupted sp^2 bonding networks. As-synthesized GO is insulating but controlled deoxidation leads to an electrically active material that is conducting. Because electrical conductivity can be recovered by restoring the π-network, one of the most important reactions of graphene oxide is its reduction to reduced graphene oxide (RGO) [1]. Thus, RGO is both conductive and has chemically active defect sites making it a promising candidate for the electroactive material in energy storage devices. Now a days, graphene-based electrode materials for supercapacitors have been reported with the superior specific capacitance. Transition metal phthalocyanines (MPcs) represent a class of macrocyclic metal compounds with unique electrochemical properties. It was stated in our previous studies that MPcs having metal-based reduction processes showed higher activities [2]. It is well documented that MPcs bearing redox active metal centers such as, Co^{2+}, Fe^{3+}, and TiO^{2+}.

Here GO were prepared according to previously reported procedures with minor changes and characterized by comparing their spectral data to those reported earlier. GO was through selectively functionalized with sodium azide to product GO-N_3 by described method and characterized by comparing their spectral data to those reported earlier. NF/RGO-N_3 electrode was constructed with the electrochemical reduction of azide-functionalized GO (GO-N_3) coated on a nickel foam(NF). This product RGO-N_3 provides a versatile reactive motif for further chemical reactions such “click chemistry (CC)” reactions. Decoration of NF/RGO-N_3 electrodes were performed with a electrode modification technique, (CC), with which TA-MPc complex was bonded to azido functional groups of RGO-N_3 on the electrodes. Reduced graphene oxide along with the MPc will be enhanced capacitance. Thereby, this study focuses on the capacitive behaviour of RGO-N_3 electrodes decorated with the MPc complex.

Microstructral, spectroscopic and elemental properties of GO, GO-N_3 and MPc were investigated. The electrochemical properties of NF/GO-N_3, NF/RGO-N_3 and NF/RGO-N_3/TA-ZnPc electrodes characterized by cyclic voltammetry (CV) to compare their capacitance and retentions. This research has been supported by Yıldız Technical University Scientific Research Projects Coordination Department. Project Number: 2014-07-02-DOP01.

[1] Dreyer D.R., Park S., Bielawski C.W., Ruoff R.S. 2010. “The chemistry of graphene oxide”, Chem. Soc. Rev., 39, 228–240.

[2] Akyüz D., Keskin B., Şahintürk U., Koca A. 2016. “Electrocatalytic hydrogen evolution reaction on reduced graphene oxide electrode decorated with cobaltphthalocyanine”, Applied Catalysis B: Environmental, 188, 217-226.

Modification of Glassy carbon electrode with electrochemically reduced graphene oxide supported Cobaltphthalocyanine for enhancing its capacitance

B. Keskin[1], U. Şahintürk[2], and A. Ekerim[2]

[1]Department of Chemistry, Faculty of Arts and Sciences, Yildiz Technical University, 34210 Istanbul,Turkey

[2]Department of Metallurgical and Materials Engineering, Faculty of Chemistry-Metallurgical, Yildiz Technical University, 34210 Istanbul, Turkey

E-mail :utkans@yildiz.edu.tr

Phthalocyanines (Pcs) are functional materials with an extended conjugated network of π-electrons[1]. Their outstanding dye properties and the ability to self-assemble, by means of π-π interactions, into highly ordered arrays can be tuned by careful design of their periphery such as quinoline moiety [2]. In this work, quinoline derivative (**3**) of tetra-1-chloro-3,4-dicyano-6-quinolin-8-yloxy substituted novel cobalt(II) phthalocyanine(CoPc) complexes were synthesized and characterized by UV-Vis, FTIR, ^{1}H NMR and Mass Spectroscopies [3]. Graphiteoxide (GO) prepared from natural graphite by improved Hummer's method is used as the starting material to electrochemically reduced graphene (ERGO). CoPc dispersion in DMF was added to GO dispersion and the resulting mixture was ultrasonicated. The CoPc/GO modified electrode was prepared by casting CoPc/GO in DMF colloid solution on a glassy carbon electrode (GCE). Then, the CoPc/GO was reduced via CVs (cyclic voltammetry) for several cycles in the electrolyte solution to prepared CoPc/ERGO modified electrode for enhanced capacitance[4]. Mass-specific capacitance of modified GCE electrode measured by CV.

This research has been supported by Yıldız Technical University Scientific Research Projects Coordination Department. Project Number: 2014-07-02-KAP01 and 2016-01-02-GEP01.

[1] Lever, A.B.P.; Leznoff, C.C.; "Phthalocyanines and their applications", Wiley, Vol 4, 1996

[2] Michal J., Kouwer Paul H. J., Rehak J., Sly J., Rowan A. E., J. Org. Chem. 74 (2009) 21–25.

[3] Çakır V., Çakır D., Göksel M., Durmuş M., Bıyıklıoglu Z., Kantekin H., J.Photochemistry and Photobiology A: Chemistry, 299 (2015) 138–151.

[4] Akyüz D., Keskin B., Şahintürk U., Koca A. 2016. "Electrocatalytic hydrogen evolution reaction on reduced graphene oxide electrode decorated with cobaltphthalocyanine", Applied Catalysis B: Environmental, 188, 217-226.

Effect of Cobalt Dopant on Electrical and Optical Properties of ZnO Thin Films

B.Coskun[1], N.Akkurt[2]

[1]Department of Physics, Kirklareli University, Kirklareli, TURKEY, burhan.coskun@klu.edu.tr

[2]Department of Chemistry, Kirklareli University, Kirklareli, TURKEY

The effect of Co doping on structural, morphological, optical, and electrical properties of zinc oxide thin films was investigated. Un-doped and Co-doped (1%, 3% and 5%) ZnO thin films were deposited on the glass substrate using sol-gel spin coating method. The X-ray diffraction analysis reveal that all the films prepared have preferential growth perpendicular to the substrate and are hexagonal wurtzite crystal structure. The Co doping creates disorder and the substantial changes in the structural properties of the ZnO film. The chemical composition of these films were confirmed by EDX measurement. The SEM micrographs show the effect of cobalt doping on the surface morphology of the films. The transmittance spectra indicates that the films are highly transparent. Using the transmittance and reflectance spectra, the band gap energy and optical constants such as refractive index and extinction coefficient were determined.

Keywords: *Zinc oxide, Bandgap, Optical properties and Surface morphology*

Acknowledgments:

This study was supported by Scientific Research Projects Unit of Kirklareli University under project number: Klubap 076

Optical and Electrical Properties of Fe Doped ZnO Thin Films

B.Coskun[1], A.Sengul[2]

[1]Department of Physics, Kirklareli University, Kirklareli, TURKEY, burhan.coskun@klu.edu.tr

[2]Department of Civil Engineering, Kirklareli University, Kirklareli, TURKEY

Un-doped and Fe-doped (1%, 3% and 5%) ZnO thin films were grown on the glass substrates. The effect of Fe doping on structural, morphological, optical, and electrical properties of these thin films was investigated using X-ray diffraction (XRD), scanning electron microscopy (SEM), UV-VIS-NIR spectrophotometer, and two probe, respectively. The chemical composition of these films were confirmed by EDX measurement. The XRD spectra reveals the structural disorder with Fe incorporation that creates the substantial changes in the structural properties of the ZnO film. The SEM micrographs show the effect of iron doping on the surface morphology of the films. Finally, the influence of doping on the band gap energy and different optical parameters was studied and results depict that Fe doping significantly change the properties of the films.

Keywords: *Zinc oxide, Bandgap, Optical properties and Surface morphology*

Acknowledgments:

This study was supported by Scientific Research Projects Unit of Kirklareli University under project number: Klubap 076

Investigation of Ageing Period on Thermal Properties of Cu-Al-Ni-Mn Shape Memory Alloy

[1]Canan AKSU CANBAY, [1]Faruk ALADAĞ, [2]Zuhal KARAGOZ GENÇ

[1]Department of Physics, Faculty of Science, University of Firat, 23119, Elazig, Turkey

[2]Department of Metallurgy and Materials Engineering, Facultyof Engineering, Adiyaman University, 02040 Adiyaman, Turkey

SME and martensitic transformation behavior of SMAs have been observed in Ni-Ti, Cu-based and Fe-based SMAs. Among the SMA systems, Cu-based alloys have been developed and have easier production procedures and lower production costs than Ni-Ti SMAs and have better SME and two-way shape memory effect (TWSME) than Fe-based alloys. Cu-based alloys are not always appropriate for cold workability. Thus, the some studies have focused to enhance the general properties and cold workability of Cu-based alloys. It is known that rare earth elements are often used as alloying element to refine the grain boundary and improve the mechanical properties.

In this work the effect of ageing period on Cu-Al-Ni-Mn SMA was thermally investigated. The differential scanning calorimetry (DSC) measurements and differential thermal analysis (DTA) were made. Enthalpy variations was investigated.

Acknowledgements: This work is financially supported by FÜBAP, Project No: FF.14.14

References

[1] Zarubova N, Gemperlova J, Gemperle A, Dlabacek Z, Sittner P, Novak V (2010) Acta Mater 58:5109-5119.

[2] Otsuka K, Wayman CM (1998), Shape Memory Materials, Cambridge University Press.

[3] Chentouf SM, Bouabdallah M, Gachon J-I, Proor E, Sari A (2009) J. Alloys Compounds 470:507-514.

[4] Colic M, Ruddolf R, Stamenkovic D, Anzel I, Vucevic D, Jenko M, Lazic V, Lojen G (2010) Acta Biometar 6:308-317.

Investigation on $Cu_{12.17}Al_{4.63}Mn$ Shape Memory Alloystrip Produced by Melt Spinning

[1]Kemal Aldaş, [1]İskender Özkul, [2]C. AksuCanbay

[1]Department of Mechanical Engineering, Faculty of Engineering, Aksaray University, 68100 Aksaray, Turkey

[2]Department of Physics, Faculty of Science, University of Firat, 23119,

Elazig, Turkey

The shape memory effect is one of the most important features of smart materials. Generally using as actuator, shape memory alloys, are commonly use in sensors device. The usage in thermal sensor, shape memory alloys can has greater displacement and temperature range compared to bimetals. This advantageous features attract notice and in our study we have produced a Cu based shape memory strip by melt spinning method. The alloy transformation temperature, which exhibits shape memory effect, have been determined with differential scanning calorimetry device. Furthermore chemical composition and microstructure of specimen has been analyzed.

References

[1] Sanchez-Arevalo FM, Aldama-Reyna W, Lara-Rodriguez AG, Garcia-Fernandez T, Pulos G, Trivi M, Villagram-Muniz M (2010) Mater Charact. 61:518-524.

[2] Rodriguez-Aseguinoloaza J, Ruiz-Larrea I, No ML, Lopez-Echarri A, San Juan JM (2008) Acta Mater 58:3711-3722.

[3] Prado MO, Decorte PM, Lovey F (1995) Scripta, Metall. Mater 33(6):878-883

[4] Kato H, Yasuda Y, Sasaki K (2011) Acta Metall 59:3955-3964

Structural Variations of Cu-Al-Ni-Mn Shape Memory Alloy by Ageing Period

Canan AKSU CANBAY, Faruk ALADAĞ
Department of Physics, Faculty of Science, University of Firat, 23119,
Elazig, Turkey

By the development of the technology shape memory alloys (SMA) such as Cu based binary and ternary systems (Cu-Zn, Cu-Al, Cu-Zn-Al, Cu-Al-Ni, Cu-Al-Mn), Ni-Ti and high temperature shape memory alloys are usually used in automotive, aerospace and medical field. The technical importance of these materials is based on their mechanical properties such as pseudoelasticity (PE) and shape memory effect (SME). Shape memory effect is related to the thermoelastic martensitic transformation exhibited by a diffusionless reconfiguration of the crystalline lattice of the material under applied temperature or stress changes.

The effect of ageing period on structure of Cu-Al-Ni-Mn SMA was investigated. The X-ray diffraction patterns and their variations according to ageing period was investigated.

Acknowledgements: This work is financially supported by FÜBAP, Project No: FF.14.14

References

[1] Lojen G, Anzel I, Kneissl A, Krizman A, Unterweger E, Kosec B, Bizjak M (2005) J Mater Process Tech162-163:220-229

[2] Izadinia M, Dehghani K (2011) Trans. Nonferrous Met. Soc. China. 21:2037-2043.

[3] Recarte V, Perez-Landazabal JI, Rodriguez PP, Bocanegra EH, No ML, San Juan J (2004) Acta Mater 52:3941-3948.

[4] Sobrero CE, La Roca P, Roatta A, Bolmaro RE, Malarria J (2012) Mater Sci Eng A. 536:207-215.

DFT and TDDFT Investigation of Electronic Properties of Aromatic Amino Acids

N. Açar[1], R. Köklü[2], C. Selçuki[2]

[1]*Department of Chemistry, Faculty of Science, 35100 Bornova, Izmir, Turkey*

[2]*Department of Biochemistry, Faculty of Science, 35100 Bornova, Izmir, Turkey*

E-mail : cenk.selcuki@ege.edu.tr

Natural amino acids are the main constituents of proteins and enzymes which are the main functional molecules in all living organisms. Among 20 natural amino acids, three of them are aromatic, namely phenylalanine (Phe), tyrosine (Tyr) and tryptophan (Trp) (Figure 1). These three aromatic amino acids (Ar-AA) have π-electronic systems which display absorption and emission. The spectroscopic properties of Ar-AA is used widely in detection of proteins and enzymes using UV-Vis and fluorescence spectroscopy techniques.

In current study, all possible neutral (**N**), zwitterionic (**ZW**), cationic (**C**), and anionic (**A**) structures of three Ar-AA will be investigated using Density Functional Theory (DFT) [1]. Calculations will be performed in gas phase for neutral structures and all other charged forms will be investigated in water using the PCM model [2] as implemented in Gaussian09 [3].

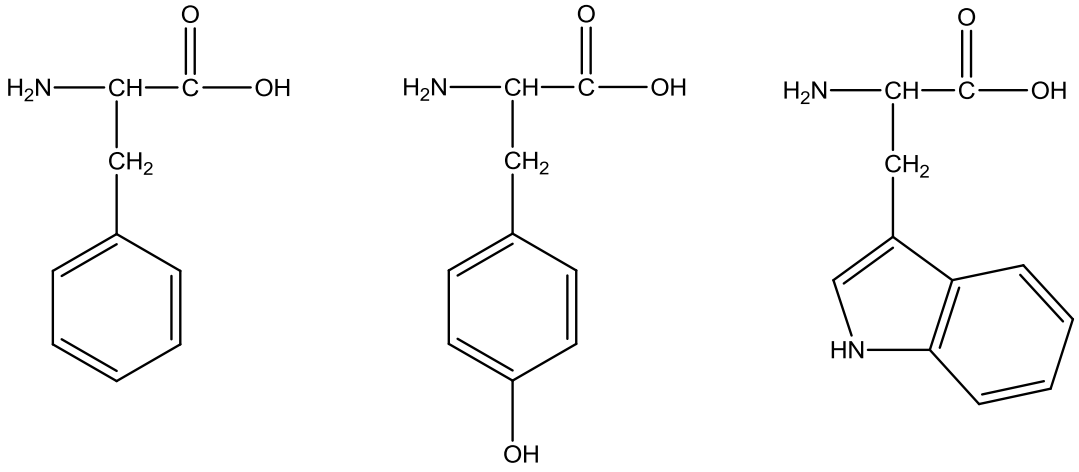

Figure 1. Neutral forms of aromatic amino acids

[1] W. Kohn, L. J. Sham, Self-consistent equations including exchange and correlation effects, Phys. Rev. 140(4A), A1133–A1138 (1965).

[2] J. Tomasi, B. Mennucci, R. Cammi, Quantum mechanical continuum solvation models, Chem. Rev. 105 2999-3093 (2005).

[3] Gaussian 09, Revision C.01, M. J. Frisch et. al. Gaussian, Inc., Wallingford CT, (2009).

DFT and TDDFT Investigation of Electronic Properties of Selected Porphyrins

N. Açar, H. Apat

Department of Chemistry, Faculty of Science, Bornova, Izmir, Turkey

E-mail : nursel.acar@ege.edu.tr

Photo-induced electron transfer and excitation energy transfer are essential processes of natural photosynthesis. Therefore, mimicking biological photosynthesis systems is important in design of artificial light-harvesting nano- and biomaterials. In order to realize artificial molecular systems for photoenergy conversion, natural photosynthetic systems are very useful examples, and various mimetic systems containing porphyrins have been synthesized to investigate the photophysical processes involved [1-5].

In current study, intramolecular charge transfer properties of selected biologically important porphyrins were investigated by quantum chemical methods. Ground state geometries and electronic transitions were calculated. Calculations were first performed in gas phase and then were repeated in water to determine the solvent effects. The investigated porphyrin derivatives are 5,10,15,20-Tetraphenyl-21H,23H-porphine (TPhP), Octaethylporhine, and 5,10,15,20-Tetrakis(4-hydroxyphenyl)-21H,23H-porphine (TPhP-OH). The effects of ethyl, phenyl and phenolic substituents on porphyrin electronic properties were investigated.

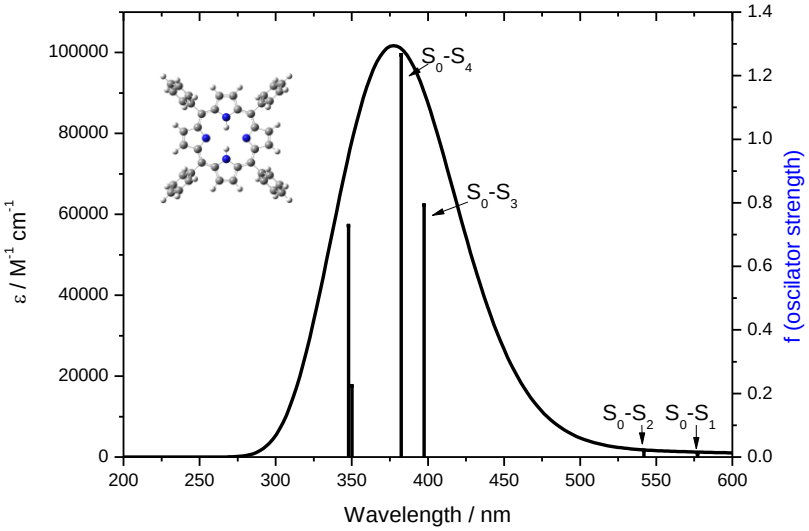

Figure 1. UV/Vis absorption spectrum of TPhP molecule calculated at B3LYP/6-311G(d,p) level in gas phase

Maximum absorption wavelength of TPP molecule is calculated as 383 nm in gas phase.

[1] M. R. Wasielewski, Photoinduced electron transfer in supramolecular systems for artificial photosynthesis, Chem. Rev. 92, 435-461 (1992).

[2] D. Gust, T. Moore, Mimicking Photosynthesis, Science 244, 35-41 (1989).

[3] A. Stockmann, J. Kurzawa, N. Acar, S. Schneider, J. Daub, R. Engl, T. Clark, Conformational Control of Photoinduced Charge Separation within Phenothiazine-Pyrene Dyads, J. Phys. Chem. A 106, 7958-7970 (2002).

[4] N. Acar, J. Kurzawa, A. Stockmann, C. Roman, S. Schneider, T. Clark, Phenothiazine-Pyrene Dyads-Photoinduced Charge Separation and Structural Relaxation in the CT-State, J. Phys. Chem. A 107, 9530-9541 (2003).

[5] Z. Shen, R. Procházka, J. Daub, N. Fritz, N. Acar, S. Schneider, Towards modelling light processes of blue-light photoreceptors. Pyrene-isoalloxazine (flavin)-phenothiazine triad: electrochemical, photophysical, investigations and quantum chemical calculations, Phys. Chem. Chem. Phys. 5, 3257-3269 (2003).

The effects of surface states (N_{ss}), series resistance (R_s) and interlayer on the current-voltage and impedance-voltage characteristics in Au/n-Si/Ag Schottky barrier diodes (SBDs)

Çiğdem BİLKAN[1,2], Şemsettin ALTINDAL[1]

[1]*Department of Physics, Faculty Sciences, Gazi University, Ankara, Turkey,*

[2]*Department of Physics, Faculty Sciences, Çankırı Karatekin University, Çankırı, Turkey,*

E-mail: cigdembilkan@gmail.com

The forward and reverse bias current-voltage (I-V), capacitance/conductance-voltage-frequency (C/G-V-f) characteristics of Au/n-Si/Ag SBDs have been investigated in detail by taking into account the effects of N_{ss}, R_s and interlayer at room temperature. The energy dependent profile of N_{ss} was extracted the forward bias I-V data by taking into account the voltage dependence of the barrier height (BH), ideality factor (n) and series resistance (R_s). The frequency dependent profile of Nss and R_s were also obtained from both the C and G/□ data by using Hill Coleman method and I-V data by using Ohm's law. The main electrical parameters such as the concentration of donor atoms (N_D), Fermi energy level (E_F), BH (□$_B$ (C-V)) were also obtained from the reverse bias C^{-2}-V plots as function of frequency. The higher values of C and G/□□at low frequencies was attributed to the surface states and surface polarization. Because, surface states could follow an external ac signal at low frequencies. The value of □$_B$ (I-V) obtained from the forward bias I-V is lower than the □$_B$ (C-V) almost each frequency. This discrepancy was attributed to the nature of measurement system, particular distribution of N_{ss} and barrier inhomogeneity. The high value of ideality factor (n□1.91) was attributed to the existence of interfacial layer, N_{ss} and barrier inhomogeneities. The obtained experimental results confirmed that the interlayer, N_{ss}, R_s and barrier inhomogeneity lead to considerably deviated from ideal case. Therefore, their effects of them must be taken into account in the calculations.

Spectrophotometric and spectrofluorometric studies of Schiff base dyes containing electron-withdrawing and electron releasing groups

Dilek BAHÇECİ

Çanakkale Onsekiz Mart University, Department of Chemistry, Polymer Synthesis and Analysis Lab.17020 Çanakkale

dilek_dilek1734@hotmail.com

Schiff base products are usually known as azomethine compounds because of the presence of azomethine bond (1). Azo compounds are the oldest and largest class of industrial synthesized organic dyes because of their versatile application in various fields, such as biomedical studies, advanced application in organic synthesis, high technology areas such as electro-optical devices, and dyeing textile fibers (2). The most common dyestuff among these are azo-group (-N=N-) containing dyes. These dyestuffs are commonly used in areas such as textile, lac-dyes, polyography, elastic, leather, plastic materials, dying of synthetic fibers and other industrial areas (3, 4). Aldehyde group containing azo dye stuff, as a result of condensation with primer amines are known to synthesize many azomethine bond containing azo dyes. These dyestuffs are used by textile industry to dye various fabrics. Imine group containing azo dyes, apart from textile industry, have significant importance to photochemistry science. It is widely known that -C=N- or -N=N- containing structures can form complexes with numerous metals efficiently, so that they can be used as metal sensors (5). Taking this information into consideration, in this study, two groups are compared: azo-azomethine dye containing electron donor methyl ($-CH_3$) and formerly synthesized. Taking all this into consideration, in this study, electron donor methyl ($-CH_3$) containing azo-azomethine dye was compared to the formerly synthesized electron accepting containing ($-SO_3H$) azo-azomethine polymers.

Keywords: Imine polymers, synthesis, characterization and thermal analysis, azo-azomethine dyes, azo dyes.

References

1. Marwani, H.M., Abdullah, M., Asiri, M.A., Khan, A.S. (2014) Arabian J of Chem., 7, 609-614.

2. Menati, S., Azadbakht, A., Azadbakht, R., Taeb, A., Kakanejadifard, A. (2013) Dyes and Pigments, 98, 499-506

3. Li, Y.X., Wu, Q.Y., Gua, D.D., Gan, X.F. (2009) Mater. Sci. Eng. B., 158, 53–57

4. Chen, W., Wu, Q.Y, Gu, H.D, Gan, X.F. (2007) Mater. Lett. 61, 4181–4184.

5. Kurtoğlu, G., Avar, B., Zengin, H., Kose, M., Sayin, K., Kurtoğlu, M. (2014) Journal of Molecular Liquids, 200,105-114.

Evaluation of electron and hole densities of organic semiconductor materials

Ebru Çopuroğlu, Tural Mehmetoğlu

Department of Physics, Faculty of Arts and Sciences, Gaziosmanpaşa University, Tokat, Turkey

Department of Electrical Engineering, Faculty of Natural Sciences and Engineering, Gaziosmanpaşa University, Tokat, Turkey

E-mail: ebrucopuroglu@gmail.com

It is well known that organic materials have prime importance in light emitted diodes and organic field effect transistors. We have established new formulae which provide us to examine the mobile electron and hole densities in organic semiconductors by using Gaussian density of states (DOS). The obtained analytical formulae are valid for arbitrary values of parameters.

Analytical evaluation of temperature dependence of optical gain coefficient in bulk semiconductors

B.A. Mamedov, E. Çopuroğlu

Department of Physics, Faculty of ArtsandSciences, Gaziosmanpaşa University, Tokat , Turkey

E-mail: ebrucopuroglu@gmail.com

The semiconductor lasers have different applications in various areas of industries such as optical-fiber communication and optical memory (audio and video disc). For this purpose we present useful analytical formula for semiconductor lasers. By using obtained formula, the temperature dependencies of optical gain coefficient have been analyzed. The accuracy of this method is tested and its efficiency illustrated with graphics.

Electrical Properties of Cu-26.04%Zn-4.01%Al Alloy

E. Aldirmaz[1], M. Evecen[1], Y. Ö. Çiftci[2], and H. Celik[3]

[1] Department of Physics, Faculty of Arts and Sciences, Amasya University, 05100 Amasya, Turkey
[2]Department of Physics, Faculty of Sciences, Gazi University Teknikokullar, 06500, Ankara, TURKEY
[3]Department of Elementary Education, Education Faculty, Kırıkkale University, Yahsihan, Kırıkkale, Turkey
ealdirmaz@gmail.com

Copper has electrical and thermal conductivity. Therefore it used to be in many fields. Cu-based alloys are used in physics, metallurgy, biomedical and engineering sciences [1, 2]. Interest of researches in alloys which belong to ternary Cu-Zn-Al system is constantly growing, because their field of application is expanding. These materials, mostly used like Cu-based shape memory materials, also have found application in catalysis, electronics, and production of metal matrix composites [3, 4]. The results of an experimental investigation of structural and electrical characteristics of Cu-Zn-Al alloy is presented in this study. The investigations were scanning electron microscope (SEM), X-ray diffraction (XRD) and electrical measurements were made at the different temperatures with typical 250 micrometer in diameter probe using a standard four-point probe D.C. method. SEM and XRD techniques have shown the presence thermally induced M18R martensite from parent phase (DO_3 super lattice) martensite structures and f.c.c. α-phase. The resistivity as a function of temperature showed a increase with temperature (above 200 °C).

Keywords: Electrical resistivity, Martensite, Scanning Electron Microscopy (SEM), X-ray Diffraction (XRD).

Acknowledgment

This study was supported financially by the Research Centre of Amasya University (Project No: FMB-BAP 16-0174).

[1] V. Torra, (ed.). Proceedings COMETT Course: the Science and Technology of Shape Memory Alloys. University of Balears Islands, Palma de Mallorca, Spain, 1989.

[2] H. Funakubo, Shape Memory Alloys. Gordon and Breach Science Publishers, 1987.

[3] L. Janke, C. Czaderski, M. Motavalli and J. Ruth, Applications of shape memory alloys in civil engineering structures: Overview, limits and new ideas, Materials and Structures, 38(5), 578 (2005).

[4] W. M. Huang, Z. Ding, C. C. Wang, J. Wei, Y. Zhao and H. Purnawali, Shape memory materials, Mater. Today, 13(7 −8), 54 (2010).

Influences of Sn and Ni on microstructuresin Cu-Zn based alloys

E. Aldirmaz[1], M. Evecen[1], Harun Celik[2]

[1]Department of Physics, Faculty of Science and Arts, Amasya University, 05100 Amasya, Turkey.

[2]Department of Elementary Education, Education Faculty, Kırıkkale University, Yahsihan Campus, 71450 Kırıkkale, Turkey.

ealdirmaz@gmail.com

Cu-Zn alloys are used in industrial application. Especially, brass ware with improved mechanical and physical properties can be produced with the addition of a third element, for example Pb (lead) and Sn (tin). Due to exposed physical and mechanical effects, metal and alloys exhibit a very surprising property. Under the various mechanical and thermodynamic conditions, microstructural changes [1, 2, 3]. The purpose of the present work is to investigate effects of thermally effect and Ni and Sn on microstructures of β Cu-Zn binary alloys. At present two different types of alloying systems are used as shape memory materials: Cu-11.89% Zn-7.68% Sn (alloy 1) and Cu-12.44%Zn-4.75%Ni (wt.%) (alloy 2) (wt.%) cu-based alloys. In SEM observations of alloy 1, dendrite and austenite phases are observed. SEM observations for alloy 2, annealing twins and austenite structures are observed. Due to Cu-based alloys are very sensitive to the thermal treatments and composition, in Cu-11.89%Zn-7.68% Sn (alloy 1), a different behaviour exists from Cu-12.44%Zn-4.75%Ni (alloy 2).

Keywords: Cu-based alloys, Austenite, Dentrite, X-ray diffraction.

Acknowledgment

This study was supported financially by the Research Centre of Amasya University (Project No: FMB-BAP 16-0174).

[1] R. Kainuma, S. Takahashi and K. Ishida, Thermoelastic martensite and shape memory effect in ductile Cu-Al-Mn alloys, Metall. Mater. Trans. A 27A, 2187 (1996).

[2] M. Peng and A. Mikula, Thermodynamic properties of liquid Cu-Sn-Zn alloys, J. Alloys Comp. 247, 185 (1997).

[3] O. Adiguzel, Martensite ordering and stabilization in copper-based shape memory alloys, Mater. Res. Bull**.** 30, 755 (1995).

[4] Y. Nakata, O. Yamamoto and K. Shimizu, Effect of aging in Cu-Zn-Al shape memory alloys, Mater. Trans. JIM 5, 429 (1993).

The Synthesis and Characterization of Mannich Bases Derived from Compounds of Including Ring 1,3,4-oxadiazole-2-thion as Potential Antimicrobial Agents

Ahmet ÇETİN, Eray ÇALIŞKAN

Department of Chemistry, Faculty of Art and Science, Bingol University, 12000, Bingol-TURKEY

email; ecaliskan@bingol.edu.tr

Abstract- Aromatic heterocycles are very important motifs in medicinal chemistry researches. 1,3,4-oxadiazole exhibit a wide range of biological activities [1]. 1,3,4-oxadiazole and their fused heterocyclic derivatives has attracted attention due to their biological importance[2,3].

In this work, various new compounds including ring 1,3,4-Oxadiazole were synthesized from the reactions of hydrazide compounds with carbon sulfur in basic medium. Mannich bases were prepared by tiyol tautomer form of 1,3,4-Oxadiazole (Scheme 1). Furthermore, structure-activity relationship was evaluated in respect to effect of different substitutions in newly synthesized 1,3,4-oxadiazole series. Then these compounds were characterized by performing of melting point, FT-IR, ^{1}H-NMR (400 MHz), and ^{13}C-NMR(100 MHz).

Keywords: 1,3,4-Oxadiazole, Mannich Bases, Thiol-Thione Tautomerism.

Introduction- Nowadays, the synthesis of polyfunctional and heteroatom bearing cyclic compounds in which possess wide range of antimicrobial and biological activity is an important field in synthetic organic chemistry.

Ring closure reaction of carbohydrazide are well-known and formation of three heteroatom bearing five-membered heterocyclic compounds such as 1,3,4-oxadiazole, 1,3,4-thiodiazole and 1,2,4- triazole are frequently synthesized [1]. Carboxylic acid carbazides give 3-arylthiocarbazide salts in presence of ethanolic KOH reaction with CS_2 and newly formed salt has given a ring closure reaction with pyridine or anhydrous NaOH in order to form 5-aryl-2-mercapto-1,2,4-oxadiazole compound [5,6]. Another study which was carried out by Cansiz *et al*. starting from 3-furil-1,2,4-triazole-5-thione compounds synthesizing mannich bases[4]. Pandaya et al. has reported that Schiff and Mannich bases synthesized from isatin derivatives exhibit antifungal and antimicrobial activity [7]. Compound 3a,b were synthesized and reported in the literature first time and showed efficient antifungal- antimicrobial activity against E. Coli, S. Aureus and B. Subtilis.

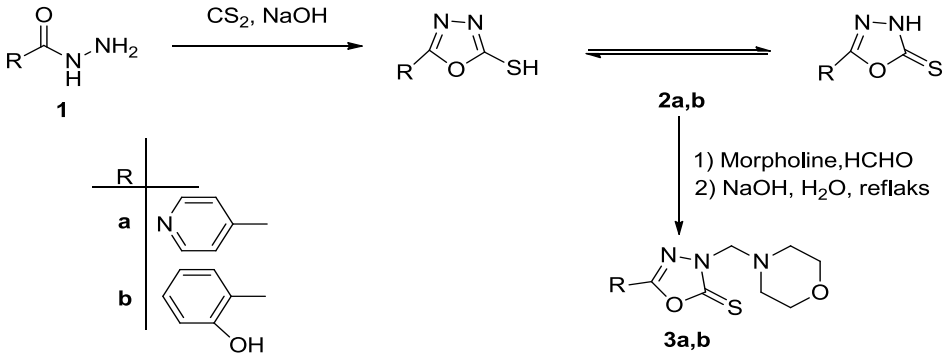

Scheme 1: Synthesized compounds

Experimental- Compounds of **2a-b** was synthesized according to the literature [6].

The synthesis of 3-(Morpholin-4-ylmethyl)-5-pyridin-4-yl-1,3,4-oxadiazole-2(3*H*)-thion (3a): A slurry consisting of (0.002 mol, 0.358 g.) 5-pyridin-4-yl-1,3,4-oxadiazole-2-thiol in ethanol (10mL) and (0.003 mol, 0.289 mL) 37 % formalin was formed. To this (0.002 mol, 0.174 mL) morpholine was added drop wise, with cooling and shaking. The reaction mixture was allowed to stand at room temperature for 1 h. with occasional shaking after which it was warmed on a steam bath for 0.5 h. At the end of period the contents were cooled and the product obtained was recrystallized from dioxane. Yield: 0.21g, 38 %, Mp 336-337 ^{0}C.

The synthesis of 5-(2-hydroxyphenyl)-3-(morpholin-4-ylmethyl)-1,3,4-oxadiazole-2(3*H*)-thione (3b): A slurry consisting 2-(5-mercapto-1,3,4-oxadiazol-2-yl) phenol (0.388 g, 2 mmoles), ethanol (10ml) and (0.289 ml, 3

mmoles) 37% formalin was made. To this morpholine (2 mmoles, 0.174 ml) was added drop wise, with cooling and shaking. The reaction mixture was allowed to stand at room temperature for 1 hour with occasional shaking after which it was warmed on a steam bath for 0.5 hour. At the end of period the contents were cooled and the product obtained was recrystallized from dioxane. Yield: 0.29 g, 46 %, m.p.: 178 ^{o}C;

Result and discussion

3-(Morpholin-4-ylmethyl)-5-pyridin-4-yl-1,3,4-oxadiazole-2(3*H*)-thion (3a)

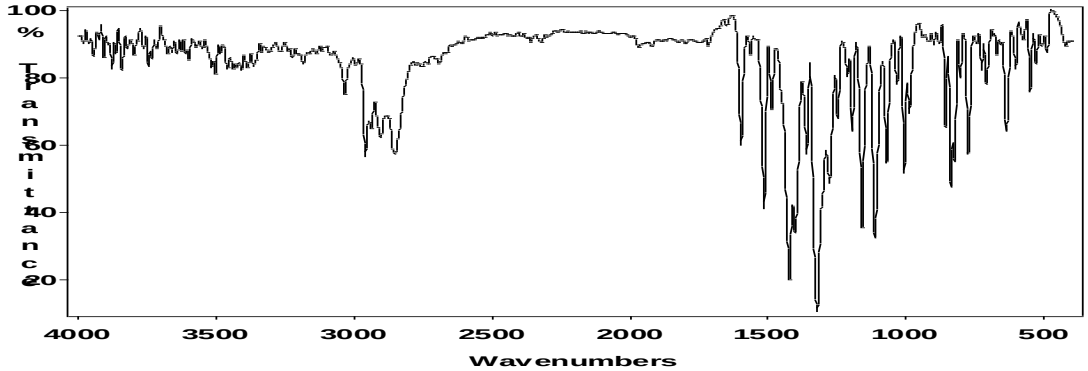

Scheme 2: FT-IR Spectrum of **3a**

FT-IR (KBr, v_{max}/cm^{-1}): 3080-3020 (Ar.C -H), 2970-2820 (Al.C -H), 1256 (C=S)

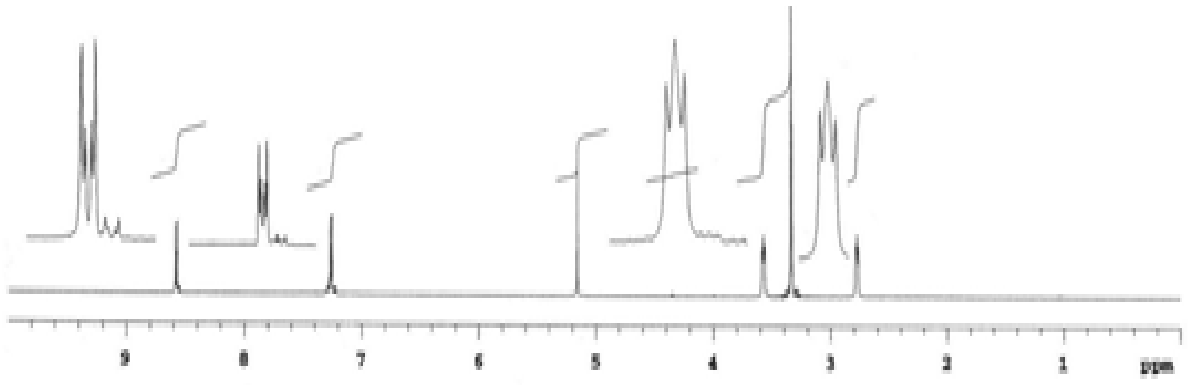

Scheme 2: ^{1}H-NMR Spectrum of **3a**

^{1}H-NMR (400 MHz, DMSO-d6, ppm) : δ 2.78 (t, J=4.45, 4H, CH_2-N-CH_2), 3.58 (t, J=4.40, 4H, CH_2-O-CH_2), 5.16 (s, 2H, N-CH_2-N), 7.22 (dd, J=5.87, 1.47, 2H, Ar. C-CH), 8.58 (dd, J=5.87, 1.47, 2H Ar. N-CH).

5-(2-hydroxyphenyl)-3-(morpholin-4-ylmethyl)-1,3,4-oxadiazole-2(3*H*)-thione (3b)

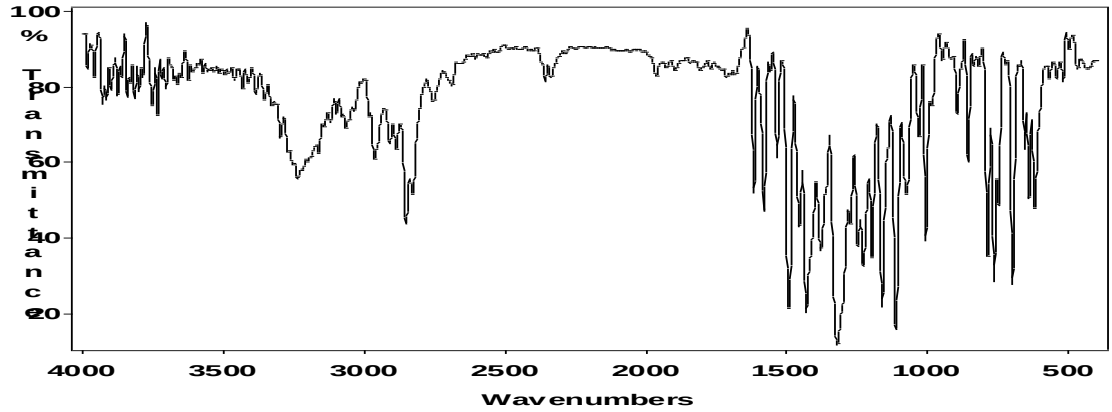

Scheme 3: FT-IR Spectrum of **3b**

FT-IR (KBr, v_{max}/cm^{-1}): 3440-3130 (OH), 3066-3000 (Ar. CH), 2970-2883 (Al. CH), 12585 (C=S)

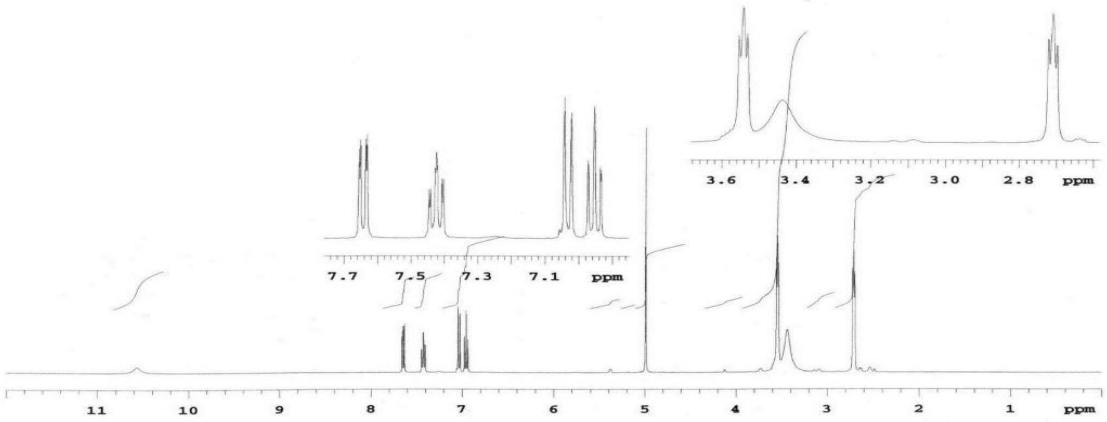

Scheme 4: ^{1}H-NMR Spectrum of **3b**

^{1}H-NMR (400 MHz, DMSO-d6, ppm) : δ 2.66 (t, J=4.46, 4H, CH_2-N-CH_2), 3.62 (t, J=4.40, 4H, CH_2-O-CH_2), 5.00 (s, 2H, N-CH_2-N), 6.93 (t, J=7.30, 1H, H_3), 7.02 (d, J=8.05, 1H, H_1), 7.49 (t, J=7.36, 1.47, 1H, H_2), 7.66 (dd, J=8.05, 1.47, 1H, H_4), 10.60 (br, 1H, OH).

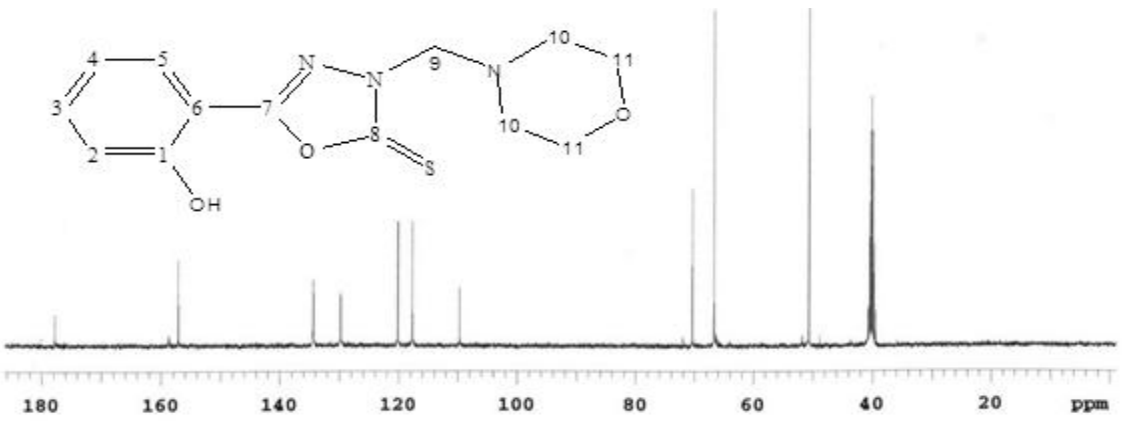

Scheme 5: ^{13}C-NMR Spectrum of **3b**

^{13}C-NMR (100 MHz, DMSO-d6, ppm) : δ C_8: 178.06, C_1: 159.04, C_7: 150.51, C_3: 138.89, C_5: 129.73, C_4: 120.00, C_2: 117.95, C_6: 109.68, C_9: 71.10, C_{10}: 51.12, C_{11}: 66.10.

Antibacterial and antifungal activity

Compounds	E.Coli (Conc.)	S. Aureus(Conc.)	B. Subtilis(Conc.)

	10 µg/ml	50 µg/ml	100 µg/ml	500 µg/ml	10 µg/ml	50 µg/ml	100 µg/ml	500 µg/ml	10 µg/ml	50 µg/ml	100 µg/ml	500 µg/ml
3a	-	+	++	++	-	+	+	++	-	+	+	++
3b	+	+	++	+++	+	+	++	+++	+	+	++	+++
Ciprofloxacin	++	++	+++	+++	+	++	+++	+++	+	++	+++	+++

Symbols: (-): < 10% inhibition, (+): 10-30% inhibition, (++): 30-60% inhibition, (+++):60-90% inhibition, Ciprofloxacin ≥ 90% inhibition

Table 1 The degree of inhibition of antibacterial activity of the synthesized compounds

Compounds	**C. Albicans (Conc.)**		**A. Niger (Conc.)**	
	50 µg/ml	100 µg/ml	50 µg/ml	100 µg/ml
3a	+	++	+	+
3b	+	++	++	++
Flucanazole	+++	+++	+++	+++

Symbols: (-) no inhibition, (+) weakly active, (++) moderately active, (+++) highly active

Table 2 Antifungal activity of compounds against C. Albicans, and A. Niger

The studied molecules (2a–b, 3a,b), were screened for antibacterial activity against E. Coli, S. Aureus and B. Subtilis by agar diffusion technique using ciprofloxacin as the reference (50 µg/ml), antifungal activity against A. Niger and C. Albicans by agar diffusion technique using fluconazole as reference (50 µg/ml). The result and observations are outlined in Table 1 and Table 2.

References

[1] F. Fülöp, E. Semega, C. Dombi, G. Bernath, Synthesis of new heterocyclic compounds as potential pharmaceutical agents, *J. Heterocyclic Chem*. 27, 951, (1990).

[2] J. R. Reid, N. D. Heindel, Improved synthesis of 5-substituted −4-amino-3-mercapto 4H 1,2,4-triazoles, *J. Heterocyclic Chem*. 13, 925, (1976).

[3] D. Rigo, D.,Couturier, Studies on pyrrolidinones. Synthesis of 5-(5-oxo-2-pyrrolidinyl)-1,3,5-oxadiazole-2-thione derivatives, *J. Heterocyclic Chem*. 22, 287, (1985).

[4] A. Cansız, S. Servi, M. Koparır, M. Altıntaş, M. Dığrak, Synthesis and antimicrobial activity of some of new 1,1,3-trisubstituted cyclobutane containing thiazoles, succinimide and phthalimide derivatives*, J. Chem. Soc. Pak.* 23, 237-239, (2001).

[5] Rehman Aziz-ur-, K. Nafeesa, MA. Abbasi, H. Kashfa, S. Rasool, I. Ahmad, S. Arshad. Synthesis, characterization and biological screening of various S-substituted derivatives of 5-(3-Nitrophenyl)-1,3,4-Oxadiazole-2-thiol. *Pak J Chem*, 3:1–8, (2013).

[6] M. Koparır, A. Çetin, and A. Cansız, 5-furan-2yl[1,3,4]oxadiazole-2-thiol and 5-furan-2yl-4H [1,2,4] triazole-3-thiol and their thiol-thione tautomerism, *Molecules*, 9(12), 204-212, (2004).

[7] S. N. Pandeya, D. Sriram, G. Nath, E. Declercq, Synthesis, antibacterial, antifungal and anti-HIV activities of Schiff and Mannich bases derived from isatin derivatives and N-[4-(4'-chlorophenyl)thiazol-2-yl] thiosemicarbazide, *Europan Journal of pharmaceutical Sciences*, 9, 25-31, (1999)

Synthesis and Investigation of Dielectric Properties of Methacrylate-Based Side-Chain Liquid Crystalline Polymers Bearing Cholesteryl Mesogen and Thiophene

Erdinç Doganci[1], Fırat Kayabaşı[2], Betul Canimkurbey[3,4], Sait Eren San[3], and Faruk Yilmaz[2]

[1]*Department of Chemistry and Chemical Processing Tech., Kocaeli Voc. Sch., Kocaeli University, Kocaeli,Turkey*

[2]*Gebze Technical University, Chemistry Department, 41400 Gebze, Kocaeli, Turkey*

[3]*Gebze Technical University, Physics Department, 41400 Gebze, Kocaeli, Turkey*

[4]*Department of Physics, Amasya University, Amasya, Turkey*

E-mail: edoganci@kocaeli.edu.tr

Recently, organic field-effect transistors (OFETs) have attracted a great deal of attention owing to their potential candidates for use in a wide range of electronic applications, such as displays, sensors, and electronic barcodes[1]. Ordered arrays of cholesterol molecules or mesogens which result in the formation of liquid crystalline polymers (LCPs) have gained importance due to the application of these polymers in opto-electronics, color information technology, bioactive materials, and biotechnology[2].

In this work, methacrylate-based side-chain liquid crystalline polymers containing cholesterol and thiophene pendant groups ()) were prepared by atom transfer radical polymerization (ATRP). Dielectric characterization of Poly(CholMMA-*co*-MTM) were investigated as the insulators for organic thin film transistors (OTFTs) (Figure 1). It is observed that dielectric properties are enhanced by increasing cholesterol content in Poly(CholMMA-*co*-MTM).

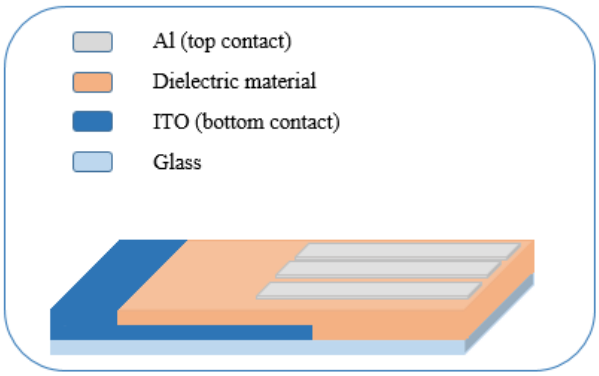

Figure 1. Schematic of Poly(CholMMA-co-MTM)- OFET device structure.

[1] Halik, M.; Klauk, H.; Zschieschang, U.; Schmid, G.; Dehm, C.; Schutz, M.; Maisch, S.; Effenberger, F.; Brunnbauer, M.; Stellacci, F. Nature 431, 963-966 (2004).

[2] Zhou, Y.; Briand, V. A.; Sharma, N.; Ahn, S-K.; Kasi, R. M. Materials, 2, 636-660 (2009).

Studies on Potential Optimization of Cu_2ZnSnS_4 Thin Film Prepared by One-Step Electrochemical Deposition Method

E. EROL[1,*], M. ÇELİK TOLU[2], B. BEZGİN CARBAS[2], F. ÖZEL[1] and S. SÖNMEZOĞLU[1]

[1]*Department of Metalurgical and Materials Engineering, Karamanoğlu Mehmetbey University, Karaman, TURKEY*

[2]*Department of Energy Systems Engineering, Karamanoğlu Mehmetbey University, Karaman, TURKEY*

E-mail : erdinceerol@gmail.com

This study focuses on one-step electrodeposition of Cu_2ZnSnS_4 (CZTS) thin film through the annealing route in a sulphur-free environment. The reduction behaviors of each Cu, Zn, Sn and S elements were investigated using the cyclic voltammetry (CV) method. The obtained reduction potentials were -0.2 V, -1.2 V, -0.6 V and -1.2 V for Cu, Zn, Sn and S elements, respectively, (vs. Ag/AgCl). The electrolyte was composed of these four elements in an appropriate stoichiometric ratio. Trisodium citrate dihydrate complexing agent was used to get closer reduction potential of these elements. Then, the optimum deposition potential was determined and the elements deposited on fluorine doped tin oxide (FTO) glass at room temperature. The annealing procedure was carried out in a sulphur-free environment, with optimum temperature for converting the amorphous structure into a kesterite crystal structure. Consequently, the kesterite crystal CZTS structure was synthesized via the one-step electrodeposition technique without sulfurization process.

Keywords: Cu_2ZnSnS_4 Thin Film, Electrochemical Deposition Method, Sulphur-Free Environment.

Acknowledgement – This study was supported by the European Union through the COST Action MP1407 “Electrochemical processing methodologies and corrosion protection for device and systems miniaturization (e-MINDS)”, and by the Scientific and Technological Research Council of Turkey (TUBITAK Grant Number 115M762) who provided financial support for this research.

Preparation and characterization of fibers and films of titanium oxide

Osman Ürper[1] Refika Budakoğlu[2] and Esra Ö. Zayim[3]

[1] Energy Institute, Istanbul Technical University, Ayazağa Kampüsü, Maslak, 34469 Istanbul, Turkey

[2] Türkiye Şişe ve Cam Fabrikaları A,Ş. Science &Technology Center, Atmospheric Coating Techologies Management, İstanbul, Turkey

[3] Istanbul Technical University, Faculty of Science and Letters, Physics Department, Istanbul, Turkey

E-mail :ozesra@itu.edu.tr

In this paper, electrospun microfibers, nanofibers and sol-gel-made films of titanium oxide were prepared by organic/inorganic blend. It is reported that this developed procedure offers several advantages over previously known procedures used to coat titanium oxide films by sol-gel process in the literature. First, it allows fabrication of films and microfibers, activating upon exposure to ultraviolet light known as photocatalytic effect. Secondly, titanium oxide fabricated via this procedure as nanofibers, microfibers and films, can be applied to numerous types of surfaces with different techniques. Microstructure and formation mechanism of the films and fibers were studied by using digital optical camera and SEM, XRD and optical measurements.

Keywords: titanium oxide; microfiber; nanofiber; film

Analysis of Reverse-Bias Transport Mechanisms in Conjugated Copolymer-Based Diodes

D. E. Yıldız[1,*], D. H. Apaydın[2], L. Toppare[2,3,4,5], A.Cirpan[2,3,5,6]

[1] Physics Department, Faculty of Arts and Sciences, Hitit University, 19030 Corum, Turkey

[2] Department of Polymer Science and Technology, Middle East Technical University, 06800 Ankara, Turkey

[3] Department of Chemistry, Middle East Technical University, 06800 Ankara, Turkey

[4] Department of Biotechnology, Middle East Technical University, 06800 Ankara, Turkey

[5] The Center for Solar Energy Research and Applications (GUNAM), Middle East Technical University, 06800 Ankara, Turkey

[6] Micro and Nanotechnology Program, Middle East Technical University, 06800 Ankara, Turkey

In this paper, thickness-dependent reverse current-voltage (I_R-V) plots obtained for conjugated copolymer based organic diodes fabricated on ITO were reinterpreted in terms of conduction mechanism. In order to analyze the reverse bias transport mechanisms in organic diodes with ITO/PEDOT:PSS/PFTBT:PC61BM/LiF/Al configuration, the thickness-dependent I_R-V measurements were applied in the thickness range between 90 and 200 nm. In this thickness range, the reverse current-voltage plots of organic diode, the thickness dependence of Polymer:PCBM was examined in terms of electrical charge transport and we observed that the reverse current was controlled these devices by Poole-Frenkel emission above 140 nm and by Schottky emission under 140 nm.

Keywords: Electronic transport, Schottky emission, Poole-Frenkel emission

To investigate the electrical properties of new silafluorene-based conjugated polymers

D. E. Yıldız[1,*], O.Erlik[2],G. Hizalan[2], L. Toppare[2,3,4,5], A.Cirpan[2,3,5,6]

[1] Physics Department, Faculty of Arts and Sciences, Hitit University, 19030 Corum, Turkey

[2] Department of Polymer Science and Technology, Middle East Technical University, 06800 Ankara, Turkey

[3] Department of Chemistry, Middle East Technical University, 06800 Ankara, Turkey

[4] Department of Biotechnology, Middle East Technical University, 06800 Ankara, Turkey

[5] The Center for Solar Energy Research and Applications (GUNAM), Middle East Technical University, 06800 Ankara, Turkey

[6] Micro and Nanotechnology Program, Middle East Technical University, 06800 Ankara, Turkey

Four new silafluorene-based conjugated polymers were used in organic diodes with ITO/PEDOT:PSS/Polymer:PCBM[70]/Ca/A configuration. The dark current-voltage I-V measurements were applied in the voltage range between (-2 V) and (2 V). The main electrical parameters were determined such as zero-bias barrier height (Φ_{Bo}), ideality factor (n), series resistance (R_s), shunt resistance (R_{sh}) and carrier mobility (μ). In addition, the forward current-voltage plots of organic diodes were examined of conduction mechanisms and we observed that the forward current was controlled these devices by the space charge limited current (SCLC).

Keywords: Space charge limited current (SCLC), Electrical properties

Electrical properties of Schottky Barrier Diodes (SBDs): A comparative Study

D. E. Yıldız, Ö. Vural, İ. H. Taşdemir

[1]Physics Department, Faculty of Arts and Sciences, Hitit University, Çorum, TURKEY

[2]Physics Department, Faculty of Arts and Sciences, Amasya University, Amasya, TURKEY

[3]Chemistry Department, Faculty of Arts and Sciences, Amasya University, Amasya, TURKEY

e-mail:desrayildiz@hitit.edu.tr

In this study, we investigated electrical properties of TiO_2/p-Si, TiO_2-Zr/p-Si, GO-TiO_2/p-Si and Rbf-TiO_2/p-Si interfaces in Schottky barrier diodes (SBDs).The Al/TiO_2/p-Si, Al/TiO_2-Zr/p-Si, Al/GO-TiO_2/p-Si and Al/Rbf-TiO_2/p-Si SBDs were fabricated and their current-voltage (I-V) measurements were carried out in the voltage range of (-4 V) – (6 V) at room temperature. A good rectifying behavior was seen from the I-V characteristics for all devices. Some electrical parameters, such as zero-bias barrier height (Φ_{Bo}), ideality factor (n), series resistance (R_s) and shunt resistance (R_{sh}) were obtained for these devices. The values of n and Φ_{Bo} were found from the forward bias I-V data as 2.66 and 0.82 eV for Al/TiO_2/p-Si (D1), 2.0 and 0.81 eV for Al/TiO_2-Zr/p-Si (D2), 2.34 and 0.78 eV for Al/GO-TiO_2/p-Si (D3) and 1.58 and 0.79 eV for Al/Rbf-TiO_2/p-Si (D4), respectively. It is clear that the obtained value of n is greater than unity especially for diode with interfacial insulator layer. Therefore, such behavior of n especially can be attributed to the interfacial layer, surface states (D_{it}) and the formation of barrier height inhomogeneity. These results show that the TiO_2-Zr, GO-TiO_2 and Rbf-TiO_2 composite insulator layer are considerably improve the Al/TiO_2/p-Si performance.

Table. 1. Same main electrical parameters of devices

	n	I_o	Φ_{Bo}	R_s (kΩ)	R_{sh} (kΩ)
TiO_2	**2.66**	**1.045×10^{-9}**	**0.82**	**402**	**16761**
TiO_2-Zr	**2.00**	**1.45×10^{-9}**	**0.81**	**841**	**9659**
GO-TiO_2	**2.34**	**4.37×10^{-9}**	**0.78**	**732**	**2238**
Rbf-TiO_2	**1.58**	**1.92×10^{-9}**	**0.79**	**846**	**5353**

Keywords: ideality factor, barrier height, series resistance, shunt resistance

The effect of surface states and series resistance on the performance Al/GO/p-Si and Al/GO-Co/p-Si Schottky Barrier Diodes (SBDs)

D. E. Yıldız, Ö. Vural, İ. H. Taşdemir

[1]Physics Department, Faculty of Arts and Sciences, Hitit University, Çorum, TURKEY

[2]Physics Department, Faculty of Arts and Sciences, Amasya University, Amasya, TURKEY

[3]Chemistry Department, Faculty of Arts and Sciences, Amasya University, Amasya, TURKEY

e-mail:desrayildiz@hitit.edu.tr

In this study, we investigated the effect of surface states and series resistance on the performance Al/GO/p-Si and Al/GO-Co/p-Si Schottky Barrier Diodes (SBDs).The Al/GO/p-Si and Al/GO-Co/p-Si SBDs were fabricated and some electrical parameters, such as zero-bias barrier height (Φ_{Bo}), ideality factor (n), series resistance (R_s) and shunt resistance (R_{sh}) were obtained for these devices. The values of n and Φ_{Bo} were found from the forward bias I-V data as 2.1 and 0.75 eV for Al/GO/p-Si (D1) and 2.1 and 0.74 eV for Al/GO-Co/p-Si (D2), respectively. In addition, density distribution profile of surface states (D_{it}) for D1 and D2 SBDs were obtained from forward bias I-V plots by taking into account the bias dependence of effective barrier height and series resistance. Experimental results show that both D_{it} and R_s values should be taken into account in the forward bias I-V plots.

Table. 1. Same main electrical parameters of devices

	n	**I_o**	**Φ_{Bo}**	**R_s (kΩ)**	**R_{sh} (kΩ)**
Al/GO/p-Si	2.10	$1.41x10^{-8}$	0.75	2.8	1680
Al/GO-Co/p-Si	2.10	$1.63 x10^{-8}$	0.74	1.0	3000

Keywords: ideality factor, barrier height, series resistance, shunt resistance, surface states

Polyoxomethalates as new therapeutic materials: From simple metal salts to metal-oxo cages

Eyüp Akgün, Muhammet Köse
Department of Chemistry, Faculty of Science and Arts, Kahramanmaraş, Turkey
E-mail: eyupakgunx@hotmail.com

Polyoxometalates are metal-oxygen cluster ions and have taken considerable interest during due to their versatile properties including size, electron transfer abilities, thermal stability and lability of lattice oxygen [1]. Unique properties of polyoxometalates have led researchers use these materials in several areas including catalysis, photochemistry, medicine and biology and material science [2]. Polyoxometalates were found to exhibit anticancer properties against to some certain cancer cells [3]. These compounds as anticancer chemotherapy drugs especially has taken inexhaustible motivation to the medicinal chemists. Thus, the anticancer activities of these polyoxometal cages become one of the frontier subjects in the pharmaceutical area. In this work, Keggin and Anderson type polyoxomethalates were prepared and characterised by the spectroscopic and analytical methods. Molecular structures of the compounds were determined by single crystal X-ray diffraction study. Photophysical properties of the structurally characterized compounds were studied by photoluminescence and UV-Vis. absorption studies both in the solid state and solutions. Molecular structures of polyoxo anion cages is shown in Figure.

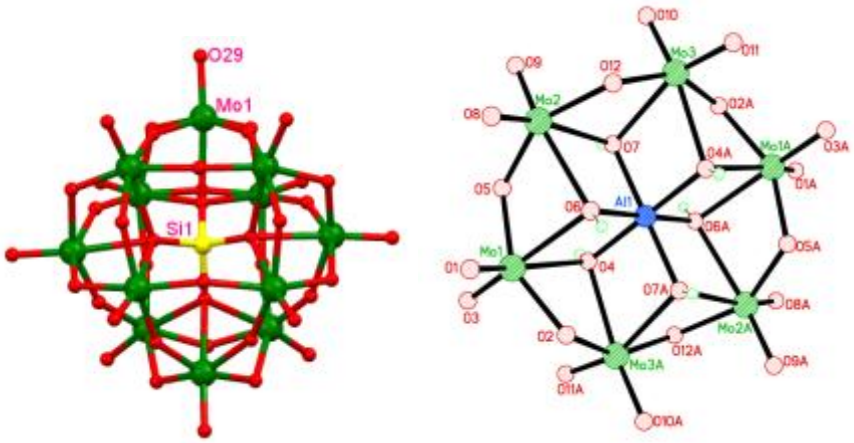

Fig: Crystal structure of $[SiMo_{12}O_{40}]^{4-}$ (left) and $[Al(OH)_6Mo_6O_{18}]^{3-}$ (right).

Acknowledgments: We are grateful to Research Council of Turkey (Tubitak Grant number: 115Z065 cost project) for financial support.

References

[1] M.T. Pope, A. Muller, Angew. Chem. Int. Ed. Engl. 30, 34 (1991).
[2] J.M. Thomas, Angew. Chem. Int. Ed. 38, 3588 (1999).
[3] H. Yanagie, A. Ogata, S. Mitsui, T. Hisa, T. Yamase, M. Eriguchi, Biomedicine & Pharmacotherapy, 60, 349 (2006).

Material properties of an azo compound for organic light-emitting diode (OLED) application

Eyüp Akgün, Muhammet Köse

Department of Chemistry, Faculty of Science and Arts, Kahramanmaraş, Turkey

E-mail: E-mail: eyupakgunx@hotmail.com

Fluorescent materials have been widely used tools in the field of science and technology. Their applications includes fluorescent probes, fluorescent paint, fluorescent indicators, and organic light-emitting diodes (OLED), have important roles in scientific research and our daily life [1]. Many types of organic fluorescent compounds have been developed to date due to their advantages such as fine adjustability of optical properties and ease of synthesis. Azobenzene compound are π-conjugated molecules and widely used as pigments [2]. Diazo compounds have potential usage for attractive fluorescent materials, considering the π-conjugated structures. Regarding the spatial arrangement of the azo group, these compounds can be either *cis* or *trans*, usually *trans* form is the more stable one [3]. The UV-induced conversion to the *cis* or *trans* configuration is a well-investigated phenomenon which allows these compounds to be used for optical storage materials. In this work, photoluminesence and electronic properties of a commercially available diazo compound 2,2'-({4-[(E)-(4-aminophenyl)diazenyl]phenyl}imino)di-ethanol were studied in detail in several solvents and in the solid state. The molecular structure of the compound was determined by single crystal X-ray diffraction study. Molecular structure of the compound is shown in Figure.

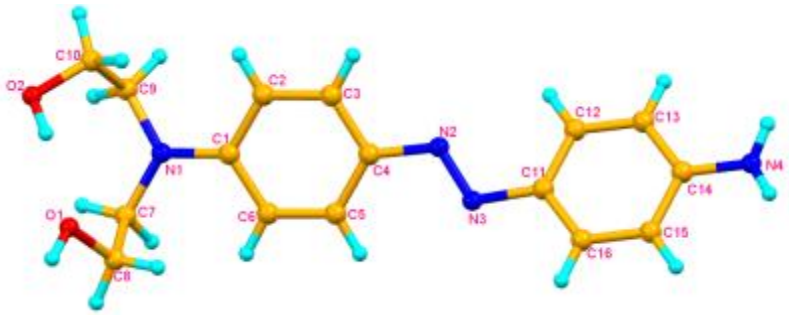

Fig: Crystal structure of 2,2'-({4-[(E)-(4-aminophenyl)diazenyl]phenyl}imino)diethanol with atom numbering.

Acknowledgments: We are grateful to Research Council of Turkey (Tubitak Grant number: 115Z065 cost project) for financial support.

References

[1] B. Valeur, Molecular Fluorescence, Wiley-VCH, Weinheim, (2002**).**

[2] J. Yoshinoa, N. Kano, T. Kawashima**,** Dalton Trans., 42, 15826 (2013**)**

[3] E. Bergmann, L. Engel, S. Sándor, Ber. Dtsch. Chem. Ges. 63, 2572(1930) .

Light Controller Solar Simulator System for Diodes

Fahrettin Yakuphanoglu

Physics Department, Faculty of Science, Firat University, Elazig, TURKEY

Nanoscience and Nanotechnology Laboratory, Firat University, Elazig, TURKEY

Here, we manufactured a light controller solar simulator system to analyze organic solar diodes, Schottky diodes, pn heterojunction diodes and all photosensors. This system can be used to determine photoresponsivity, photosensitivity, photocurrent gain I_{on}/I_{off} ratio, stability of current, photoconductive, photovoltaic mechanism, photocapacitor behavior and etc.

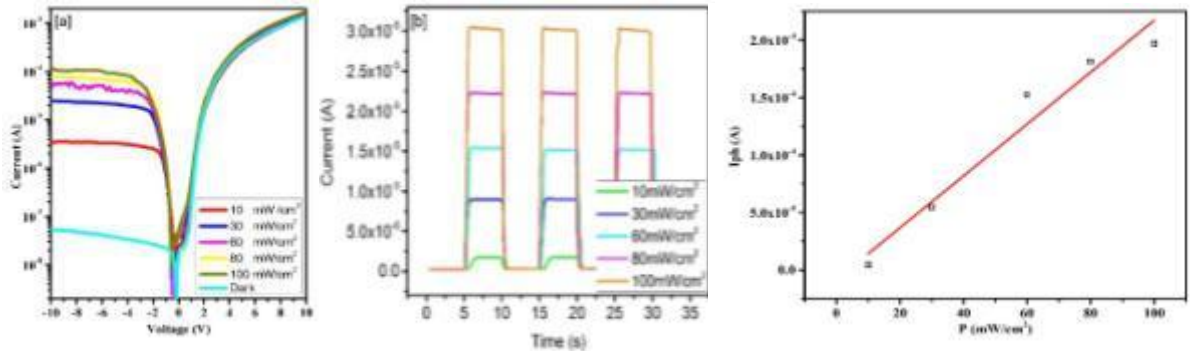

Keywords: Diodes, Solar Simulator

Wavelength Controller Solar Simulator System for all electronic devices

Fahrettin Yakuphanoglu

Physics Department, Faculty of Science, Firat University, Elazig, TURKEY

Nanoscience and Nanotechnology Laboratory, Firat University, Elazig, TURKEY

Here, we manufactured a wavelength controller solar simulator system to analyze organic solar cells, dye sensitized solar cells, silicon solar cell, quantum dots solar cells. The system has the following capabilities; current-time, quantum efficiency-wavelength, Responsivity-wavelength at various bias voltages, current-voltage under various wavelengths, current-voltage under constant wavelength for various light intensities and so on. The system can be also used to determine all electronic parameters of the all photodetectors and photodiodes.

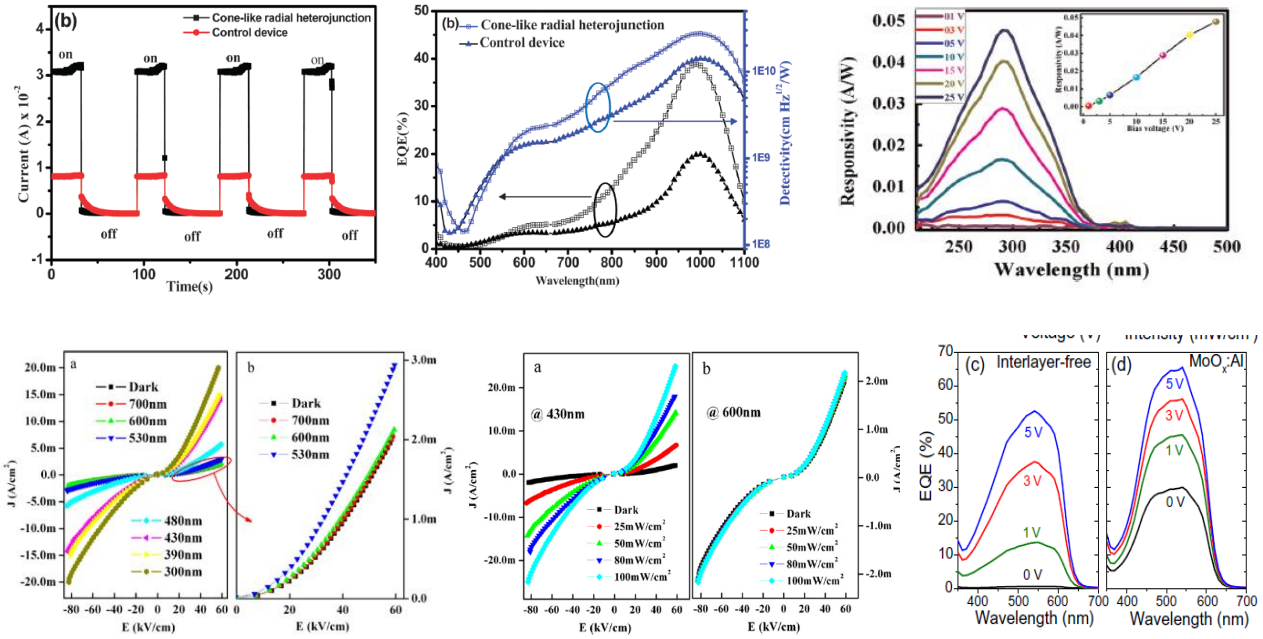

Keywords: Solar Cells, Solar Simulator

Investigation of adsorption and corrosion inhibitive properties of 5-((4-chloro-2-methylphenoxy)methyl)-1,3,4-thiadiazole-2-amine films on mild steel in HCl solution

Ramazan Solmaz, Ahmet Çetin
Bingöl University, Science and Letters Faculty, Chemistry Department, 12000, Bingöl, Turkey
E-mails: rsolmaz@bingol.edu.tr, acetin74@hotmail.com

Abstract

Adsorption of 5-((4-chloro-2-methylphenoxy)methyl)-1,3,4-thiadiazole-2-amine (CMMTA) on mild steel surface from 1 M HCl solution and its inhibition efficiency against corrosion were studied with the help of electrochemical methods. The mild steel specimens were exposed to 1 M HCl solution in the absence and presence of 1 mM CMMTA and the change of its open circuit potential as a function of exposure time (E_{ocp}-t) was graphically monitored. Electrochemical kinetics parameters were evaluated by potentiodynamic polarization measurements. The metal-film/solution interface was investigated by electrochemical impedance spectroscopy (EIS). The resistance of the steel in the absence and presence of the inhibitor were determined from EIS and linear polarization measurements. It was found that CMMTA has great corrosion protection ability for mild steel. The high inhibition efficiency of this compound was explained by its adsorption on the metal surface and a protective film formation on the steel surface.

Keywords: 5-((4-chloro-2-methylphenoxy)methyl)-1,3,4-thiadiazole-2-amine, mild steel, adsorption, corrosion inhibition.

1. Introduction

The study of adsorption of organic molecules at the metal/solution interface is of great interest in developing and understanding of many electrochemical processes such as double layer, electro-organic synthesis, electro-kinetics, as well as electrocatalysis [1, 2]. Corrosion resisting properties of the metals can also be markedly changed by the adsorption of organic molecules on metal surfaces and their inhibitory efficiencies are mainly depend on their adsorption ability on metal surface. Therefore, the determination of relation between adsorption and corrosion inhibition is very important. The adsorption of organic molecules at the metal/solution interface takes place through the replacement of water molecules according to following equation [3].

$$Org_{(sol)} + xH_2O_{(ads)} \leftrightarrow Org_{(ads)} + xH_2O_{(sol)} \quad (1)$$

Herein, $Org_{(sol)}$ and $Org_{(ads)}$ are organic molecules in solution and adsorbed on metal surface, respectively. x is the number of water molecules replaced by organic molecules.

Corrosion is an important problem which resulting a terrible waste of both resources and money during the application of metallic materials. Extending the life of equipment could be achieved by controlling corrosion. By doing this, the dissolution of environmentally toxic metals from the components could also be limited. Literature survey shows that the use of organic inhibitors is one of the most practical methods for protection of metals against corrosion. Organic inhibitors act generally by adsorption and a film formation on surface of metals. Their adsorption on metal surface can change the corrosion resistance properties of metals. Organic inhibitors bearing heteroatoms with high electron density such as sulphur, nitrogen, oxygen as well as multiple bonds, which are considered as adsorption centers, are effective inhibitors for the corrosion of metals [4-9].

The purpose of this study is to investigate adsorption of CMMTA on mild steel in 1 M HCl solution and its corrosion inhibition properties. For this aim, electrochemical studies such as E_{ocp}-t, potentiodynamic polarization, EIS and linear polarization resistance (LPR) techniques were used.

2. Experimental

The working electrode was a mild steel specimen, which was cut from a cylindrical mild steel disc to a length of about 5 cm. The mild steel electrode was covered with a polyester block except its only bottom surface, which has 0.785 cm^2 surface area. The surface of the steel was mechanically abraded using different grades of sand papers, which ended with the 1200 grade. Then, the electrodes were washed with distilled water and ethanol, immersed into the ultrasonic bath to remove possible corrosion products or metal particles from the surface, washed once again with ethanol and water. After drying with a filter paper, they were immersed into the test solutions as quickly as.

The test solutions were 1 M HCl solution without and with the addition of 1.0 mM CMMTA, whose chemical structure is given in Fig. 1. The corrosive solutions were opened to atmosphere, and the temperature was controlled thermostatically at 298 K during the electrochemical measurements.

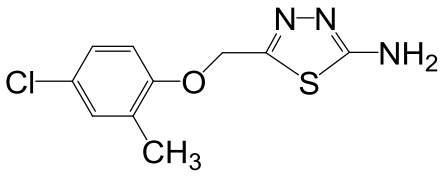

Fig. 1. Chemical structure of CMMTA

The electrochemical measurements were carried out using a CHI 660D A.C. Electrochemical Analyzer under computer control. The experiments were conducted in an electrochemical cell with three-electrode configuration. A platinum sheet with 2 cm^2 surface area and an Ag/AgCl (3 M KCl) were used as the auxiliary and the reference electrodes, respectively. The working electrode was exposed into the test solutions for 1 hour and open circuit potential of the electrode was monitored as a function of exposure time. After this time period, a steady-state open circuit potential (E_{ocp}) was obtained. The EIS experiments were carried out in the frequency range from 100 kHz to 0.01 Hz at E_{ocp} with perturbation amplitude of 0.005 V peak-to-peak. LPR measurements were carried out by recording the electrode potential ±0.010 V around E_{ocp} starting from cathodic potentials with a scan rate of 1 mV s^{-1}. The polarization resistance (R_p) of mild was calculated from the slope of the current-potential curves according to following equation:

$$R_p = \frac{S\mathrm{d}E}{\mathrm{d}i} \qquad (2)$$

In this equation, S is the surface area of the electrode which was exposed to the electrolytes, E is the difference in applied potential and di is the difference in the current.

The potentiodynamic polarization curves were conducted starting from cathodic potentials to the anodic domain with a constant scan rate of 1 mV s^{-1}.

3. Results and discussion

The representative potentiodynamic polarization curves of the mild steel electrode obtained in 1 M HCl solution in the presence of 1.0 mM CMMTA is given Fig. 2. For comparison, that of blank solution was also obtained and presented in the same figure. It can clearly be seen from the figure that addition of the inhibitor to the aggressive solution markedly reduces both anodic metal dissolution reaction and cathodic hydrogen evolution reaction. Corrosion potential of the steel in the absence and presence of CMMTA are nearly remained the same, -0.468 and -0.472 V Ag/AgCl), respectively. Therefore, it can be concluded that CMMTA could be classified as mixed type corrosion inhibitor [10].

Corrosion current densities (i_{corr}) were determined by the extrapolation of the linear portions of the current-potential curves to the corresponding corrosion potentials. The i_{corr} values in the absence and presence of the inhibitor are 0.762 and 0.002 mA cm^{-2}, respectively. The inhibition efficiency (I %) was calculated from the corresponding current densities according to following equation;

$$I\% = \left(\frac{i_{corr} - i'_{corr}}{i_{corr}} \right) x100 \qquad (3)$$

where, i_{corr} and i'_{corr} are corrosion current densities in the absence and presence of the inhibitor, respectively. It was found that this compound has 99.7% inhibition efficiency. The great inhibition efficiency was explained by formation of a protective organic film on the metal surface.

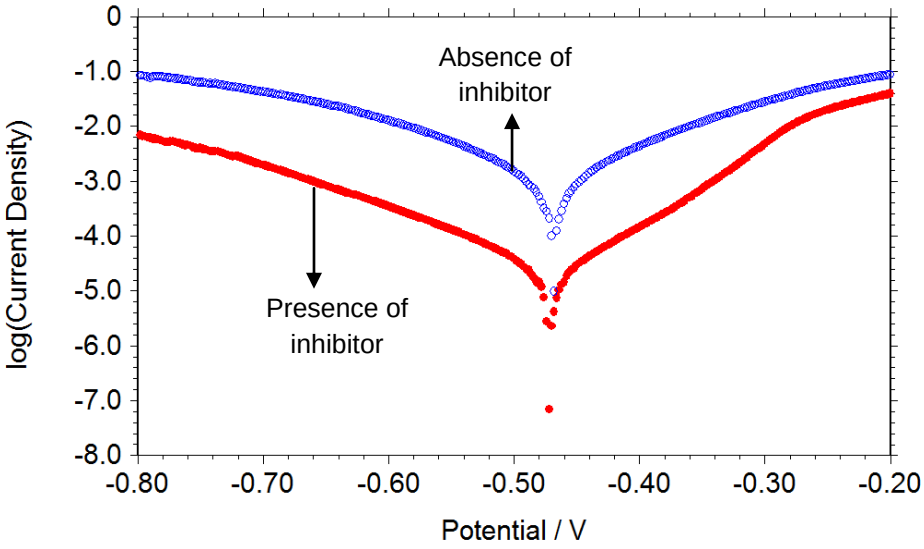

Fig. 2. Potentiodynamic polarization plots of mild steel in 1 M HCl solution in the absence (○) and presence of 1 mM CMMTA (●)

The cathodic current-potential curves in the absence and presence of CMMTA (Fig. 2) are almost giving rise to parallel lines. This observation suggests that the addition of CMMTA to 1 M HCl solution does not modify the hydrogen evolution mechanism, and the reduction of H^+ ions at the mild steel surface take place mainly through a charge transfer mechanism [11, 12].

In contrary to the cathodic inhibition, anodic inhibition reaction was potential-dependent. Although, CMMTA inhibits metal dissolution markedly at lower anodic overpotentials, this effect slightly reduces as the potential was screened to more anodic potentials. This effect more probably arises from the excess dissolution of iron, which leads to removing the film from the metal. The similar results have also been reported in literature for the corrosion inhibition of the metals with the formation of a protective layer of adsorbed inhibitor molecules at the metal surface [13].

The representative Nyquist and log(f)-log(Z) plots of the mild steel electrode obtained in 1 M HCl solution in the absence and presence of the inhibitor are shown in Fig. 3. Nyquist plot of the steel in the absence of the inhibitor shows a capacitive loop at high and low frequencies and followed an inductive loop at low frequencies. The high and medium frequency behaviors suggest that corrosion reaction is charge transfer

controlled [14]. These data are good in agreement with the polarization plots. The low frequency inductive loop could be assigned to the relaxations of corrosion products from the surface. The addition of the organic compound to the solution changes the appearance of the Nyquist plot, which shows only one capacitive loop. The addition of inhibitor does not change the corrosion reaction [15] and reduces dissolution of metal. The diameter of Nyquist plots which corresponds to polarization resistance greatly increases after the addition of the inhibitor. The inhibition efficiency calculated from EIS measurements is around 97.6%. The similar observations could be extracted from the Bode plots.

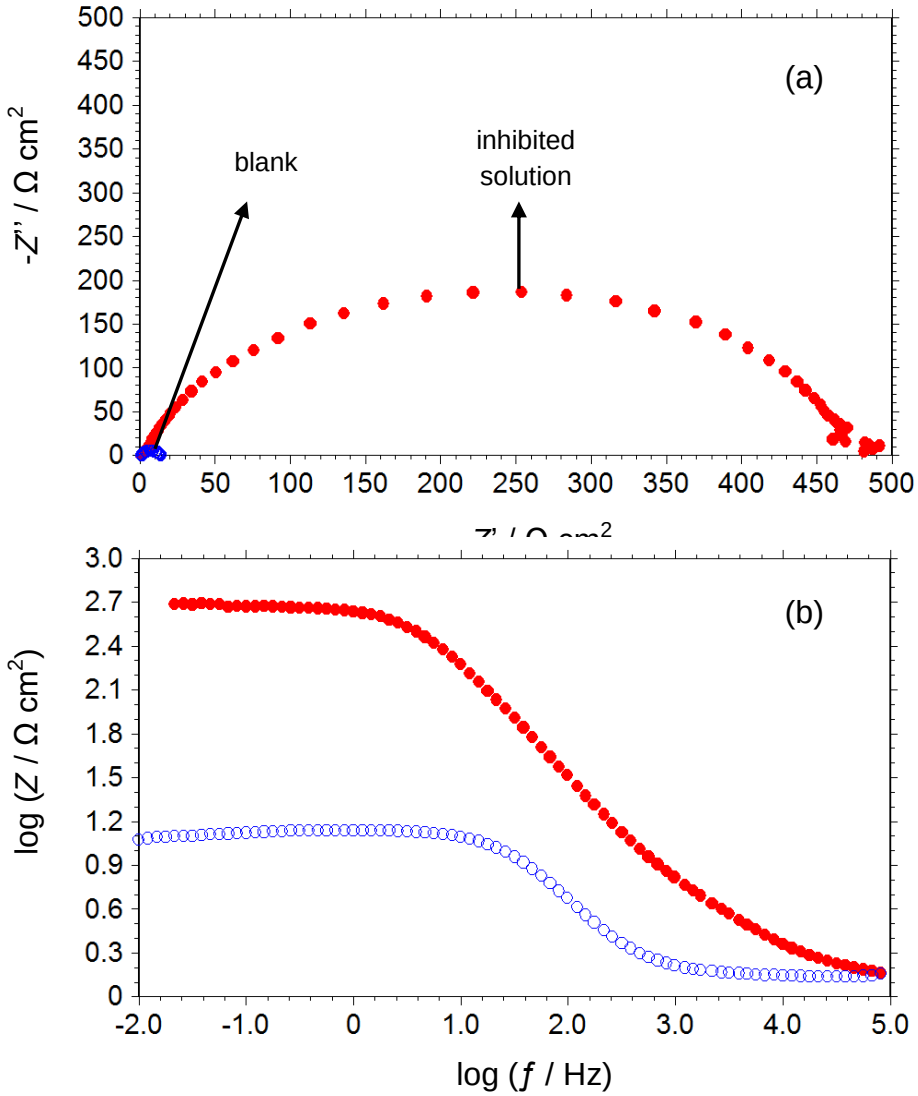

Fig. 3. Nyquist (a) and Bode (b) plots of mild steel in 1 M HCl solution the absence (○) and presence of 1 mM CMMTA (●)

The I % was calculated from polarization resistance (R_p) using the following equation;

$$I\% = \left(\frac{R_p^{'} - R_p}{R_p^{'}} \right) x100 \qquad (3)$$

In this equation, R_p and $R_p^{'}$ are polarization resistance of the steel in the absence and presence of CMMTA, respectively.

The adsorption and corrosion resistance of the inhibitor was also studied with the help of LPR technique using equation 1. The calculated R_p values are 11.5 and 473 Ω cm^{-2}, respectively. The higher R_p value in the inhibited solution indicates great inhibition efficiency, which could be explained by adsorption of CMMTA molecules on the mild steel surface and blocking the surface against the corrosive attack efficiently.

E_{ocp-t} curves of the mild steel specimen in 1 M HCl solution the absence and presence of 1 mM CMMTA (●) are presented in Fig. 4. It can clearly be seen from this figure that the addition of CMMTA to the aggressive solution shifts the E_{ocp} to nobler direction, which is indicative of a protective film formation. E_{ocp} values of the steel in both inhibited and un-inhibited solutions nearly remained constant after 1 h exposure. An initial increase in the absence of the inhibitor could be assigned to dissolution of active metal from the surface.

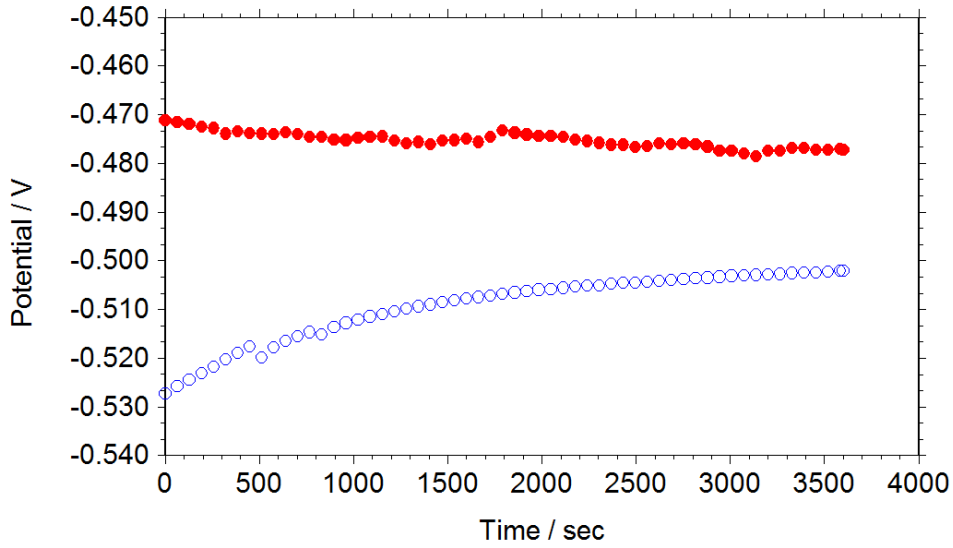

Fig. 4. Chang of open circuit potentials of mild steel in 1 M HCl solution in the absence (○) and presence of 1.0 mM CMMTA (●) as a function of time.

4. Conclusions

Adsorption of 5-((4-chloro-2-methylphenoxy)methyl)-1,3,4-thiadiazole-2-amine (CMMTA) on mild steel surface from 1 M HCl solution and its inhibition efficiency against corrosion were studied using electrochemical methods. From the data obtained, following conclusions could be highlighted;

1. The CMMTA adsorbs on the steel surface from 1 M HCl solution and forms a protective film formation.
2. Formation of the protective film over the surface performs great inhibition efficiency against the corrosion.
3. The inhibitor affects both anodic and cathodic reactions, namely this compound is mixed type corrosion inhibitor.

Acknowledgements

The authors are greatly thankful to Bingöl University Scientific Research Projects (BÜBAP) Coordination Unit and Bingöl University Central Laboratory.

References

[1] M. Özcan, R. Solmaz, G. Kardaş, I. Dehri, Adsorption properties of barbiturates as green corrosion inhibitors on mild steel in phosphoric acid, Colloid Surface A 325, 57 (2008).
[2] O. K. Abiola, Adsorption of 3-(4-amino-2-methyl-5-pyrimidyl methyl)-4-methyl thiazolium chloride on mild steel, Corros. Sci. 3078, 48 (2006).
[3] J.O'M. Bockris, A. K.N. Reddy, Modern Electrochemistry, Volume 2, Published by Plenum Publishing Corporation,, 227 West 17th , Street, New York, 1976.
[4] I.B. Obot, N.O. Obi-Egbedi, S.A. Umoren, Antifungal drugs as corrosion inhibitors for aluminium in 0.1 M HCl, Corros. Sci. 51, 1868 (2009).
[5] R. Solmaz, E. Altunbaş, G. Kardaş, Investigation of adsorption and corrosion inhibition effect of 1,1'-Thiocarbonyldiimidazole on Mild Steel in Hydrochloric Acid Solution, Prot. Met. Phys. Met. 47, 262 (2011).
[6] A. Chetouani, A. Aouniti, B. Hammouti, N. Benchat, T. Benhadda, S. Kertit, Corrosion inhibitors for iron in hydrochloric acid solution by newly synthesized pyridazine derivatives, Corros. Sci. 45, 1675 (2003).
[7] S.A. Abd El Maksoud, Studies on the effect of pyranocoumarin derivatives on the corrosion of iron in 0.5 M HCl, Corros. Sci. 44, 803 (2002).
[8] G. Kardas, R. Solmaz, Electrochemical investigation of barbiturates as green corrosion inhibitors for mild steel protection, Corros. Rev. 24, 151 (2006).
[9] A. Doner, E.A. Sahin, G. Kardaş, O. Serindağ, Investigation of corrosion inhibition effect of 3-[(2-hydroxy-benzylidene)-amino]-2-thioxo-thiazolidin-4-one on corrosion of mild steel in the acidic medium, Corros. Sci. 66, 278 (2013).
[10] L. Li, X. Zhang, J. Lei, J. He, S. Zhang, F. Pan, Adsorption and corrosion inhibition of Osmanthus fragran leaves extract on carbon steel, Corros. Sci. 63, 82 (2012).
[11] M. Lebrini, M. Lagrenee, H. Vezin, L. Gengembre, F. Bentiss, Electrochemical and quantum chemical studies of new thiadiazole derivatives adsorption on mild steel in normal hydrochloric acid medium, Corros. Sci. 47, 485 (2005).
[12] A.Y. Musa, A.A.H. Kadhum, A.B. Mohamad, M.S. Takriff, Experimental and theoretical study on the inhibition performance of triazole compounds for mild steel corrosion, Corros. Sci. 52, 3331 (2010).
[13] F. Bentiss, M. Traisnel, H. Vezin, H.F. Hildebrand, M. Lagrenee, 2,5-Bis(4-dimethylaminophenyı)-1,3,4-oxadiazole and 2,5-bis(4-dimethylaminophenyl)-1,3,4-thiadiazole as corrosion inhibitors for mild steel in acidic media, Corros. Sci. 46, 2781 (2004).
[14] Q.B. Zhang, Y.X. Hua, Corrosion inhibition of mild steel by alkylimidazolium ionic liquids in hydrochloric acid, Electrochim. Acta 54, 1881 (2009).
[15] S. John, A. Joseph, Electro analytical, surface morphological and theoretical studies on the corrosion inhibition behavior of different 1,2,4-triazole precursors on mild steel in 1 M hydrochloric acid, Mater. Chem. Phys. 133, 1083 (2012).

Synthesis and Characterization of Poly(phenols) Containing Naphthalene Unit

Fatma Zehra Yener, İsmet Kaya

Çanakkale Onsekiz Mart University, Faculty of Sciences and Arts, Department of Chemistry, Polymer Analysis Laboratory, 17020 Çanakkale.

E-mail: *fatmazehraynr@gmail.com*

Polymeric materials have a very important place in human life. Space vehicles from auto parts, water pipes of the toy, very soft or hard, or too light are used in the construction of many heavy material. Poly(azomethine)s are known as poly(Schiff base) or polyimines. Classical synthesis mechanism for these polymers primarily based on polycondensation reactions. Dialdehydes or diketons from Schiff base of the polymer entering the condensation reaction with diamines. Although the resulting polymers solubility in organic solvents is weak, thermal properties are very good and used in many fields. These molecules are high of strongly and thermal conductivity because of conjugation and a large number of aromatic heterocyclic in structure. These materials are an attractive class of high-performance polymers that show interesting properties which are associated basically with their conjugated backbone. They have good thermal stability, mechanical strength, nonlinear optical, the ability to form metal chelates, semiconducting, environmental stability, and fibre-forming properties [1].

Derivatives of poly(phenols) containing naphthalene unit were synthesized via chemical oxidative polymerization method of Schiff base of different aromatic aldehydes with 1,5-diaminonaphthalene as the monomers. The structures of monomers and polymers were confirmed FT-IR, ^{1}H-NMR, ^{13}C-NMR, UV-Vis spectral techniques. The characterization was undertaken by GPC, TGA, DSC, SEC, CV and fluorescence analyses. In addition, morphological properties of these compounds were determined with SEM analyses.

Keywords: Schiff base polymers; oxidative polycondensation, azomethine polymers, thermal stability

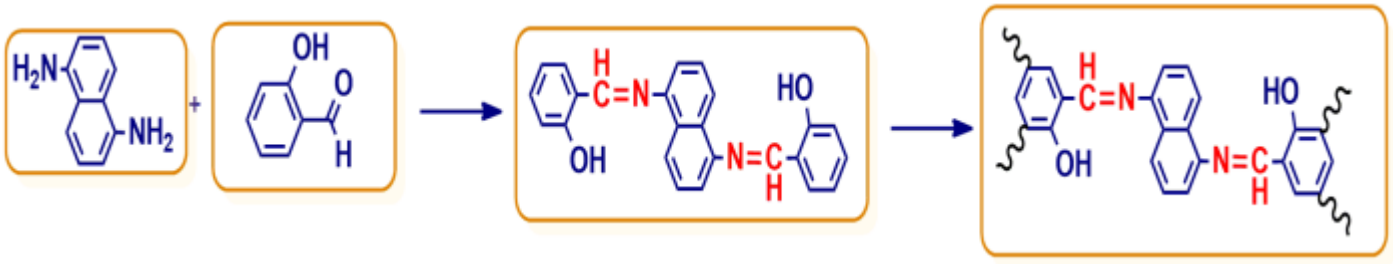

[1] M. Grigoras, G. Stoica, I. Cianga, C.I. Simionescu (1997). Synthesis and characterization of some pyrrole-based aldimine monomers. *Revue Roumaıne de Chimie,* **42(10):** 993-998.

Synthesis, Structural Characterization of Azo-imine Compound and Investigation of Their Electrochemical and Photoluminescence Properties

G. Ceyhan[1], M. Tümer[2]

[1]*Research and Development Centre for University-Industry-Public Relations, Kahramanmaras¸ Sütçü İmam University, 46100, Kahramanmaras¸ Turkey*

[2]*Department of Chemistry, Faculty of Science and Arts, Kahramanmaraş, Turkey*

E-mail: gceyhan@ksu.edu.tr

Synthesis of azo-imine compound with luminescence properties has attracted much attention in recent years due to their importance in designing sensors and optical materials [1]. Azo compound is of interest for application in detection of ions in solution. A new azo ligand has been utilized as chemosensors for anions and cations [2–3] but there are scarcity of luminescent azo ligand which can act as efficient sensors for anions [2]. Mostly, these compounds have heterocycle rings and pharmacologic properties. Schiff bases are interesting compounds because of variety of the biological properties. Antibacterial, anticonsulvant, anti-inflammatory, anticancer, anthihypertansive, antifungal, anti-HIV, hypnotic and herbicidal properties of these compounds were determined. For example, these are silver complexes that used in the scare treatment, zinc antiseptic creams, bizmuth drugs that used in the peptic ulcer and the metal complexes that used as anti-HIV drugs. In this work, photoluminesence and electronic properties of a commercially available diazo compound L8 were studied in detail in several solvents and in the solid state. The molecular structure of the compound was determined by single crystal X-ray diffraction study. Molecular structure of the compound is shown in Figure.

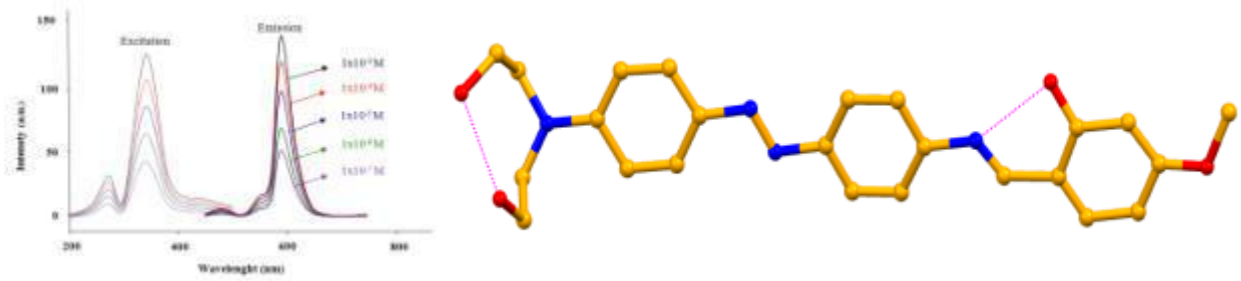

Fig: Crystal structure of L8 with photoluminescence spectrum .

Acknowledgments: We are grateful to Research Council of Turkey (Tubitak Grant number: 115Z065 cost project) for financial support.

References

[1] J. Shinar (Ed.), Organic Light-Emitting Devices: A Survey, Springer-Verlag, NY,(2004).

[2] A. Hens, P. Mondal, K.K. Rajak, Polyhedron 85, 255, (2015).

[3] J. Wang, C.-S. Ha, Tetrahedron 66, 1846, (2010).

Synthesis, Structural Characterization of Organic-Inorganic Hybrids and Investigation of Their Biological Properties

G. Ceyhan[1], F. Tümer[2]

[1]*Research and Development Centre for University-Industry-Public Relations, Kahramanmaras¸ Sütçü İmam University, 46100, Kahramanmaras¸ Turkey*

[2]*Department of Chemistry, Faculty of Science and Arts, Kahramanmaraş, Turkey*

E-mail: gceyhan@ksu.edu.tr

Polyoxometalates (POMs), generally, are polynuclear metal-oxo polyanions that composed of the oxygen and d-group elements in the high oxidation steps (wolfram, molybdenum, vanadium etc.) [1]. Because of their redox properties and magnificent stabilities, POMs have been extensively used in the catalytic reactions as catalyst. In addition to, they have also suitable structural properties for obtaining of the functional materials because of they may obtained in the nano-size and contain a lot of metal atoms. The advantage, the hybrid materials are composed by interaction of the POMs and organic molecules [2]. By modified the side groups in the hybrid materials, the obtained compounds are used for the identification of target biomacromoleculars and extremely important for developing of the drug formulation. In addition to POMs catalytic, magnetic, electronic and nanotechnological applications, their antibacterial, anticancer and antiviral applications are very important [3]. We synthesized a novel bifunctional imine compound and characterized it by the analytical and spectroscopic methods. The electrochemical properties of the compound was investigated in DMSO solution and at different scan rates. The compound showed reversible and irreversible redox potentials in the positive regions. The solution / solid state electronic and photoluminescence spectra of the compound were investigated and different bands determined in its spectra.

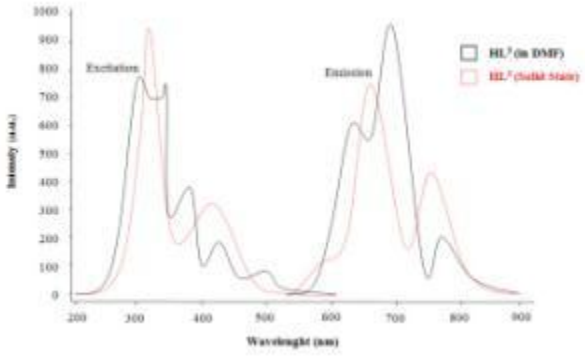

Fig: Photoluminescence spectra of various compounds.

Acknowledgments: We are grateful to Research Council of Turkey (Tubitak Grant number: 115Z065 cost project) for financial support.

References

[1] Mirkhani V., Moghadam M., Tangestaninejad S., Mohammadpoor-Baltork I., Rasouli N. 2008. “Oxidation of alkanes with hydrogen peroxide catalyzed by Schiff base complexes covalently anchored to polyoxometalate”, Catalysis Communications 9 (2008) 2171–2174.

[2] Lin S., Wu Q., Tan H., Wang E., “A new organic–inorganic hybrid based on Mn–salen and decavanadate”, Journal of Coordination Chemistry, 64(21) (2011) 3661–3669.

[3] Eds.: Pope M. T., Muller A. 1994. “Polyoxometalates: from Platonic Solids to Anti-Retroviral Activity”, Kluwer: Dordrecht, The Netherlands, 337-359, 373-387.

Syntheses, Characterizations And Molecular Modelling of Heteronuclear Complexes with 1-Ethylimidazole for Molecular Electronic Applications

G.S. Kürkçüoğlu[1], İ. Kavlak [2]

[1]Department of Physics, Faculty of Arts and Sciences, Eskişehir Osmangazi University, Eskişehir, Türkiye

[2]Department of Physics, Graduate School of Natural and Applied Sciences, Eskişehir Osmangazi University, Eskişehir, Türkiye

E-mail: gkurkcuo@ogu.edu.tr

In this study, 1-ethylimidazole and its tetracyanopalladate(II) complexes containing Zn(II) and Cd(II) ions were investigated of structural, spectral and electric responses properties. The geometrical parameters, vibration wave numbers and transition energies were obtained by x-ray diffractometer, FT-IR and UV-spectrometers, respectively. The obtained experimental data were compared with the effects of theoretical appropriate basis sets. Fundamental vibrations were assigned on the basis of the potential energy distribution (PED) of the vibration modes in the FT-IR and Raman spectra of 1-ethylimidazole and the complexes. Additionally, electronic transition energies and HOMO-LUMO energy levels have been calculated with time depended on density functional theory (TD-DFT) approach. HOMO-LUMO energy levels of the 1-ethylimidazole and the complexes were given in Figure 1. Furthermore, the non-linear optical properties such as the first order hyperpolarizability (β_0) and their related properties (α_0 and Δ_α) were also computed. The charge density distribution of studied compounds and their chemical reactivities have been studied by mapping molecular electrostatic potential surface (MEPs). Mulliken atomic charges, molecular electrostatic potential surfaces, electric response properties and dipole moments, electric multipole moments and polarizability of 1-ethylimidazole and the complexes were calculated by DFT-B3LYP method at LANL2DZ, SDD, CEP-121G basis sets in gaseous phase. A good correlation was found via comparison of the experimental and theoretical data of 1-ethylimidazole and the complexes. As can be seen from Figure 1, we estimate the LUMO and exciton binding energies of a wide range of organic semiconductors.

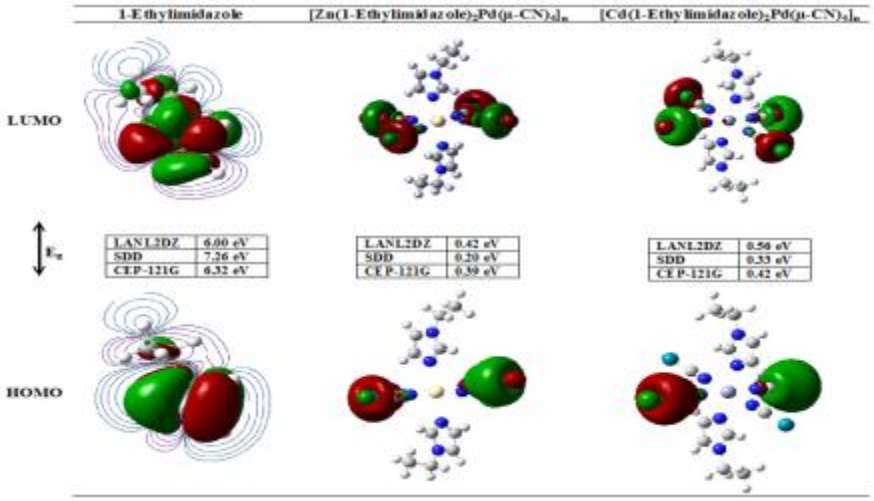

Figure 1. HOMO-LUMO energy levels of 1-ethylimidazole and the complexes.

This work was supported by the Research Fund of Eskisehir Osmangazi University. Project no: 201519047.

Theoretical and Experimental Studies of Molecular Structure and Electronic Transition Energies On PTCDA as Organic Semiconductor

G.S. Kürkçüoğlu[1], İ. Kavlak[2]

[1]*Department of Physics, Faculty of Arts and Sciences, Eskişehir Osmangazi University , Eskişehir, Türkiye*

[2]*Department of Physics, Graduate School of Natural and Applied Sciences, Eskişehir Osmangazi University, Eskişehir, Türkiye*

E-mail: gkurkcuo@ogu.edu.tr

Organic light-emitting diodes (OLEDs) are currently under intense investigation for use in next-generation display technologies. Research into the fundamental properties of the materials used in OLEDs, such as structure and vibration modes, will help provide experimental probes which are required to gain insight into the processes leading to device degradation and failure. Calculations using the hybrid B3LYP functional and the LANL2DZ basis set were carried out assign the FT-IR bands of the perylene-3,4,9,10-tetracarboxylic dianhydride (PTCDA). The ground-state and excited-state geometries were optimized by the DFT method with B3LYP. TD-DFT calculations using the B3LYP functional with the same basis set, associated with the polarized continuum model (PCM) in dichloromethane (CH_2Cl_2) media, were determined to obtain the vertical excitation energies of singlet (S_n) and triplet (T_n) states. Furthermore, HOMO and LUMO energy levels, non-linear optical properties and frontier orbital contours have been investigated by DFT calculations and the comparison with experimental ones. The HOMO and LUMO energy levels of PTCDA were given in Figure 1. As can seen from Figure 1, excellent agreement was found between the theoretical and experimental data. Our calculations provide new interpretation of spectroscopic properties of organic semiconductors critical to optoelectronics.

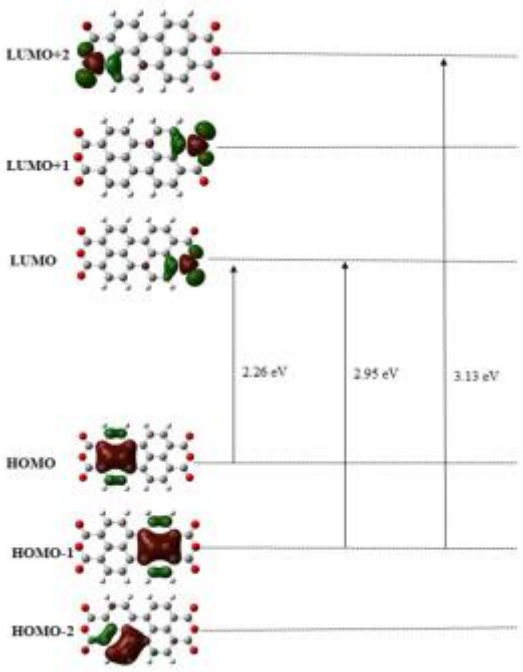

Figure 1. The plot of the HOMO and LUMO energy levels of PTCDA

Spectral, Thermal, Electrical And Magnetic Properties Of Cyanide Complexes Containing Tetracyanonickelate(II) and 2-Pyridinemethanol

G.S. Kürkçüoğlu[1] and E. Sayın[2]

[1]Department of Physics, Faculty of Arts and Sciences, Eskişehir Osmangazi University , Eskişehir, Türkiye

[2]Department of Physics, Graduate School of Natural and Applied Sciences, Eskişehir Osmangazi University, Eskişehir, Türkiye

E-mail: gkurkcuo@ogu.edu.tr

Three new heteropolynuclear cyanide complexes, $[M(H_2O)(hmpH)Ni(CN)_4]_2 \cdot nH_2O$, (M = Fe(II), Co(II) and Ni(II); n = 12 for Fe, 2 for Co and Ni; hmpH = 2-pyridinemethanol) have been synthesized and characterized by elemental, thermal analysis, FT-IR and Raman spectral, electrical conductivity and magnetic susceptibility measurement techniques. General information was acquired about structural properties of the complexes from FT-IR and Raman spectra by considering changes at characteristic peaks of the cyanide, aqua and hmpH ligands. As a result of these analyses, the Ni(II) ion is four coordinated with four cyanide-carbon atoms in a square planar geometry, while the M(II) ions exhibit a distorted octahedral coordination by two different N- and O- atoms from two hmpH ligands, two aqua ligands and six bridging cyanide ligands. Additionally, electrical properties of the complexes are measured by the standard four-point probe method. The magnetic data of the complexes were recorded with Evans method at room temperature. The thermal behaviors of these complexes have been also investigated in the range of 30-1000 °C using TG, DTG and DTA methods. These type complexes are used in the design and construction of magnetic receptors, sensors, electrochromic devices (ECD), organic light emitting diodes (OLED).

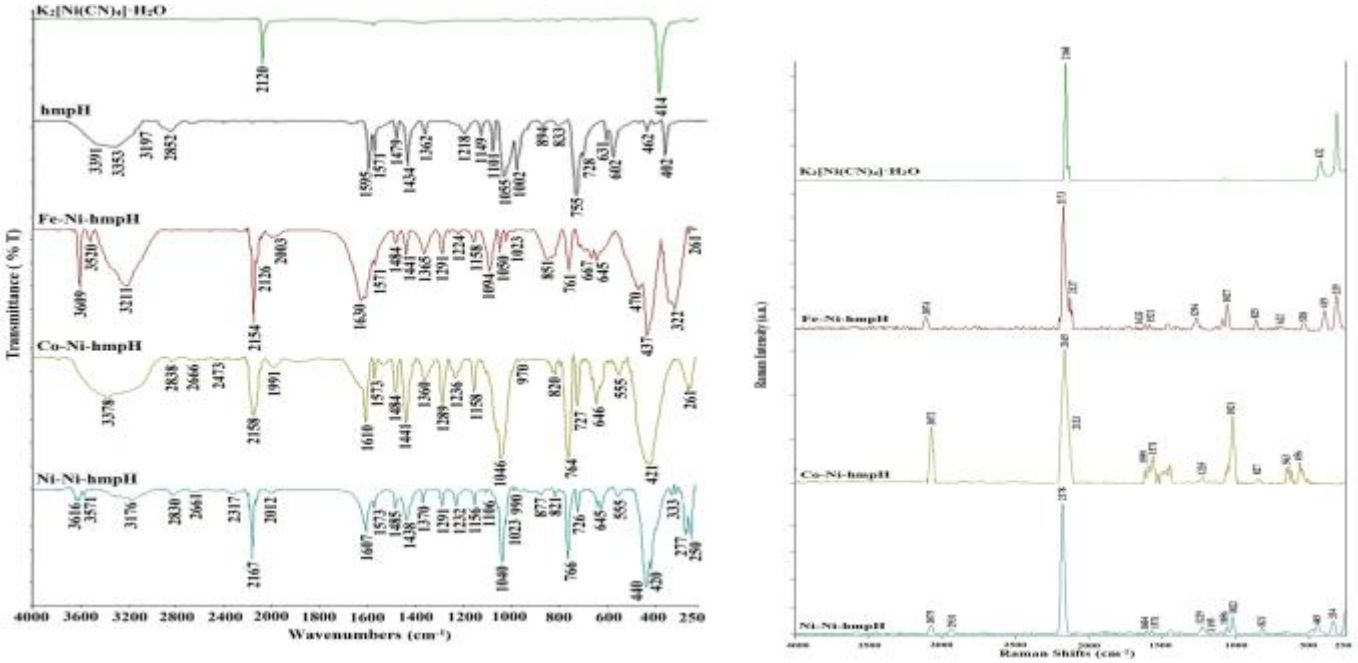

Figure 1. The FT-IR and Raman spectra of the complexes.

Drying Behavior of Poly(4-vinylphenol) (PVP)

H.O. DEMIR[1*], Z. MUTLU[2], A. YILDIRIM[2] and M. CAKMAK[2]

[1]*Department of Chemistry, Faculty of Science and Arts, Kahramanmaraş Sütçü İmam University, 46050 Kahramanmaraş, Turkey*

[2] *Department of Polymer Engineering, University of Akron, 44325-0301, Akron, OH, USA*

E-mail: okkesdemir@gmail.com

Organic field effect transistors (OFETs) have garnered significant interest for use in low cost, lightweight, and flexible electronics compared with conventional inorganic TFTs. One common feature of OFET materials is the inclusion of an aromatic or otherwise conjugated π-electron system, facilitating the delocalization of orbital wave functions. Much of the research effort within the field of flexible OTFTs has focused on the mobility of the semiconductor. However, a great deal of effort is being directed toward generating improved gate dielectrics for low voltage alternatives to silicon-based technologies. The insulator layer, especially the insulator/semiconductor interface, has a significant effect on the performance of OTFTs, because OTFTs operate in the accumulation region and the modulated charge lies within the area (about 10 nm thick) close to the interface. Therefore, many groups have made much effort to improve the interface properties between the dielectrics and the semiconductor. The most common gate dielectrics used in both academia and industry are poly(4-vinylphenol) (PVP) layers (typically 40-600 nm thick).

Based on this background information, we employed birefringence technique to track the structural response of PVP films at molecular level. The drying behavior of poly(4-vinylphenol) in dimethylformamide (DMF) with and associated anisotropy development were determined using a real-time measurement system that tracks weight loss, thickness, in and out of plane birefringence [1]. Initially optically isotropic cast films develop out of plane optical anisotropy below a critical solvent concentration.

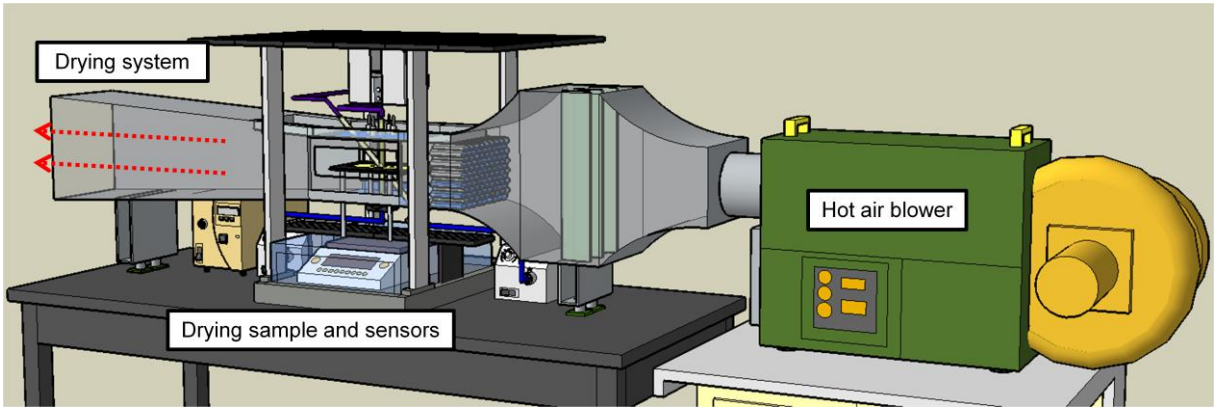

[1] Unsal, E., Drum, J., Yucel, O., Nugay, I. I., Yalcin, B., & Cakmak, M. (2012). *Review of Scientific Instruments*, *83*(2), 025114.

The Fabrication and Analyses of Ni/Poly[3-(1-(2-phenylhydrazono)ethyl)phenol]/*n*-Si Heterojunction using Room Temperature Current-Voltage Characteristics

H.O. Demir[1*], Z. Caldıran[2], K. Meral[3] and S. Aydogan[2]

[1]*Department of Chemistry, Faculty of Science and Arts, Kahramanmaraş Sütçü İmam University, 46050 Kahramanmaraş, Turkey*

[2]*Department of Physics, Faculty of Science, Atatürk University, 25240 Erzurum, Turkey*

[3]*Department of Chemistry, Faculty of Science, Atatürk University, 25240 Erzurum, Turkey*

E-mail: okkesdemir@gmail.com

The field of organic electronics is growing tremendously due to low cost processing and flexibility compared to other conventional inorganic materials. The conjugated polymers are in the heat of this field, in which they have been utilized in the electronics and optoelectronic applications. The known conjugated polymer poly[3-(1-(2-phenylhydrazono)ethyl)phenol] (poly[3-PHEP]) is considered an attractive material because of its active hydroxyl groups [1]. The survey on the literature reveals that no other information on Ni/Poly(3-PHEP)/*n*-Si structure has been reported.

A Ni/Poly(3-PHEP)/n-Si heterojunction was formed by growth of poly(3-PHEP) on *n*-type Si via spin coating film technique and by sputtering of Ni on the polymer coated surface with DC magnetron sputter. Current-voltage measurements of Ni/Poly(3-PHEP)/*n*-Si device performed at room temperature showed nearly ideal rectifying behavior in terms of ideality factor. Thus, the analyses of its experimental current-voltage were carried out by Thermionic Emission (TE) theory. The ideality factor and the barrier height of the device were determined as 1.09 and 0.63 eV, respectively. Furthermore, the barrier height value of the device was calculated as 0.63 eV from Norde method, too. We expect that poly(3-PHEP) as an active material may be a novel candidate for heterojunction applications in future.

[1] H. O. Demir, Journal of Applied Polymer Science, 127(6), 5037-5044 (2013).

Electrical properties of Ag/0.6 wt % nanographene oxide doped poly(vinyl alcohol)/p-Si structures at room temperature

H. Özerli[1], M. G. Aydın[1], İ. Karteri[1] and Ş. Karataş[2]

[1]*Department of Materials Science and Engineering, Kahramanmaras Sutcu Imam University, Kahramanmaraş, Turkey*

[2]*Department of Physics, Kahramanmaras Sutcu Imam University, Kahramanmaraş, Turkey*

E-mail: halilozerli@gmail.com

In present study, we fabricated an Ag/nGO-PVA/*p*-Si heterojunction. The electrical characteristics of the Ag/nGO-PVA/*p*-Si heterojunction structure were investigated by current–voltage (*I–V*) and capacitance-voltage (*C-V*) under dark and illuminated conditions at room temperature. The main parameters such as ideality factors (*n*), barrier heights (Φ_{b0}), series resistances (R_S), and the density of interface states (N_{SS}) have been investigated using current–voltage measurements, in dark and under illumination conditions at room temperature. The difference between the barrier heights obtained from the *I–V* and *C–V* characteristics has been discussed in dark and under illumination conditions. The barrier height, ideality factor and series resistance of the Ag/nGO-PVA/*p*-Si Schottky heterojunction have been also determined using Cheung's and Norde methods. In addition, the interface state density (N_{SS}) as a function of energy distribution (E_{SS}- E_V) was extracted from the forward-bias *I–V* measurements by taking into account the bias dependence of the effective barrier height and series resistance.

[1] İ. Karteri, Ş. Karataş¸ F. Yakuphanoğlu, Appl. Surf. Sci.318, 74 (2014).

[2] E.H. Rhoderick, R.H. Williams, Metal-Semiconductor Contacts. Clarendon, Oxford, 1988.

[3] S.M. Sze, Physics of Semiconductor Devices, second ed.. Willey & Sons, New York, 1981.

Acknowledgements

We would like to thank Kahramanmaraş Sütcü Imam University for financial support of the research program. (Project No: 2015/3-90M). Authors thanks to Kahramanmaraş Sütcü Imam University for financial supporting.

Synthesis, Characterization, Electrical and Dielectric Properties of MWCNT-SiO_2-ZnO Nonocomposite

H. Özerli[1], M. Çaylar[1,2], İ. Karteri[1], S. Uruş[2] and Ş. Karataş[3]

[1]*Department of Materials Science and Engineering, Kahramanmaras Sutcu Imam University, Kahramanmaraş, Turkey*

[2]*Department of Chemistry, Kahramanmaras Sutcu Imam University, Kahramanmaraş, Turkey*

[3]*Department of Physics, Kahramanmaras Sutcu Imam University, Kahramanmaraş, Turkey*

E-mail: halilozerli@gmail.com

Investigation of carbon nanotubes (CNT) has exposed the new nano-material concept. Some of usage area of carbon nano tubes is in the production of electronic circuit elements, military and medical technology. The strength and flexibility of carbon nanotubes make important that the usage of them in nanotechnology engineering for the production of nano-sized structures. In this study, a new diode was chemically synthesized and characterized from a nano-composite structure of MWCNT (multiwalled carbon nanotube)-SiO_2-ZnO/p-Si/Al. FT-IR, XRD, TGA and SEM techniques were used for the characterization of MWCNT-SiO_2-ZnO nano-composite. Besides, electric and dielectric properties of this nano-composite were investigated. Additionally, the properties of current-potential (IV) and capacitance-potential (CV) were studied in detail. According to the results, obtained MWCNT-SiO_2-ZnO nano-composite has an significant properties in electronic technology.

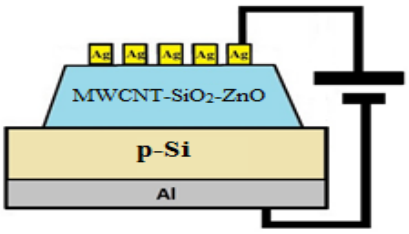

Figure 1. Schematic view of MWCNT-SiO_2-ZnO/p-Si/Al diode.

References:

[1]. Liu Z., Shi Q., Peng F., Wang H., Yu H., Li J., Wei X., Catalysis Communications 22 (2012) 34 – 38.

[2]. Chen X. , Wu X. , Zou J., Liu J., Chen J., Materials Science and Engineering B 176 (2011) 425–430.

[3]. Muleja A.A., Mbianda X.Y., Krause R.W., Pillay K., Carbon 50 (2012) 2741 – 2751.

Acknowledgements

We would like to thank Kahramanmaraş Sütcü Imam University for financial support of the research program. (Project No: 2015/3-90M and 2015/2-13 YLS). Authors thanks to Kahramanmaraş Sütcü Imam University for financial supporting.

Frequency dependent of capacitance-voltage (*C-V*) and conductance-voltage (*G/ω-V*) characteristics of Ag/GO-PVA/p-Si Structure

Merve Gül Aydin[1], İbrahim Karteri[1], Halil Özerli[1] and Şükrü Karataş[1,2]

[1]*Kahramanmaras Sutcu Imam University, Department of Materials Science and Engineering, 46100-Kahramanmaraş, Turkey*

[2]*Kahramanmaraş Sütçü İmam University, Faculty of Sciences and Arts, Department of Physics, 46100-Kahramanmaraş, Turkey*

Email: halilozerli@gmail.com

In this study, the nanographene oxide (nGO) powders were prepared by improved Hummers method and the 0.6 wt% nGO doped poly(vinyl alcohol) (PVA) are successfully prepared and coated onto *p*-Si substrates under various conditions in order to fabricated an Ag/nGO-PVA/p-Si heterojunction. The structure and morphology of as obtained nGO-PVA/p-Si were analyzed through SEM and EDX. Furthermore, it was investigated frequency and voltage dependent electrical and dielectric properties of Ag/GO-PVA/p-Si structure using capacitance-voltage (*C-V*) and conductance-voltage (*G/ω-V*) characteristics in the frequency range 10 kHz–1 MHz in the room temperature. The frequency and voltage dependence of the dielectric constant (ε'), dielectric loss (ε''), dielectric loss tangent ($\tan\delta$) and ac electrical conductivity (σ_{ac}) were calculated from the *C–V* and *G/ω–V* measurements and these figures plotted as a function of frequency.

Acknowledgements

We would like to thank Kahramanmaraş Sütcü Imam University for financial support of the research program. (Project No: 2015/3-90M). Authors thanks to Kahramanmaraş Sütcü Imam University for financial supporting.

Growing of Iron-Doped Copper Oxide Thin Films And Analysis of Electrical And Optical Properties

Murat Tokuş[1], Yusuf Selim Ocak[2,3], Ahmet Tombak[4], Halil Özerli[5] and Şükrü Karataş[5,6]

[1]*Department of Physics, Faculty of Science, Dicle University, Dicle, Turkey*

[2]*Science and Technology Application and Research Center, Dicle University, Diyarbakir, Turkey*

[3]*Dicle University, Faculty of Education, Department of Science, Diyarbakir, Turkey*

[4]*Department of Physics, Faculty of Science, Batman University, Batman, Turkey[2]*

[5]*Department of Materials Science and Engineering, Kahramanmaras Sutcu Imam University, Kahramanmaraş, Turkey*

[6]*Sütçü İmam University, Faculty of Science and Arts, Department of Physics, Kahramanmaraş, Turkey*

Email: *halilozerli@gmail.com*

CuO is a semiconductor which has a direct band gap and promising properties. Its polycrystalline structure has been used for hundreds of years. Copper oxides (CuO) have been extensively studied for applications in sensors, solar cells, photocatalysis and lithium-ion batteries because of certain key properties and functionalities. CuO can be produced by several methods such as chemical vapor deposition, spray technique, vacuum arc deposition and magnetron sputtering.

The crystalline properties of the films were characterised by X-ray diffraction (XRD). The surface morphology of the films was investigated using atomic force microscopy (AFM). The absorbance and transmittance of the undoped and Fe-doped CuO films were measured using a Shimadzu UV–3600 spectrophotometer over 300–1100 nm. The electrical properties of the films were evaluated with the Ecopia HMS–3000 Hall Measurement System using the van der Pauw method at room temperature in a 0.58 T magnetic field. Hall effect measurements established that the films displayed p-type conductivity. The band gaps of the films calculated using Tauc's plots.

Keywords: Cupper Oxide, thin films, doping, optical Properties

Acknowledgements

We would like to thank Kahramanmaraş Sütcü Imam University for financial support of the research program. (Project No: 2015/1-40YLS). Authors thanks to Kahramanmaraş Sütcü Imam University for financial supporting.

Molecular structure, spectroscopic and quantum chemical studies on tris(trimethylsilyl)cyanurate

Hasan Tanak[1]

[1] *Department of Physics, Faculty of Arts and Sciences, Amasya University, 05100 Amasya, Turkey*

E-mail : hasantanak@gmail.com

1,3,5-Triazine and their substituted derivatives have been known for a long period of time. They have found widespread applications in the pharmaceutical, textile, plastic, and rubber industries, and are used as pesticides, dyestuffs, optical bleaches, explosives, and surface active agents [1]. They have electron-transporting behavior and utilization in organic light-emitting diodes [4]. They also possess π-interaction abilities and can be involved in intricate H-bond networks for applications in organic and supramolecular chemistry [2]. As s-triazine and tri-s-triazine derivatives attracted attention, tris(trimethylsilyl)cyanurate and its analog tris(trimethylsilyl)cyamelurate are used as precursors to synthesize versatile organic-inorganic hybrid polymers through sol-gel transitions [3].

In this study, the molecular structure, vibrational spectra and assignments, ^{13}C and ^{29}Si NMR spectra, molecular electrostatic potential and frontier molecular orbital energies have been investigated on tris(trimethylsilyl)cyanurate using the densitiy functional theory calculations.

Acknowledgment, this study was supported financially by the Research Centre of Amasya University (Project No: FMB-BAP 16-0175).

[1] G. Blotny, Recent applications of 2,4,6-trichloro-1,3,5-triazine and its derivatives in organic synthesis, Tetrahedron 62, 9507 (2006).

[2] N.E.A. El-Gamel, J. Brand and E. Kroke, Synthesis, spectroscopic characterization, and X-ray crystal structure of tris(trimethylsilyl)cyanurate, J. Coord. Chem. 62, 1278 (2009).

[3] N.E.A. El-Gamel, M. Schwarz, E. Brendler and E. Kroke. s-Triazine and tri-s-triazine based organic-inorganic hybrid gels prepared from chlorosilanes by exchange reactions, Chem. Commun., 45, 4741 (2006).

DFT computational studies of Benzyl 2-methyl-3-[(*E*)-(thiophen-2-yl)methylidene]

Hasan Tanak[1]

[1] *Department of Physics, Faculty of Arts and Sciences, Amasya University, 05100 Amasya, Turkey*

E-mail : hasantanak@gmail.com

Schiff bases having imine groups (C = N) and benzene rings in the main chain alternately, and being π-conjugated, exhibit interest as materials for wide spectrum applications, particularly as corrosion inhibitors, catalyst carriers, metal ion complexing agents and thermo-stablematerials [1]. Many Schiff bases are known to be medicinally important and are used to design medicinal compounds. They are known to exhibit anticonvulsant, antiinflammatory activities. In addition some Schiff bases show pharmacologically useful activities like anticancer, anti-hypertensive and hypnotic activities, anti-tuberculosis, antifeedant etc. Schiff bases belongs to a widely used group of organic intermediates important for production of specially chemicals, e.g. pharmaceutical or rubber additives, as amino protective groups in organic synthesis. They also have used as liquid crystals, in analytical, medical and polymer chemistry [2].

In this study, the molecular structure, atomic charges, molecular electrostatic potential and frontier molecular orbital energies have been investigated of Benzyl 2-methyl-3-[(*E*)-(thiophen-2-yl)methylidene]dithiocarbazate using the densitiy functional theory calculations.

Acknowledgment, this study was supported financially by the Research Centre of Amasya University (Project No: FMB-BAP 15-091).

[1] H. Tanak, Molecular structure, spectroscopic (FT-IR and UV-Vis) and DFT quantum-chemical studies on 2-[(2,4-Dimethylphenyl)iminomethyl]-6-methylphenol, Mol. Phys. 112, 1553 (2014).

[2] O.G. Bhusnure, S.B. Zangade, S.B. Chavan, Y.B. Vibhute, Comparative study of conventional and microwave assisted synthesis of novel Schiff bases and their antimicrobial screenings, J. Chem. Pharm. Res. 2, 234 (2010).

Electrodeposition of CuInS ternary thin film: Deposition Potential and Time Effect on Optical Properties

H.Yildirim, A. Peksoz

Department of Physics, Faculty of Sciences and Arts, Bursa, Turkey

E-mail :yildirim84hasan@gmail.com

CuInS ternary thin films were successfully grown on indium thin oxide (ITO) coated glass substrate at the room temperature. The deposition bath consisted of aqueous solutions of 10 mM $CuCl_2$, 20 mM $InCl_3$, 20 mM $Na_2S_2O_3$ as precursors, and 200 mM LiCl. The pH of the electrolyte was adjusted to 2.0 using HCl. Cyclic voltammograms were carried out to characterize using a standard three-electrode cell. The voltammogram of the deposition bath were recorded applying a scan rate of 20 mV/s (Figure 1). Three different CIS films were produced by chronoampermetry technique: First film was produced at a cathodic potential of -1.1 V for a deposition time of 10 min, second film was at -0.9V for 5 min, and third film was at -0.25 V for 2.5 min and -1.1 V for 2.5 min. The produced CIS films exhibited p-type semiconductor properties. The band gap values of the films were calculated to be 1.52, 1.41 and 1.45 for the first, second and third film respectively.

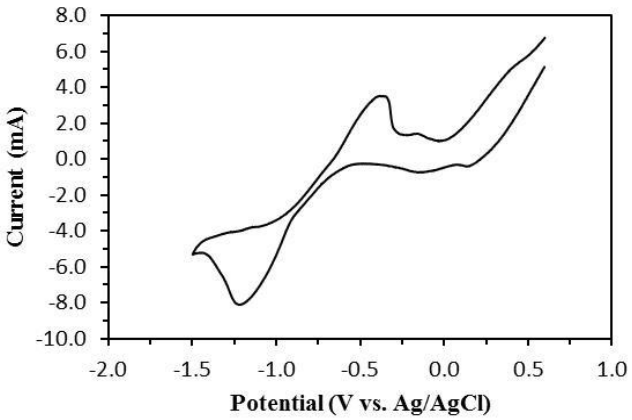

Figure 1. Cyclic voltammogram of the solution consist of 10 mM $CuCl_2$, 20 mM $InCl_3$, 20 mM $Na_2S_2O_3$ and 200 mM LiCl.

A compare study on dielectric properties, electric conductivity and electrical modulus of Au/n-SiC structures with three different thickness interfacial (Zn-dopped PVA) layers as function of thickness and frequency at room temperature

Havva Elif Lapa[1], Mohammad Hussein Ali Al-Dharob[1], Ali Kökce[1], Ahmet Faruk Özdemir[1], İbrahim Uslu[2], Şemsettin Altındal[3]

[1]Department of Physics, Faculty of Sciences and Arts, Süleyman Demirel University, Isparta, TURKEY

[2]*Department of Chemistry Education, Faculty of Education, Gazi University, Ankara, TURKEY*

[3]*Physics Department, Faculty of Sciences, Gazi University, Ankara, TURKEY*

E-mail:elif_l87@hotmail.com

Au/n-SiC organic structures with three different thickness interfacial (Zn-dopped PVA) layers (50, 150 and 500 nm) which are coated by electro-spinning method were fabricated. The frequency and interfacial layer thickness dependence dielectric constant (ε'), dielectric loss (ε''), loss tangent (tanδ), real (M') and imaginary (M'') components of the complex electrical modulus and electrical conductivity (σ_{ac}) of these structures have been investigated and compared in the frequency range of 1kHz-500kHz at room temperature. All these parameters were calculated from the capacitance (C) and conductance (G/ω) data in the accumulation region. Experimental results show that all these parameters were found a strong function of frequency and thickness relatively at low frequencies. While the values of ε' and ε'' decrease with increasing frequency almost exponentially, σ_{ac} increases especially at high frequency. The change in σ_{ac} with frequency at low and intermediate frequencies was corresponding to the dc conductivity and at ac conductivity, respectively. The double logarithmic σ vs f plots for three samples have three distinct linear regimes with different slopes and it is evident that there exist three different conduction mechanisms which corresponding to the low, intermediate and high frequency regions, respectively. In order to determine of the conduction and polarization mechanisms, the values of M' and M'' versus frequency were also calculated from the ε' and ε'' data for each sample and they were quite sensitive to frequency and thickness.

Keywords: Au/n-SiC (MS) structures (Zn-dopped PVA) interfacial organic layer; Impedance spectroscopy; Frequency and thickness dependences; Dielectric properties and electric modulus.

On the dielectric relaxation, electric modulus and ac electrical conductivity usingimpedance spectroscopy method in Au/Zn-dopped PVA/ n-SiC (MPS) organic structures

Havva Elif Lapa[1], Mohammad Hussein Ali Al-Dharob[1], Ali Kökce[1], Ahmet Faruk Özdemir[1], İbrahim Uslu[2], Şemsettin Altındal[3]

[1] Department of Physics, Faculty of Sciences and Arts, Süleyman Demirel University, Isparta, TURKEY

[2] *Department of Chemistry Education, Faculty of Education, Gazi University, Ankara, TURKEY*

[3]*Physics Department, Faculty of Sciences, Gazi University, Ankara, TURKEY*

E-mail:elif_l87@hotmail.com

Dielectric, electric modulus and ac electrical conductivity properties of the Au/Zn-dopped PVA/ n-SiC (MPS) organic structures were investigated by using impedance spectroscopy in a wide frequency and applied bias voltage ranges at room temperature. The frequency and voltage dependence of forward and reverse bias capacitance-voltage (*C*-*V*) and conductance-voltage (G/ω-*V*) data are analyzed in the framework of conductivity and electric modulus formalisms. Both these formalisms show qualitative similarities in relaxation time and surface states (N_{ss}). The values of dielectric constant (ε'), dielectric loss (ε''), dielectric loss tangent (tanδ), real and imaginary parts of electric modulus (M' and M'') and ac electrical conductivity (σ_{ac}) were found considerably sensitive both to the frequency and applied bias voltage in depletion region. The observation peaks in the tanδ, M' and M'' versus V plots especially at low and intermediate frequencies was attributed to the dielectric relaxation processes. Changes in these parameters with frequency are quite large at low and intermediate frequencies due to the charges at surface states (N_{ss}) and their relaxation times, surface and dipole polarizations. It is clear that the surface and dipole polarizations can be more easily occur at low frequencies and the majority of charges at surface states between (Zn-dopped PVA) and n-SiC contributes to the deviation of dielectric properties of Au/Zn-dopped PVA/n-SiC (MPS) organic structures.

Keywords: Au/Zn-dopped PVA/n-SiC (MPS) structures; Impedance spectroscopy method; Frequency and voltage dependences; Dielectric relaxation; Electric modulus and conductivity.

Current-Conduction Mechanisms (CCMs) in Au/ZnO/n-Si Schottky Barrier Diodes in Wide Temperature Range

[1]YosefBadali, [2]Gamze Kaya, [3]Afsoun Nikravan, [4]Şemsettin Altındal, [5]İbrahim Uslu

[1]Department of Advanced Technologies, Institute of Science and Technology, Gazi University, Ankara, Turkey

[2]Department of Chemistry, Institute of Science and Technology, Gazi University, Ankara, Turkey

[3]Department of Environmental Engineering, Institute of Science, Hacettepe University, Ankara, Turkey

[4]Department of Physics, Faculty of Science, Gazi University, Ankara, Turkey,

[5]Department of Chemistry Education, Gazi Faculty of Education, Gazi University, Ankara, Turkey

profibrahimuslu@gmail.com

Current-voltage (I-V) characteristics of Au/ZnO/n-Si SBDs have been investigated in the temperature range of 80-400 K with 20 K steps. Here, zinc oxide (ZnO) has been used as an interfacial layer between metal and semiconductor. The reverse saturation current (I_o), ideality factor (n), zero-bias barrier height (Φ_{Bo}) were determined from the forward bias I-V data and they were found a strong function temperature. The values of Φ_{Bo} increase with the increasing temperature whereas the value of n decrease. An abnormal decrease in the Φ_{Bo} and increase in the n with decreasing attempted to draw Φ_{Bo} versus q/2kT plots to obtain evidence of a Gaussian distribution (GD) of the barrier heights (BHs). The mean values of BH and standard deviation (δs) were found as 1.156 eV and 0.167 V for region I (220-400 K) and 0.526 eV and 0.072V for region II (80-200 K), respectively. Hence, it has been concluded that the temperature dependent of the forward bias I-V characteristics of Au/ZnO/n-Si SBD can be successfully explained on the basis of TE theory with double GD of the BHs between metal and semiconductor. In very recently, similar results have been reported in the literature [1-4].

References

[1] A. Kumar, S. Vinayak, R. Singh, Current Applied Physics, 13 (2013) 1137.

[2] H. Tecimer, A. Türüt, H. Uslu, Ş. Altındal, İ. Uslu, Sensors and Actuators A: Physical, 199 (2013) 194.

[3] E. Marıl, A. Kaya, H.G. Çetinkaya, S. Koçyiğit, Ş. Altındal, Material Science in Semiconductor Processing, 39 (2015) 332.

[4] B. Prasanna Lakshmi, M. Siva Pratap Reddy, A. Ashok Kumar, V. Rajagopal Reddy, Current Applied Physics, 12 (2012) 765.

Influence Of Frequency And Applied Voltage On Dielectric Properties, Electric Modulus And Electrical Conductivity In Ag/%3Ru doped PVP/n-Si Structures

[1]Gamze Kaya, [2]YosefBadali, [3]Afsoun Nikravan , [4]Şemsettin Altındal, [5]İbrahim Uslu

[1]Department of Chemistry, Institute of Science and Technology, Gazi University, Ankara, Turkey

[2]Department of Advanced Technologies, Institute of Science and Technology, Gazi University, Ankara, Turkey

[3]Department of Environmental Engineering, Institute of Science, Hacettepe University, Ankara, Turkey

[4]Department of Physics, Faculty of Science, Gazi University, Ankara, Turkey,

[5]Department of Chemistry Education, Gazi Faculty of Education, Gazi University, Ankara, Turkey

profibrahimuslu@gmail.com

In this study, the frequency and voltage dependence of dielectric constant (ε'), dielectric loss (ε'), loss tangent (tanδ), ac electrical conductivity (σ_{ac}), real and imaginary parts of electric modulus (M' and M'') of Ag/%3Ru doped PVP /n-Si structures have been investigated in the wide frequency range of 0.5 kHz-5 MHz by using impedance spectroscopy method which is including

A set of capacitance/conductance-voltage-frequency(C-V and G/ω-V) plots. There was observed a large dispersion in the C-V and G/ω-V plots due to the existence of surface states (N_{ss}), interfacial organic layer and between metal and semiconductor. Surface and dipole polarization especially at low frequencies. Thus, similar results were also observed the dielectric observed and electric modulus as function of frequency. In the other words, both the obtained experimental results confirmed that the all of these parameters are strong function of frequency and voltage. In addition, the values of ε', ε'' and tanδ show a steep decrease with increasing frequency for each forward bias voltage, whereas the values of σ_{ac} increase with increasing frequency. As a result, the change in the ε', ε", tanδ, M', M" and σ_{ac} is a result of restructuring and reordering of charges at M/S interface under external electric field.

Keywords*:* Ag/%3Ru doped PVP/n-Si (MPS) structure; Impedance spectroscopy method; Dielectrical relaxation; Electric modulus and conductivity

Illumination intensity effects on the electrical characteristics of Al–TiW–Pd2Si/n-Si Schottky structures

İlbilge Dökme

Department of Science Education, Gazi Education Faculty, Ankara/Turkey

ilbilgedokme@gazi.edu.tr

The thin film of TiW alloy was deposited on Pd_2Si–n-Si to form a diffusion barrier between aluminum (Al) and Pd_2Si–n-Si as distinct from conventional metal–Si compounds–n-Si structures. Illumination intensity effects on the electrical characteristics of fabricated Al–TiW–Pd_2Si/n-Si Schottky structures have been investigated in this study. The electrical parameters such as ideality factor (n), zero-bias-barrier height (Φ_{B0}), series resistance ($_{Rs}$), depletion layer width (W_D) and dopping concentration (N_D) of Al–TiW–Pd_2Si/n-Si Schottky barrier diodes (SBDs) have been investigated by using the forward and reverse bias current–voltage (I–V), capacitance–voltage (C–V) and conductance–voltage (G/ω-V) measurements in dark and under illumination conditions at room temperature. The values of C and G/ω increase with increasing illumination intensity due to the illumination induced electron–hole pairs in the depletion region. The density of interface states (N_{ss}) distribution profiles as a function of ($E_c - E_{ss}$) was extracted from the forward I–V measurements by taking into account the bias dependence of the effective barrier heights (Φ_e) for device in dark and under various illumination intensities. The high values of N_{ss} were responsible for the nonideal behavior of I–V, C–V and G/ω characteristics. The values of Rs obtained from Cheung and Nicollian methods decrease with increasing illumination intensity. The high values of n and R_s have been attributed to the particular distribution of N_{ss}, surface preparation, inhomogeneity of interfacial layer and barrier height at metal/semiconductor (M/S) interface. As a result, the characteristics of Schottky barrier diodes are affected not only in N_{ss} but also in R_s, and these two parameters strongly influence the electrical parameters.

The frequency and voltage dependent electrical characteristics of Al-TiW-Pd2Si/n-Si structure

İlbilge Dökme

Department of Science Education, Gazi Education Faculty,Ankara/Turkey

ilbilgedokme@gazi.edu.tr

The forward and reverse bias capacitance–voltage (*C*-*V*) and conductance–voltage (*G*/*w*-*V*) characteristics of Al-TiW-Pd_2Si/n-Si structures have been investigated over a wide frequency range of 5 kHz – 5 MHz. These measurements allow to us the determination of the interface states density (N_{ss}) and series resistance (R_s) distribution profile. The effect of R_s on *C* and *G* is found noticeable at high frequencies. The *C*-*V*-*f* and *G*/*w*-*V*-*f* characteristics of studied structures show fairly large frequency dispersion especially at low frequencies due to N_{ss} in equilibrium with the semiconductor. The N_{ss} profile was obtained both forward bias current-voltage (*I*-*V*) and low frequency (C_{LF})-high frequency (C_{HF}) method. In addition, the energy distribution of N_{ss} was obtained from the forward bias *I*-*V* characteristics by using into account the bias dependent of the ideality factor and effective barrier height (Φ_e). The plot of series resistance vs voltage for the low frequencies gives a peak, decreasing with increasing frequencies. The frequency dependent *C*-*V* and *G*/*w*-*V* characteristics confirm that the R_s and N_{ss} of the Al-TiW-Pd_2Si/n-Si structures are important parameters that strongly influence the electric parameters in device.

Keywords: MS structure; frequency dependent; interface states; series resistance; Pd_2Si/n-Si contacts

Electrical characteristics of Al/p-Si structures with two different thickness TiO2 interfacial insulator layer

İlbilge Dökme

Department of Science Education, Faculty of Gazi Education, Ankara, Turkey

ilbilgedokme@gazi.edu.tr

The purpose of present study was to fabricate the Metal/Insulator/Semiconductor (MIS) with two different thickness titanium dioxide (TiO_2) interfacial layer and determine electrical characteristics of them. The current-voltage (*I-V*), capacitance-voltage (*C-V*) and conductance-voltage (*G/w-V*) were measured for fabricated two Al/TiO_2/p-Si electronic structures. Device parameters such as ideality factor (*n*), saturation current (I_o), zero bias barrier height (Φ_B), series resistance (R_s), interface states density (N_{ss}) were calculated from *I-V* data. The change of *C-V* ve *G/w-V* with frequency was analyzed and some atomic and electrical parameters calculated from these data. It is found that interfacial layer thickness influenced interface states density profile and series resistance. Moreover, diode parameters are very sensible the thickness of interfacial layer.

Keywords: MIS structure; interface states; series resistance; TiO_2 interface layer

Frequency and gate voltage effects on the dielectric properties and electrical conductivity of Al/TiO_2/p-Si structures

İlbilge Dökme

Department of Science Education, Faculty of Gazi Education, Ankara, Turkey

ilbilgedokme@gazi.edu.tr

Dielectric properties and electrical conductivity of Al/TiO_2/p-Si metal-Insulator-Semiconductor (MIS) structures in the frequency range of 10 kHz-5 MHz and gate voltage range of (-4 V)-(4 V) have been investigated in detail by using experimental *C-V* and *G/w-V* measurements. Also, the imaginary part of electric modulus (M″) shows a peak and the peak position shifts to higher frequency with increasing applied voltage. Experimental results indicate that the dielectric constant (ε') and dielectric loss (ε'') are almost found to decrease while the ac electrical conductivity (σ_{ac}) and the real part of electric modulus (M′) increase with increasing frequency. It can be concluded that the interfacial polarization can be more easily occurred at low frequencies, and the majority of interface states at metal semiconductor interface, consequently contributes to deviational of dielectric properties of Al/TiO_2/p-Si structures. In addition the results indicated that the interfacial polarization can be more easily occurred at low frequencies.

Keywords: MIS structure; frequency dependent; dielectric; Al/TiO_2/p-Si

Ab-initio calculations of semiconductor LiScGe compound

Y.Ö. Çiftci[1] and İ.Ö. Alp[2]

[1,2]Gazi University, Department Of Physics, Ankara, TURKEY

E-mail: iremoner@gazi.edu.tr

Semiconducting ternary half-Heusler (HH) compounds with narrow band gaps have turned out to be an important class of materials in recent years due to their wide range of interesting physical properties (e.g. high melting point, large thermal conductivity, large thermopower and unusual magnetic properties, etc.) [1]. They crystallize in MgAgAs structure with the *F*43m space group. In this study, we focus on structural, electronic, elastic, lattice dynamic and optic properties of LiScGe using *ab-initio* density-functional theory (DFT) within the generalized gradient approximation (GGA) for the exchange-correlation potential. Our computed structural results are in reasonable agreement with the literature. The band gap of this compounds is predicted to be 0.78 eV (see Fig.1). Our elastic results prove that this compound are mechanically stable. The obtained phonon spectra for LiScGe does not exhibit any significant imaginary branches of the phonon spectrum. Further analysis of the optical response of the dielectric functions, optical reflectivity, refractive index, extinction coefficient and electron energy loss delves into for the energy range of 0–30 eV.

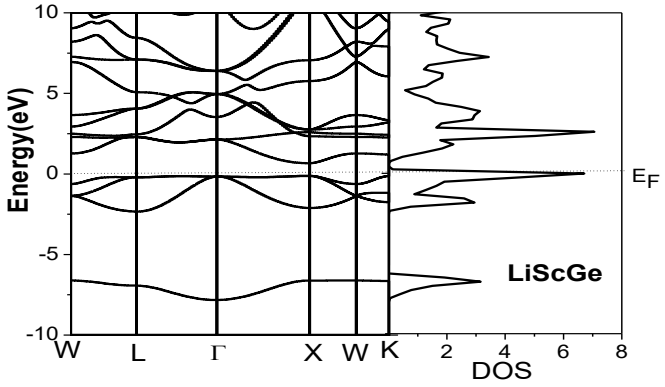

Figure 1. Calculated electronic band structure and density of states for LiScGe

[1] P. Larson, S.D. Mahanti, S. Sportouch and M. G. Kanatzidis, Electronic structure of rare-earth nickel pnictides: Narrow-gap thermoelectric materials, Phys. Rev. B 59, 15660 (1999).

Synthesis of polyfluoro substituted new Co(II), Fe(II) phthalocyanines and their usage as catalysts for aerobic oxidation of benzyl alcohol

Ayşe Aktaş[1], İrfan Acar[2], Ece Tuğba Saka[1], Zekeriya Bıyıklıoğlu[1]

[1] *Department of Chemistry, Karadeniz Technical University, Trabzon, Turkey*

[2] *Department of Energy Systems Engineering, Karadeniz Technical University, Trabzon, Turkey*

acar_irfan_2000@yahoo.com

The investigations on phthalocyanine compounds have been increased owing to their fascinating applications areas such as molecular conductors and semiconductors, nanotechnology, gas sensors, liquid crystals, photosensitizers in photodynamic therapy and catalysis. It is main importance to synthesize target compounds which achieved by attaching suitable functional groups to peripheral or non-peripheral position to phthalocyanine ring and various metal ion inserted Pc core [1,2]. Catalytic oxidation of benzyl alcohol (BzOH) to benzaldehyde (BzH) has attracted much attention both in the laboratory and in the chemical industry [3,4]. In this study, novel metallophthalocyanine complexes (Co and Fe) were synthesized using the phthalonitrile derivative. All proposed structures were supported by using spectroscopic methods. In this contribution, the influence of different parameters on the oxidation of benzyl alcohol with Co(II) and Fe(II) phthalocyanine catalysts were systematically investigated. The optimal conditions were determined for benzyl alcohol oxidation. The advantage of this method compared to other methods that the phthalocyanine complexes act active catalysts at a lower temperature which may cause the benzyl alcohol conversion.

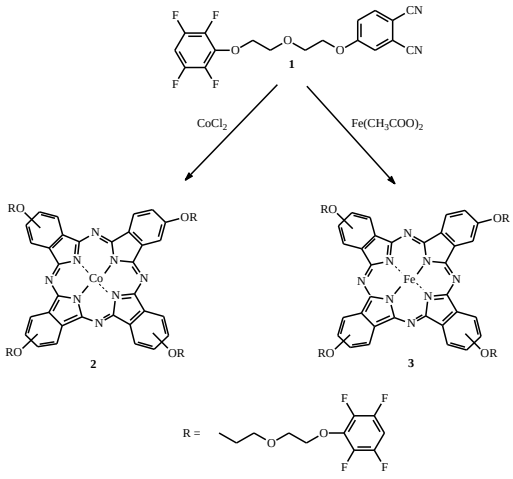

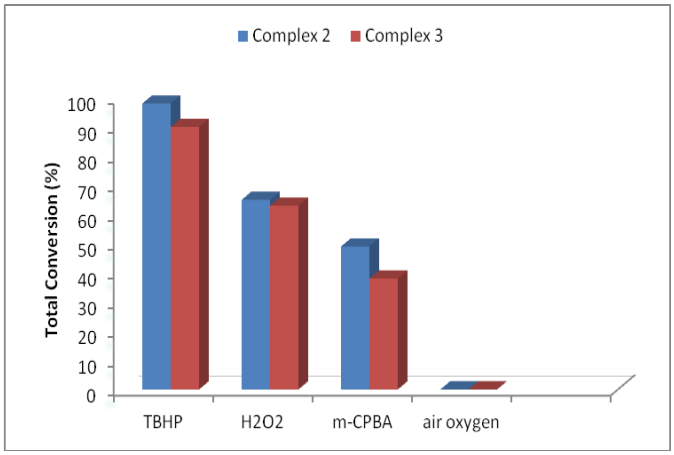

[1] T. Inabe, K. Morimoto, Wide variety of dimensionality in phthalocyanine based molecular conductors, Synth. Met. 86, 1799 (1997).

[2] O. M. Bankole, J. Britton, T. Nyokong, Photophysical and non-linear optical behavior of novel tetra alkynyl terminated indium phthalocyanines: Effects of the carbon chain length, Polyhedron 88, 73 (2015).

[3] R.A. Sheldon, J.K. Kochi, Metal-Catalyzed Oxidation of Organic Compounds (Academic, New York, 1981).

[4] S. Tsuruya, H. Miyamoto, T. Sakae, M. Masai, Oxidation of benzyl alcohol over Co(II)NaY zeolites, J. Catal. 64, 260 (1980).

Peripherally tetra-{2-(2,3,5,6-tetrafluorophenoxy)ethoxy} substituted cobalt(II), iron(II) metallophthalocyanines: synthesis and their electrochemical, catalytic activity studies

Ayşe Aktaş[1], İrfan Acar[2], Zekeriya Bıyıklıoğlu[1], Ece Tuğba Saka[1]

[1] *Department of Chemistry, Karadeniz Technical University, Trabzon, Turkey*

[2] *Department of Energy Systems Engineering, Karadeniz Technical University, Trabzon, Turkey*

acar_irfan_2000@yahoo.com

Phthalocyanines (Pcs) having conjugated 18 π electron system, exhibit growing attention as a subject for their excellent physical and chemical properties which highly resist to heat, light, non-oxydizing acids and bases. Unsubstituted phthalocyanines are insoluble in organic solvents. Especially, fluorinated metallophthalocyanines are known good solubility different solvent for example polar and apolar solvents [1,2]. Fluorine substituted phthalocyanines affect the electronic structure, reactivity and application of phthalocyanines [3]. In this study, new Co^{II} Pc and Fe^{II} Pc have been synthesized for the first time and their structures have been characterized by using IR, ^{1}H NMR, mass and UV–Vis spectroscopy techniques. Electrochemical properties of Fe^{II}Pc and Co^{II}Pc were investigated by using cyclic voltammetry (CV) and square wave voltammetry (SWV) techniques. Also Co(II) and Fe(II) phthalocyanine complexes (2, 3) were examined as a catalyst for the oxidation of benzyl alcohol with changing different parameters to determine the optimal conditions.

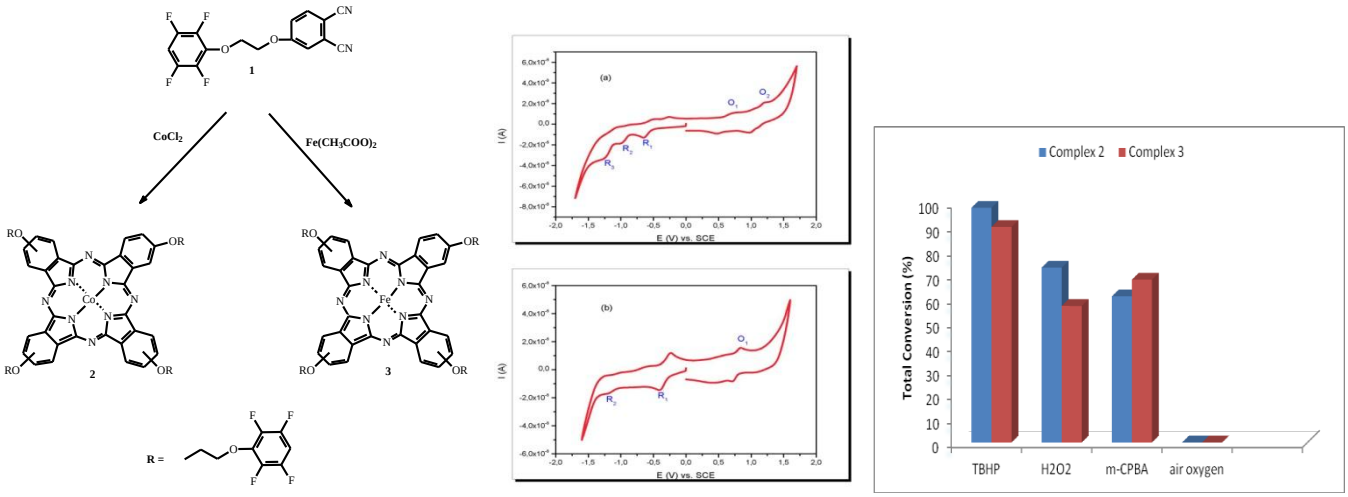

[1] C. C. Leznoff, A. B. P. Lever Mc Keown, Phthalocyanines: properties and applications, VCH: New York, 1989.

[2] M. Özçeşmeci, E. Hamuryudan, The synthesis and characterization of functionalized polyfluorinated phthalocyanines, Dyes and Pigments 77, 457 (2008).

[3] İ. Gürol, G. Gümüş, V. Ahsen, Synthesis and characterization of novel fluoroether-substituted phthalocyanines, J. Fluorine Chem. 142, 60 (2012).

Simulation of Flexural Behavior of Nanocantilever using Molecular Dynamics Method

R. Ahmadi [1] and M.Tahmasebipour [2]

[1]Department of Mechanical Engineering, Islamic Azad University, Parand branch, Parand, Tehran, Iran

[2]Faculty of New Sciences and Technologies, University of Tehran, Tehran, Iran

E-mail :tahmasebipour@ut.ac.ir

Simulation of nano-scaled systems requires accurate and efficient methods proportional with the dimensions and physical properties of the studied system, which can generate reliable results through due consideration of nanoscale intermolecular and interatomic interactions. Exhibiting a higher accuracy than that offered by other computational methods, MD is frequently used for simulating nanosystems. This study implements MD method to simulate the flexural behavior of gold nanocantilevers using the EAM potential. The nanocantilever used in this study is a beam with a square cross section (3x3 nanometers) and a length of 9 nanometers. By applying different mechanical loads to this beam, we determined its flexural behavior including deflection, bending angle, shear force distribution, as well as the bending moment along the beam and simulated the induced cross sectional stresses (both compressive and tensile). Fig. 1 shows the graphical display of the nanocantilever bending under the applied mechanical loads.

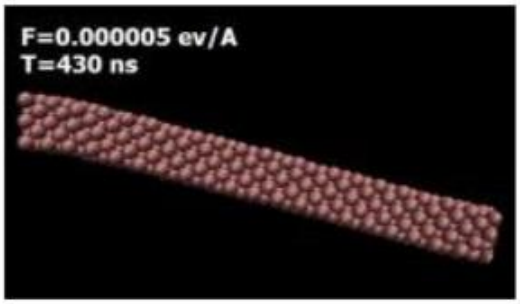

Fig. 1 nanocantilever bending under the applied mechanical load

Two diodes model and (CdSe-PVA) interfacial layer effect on the forward bias current-voltage (I-V) characteristics of Au/CdSe-PVA/n-Si Schottky barrier diodes

Şemsettin Altındal[1], Çiğdem Bilkan[1,2]

[1]*Department of Physics, Faculty Sciences, Gazi University, Ankara, Turkey,*

[2]*Department of Physics, Faculty Sciences, Çankırı Karatekin University, Çankırı, Turkey*

E-mail: altundal@gazi.edu.tr

The electrical characteristics of fabricated Au/CdSe-PVA/n-Si Schottky barrier diodes (SBDs) have been investigated at room temperature by using the forward and reverse bias current-voltage (I-V), capacitance/conductance-voltage (C/G-V) characteristics. The main electrical parameters such as reverse saturation current (I_s), ideality factor (n), zero bias barrier height (Φ_{Bo}), series and shunt resistances (R_s and R_{sh}) of the diode were obtained from the forward bias I-V data. In addition, the energy dependent values of N_{ss} were extracted from these data by taking into account voltage dependence of barrier height (BH) and n. The exponential growth of the N_{ss} from midgap energy of the Si towards the bottom of the conductance band (E_c) is very apparent. The voltage dependent resistance (R_i) was obtained both the Ohm's law using I-V data and Nicollian and Brews method using impedance data and compared. The obtained high value of n and R_s were attributed to the particular distribution of N_{ss} at M/S interface, surface and fabrication processes, barrier inhomogeneity and interfacial. C-V and G/ω-V plots were drawn and they show inversion, depletion and accumulation regions. Experimental results confirmed that the existence of interlayer, N_{ss} and R_s are quite effective on electrical characteristics of the SBDs and CdSe-PVA interlayer can be used as an alternative material to replace the conventional SiO_2 at M/S interface.

Organic Solar Cells Using Polymers with Different Band Gaps

Y. Altin[1], S. Gungor[1], I. Borazan[2,3], A. Demir[2,3] and A. Bedeloglu*[1]

[1]*Department of Fiber and Polymer Engineering, Bursa Technical University, Bursa, Turkey*

[2]*Faculty of Textile Technologies and Design, Istanbul Technical University, Istanbul, Turkey*

[3] *TEMAG Laboratory, Istanbul Technical University, Istanbul, Turkey*

E-mail : ayse.bedeloglu@btu.edu.tr

Polymer-based organic solar cells are attracting great attention since they can be produced via low-cost techniques and have many interesting properties including flexibility, semi-transparency, easy integration and lightweight. However, as conventional wide band gap polymers for light absorbing layer lack adequate efficiency to collect sun light and stability in air, they significantly affect the power conversion efficiency of organic solar cells. Therefore, in this study, low band gap polymers were used to produce more stable and efficient organic solar cells. P3HT as wide band gap polymer and PTB7 and PCDTBT as low band gap polymers were combined to get an optimum photoactive layer in the organic solar cell with increased efficiency. Obtained devices were characterized by measuring optical, photoelectrical and morphological properties.

This study was supported by Turkish Scientific and Technical Research Council, TUBITAK, Project No: 113M950.

Purification and Characterization of Turkey Liver Mitochondrial TrxR

Yusuf TEMEL[a], Mehmet ÇİFTCİ[b], Ö.İrfan KÜFREVİOĞLU[c]

[a]Solhan Health Services Vocational School, Bingöl University, 12000 Bingöl

[b]Faculty of Arts and Sciences, Bingöl University, 12000 Bingöl

[c]Faculty of Science, Atatürk University, 25100 Erzurum

Thioredoxin reductase enzyme (**TrxR**), thioredoxin protein (**Trx**) and NADPH called thioredoxin system which found in almost all living organisms [1]. This system which has important roles in DNA synthesis, the prevention of damage to the cell caused by oxidative stress in cell proliferation, apoptosis, the protection of the cell from the damaging effects of peroxides and the stimulation of transcription factor activity is of great importance for the cell [1,2].

Herein, the turkey liver mitochondrial **TrxR** enzyme with 3,07 EU x mg^{-1} specific activity was purified 990-fold in a yield of 2,05 % by using 2',5'-ADP Sepharose 4B affinity chromatography. SDS-polyacrylamide gel electrophoresis was done to control the purity of enzyme and to determine the molecular mass of subunits, and a single band was observed. The subunit molecular mass was determined to be about 45,5 kDa. The molecular mass of the enzyme's natural state was found to be 88 kDa using Sephadex-G 150 gel filtration chromatography. Furthermore, we have determined characterization properties of Turkey liver mitochondrial **TrxR**.

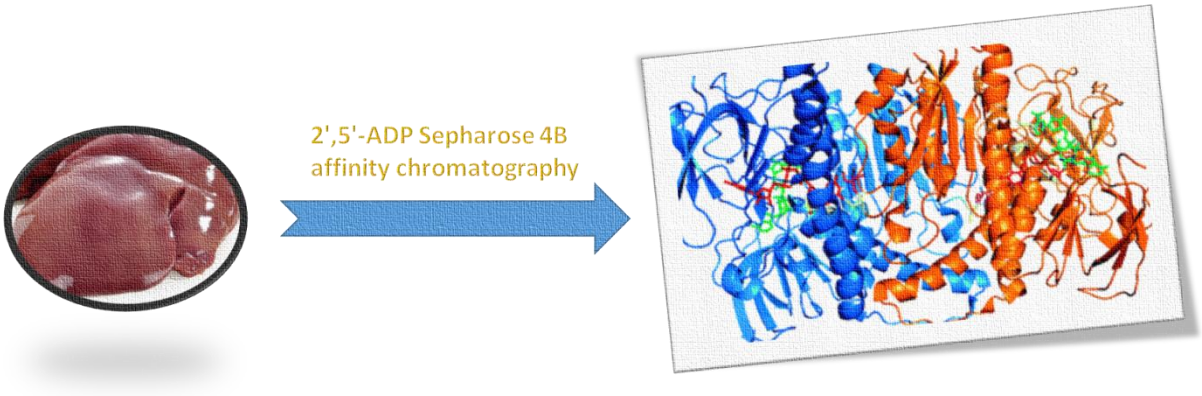

http://www.ebi.ac.uk/pdbe-srv/view/images/entry/1h6v600.png

References

[1] E.S Arner and A. Holmgren . Semin Cancer Biol. 16, 420–426. (2006)

[2] Kohárýová M., Kollárová M. Gen. Physiol. Biophys. 27**,** 71–84 (2008)

Purification of 6PGD enzyme from rat erythrocytes

Yusuf Temel [1], Mehmet Çiftci [2]

[1]Department Of Health Services, Vocational Schools, , Bingöl, Turkey

[2]Department of Chemistry, Art and Science Faculty, Bingöl, Turkey

E-mail : ytemel@bingol.edu.tr

Abstract: Pentose phosphate pathway consists of two stages including oxidative and non-oxidative. The aim of this metabolic pathway occurring in the cytosol to produce for reductive biosynthesis events **NADPH** and in the structure of various compounds ribose 5-phosphate. 6-Phosphogluconate dehydrogenase (**6PGD**; E.C.1.1.1.44) enzyme is involved in the synthesis of metabolic intermediates vital importance for life. For example, the **6PGD** is an important enzyme in pentose phosphate pathway that catalyzes the second step of the oxidative metabolic pathways. Herein, we purified the **6PGD** in 61.5% yield from rat erythrocytes with a specific activity of 1,37 EU mg^{-1} using 2′,5′-ADP sepharose 4B affinity chromatography one step. As a result of purifications, the overall purification was determined to be approximately 244,7 fold. A single band and obtained approximately 59,8 kDa was observed from SDS–polyacrylamide gel electrophoresis.

INTRODUCTION

There are two main functions of the pentose phosphate pathway in cells, which are the synthesis of ribose 5-phosphate that are required for DNA, RNA and ribonucleotide synthesis of the reducing power NADPH which is used in reduction reactions [1]. Also, phosphorylated carbohydrates such as erythrose-4-phosphate are synthesized which is vital for synthesis of aromatic amino acids and vitamins and sedoheptulose-7-phosphate that as a component of the bacterial cell wall [2].

6-Phosphogluconate dehydrogenase enzyme (**6PGD**; E.C.1.1.1.44) catalyzes conversion reaction 6-phosphogluconate to D-ribulose 5-phosphate in the presence of $NADP^+$ which is third step of the pentose phosphate pathway [3]. **NADPH** is one of the products resulting from these reactions plays a role biosynthesis of fatty acid, cholesterol, L-ascorbic acid, nitric oxide, the reduction of peroxides, drug and xenobiotic detoxification and reduction of glutathione in cells [2,4]. Reduced glutathione (GSH) and GSH-dependent enzymes protect cell versus internal and the external of the origin of the toxic compounds and reactive oxygen species (**ROS**) [5]. Hence **6PGD** is classified in the antioxidant enzyme class [6]. In the absence of the enzyme is determined hemolytic anemia, deficiency in the number of reticulocytes, jaundice and hemolytic epidemic events, also, observed increase in pyruvate kinase activity and decrease in GSH level. Consequently shortens the life time of the erythrocytes [6].

6PGD enzyme has been purified many resources from bacteria to mammals. This enzyme was first purified from sheep liver by Villet and Dalziel [7], then it has been purified and caracterizated many resources such as human erythrocytes [8,16], rat liver, mammary gland of rabbit [15], pork liver [9], parsley leaves [10], rat erythrocytes [11], rat heart and lung tissues [12], chicken liver [13], cat erythrocytes [14] and rainbow trout gill [17].

In the present study having great importance in metabolism 6PGD enzyme was purified in a single step using affinity chromatography of rat erythrocytes.

RESULTS AND DISCUSSION

The pentose phosphate pathway enzymes of 6PGD has an important role in the metabolism. Even though less severe hemolytic cases were detected in the absence of enzymes. 6PGD is an inhibitor of phospho-glucose isomerase and it is accumulation in cell leads to inhibits glycolysis path. For this reason, it may be used the target enzyme in antimicrobial chemotherapys [21]. 6PGD enzyme was purified from rat erythrocytes and purification of enzyme was performed by single step which is 2′,5′-ADP Sepharose 4B affinity gel chromatography. The enzyme was obtained to have a specific activity of 1.37 EU/mg protein with a yield of 61,5% and 244.7 of purification fold (Table 1).

Table 1. Purification table of 6PGD of rat erythrocytes.

Purification Steps	Activity (EU/ml)	Protein (mg/ml)	Total Activity (EU)	Total Protein (mg)	Specific Activity (EU/mg)	Yield (%)	Purification fold	Totalv volume (ml)
Hemolysate	0.0695	12.35	0.208	37.05	0.0056	100	1	3
2',5'- ADP Sepharose- 4B chromatography	0.0642	0.0467	0.128	0.0934	0.37	61.5	244.7	2

Until now, enzyme has been purified using different methods such as DEAE cellulose, CMC-cellulose and ammonium sulfate precipitation methods of mammals tissue [7], high-speed centrifugation, ammonium sulfate precipitation, and 2',5'-ADP Sepharose 4B affinity chromatography methods of using from rat erythrocytes [11], using 2',5'-ADP Sepharose 4B affinity chromatography by single step of rat heart and lung tissue [12], ammonium sulphate precipitation, 2',5'-ADP Sepharose 4B affinity chromatography and Sephadex G-200 gel filtration chromatography of chicken liver [13], 2',5'-ADP Sepharose 4B affinity chromatography of cat erythrocyte [14], ammonium sulphate precipitation and 2',5'-ADP Sepharose 4B affinity chromatography of human erythrocyte [16]. All these steps have been used costly and requires a long time. In the present study were obtained in high purity enzyme in a short time and at low cost by single step. The purity of the **6PGD** enzyme obtained from rat erthrocyte was controlled by **SDS-PAGE** method. Purity of enzyme was determined by the observation of a single band in the gel (Figure 1a). The molecular mass of the subunit of the enzyme was calculated to be about 59,8 kDa by this method. In different study reported that the molecular weight of the native enzyme was found to by Sephadex G-200 chromatography at 111 kDa and it was a homodimeric structure [11]. It is reported from various resources in the literature that the purified **6PGD** enzyme is homodimeric or homotetrameric structure and the subunits molecular masses are between 33 and 60 kDa [7-17]. The molecular weight of rat erythrocyte 6PGD enzyme is similar to the rat liver and rabbit mammary gland. SDS-PAGE method was used for purity and determine subunits molecular weight of the enzyme (Figure 1a). Using standard protein and 6PGD enzyme, R_f values were calculated, and R_f-Log MW graph was prepared by Laemmli procedure, obtained molecular weight of approximately 59,8 kDa for 6PGD enzyme (Figure 1b).

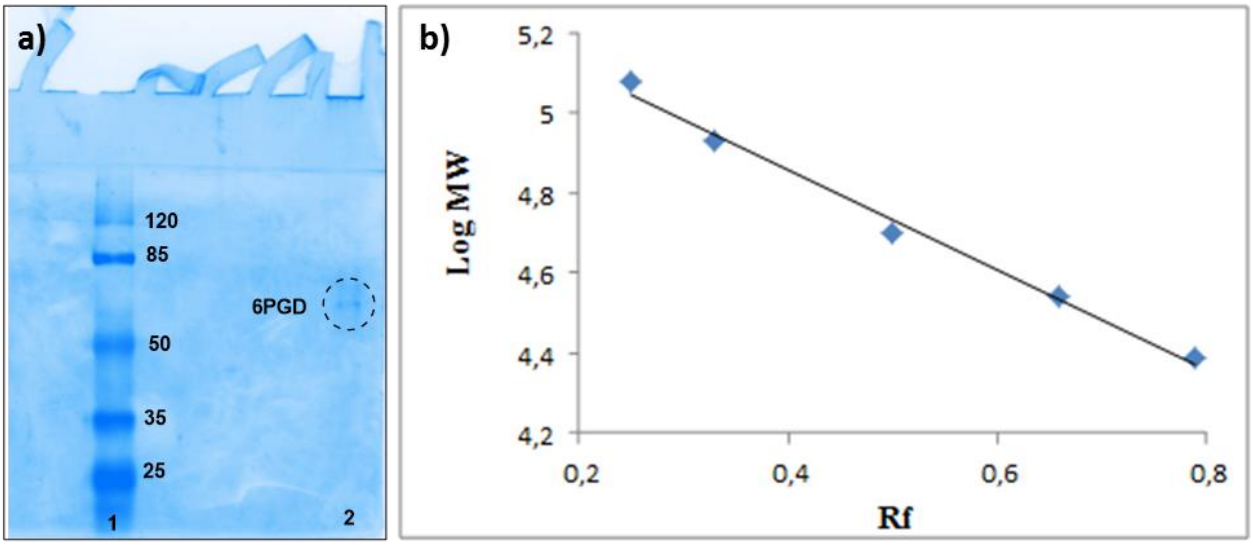

Figure 1. a) SDS-polyacrylamide gel electrophoresis of 6PGD purified by affinity gel (Lane 1: Standard proteins; Lane 2: **6PGD**) and **b)** Standard graph used for the determination of molecular weight of 6PGD enzyme by the method SDS-PAGE

MATERIAL AND METHOD

Chemicals

The chemicals used were purchased from Sigma and Merck. 2′,5′-ADP Sepharose 4B was purchased from Pharmacia.

Preparation of hemolysate

Fresh blood samples from rats, placed in EDTA-containing tubes, were centrifuged (15 min, 2.500×g) and plasma were removed. The precipitate (red blood cells) washed three times with KCl (0.16 M) and hemolyzed with 5 volume of cold-water. Then, to remove the cell membranes, and intact cells 30 minutes centrifugation at 10.000×g were performed. All procedures were carry out at 4˚C.

2′,5′-ADP Sepharose 4B Affinity Chromatography

The dried 2′,5′-ADP Sepharose 4B gel (2 g) was weighed for 10 ml column volume. The gel washed with 300 ml distilled water. The gel was treated with 50 mM KH_2PO_4 +1 mM EDTA + 1mM DTT (pH 7.3) buffer and packed in column (10 cm). And the gel was equilibrated same buffer. After the sample was passed through the column, the elution column was washed with equilibration buffer until the absorbance difference 0.05 in 280'nm. Elution was carried out with 80 mM K-fosfat + 10 mM EDTA + 80 mM KCl + 5 mM $NADP^+$ (pH 7.3). All procedures were carry out at 4˚C.

Activity determination

The activity of **6PGD** enzyme was measured according to Beutlers method [18].

Protein determination

To quantify the amount of proteins in the samples, Bradford method [19] has been relied on, by which the amount of proteins were determined spectrophotometrically at 595 nm using boving serum albumin as a standard protein.

SDS polyacrylamide gel electrophoresis

6PGD enzyme purities were guranted using SDS polyacrylamide gel electrophoresis by Laemmli method which described previously [21] 10% and 3% of acrylamide used for both running and stacking gels respectively with 0.1% of SDS.

Conculation

In conclution, we purified **6PGD** enzyme from rat erythrocytes by a single step which is 2′,5′-ADP sepharose 4B affinity chromatography. Thus, we have obtained the enzyme in high purity, economic and effective method and in very short time compared with other studies. Hereby, the study would be investigation of the effect of organic compounds on purified 6PGD enzyme activity from rat eryhtrocytes in the future.

References

[1] H. A. Krebs and L.V. Eggleston, The regulation of the pentosephosphate cycle in rat liver. In: Weber G (ed). Adv Enzymeregul. Oxford: Pergamon Press Ltd, 12, 421-33. (1978).

[2] T. Wood, Distribution of the pentose phosphate pathway in living organisms. Cell Biochem Funct. 4, 235-40. (1986).

[3] M. Çiftci, Ş. Beydemir, H. Yilmaz, E. Bakan, Effects of some drugs on rat erythrocyte 6-phosphogluconate dehydrogenase: an in vitro and in vivo study. Polish J. Pharmacol. 54, 275-280. (2002)

[4] D. L. Nelson, M.M. ve Cox, Lehninger Biyokimya İlkeleri (Çeviri: N. Kılıç) Palme Yayıncılık, Madison. 243-245 (2005).

[5] W. G. Siems, O. Sommerburg, T. Grune, Erythrocyte free radical and energy metabolism. Clin Nephrol. 53, 9-17. (2000).

[6] R. A. Kozar, C. J. Weibel, J. Cipolla, A. J. Klein, M. M. Haber, M. Z. Abedin, S. Z. Trooskin, Antioxidant enzymes are induced during recovery from acute lung injury. Crit. Care Med. 28, 2486-2491. (2000)

[7] R. H. Villet and K. Dalziel, Purification and properties of 6-phosphogluconate dehydrogenase from sheep liver. Biochem J. 115, 639-643. (1969).

[8] F. Dallocchio, F. Matteuzzi, T. Bellini, Half-site reactivity in 6- phosphogluconate dehydrogenase from human erythrocytes. Biochem J. 227, 305-310. (1985).
[9] M. A. Rosemeyer, The biochemistry of glucose-6-phosphate dehydrogenase and glutathione reductase. Cell Biochemistry and Function. 5, 79-95. (1987).
[10] H. Demir, M. Çiftci, Ö. İ. Küfrevioğlu, Purification of 6-phosphogluconate dehydrogenase from parsley (Petroselinum hortense) leaves and investigation of some kinetic properties. Prep Biochem Biotechnol. 33, 39-52. (2003).
[11] Ş. Beydemir, M. Çiftci, H. Yılmaz, Ö.İ. Küfrevioğlu, 6-phosphogluconate dehydrogenase: purification, characterization and kinetic properties from rat erythrocytes. Turk J Vet Anim Sci. 28, 707-714 (2004).
[12] Ş. Adem, and M. Çiftci, Purification and biochemical characterization of glucose 6-phosphate dehydrogenase, 6-phosphogluconate dehydrogenase and glutathione reductase from rat lung and inhibition effects of some antibiotics. J Enzyme Inhib Med Chem. 1475-6374. (2015)
[13] M. Erat, Purification of 6-phosphogluconate dehydrogenase from chicken liver and investigation of same kinetic properties. Prep. Biochem. Biotechnol., 35, 5369. (2005).
[14] S. Kılıç, PhD thesis, Van Kedisi'nden 6-Fosfoglukanat Dehidrogenaz Enziminin Saflaştırılması Karekterizasyonu, Kinetiği, İnhibisyonu ve HPLC İle Tayin Yönteminin Geliştirilmesi. Yüzüncü Yıl Üniversitesi Fen Bilimleri Enstitüsü.(2007).
[15] S. A. Betts, J.R. Mayer, Purification and properties of 6-phosphogluconate dehydrogenase from rabbit mammary gland. Biochem J. 151, 263-270. (1975).
[16] F. Ozabacıgil PhD thesis, İnsan Eritrosit 6-Fosfoglukanat Dehidrogenaz Enziminin Saflaştırılması, Bazı İlaçların Enzim Aktivitesi Üzerine İn Vitro ve Tavşanlarda İn Vivo Etkisinin İncelenmesi. Atatürk Üniversitesi Sağlık Bilimleri Enstitüsü (2005).
[17] A. Öztürk, Master Thesis. Investigations On Purification And Characterization Of 6-Phosphogluconate Dehydrogenase From Rainbow Trout Gills And Inhibition Effects Of Some Metal Ions On The Enzyme Activity. Atatürk Üniversitesi Fen Bilimleri Enstitüsü (2015).
[18] E. Beutler, Red Cell Metabolism Manuel of Biochemical Methods. Academic Press, 68-70. London, (1971).
[19] M. M. Bradford, A rapid and sensitive method for the quantition of microgram quantities of protein utilizing the principle of protein-dye binding. Anal. Biochem. 72, 248-251. (1976)
[20] U. K. Laemmli, Cleavage of structural proteins during assembly of the head of bacteriophage T4. Nature. 227, 680-683. (1970)

Purification of 6PGD Enzyme from Rat Erythrocytes

Yusuf Temel [1], Mehmet Çiftci [2]

[1]*Department Of Health Services, Vocational Schools, , Bingöl, Turkey*

[2]*Department of Chemistry, Art and Science Faculty, Bingöl, Turkey*

E-mail : ytemel@bingol.edu.tr

Pentose phosphate pathway consists of two stages which are oxidative and non-oxidative. The aim of this metabolic pathway occurring in the cytosol to produce for reductive biosynthesis events NADPH and in the structure of various compounds ribose 5-phosphate[1].

6-Phosphogluconate dehydrogenase (**6PGD**; E.C.1.1.1.44) enzyme is involved in the synthesis of metabolic intermediates which is vital importance for life. For example, the **6PGD** is an important enzyme in pentose phosphate pathway that catalyzes the second step of the oxidative metabolic pathways[2]. Caused any inconvenience in the study of this enzyme would be serious risks for life. Moreover, 6-phosphogluconate accumulation in the cell are also negatively affects the metabolism of energy pathways glikolisis. Therefore, the having important position of this enzyme was suggested that could be used as targets for chemotherapy[3]. Due to the importance of the enzyme It has being continued that purification characterization, and kinetics studies of various sources in these days.

Herein, we purified the **6PGD** in 61.5% yield from rat erythrocytes with a specific activity of 1,37 EU mg^{-1} using 2',5'-ADP sepharose 4B affinity chromatography one step. As a result of purifications, the overall purification was determined to be approximately 244,7 fold. A single band and obtained approximately 59,8 kDa was observed from SDS–polyacrylamide gel electrophoresis. Hereby, it would be investigation of the effect of activity on purified rat erythrocyte 6PGD enzyme of organic compounds in the future.

References

[1] E. Keha and O.I. Küfrevioğlu, Biyokimya, Aktif yayınevi, Erzurum (2004).

[2] B. Tandogan and N.N. Ulusu, 6-fosfoglukonat dehidrogenaz: Moleküler ve kinetik özellikleri. Türk Biyokimya Dergisi, 28(4): 268-273. (2003).

[3] M.P. Barrett The pentose phosphate pathway and parasitic protozoa. Parasitol Today. Jan;13(1):11-6. (1997)

Synthesis and electropolymerization properties of cobalt, manganese and titanium phthalocyanines bearing {[4-(2-morpholin-4-ylethoxy)benzyl]oxy} groups

Ü.E. Özen[1], T. Keleş[2], Z. Bıyıklıoğlu[2], A. Koca[1]

[1]Department of Chemical Engineering, Marmara University, İstanbul, 34722, Turkey

[2] Department of Chemistry, Karadeniz Technical University, Trabzon, 61080, Turkey

E-mail :zekeriya_61@yahoo.com

Phthalocyanines (Pcs) are important compounds due to not only their blue-green color but also their electronic properties. They have been proposed and used in various technological areas such as liquid crystals, electronic devices, gas and chemical sensors, electrochromic and electroluminescent displays, non-linear optics, photovoltaics and semiconductors [1]. Metallophthalocyanines are also interesting electrochromic materials as monomer and polymeric conductive films due to their high chemical and thermal stability. Modifications of metallophthalocyanines with functional substituents extend the redox richness and versatility of their electrochemical applications in different fields, such as electrocatalytic, electrosensing and electrochromic applications [2]. In this study, we designed and synthesized a novel series of peripherally tetra-{[4-(2-morpholin-4-ylethoxy)benzyl]oxy} substituted metallophthalocyanines bearing electropolymerizable ligand for the first time. This study was supported by The Scientific & Technological Research Council of Turkey (TÜBİTAK, project no: 114Z914).

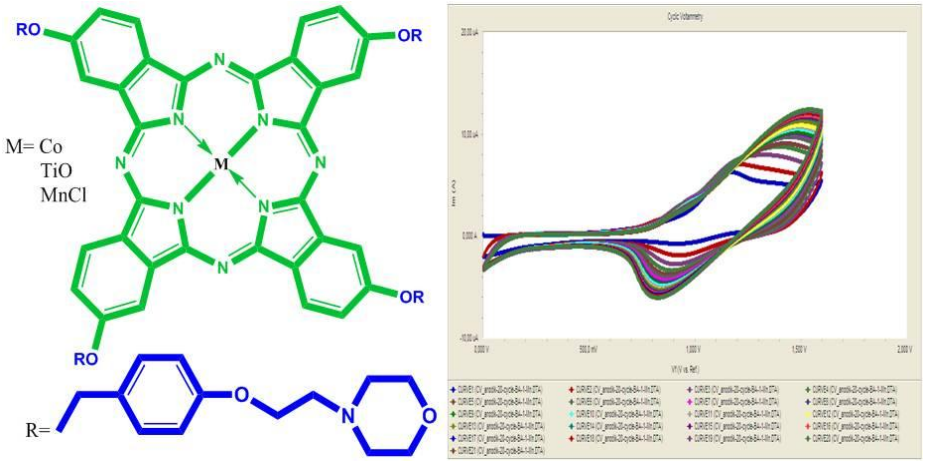

[1] M. Ince, M. V. Martinez-Diaz, J. Barbera, T. Torres, Liquid crystalline phthalocyanine–fullerene dyads, J. Mater. Chem. 21, 1531 (2011).

[2] A. Lever, E. Milaeva, The Phthalocyanines, properties and applications, vol. 2, VCH, New York, pp. 162 (1992).

Electropolymerizable, non-aggregated axially disubstituted silicon naphthalocyanines and their electrochemical properties

Z. Bıyıklıoğlu[1], H. Alp[1]

[1]*Department of Chemistry, Karadeniz Technical University,Trabzon, 61080, Turkey*

E-mail :zekeriya_61@yahoo.com

Metallophthalocyanines (MPcs) are a class of macrocyclic compounds which are very versatile because they possess a highly conjugated π-electron system. They were first developed as industrial pigments, and have been diversely applied in various fields, including electrochromism [1], photodynamic therapy [2]. Axial substitution is an attractive feature for phthalocyanines because of following reasons: (i) having different substituents macrocycle prevents aggregation and increases the solubility of phthalocyanines, (ii) the ligands can be highly functionalized, (iii) silicon phthalocyanines are resistant under chemical treatments. In this study, we designed and synthesized a novel series of axially disubstituted silicon phthalocyanines. Electrochemical and electropolymerization properties of the silicon naphthalocyanines were studied by cyclic and square wave voltammetry. Also, aggregation behavior of silicon naphthalocyanines were investigated in different solvents and concentrations.

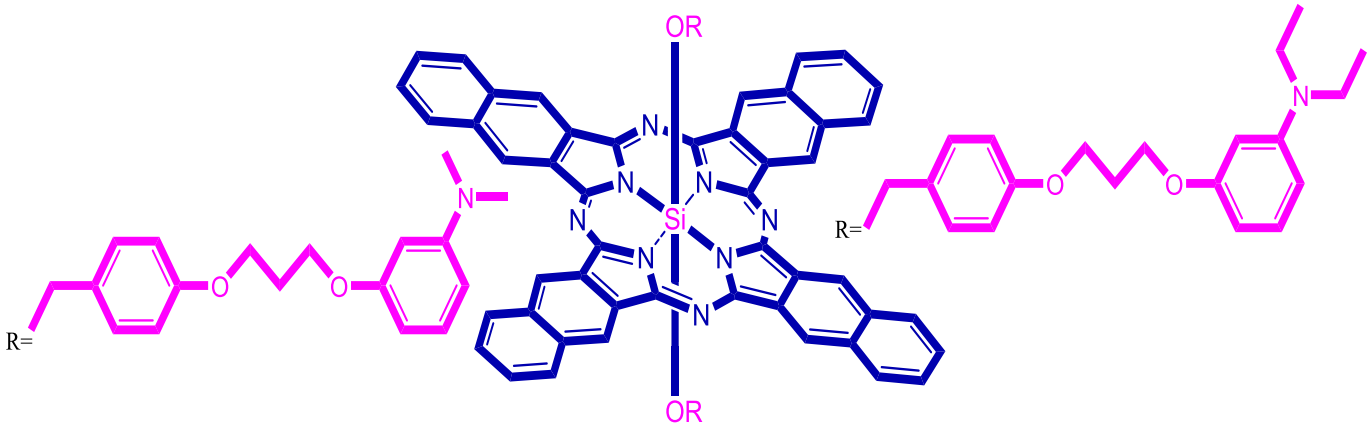

[1] F. Demir, Z. Bıyıklıoğlu, A. Koca, Electrochromism of Electropolymerized Metallophthalocyanines, J. Electrochem. Soc. 161, G1 (2014).

[2] W.S.G. Medina, N.A.G. dos Santos, C. Curti, A.C. Tedesco, A.C. dos Santos, Effects of zinc phthalocyanine tetrasulfonate-based photodynamic therapy on rat brain isolated mitochondria, Chem. Biol. Inter., 179, 402 (2009).

Thermal characterization of semi conductive Polypropylene blends with different J-AP contents

Fatih DOĞAN[a,b], Kevser TEMİZKAN[a], İsmet KAYA[a]

*[a]Polymer Synthesis and Analysis Laboratory, Department of Chemistry, Çanakkale Onsekiz Mart University, Çanakkale, 17020, Turkey, *e mail:fatihdogan_tr@hotmail.com*
[b]Faculty of Education, Secondary Science and Mathematics Education, Çanakkale Onsekiz Mart University, 17100, Çanakkale, Turkey

Abstract

Enzymatic polymerization of 7-amino-4-hydroxy-2-naphthalene sulfonic acid (J-AP) was first carried out as literature. Different series of polypropylene/J-AP blends were then prepared via melt blending in a twin screw extruder. The effects of J-AP loading ratio on the thermal stability of the blends were analyzed. The results showed that the addition of J-AP into PP matrix increases the activation energies related to the thermal degradation of the blends. Increasing the J-AP ratio in PP content caused significant changes in the solid state decomposition mechanism of blends. The reaction process and kinetic parameters related to the solid state decomposition of corresponding blends were investigated by thermogravimetric analysis (TG) technique at a single heating rate. TG/DTG-DTA curves showed that the thermal decomposition occurred mainly in one stages. The kinetic parameters such as the activation energy *E*, frequency factor *A* and reaction order *n* related to solid state decomposition stage of blends were calculated by using the methods based on single heating rates such as Coats-Redfern (CR), MacCallum Taner (MT) and van Krevelen (vK). We also calculated the thermodynamic parameters such as entropy change $\Delta H^{\neq}$, enthalpy change $\Delta S^{\neq}$ and Gibbs free energy $\Delta G^{\neq}$, related to the thermal decomposition by TG technique. The activation energy values from so-called methods were very close with each other. The mean activation energy related to the thermal decomposition of blends was found to change between about 220 -240 kJ/mol.

***Keywords*:** activation energy; 7-amino-4-naphthol-2-sulfonic acid; thermal decomposition

Introduction

Polypropylene (PP) is one of the most important industrial polymers due to its relatively low cost, regular chain structure, biocompatibility, and good mechanical performance in many industrial and biomedical applications. Moreover it has a high melting point, low density, regular chain structure and low energy demand for processing and is relatively stiff, cheap and versatile. Because of processing easily and using in different materials PP suits a wide spectrum of end-use applications in industry. However, it always consist certain shortcomings such as poor oxygen barriers, low dimensional and thermal stability that can limit universal applications in areas requiring high

performance. From this perspective, material properties of PP are far from ideal. This has led to research into using additives to make PP composites with desired physical properties. These properties make it one of the most popular polymers in engineering applications. In this study, different series of Polypropylene/J-AP blends were prepared via melt blending in a twin screw extruder. The effects of J-AP loading ratio on the thermal performances of the blends were analyzed. The results showed that the addition of J-AP into PP changed the thermal properties of the blends.

Kinetic Theory

The following general equation is used to describe kinetics of thermally induced reactions in the solid state,

$$\beta \frac{d\alpha}{dT} = A\, f(\alpha)\, \exp(\frac{-E}{RT}) \quad (1)$$

where *α, β, A, f(α)* are the degree of conversion, the linear heating rate, pre-exponential factor, and the differential conversion function, respectively. In kinetic calculating, many different reaction models can be used to determine the kinetic parameters and thermodynamic parameters related to the solid state decomposition. In this study, the so-called parameters related to the solid state decomposition of polypropylene/J-AP blends were calculated from methods based on a single heating rate given in the literature. These methods are those of CR[1], HM[2], MC[3], vK[4], MKN[5] and WHYC[6], and generally expressed by following equations

The Coats-Redfern method

$$\ln[\frac{g(\alpha)}{T^2}] = \ln[\frac{AR}{\beta E}(1-\frac{2RT}{E})] - (\frac{E}{RT}) \quad (2)$$

The van Krevelen method

$$\ln g(\alpha) = \ln\left[\frac{A(0.368/T_m)^{\frac{E_a}{RT_m}}}{\beta(\frac{E_a}{RT_m}+1)}\right] + (\frac{E_a}{RT_m}+1)\ln T \quad (3)$$

The MacCallum-Tanner method

$$\log g(\alpha) = \log(\frac{AE}{\beta R}) - 0.4828E^{0.4351} - (\frac{0.449+0.217E}{10^{-3}T}) \quad (4)$$

Madhusudanan-Krishnan-Ninan method

$$\ln\left(\frac{g(\alpha)}{T^{1.9206}}\right) = \left[\ln\frac{AR}{\beta E} + 3.7678 - 1.92061\ln E\right] - 0.12040\left(\frac{E}{RT}\right) \quad (5)$$

Horowitz-Metzger method

By using Θ=T-Tm

$$\ln(g(\alpha))=\ln\frac{ART_m^2}{\beta E}-\frac{E}{RT_m}+\frac{E\theta}{RT_m^2} \quad (6)$$

Wanjun-Yuwen-Hen-Cunxin method

$$\ln\left(\frac{g(\alpha)}{T^{1.8946}}\right)=\left[\ln\frac{AR}{\beta E}+3.6350-1.89461\ln E\right]-1.0014\left(\frac{E}{RT}\right) \quad (7)$$

In the equations above, *g(α), T_m , E, R,* are the integral function of conversion, DTG peak temperature, activation energy and gas constant, respectively. From the linear plots of the left-hand side of kinetic equations against 1/*T* the kinetic parameters can be estimated. For vK equation the left-hand side is plotted against ln*T*. The values *E* and *A* were calculated from the slope and intercept of the straight lines, respectively.

Material and Methods

7-amino-4-hydroxy-2-naphthalene sulfonic acid, hydrochloric acid (HCl, 37%) and other all chemical compounds were supplied from Merck Chem. Co. (Germany) and they were used as received. HRP was purchased from Sigma Chemical Company and had a specific activity of 259 purpurogallin units/mg and RZ = 3.0 and used directly as supplied. Polypropylene was supplied as pellets by Petkim Petrochemical Company (Aliaga, Izmir, Turkey). The specific gravity of the PP is 0.905g/cm_3, melt flow index of 0.3-0.5g/10 min (2.16kg, 230 ± 0.5 °C).

Synthesis of poly(7-amino-4-hydroxy-*naphthalene*-2-sulfonic acid)

A typical procedure of enzymatic polymerization is performed as described in follow[7]. 7.5 mmol monomer (J-AM) and 10 mg HRP were added to 35 mL 1,4-dioxane solution containing 15 mL sodium phosphate buffer (pH :7) in a 100 mL three-necked round bottom flask at room temperature. H_2O_2 solution of 30% was added into drop wise to the reaction mixture over a period of 5 h. After vigorously stirring for 10 h, black precipitate was collected by filtration, washed periodically with ether (3 x 30 mL) to remove unreacted monomer and then dried in a vacuum oven at 55 ^{0}C for 24 h (yield: 92%). The synthetic pathway is outlined in Scheme 1. The FT-IR results of J-AP are also illustrated in Figure 2. FT-IR (cm^{-1}): Region 3800-2700, (stronger hydrogen bonding), 3387(-NH), 1635 (–C=N), 1484 (–C=C-aromatic), 1446 (–C=C- aromatic), 1381 (phenolic –OH), 1274, 1230, 1150, 1140.

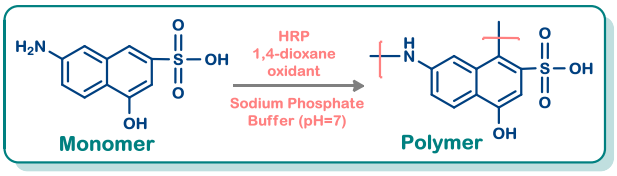

Scheme 1. Synthetic pathway for J-AP

Preparation of polypropylene/J-AP blends (J-AP$_n$)

Polypropylene blends containing J-AP with of 0.5, 1 and 3 wt.% loading level (J-AP$_{0.5}$, J-AP$_1$ and J-AP$_3$) were prepared by means of a single-screw extruder (Collin E 30P, Ebensburg, Germany) which has a diameter of 30 mm and length to diameter ratio of 20. The mixing temperature rose from 190 ºC in the feed throat to 230 ºC in the die section of the extruder. All compounds were produced as approximately 70 µm thick and 10 cm wide films. All of the blends were prepared under same conditions.

Instrumental techniques

Thermogravimetric analysis was performed with TGA-DTA Perkin-Elmer Diamond system apparatus. The thermal measurements were carried out from the ambient temperature up to 1000 °C at heating rates of 5, 10, 15, 20°C /min. TGA-DTG and DTA curves were recorded in dynamic nitrogen atmosphere at a flow rate of 200 mL/min. For thermogravimetric analysis, the polymer sample was evaluated in the form of 4 mg weight. A platinum crucible was used as a sample container. Al_2O_3 was used as a reference material

Result and Discussion

The kinetic analysis of J-AP$_n$ blends was investigated by thermogravimetric analysis from ambient temperature to 1000 ^{0}C in N_2. Typical TG, DTG and DTA curves obtained at heating rates of 5, 10, 15 and 20 °C /min for all the blends are shown in Figure 1.

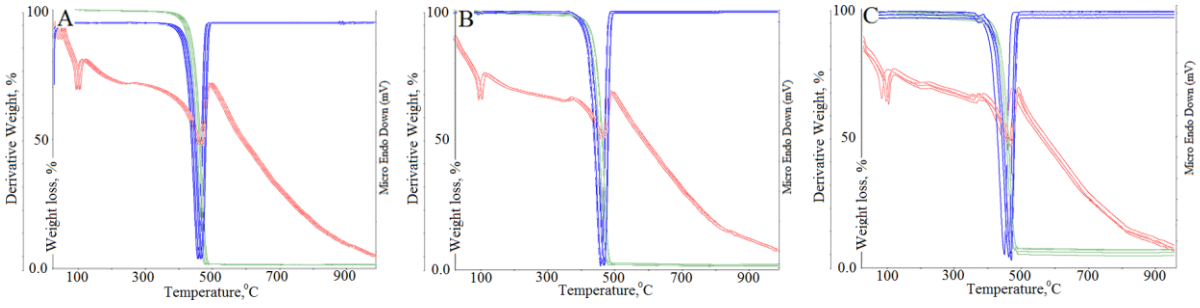

Figure 1. Typical TG, DTG and DTA curves for J-AP$_{0.5}$ (a), J-AP$_1$ (b) and J-AP$_3$ (c)

All the TG thermograms displayed that J-AP$_n$ blends decomposed in one stage over the temperature range 320-550 ^{0}C with a mass loss nearly 92.6 % in weight. Also the corresponding DTA profiles presented two endothermic peaks for J-AP$_n$ blends. The maxima of these peaks were attributed to the melting point and thermal decomposition of J-AP$_n$ blends. All thermograms and decomposition processes were similar in J-AP$_n$ blends. The thermal stability in J-AP$_n$

blends increased with an increase of J-AP loading ratio in PP. Thermal data obtained at heating rates of 5, 10, 15, 20 °C min^{-1} were evaluated by the methods based on a single heating rates for kinetic and thermodynamic analysis. The kinetic parameter such as reaction order, *n*, activation energy, *E*, pre-exponential factor, *A*, and thermodynamic parameters such as entropy change $\Delta H^{\neq}$, enthalpy change $\Delta S^{\neq}$ and Gibbs free energy $\Delta G^{\neq}$ were determined by the linearization curves related to the thermal decomposition of J-AP_n blends. In this study, the several methods based on a single heating rate were used in the kinetic and thermodynamic analysis. The linearization curve related to the decomposition step of each J-AP_n blends was obtained using the least squares method. From the TG/DTG and DTA curves, the kinetic and thermodynamic parameters of the decompositions were elucidated by the methods with higher linear regression coefficient. The so-called parameters related to solid state decomposition of the J-AP_n blends were calculated by the software developed in our laboratory using PHP Web programming language. Furthermore, for all of the methods, it is possible to determination of the pre-exponential factor and reaction order is possible from the expression of $g(\alpha)$ in eqns. where $n \neq 1$:

$$g(\alpha) = \frac{1-(1-\alpha)^{1-n}}{1-n}$$

By using the aforementioned methods above, kinetic triplets can be calculated from the linearization curves of Arrhenius plots related to the decomposition steps of the J-AP_n blends. *n*, *E*, *A*, $\Delta H^{\neq}$, $\Delta S^{\neq}$, $\Delta G^{\neq}$ obtained by all the methods using in this study was presented in Table 1. The results obtained by different methods are in good agreement with each other. The value of correlation coefficients of linearization curves obtained for the decomposition step of the J-AP_n blends was found to be approximately 1.00. The thermodynamic parameters such as $\Delta G^{\neq} \Delta H^{\#}$, $\Delta S^{\#}$, and $\Delta G^{\#}$, of the decomposition steps were also calculated from the following equations:

$$\Delta S^{\#} = 2.303 \log\left(\frac{Ah}{kT}\right) R \; ; \; \Delta H = E - RT; \quad \Delta G^{\#} = \Delta H - T\Delta S^{\#}$$

Where *h, T* and *A* are the Planck constant, temperature at the maximum rate of weight loss, pre-exponential factor.

Table 1. The Kinetic and thermodynamic data on the decomposition step of J-AP_n

	J-$AP_{0.5}$ blend							J-AP_1 blend							J-AP_3 blend						
Heating rate	Methods	*n*	E	lnA	$\Delta S^{\#}$	$\Delta H^{\#}$	$\Delta G^{\#}$	Methods	*n*	E	lnA	$\Delta S^{\#}$	$\Delta H^{\#}$	$\Delta G^{\#}$	Methods	*n*	E	lnA	$\Delta S^{\#}$	$\Delta H^{\#}$	$\Delta G^{\#}$
5 ^{0}C/min	WHYC	1.6	218.8	-42.7	-612.5	189.3	615.4	WHYC	1.8	215.7	-30.8	-653.9	193.7	509.4	WHYC	1.9	231.2	-62.9	-823.3	144.0	328.6
	CR	1.6	217.5	-41.6	-631.0	184.7	644.3	WHYC	1.8	215.7	-36.1	-653.1	194.3	504.3	WHYC	1.8	231.0	-62.3	-823.0	144.5	327.6
	MC	1.6	219.6	-42.4	-636.1	180.3	626.9	MKN	1.8	216.9	-34.2	-653.6	193.3	504.2	HM	1.8	232.1	-62.2	-825.6	143.2	327.2
	HM	1.5	217.7	-43.7	-678.3	182.5	620.8	HM	1.8	217.7	-33.1	-657.8	192.8	502.8	MC	1.8	231.3	-63.0	-823.7	143.8	327.7
	MKN	1.5	219.1	-43.5	-625.7	189.7	620.6	MC	1.7	219.1	-33.2	-655.7	193.7	500.1	MKN	1.8	231.1	-63.4	-824.7	144.7	326.4
	vK	1.4	214.9	-45.5	-631.5	183.3	629.9	vK	1.7	219.4	-35.2	-653.1	192.3	502.9	vK	1.7	234.2	-65.2	-823.6	144.3	325.2
10 ^{0}C/min	CR	1.8	222.8	-40.8	-719.9	181.7	623.9	WHYC	1.8	216.9	-27.3	-656.3	182.4	498.7	CR	1.9	237.2	-56.8	-826.7	135.1	308.2
	WHYC	1.8	223.4	-40.4	-734.6	187.5	634.6	WHYC	1.8	214.3	-24.5	-654.7	182.5	494.3	WHYC	1.9	237.3	-56.8	-833.0	134.6	307.8
	MKN	1.8	221.6	-41.3	-728.5	186.4	646.9	vK	1.8	216.1	-24.1	-658.5	181.3	498.9	MC	1.9	237.5	-56.2	-835.6	136.2	306.2
	MC	1.7	221.2	-41.6	-775.7	189.0	618.8	MC	1.8	212.1	-24.6	-655.3	181.8	498.7	MKN	1.8	235.3	-55.3	-833.7	133.7	305.5
	HM	1.7	225.4	-40.1	-730.3	183.3	622.2	MKN	1.7	213.5	-24.5	-650.3	181.4	496.2	HM	1.8	235.3	-55.7	-834.7	134.6	305.4
	vK	1.6	226.6	-40.6	-783.5	180.1	630.1	HM	1.7	215.6	-24.4	-653.2	180.0	493.8	vK	1.7	234.4	-55.4	-833.6	133.7	305.7
15 ^{0}C/min	MC	1.9	225.0	-39.6	-728.3	174.0	638.7	CR	1.9	222.2	-24.7	-661.6	175.0	486.9	MKN	2.0	233.3	-44.2	-839.0	124.0	295.1
	WHYC	1.8	224.3	-38.7	-731.2	166.7	646.1	WHYC	1.9	224.3	-24.7	-661.2	176.3	486.1	WHYC	1.9	232.3	-44.3	-848.7	124.7	295.4
	MKN	1.8	223.4	-38.9	-725.1	160.7	642.9	MKN	1.9	224.4	-24.2	-665.0	172.7	486.9	MKN	1.9	231.6	-44.1	-848.4	123.3	294.2
	MC	1.8	223.1	-37.2	-772.1	167.5	619.3	vK	1.8	222.5	-24.2	-662.4	177.4	487.3	HM	1.9	231.2	-43.3	-848.3	123.4	294.6
	HM	1.7	225.0	-38.8	-733.3	165.0	622.1	MC	1.8	222.3	-24.6	-663.3	175.3	485.1	MC	1.9	231.0	-43.1	-847.6	124.0	294.3
	vK	1.7	227.2	-39.6	-723.5	166.1	627.7	HM	1.8	221.1	-24.6	-663.6	176.0	487.7	vK	1.9	230.4	-43.8	-847.5	123.2	293.0
20 ^{0}C/min	WHYC	2.0	228.3	-37.2	-735.7	171.8	641.0	WHYC	2.0	224.4	-22.0	-669.4	168.9	481.3	WHYC	2.1	230.7	-42.9	-858.3	111.1	281.0
	CR	1.9	229.1	-37.6	-735.0	178.7	645.4	WHYC	1.9	223.1	-22.6	-665.1	168.1	482.3	WHYC	2.0	230.3	-42.4	-858.3	110.6	280.3
	MKN	1.9	228.8	-37.1	-734.4	170.3	648.3	MC	1.9	223.6	-22.1	-664.8	163.8	481.3	MKN	2.0	230.4	-42.5	-858.5	110.4	280.2
	MC	1.9	227.6	-37.6	-772.1	178.1	620.6	MKN	1.9	221.7	-22.4	-662.1	168.0	483.8	MC	1.9	230.2	-41.2	-858.7	110.2	280.4
	HM	1.8	226.3	-38.6	-736.4	175.2	620.6	vK	1.9	220.3	-22.6	-666.3	165.2	482.6	vK	1.9	230.1	-41.1	-857.1	110.0	279.7
	vK	1.8	227.4	-37.3	-719.5	178.3	628.7	HM	1.8	221.3	-22.2	-669.5	168.0	480.1	HM	1.9	229.8	-40.4	-857.0	109.1	279.6

E, kJ mol^{-1}; lnA, s^{-1}; $\Delta S^{\#}$, J $mol^{-1}K^{-1}$; $\Delta H^{\#}$ and $\Delta G^{\#}$, kJ mol^{-1}

Conclusions

Polypropylene blends with containing different amounts of J-AP filler were prepared by melt-blending with a single-screw extruder. The effect of J-AP filler on thermal stability, thermal decomposition process as well as kinetic and thermodynamic parameters of prepared blends was investigated. The activation energies of the thermal decomposition by the CR**,** HM, MC, vK, MKN and WHYC methods in N_2 were found to be approximately 218 kJ/mol for J-$AP_{0.5}$ blend, 216 kJ/mol for J-AP_1 blend and 232 kJ/mol for J-AP_3 blend. In conclusion *i*) J-AP_n blends are more stable than virgin PP *ii*) J-AP_3 blends appear to be more stable than corresponding analogs containing J-$AP_{0.5}$ and J-AP_1 *iii*) structurally similar blends have similar thermal decomposition curves; *iv*) kinetic and thermodynamic parameter generally increases with an increase of heating rate.

Acknowledgments

This work was financially supported by the TUBITAK Grants Commission (Project No: KBAG- 113Z587).

References

1. Coats AW. Redfern JP. (1964). Kinetic parameters from thermogravimetric Data. *Nature*. Vol.201.68-69

2. Horowitz HH. Metzger G. (1963). Interpretation of thermogravimetric traces. *Fuel*. 42(5). 418-420.

3. MacCallum JR. Tanner J. (1970). Derivation of rate equations used in thermogravimetry. *Nature*. 225 (5238). 1127-1128.

4. Van Krevelen DW. Van Heerden C. Huntjons FJ. (1951). Physicochemical aspects of the pyrolysis of coal and related organic compounds. *Fuel*. 30. 253-259.

5. Wanjun T. Yuwen L. Hen Z. Cunxin W. (1993). New approximate formula for Arrhenius temperature integral. *ThermochimActa* 408. 39-43.

6. Madhusudanan PM. Krishnan K. Ninan KN. (1993). New equations for kinetic analysis of non-isothermal reactions. *ThermochimActa* 221 13-21.

7. Bilici A. Kaya İ. Yıldırım M. Doğan F (2010). Enzymatic polymerization of hydroxy-functionalized carbazole monomer. *Journal of Molecular Catalysis B: Enzymatic* 64. 89–95

Thermokinetic properties of semiconductive polypropylene matrix

Fatih DOĞAN[a,b], Kevser TEMİZKAN[a], İsmet KAYA[a]

*[a]Polymer Synthesis and Analysis Laboratory, Department of Chemistry, Çanakkale Onsekiz Mart University, Çanakkale, 17020, Turkey, *e mail:fatihdogan_tr@hotmail.com*
[b]Faculty of Education, Secondary Science and Mathematics Education, Çanakkale Onsekiz Mart University, 17100, Çanakkale, Turkey

Abstract

This paper presents thermokinetic properties of the semi-conducting polypropylene (PP) blended with of poly(1-amino-2-naphthol-4-sulfonic acid), (PANSA). PANSA were synthesized under different reaction conditions. PP matrix with PANSA was formed in twin screw extruder by melt blending method. The loadings of the conducting polymer into PP matrix were from 0.5 to 3.0 wt %. The conductivity of the thin films of PP/PANSA matrix was determined to be in the range of 10^{-9}-10^{-11} S/cm, showing its potential use in the electronic equipment. However, thermal decomposition kinetics of PP/PANSA matrix was investigated by TG. Thermokinetic properties were determined by nonisothermal analysis under nitrogen atmosphere at different heating rates of 10, 15, 20 and 25 ^{0}C/min. The thermal degradation of PP/PANSA matrix occurred only one stage process. The methods based on a single heating rate such as Coats-Redfern (CR), van Krevelen (vK), MacCallum-Tanner (MC), Madhusudanan-Krishnan-Ninan (MKN), Horowitz-Metzger (HM) and Wanjun-Yuwen-Hen-Cunxin (WHYC) was used to calculate the activation energy of thermal degradation. The thermodynamic parameters such as entropy change $\Delta H^{\neq}$, enthalpy change $\Delta S^{\neq}$ and Gibbs free energy $\Delta G^{\neq}$, related to the thermal decomposition was also calculated by TG technique. The activation energy values calculated from all of the methods, representing different classes, are found to be very close to each other.

***Keywords*:** activation energy; 1-amino-2-naphthol-4-sulfonic acid; thermal decomposition

Introduction

Heating process in thermogravimetric analysis (TG) may be either at constant temperature (isothermal) or by changing the temperature linearly in time (non-isothermal). A number of kinetic models were proposed in the literature using both kinds of heating process and kinetic modelling for non-isothermal heating process were classified by Flynn and Wall as follows:

i- Integral methods: Coats and Redfern method[1], Horowitz and Metzger method[2], Madhusudanan-Ninnan-Kirschan method[3], Wanjun-Yuwen-Hen-Cunxin method[4]
ii- Differential methods: van Krevelen method[5], Kissinger method, Friedman method

iii- Difference-differential methods: MacCallum-Tanner method[6].

Almost all of the methods mentioned above are based on expressions requiring high level of mathematical knowledge. One or more kinetic methods are used in determining kinetic parameters such as reaction order, *n*, activation energy, *E*, pre-exponential factor, *A* and thermodynamic parameters such as entropy change, $\Delta S^{\neq}$ of any material in investigation because of both difficulty in application of mathematical expressions and tedious and time-consuming processes related to the methods chosen for determining the thermal step parameters of any material. So, reliability of the result decrease because obtained kinetic and thermodynamic parameters are not compared to those obtained with various kinetic methods. Thus, in order to solve this problem an algorithm including all the aforementioned methods above can be suggested. This algorithm is also able to use isothermal and non-isothermal functions, to give the best decomposition mechanism, the best kinetic method according to linear regression coefficient of Arrhenius plots, and kinetic and thermodynamic parameters of oxidation reactions. In this work, we tested a software program called "**Thermal Analyses Version 1.0.0**" written in PHP web-developing language previously design by Doğan and Yürekli[7] using different series of Polypropylene/PANSA blends. Thermal behaviors of Polypropylene/PANSA blends and their solid-state decomposition kinetics were investigated from the thermogravimetric curves by using the software. Each method was used individually in the investigation.

Materials

Here, the polyaminonaphtol *sulfonic acid* particles were carried out in an aqueous basic medium. Therefore, *1-amino-2-hydroxy-naphthalene-4-sulfonic acid* (99%, ACS reagent), hydrogen peroxide (30% aqueous solution), potassium hydroxide (≥ 85%, ACS reagent, as pellet), hydrochloric acid (37%, AR grade) and all solvents used in the oxidative process were supplied from Merck Chem. Co. (Germany). Sodium hypochlorite (30% aqueous solution) was obtained from Paksoy Chemical Co. (Turkey). All the chemicals were used as received.

Synthesis of polyaminonaphtol *sulfonic acid* particles (PANSA)

The PANSA nanoparticles were synthesized by *oxidative polymerization technique* in an aqueous alkaline medium, as follows[8]. NaOCl *were used* as oxidants in *polymerization procedures* (Scheme 1). Trifunctional monomer, ANSA (0.24 g, 0.001 mol) was dissolved in an aqueous solution of 10 mL containing 0.1 M KOH (10%, 0.001 mol) at room temperature for 1 h. The reactions were performed by a dropping funnel containing a solution of NaOCl in a refluxing system. After completion of the reaction, the mixture was cooled to room temperature and then neutralized by the equimolar amount of HCl solution (10%, 0.001 mol). PANSA nanoparticles were precipitated as black-colored particles in powder form and then separated by filtration. The precipitated particles were washed with hot 50 mL water to separate the mineral salts and unreacted monomer and then dried in a vacuum oven at 45 °C for 24 h (yield: 86%).

IR: 3460, 3380 (Ar-NH_2), 3215(OH, intramolecular hydrogen bonding), 1674 (C=O), 1639 (C=N), 1578 (Ar), 1285, 1344 (C-N), 1381 (OH), 1218 (C-O), 1044, 1159 (SO_3), 725, 760 cm^{-1} (CH for substituted naphthalene ring)

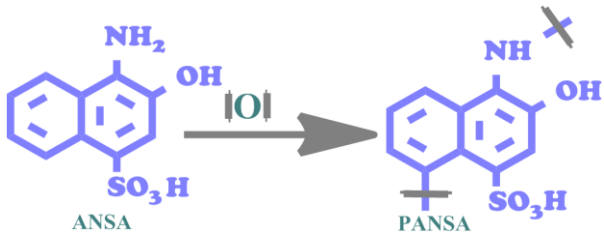

Scheme 1. Synthetic route for PANSA

Preparation of Polypropylene/PANSA (PP_n)

Polypropylene blends containing PANSA with of 0.5, 1 and 3 wt.% loading level ($PP_{0.5}$, PP_1 and PP_3) were prepared by means of a single-screw extruder (Collin E 30P, Ebersberg, Germany) which has a diameter of 30 mm and length to diameter ratio of 20. The mixing temperature rose from 190 ºC in the feed throat to 230 ºC in the die section of the extruder. All compounds were produced as approximately 70 µm thick and 10 cm wide films. All of the blends were prepared under same conditions.

Instrumental techniques

Thermogravimetric analysis was performed with TGA-DTA Perkin-Elmer Diamond system apparatus. The thermal measurements were carried out from the ambient temperature up to 1000 °C at heating rates of 5, 10, 15, 20°C /min. TGA-DTG and DTA curves were recorded in dynamic nitrogen atmosphere at a flow rate of 60 ml/min. For thermogravimetric analysis, the polymer sample was evaluated in the form of 4 mg weight. A platinum crucible was used as a sample container. Al_2O_3 was used as a reference material

Result and Discussion

The thermal decomposition of PP_n blends is adopted for the kinetic research. The kinetic analysis of PP_n blends was investigated by thermogravimetric analysis from ambient temperature to 1000 ^{0}C in N_2. Typical TG, DTG and DTA curves obtained at heating rates of 5, 10, 15 and 20 °C /min for all the blends are shown in Figure 1. The Energy of activation of thermal decomposition process for PP_n blends was performed by single heating rate kinetics. All TG curves of PP_n blends displayed that the thermal decomposition occurred mainly in one stages over the temperature range 310-560 ^{0}C with a mass loss nearly 96.7 % in weight. Also the corresponding DTA profiles presented two endothermic peaks for PP_n blends. The maxima of these peaks were attributed to the melting point and thermal decomposition of PP_n blends. All thermograms were repeated until a similar character. The influence of the heating rate on the kinetic and thermodynamic parameter related to the solid state decomposition kinetics was also determined. Thus, increasing the heating rate increased both the thermal degradation rate and the residual weight at 1000 °C, as well as initial degradation temperature

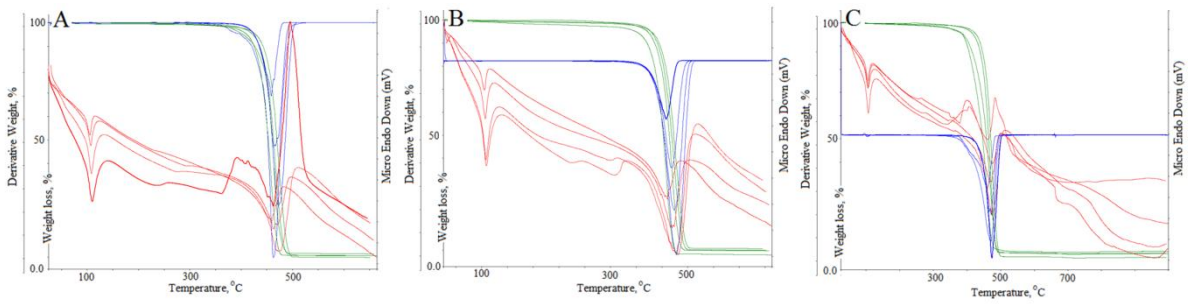

Figure 1. Typical TG, DTG and DTA curves for $PP_{0.5}$ (a), PP_1 (b) and PP_3 (c)

The decomposition processes obtained by the thermograms given in Figure 1 were similar in PP_n blends. The thermal stability in all the PP_n blends increased with an addition of PANSA into PP. The kinetic and thermodynamic data was obtained from TG curves at different heating rates of 5, 10, 15, 20 °C min^{-1}, and analyzed by the methods based on a single heating rate in the kinetic and thermodynamic calculations. The linearization straight of Arrhenius plots drawing form TG curves of PP_n blends was used to determined the kinetic parameter such as reaction order, *n*, activation energy, *E*, pre-exponential factor, *A*, as well as thermodynamic parameters such as entropy change $\Delta H^{\neq}$, enthalpy change $\Delta S^{\neq}$ and Gibbs free energy $\Delta G^{\neq}$. The kinetic parameters and thermodynamic parameters were calculated from CR, HM, vK, MC, MKN and WHYC methods by software. The algebraic expression of integral *g(α)* functions for the most common mechanism operating in solid-state decomposition tested in the present work are given below as.

The Coats-Redfern method

$$\ln[\frac{g(\alpha)}{T^2}] = \ln[\frac{AR}{\beta E}(1-\frac{2RT}{E})] - (\frac{E}{RT}) \quad (1)$$

The van Krevelen method

$$\ln g(\alpha) = \ln\left[\frac{A(0.368/T_m)^{\frac{E_a}{RT_m}}}{\beta(\frac{E_a}{RT_m}+1)}\right] + (\frac{E_a}{RT_m}+1)\ln T \quad (2)$$

The MacCallum-Tanner method

$$\log g(\alpha) = \log(\frac{AE}{\beta R}) - 0.4828E^{0.4351} - (\frac{0.449+0.217E}{10^{-3}T}) \quad (3)$$

Madhusudanan-Krishnan-Ninan method

$$\ln\left(\frac{g(\alpha)}{T^{1.9206}}\right) = \left[\ln\frac{AR}{\beta E} + 3.7678 - 1.92061\ln E\right] - 0.12040\left(\frac{E}{RT}\right) \quad (4)$$

Horowitz-Metzger method

By using Θ=T-Tm

$$\ln(g(\alpha)) = \ln\frac{AR T_m^2}{\beta E} - \frac{E}{RT_m} + \frac{E\theta}{RT_m^2} \quad (5)$$

Wanjun-Yuwen-Hen-Cunxin method

$$\ln\left(\frac{g(\alpha)}{T^{1.8946}}\right) = \left[\ln\frac{AR}{\beta E} + 3.6350 - 1.89461\ln E\right] - 1.0014\left(\frac{E}{RT}\right) \quad (6)$$

In the equations above, *g(α), T_m* , *E, R,* are the integral function of conversion, DTG peak temperature, activation energy and gas constant, respectively. The kinetic parameters can be calculated from the slope and intercept of the straight lines drawing for the left-hand side of kinetic equations (Eqs 1, 2, 3, 4, 5 and 6) against 1/T for above methods. Values of the kinetic parameters obtained for each decomposition stage in PP_n blends are listed in Table 1. The six different kinds of kinetic functions given in Table 1 are arranged by higher linear regression coefficient using the least squares method. The value of correlation coefficients of linearization curves obtained for the decomposition step of the PP_n blends was found to be approximately 1.00. On the other hand the thermodynamic parameters containing $\Delta G^{\neq}$, $\Delta H^{\#}$, $\Delta S^{\#}$, and $\Delta G^{\#}$, of the decomposition steps were also calculated from the following equations:

$$\Delta S^{\#} = 2.303\log\left(\frac{Ah}{kT}\right)R \;;\; \Delta H = E - RT;\quad \Delta G^{\#} = \Delta H - T\Delta S^{\#}$$

Where *h, T* and *A* are the Planck constant, temperature at the maximum rate of weight loss, pre-exponential factor. The kinetic and thermodynamic parameters related to solid state decomposition of the PP_n blends were calculated by the PC-software designed in our laboratory using PHP Web programming language. Thus, one should note that there is a good agreement between the results obtained for the activation energy of PP_n blends

Table 1. The Kinetic and thermodynamic data on the thermal decomposition step of PP_n

	$PP_{0.5}$ blend							PP_1 blend							PP_3 blend						
Heating rate	methods	*n*	E	lnA	$\Delta S^{\#}$	$\Delta H^{\#}$	$\Delta G^{\#}$	methods	*n*	E	lnA	$\Delta S^{\#}$	$\Delta H^{\#}$	$\Delta G^{\#}$	methods	*n*	E	lnA	$\Delta S^{\#}$	$\Delta H^{\#}$	$\Delta G^{\#}$
5 ^{0}C/dk	WHYC	2.1	180.3	-29.6	-587.5	186.6	416.3	WHYC	2.0	186.3	-38.1	-614.0	202.1	433.0	WHYC	1.7	216.8	-49.1	-723.6	175.6	498.96
	CR	2.1	180.3	-31.6	-591.3	186.8	414.5	CR	1.8	185.1	-37.8	-613.1	202.9	434.6	CR	1.8	215.3	-49.3	-723.7	174.3	497.2
	MC	2.1	179.4	-31.3	-596.1	184.3	416.0	HM	1.8	186.9	-37.2	-613.4	203.3	434.2	vK	1.8	215.1	-48.7	-725.6	173.7	497.6
	MKN	2.2	177.7	-31.7	-598.7	184.6	420.7	MKN	1.8	186.3	-37.0	-612.8	202.9	432.7	HM	1.8	214.7	-48.0	-723.3	173.8	497.7
	HM	2.2	177.0	-30.5	-595.3	185.7	420.2	MC	1.7	189.1	-36.2	-612.3	203.7	430.1	MKN	1.8	214.1	-47.1	-723.8	172.8	496.7
	vK	2.2	174.7	-31.1	-591.5	183.2	419.3	vK	1.7	188.8	-35.8	-613.0	202.7	432.2	MC	1.7	214.8	-46.2	-723.6	171.3	495.2
10 ^{0}C/dk	CR	2.1	184.8	-27.9	-607.6	174.7	428.2	MKN	2.1	189.1	-36.7	-618.7	198.0	447.8	CR	1.9	224.3	-40.0	-731.7	180.7	508.7
	MKN	2.1	183.4	-28.5	-604.4	177.5	434.6	CR	1.8	188.2	-35.5	-617.6	198.2	447.3	WHYC	1.9	224.3	-40.8	-733.4	179.2	507.7
	WHYC	2.1	181.7	-28.3	-608.5	176.7	436.1	MC	1.8	186.1	-35.8	-618.5	198.1	448.1	HM	1.9	223.7	-39.6	-732.6	179.2	506.2
	MC	2.1	181.3	-28.8	-605.3	177.0	438.9	vK	1.8	184.0	-34.6	-617.4	198.1	448.8	MKN	1.8	223.5	-39.3	-732.7	178.8	505.8
	HM	2.2	180.8	-28.1	-603.0	176.2	442.2	WHYC	1.7	183.5	-34.7	-615.3	198.1	446.2	MC	1.8	223.5	-38.4	-734.8	177.6	505.4
	vK	2.2	179.7	-29.7	-603.5	180.1	440.0	HM	1.7	181.8	-33.4	-613.7	197.8	443.5	vK	1.7	222.4	-38.2	-731.6	176.1	505.3
15 ^{0}C/dk	MC	2.2	196.7	-22.7	-612.8	162.1	437.5	CR	2.2	192.2	-33.1	-629.0	194.4	461.6	WHYC	1.9	228.0	-37.1	-743.1	164.0	519.61
	WHYC	2.2	196.2	-22.5	-611.2	163.3	436.1	WHYC	1.9	193.3	-33.7	-629.2	194.1	460.1	MKN	1.9	228.6	-36.7	-744.7	164.6	518.2
	vK	2.2	196.4	-22.9	-614.0	163.4	435.3	MC	1.9	194.0	-33.0	-629.1	192.2	459.7	CR	1.9	228.6	-36.1	-743.7	163.7	517.2
	CR	2.2	195.0	-22.7	-612.1	163.5	434.3	vK	1.8	192.5	-34.2	-627.3	192.6	457.3	HM	1.9	227.7	-36.8	-743.3	163.4	516.7
	HM	2.3	194.0	-23.8	-613.5	164.2	432.8	MKN	1.8	193.8	-33.7	-626.3	191.8	455.3	MC	1.9	227.0	-35.1	-743.8	164.8	514.3
	MKN	2.3	193.7	-24.1	-613.6	165.1	431.7	HM	1.8	191.1	-32.6	-625.7	190.7	457.2	vK	1.9	225.2	-34.6	-742.5	163.2	513.2
20 ^{0}C/dk	WHYC	2.2	195.4	-18.2	-632.7	151.2	441.8	WHYC	2.4	205.8	-27.3	-636.4	183.3	777.0	MKN	2.1	230.7	-34.7	-754.7	153.6	527.06
	CR	2.2	195.1	-17.3	-633.3	152.3	642.7	CR	1.9	204.1	-27.4	-635.8	182.3	782.9	WHYC	2.0	230.8	-34.3	-754.7	153.6	527.8
	MKN	2.2	195.7	-17.1	-634.4	152.3	642.3	MKN	1.9	203.8	-27.2	-634.0	183.8	783.3	MC	2.0	230.2	-33.4	-753.4	152.5	526.2
	MC	2.2	194.6	-17.7	-677.5	154.8	642.1	MC	1.9	201.7	-26.4	-633.1	182.0	783.0	CR	1.9	230.4	-33.2	-752.5	152.3	525.6
	HM	2.3	194.6	-18.6	-636.4	155.2	638.8	vK	1.9	200.0	-26.7	-633.7	181.7	780.6	vK	1.9	229.1	-32.7	-752.1	150.0	524.7
	vK	2.3	193.4	-17.3	-629.9	157.2	634.7	HM	1.8	201.3	-24.2	-632.5	180.0	778.7	HM	1.9	227.6	-30.4	-750.0	149.7	524.1

E, kJ mol^{-1}; lnA, s^{-1}; $\Delta S^{\#}$, J mol^{-1}K^{-1}; $\Delta H^{\#}$ and $\Delta G^{\#}$, kJ mol^{-1}

Conclusions

Polypropylene/PANSA blends involving different amounts (0.5, 1 and 3 wt%) of PANSA were prepared by melt-blending with a single-screw extruder. The effect of addition of PANSA on thermal decomposition process and kinetic parameters, such as activation energy and pre-exponential factor of Polypropylene/PANSA blends was studied. The kinetics of the thermal decomposition of blends was investigated by using the software from thermogravimetric analysis in dynamic nitrogen atmosphere at different heating rates. In determining the kinetic and thermodynamic parameters of the decomposition CR, HM, MC, vK, MKN and WHYC methods based on a single heating rate was used. Among these methods, the best one was examined according to the linear regression coefficient of Arrhenius plots. Accordingly,

The software so-called "**Thermal Analysis Version 1.0.0**." led to gathering a number of kinetic methods mentioned in the literature;

i- save both time and labor through obtaining the kinetic and thermodynamic parameters which used to be achieved by using tedious and time-consuming procedures by transferring the kinetic models into the computer prior to this software;

ii- and increasing the reliability of the results by means of more accurate comparisons of the kinetic and thermodynamic parameters obtained according to a wide variety of kinetic methods

On the other hand the activation energies of the thermal decomposition in N_2 by software were found to be approximately 190 kJ/mol for $PP_{0.5}$ blend, 195 kJ/mol for PP_1 blend and 220 kJ/mol for PP_3 blend.

Acknowledgments

This work was financially supported by the TUBITAK Grants Commission (Project No: KBAG- 113Z587).

References

1. Coats AW. Redfern JP. (1964). Kinetic parameters from thermogravimetric Data. *Nature*. Vol.201.68-69

2. Horowitz HH. Metzger G. (1963). Interpretation of thermogravimetric traces. *Fuel*. 42(5). 418-420.

3. Wanjun T. Yuwen L. Hen Z. Cunxin W. (1993). New approximate formula for Arrhenius temperature integral. *ThermochimActa* 408. 39-43.

4. Madhusudanan PM. Krishnan K. Ninan KN. (1993). New equations for kinetic analysis of non-isothermal reactions. *ThermochimActa* 221 13-21.

5. Van Krevelen DW. Van Heerden C. Huntjons FJ. (1951). Physicochemical aspects of the pyrolysis of coal and related organic compounds. *Fuel*. 30. 253-259.

6. MacCallum JR. Tanner J. (1970). Derivation of rate equations used in thermogravimetry. *Nature*. 225 (5238). 1127-1128.

7. Doğan F, (2006) "Development of a computer program related to the methods of kinetic analysis of Thermogravimetric data and its application to the kinetics of thermal decomposition and degradation of polymers, PhD. Thesis, Ege University, Izmir, Turkey.

8. Doğan F., Kaya İ. and Temizkan K., (2015), Synthesis route to regioselectively functionalized bifunctional polyarene, *Polymer International*, 64 (11), 1639–1648

XRD Raman analysis and optical properties of CdS and CdS:Ce films

T. Hurma[a*], S. Köse[b]

[a] Department of Physics, Anadolu University, TR-26470, Eskişehir, Turkey

[b]Department of Physics, Eskişehir Osmangazi University, TR-26480, Eskişehir, Turkey.

CdS and CdS:Ce films have been deposited by ultrasonic spray pyrolysis method. The effect of cerium incorporation on structural and optical properties of CdS films have been investigated. The XRD analysis showed that the hexagonal structure of CdS is not much affected with respect to Ce doping. The films exhibit the Raman peaks centered around 110, 294 and 590 cm^{-1} and the peak profiles are almost symmetric. The SEM measurements showed that the surface morphology of the CdS film was affected from the Ce incorporation. The optical properties of CdS:Ce film changed compared to CdS film. The average optical transmittance value of the CdS:Ce film was higher than CdS film in the visible region .

A Few Minute Microwave-assisted Chemical Bath Deposition of Nanotube Mg doped ZnO

M. Caglar[1], K. Gorgun[2], Y. Caglar[1], S. Ilican[1]

[1]*Department of Physics, Faculty of Science, Anadolu University,Eskisehir, Turkey*

[2]*Department of Chemistry, Faculty of Arts and Sciences, Eskisehir Osmangazi University,Eskisehir, Turkey*

E-mail :mcaglar@anadolu.edu.tr

As one of the noticeable materials, nanostructured zinc oxide (ZnO) has been significantly investigated for its versatile physical and chemical properties. Compared the deposition techniques used to obtain ZnO nanotubes, low-temperature solution growth process comes forward because of its simplicity and ease of fabrication. A rapid synthesis technique, known as, microwave-assisted chemical bath deposition (MW-CBD) is evolving in recent times for preparation of nanostructured films and particles. Doping process has been used to control the properties of semiconductors in most electronic devices. Especially for ZnO, Mg can be considered as an important dopant due to the similarity of ionic radii of Zn and Mg. In this work, Mg doped ZnO films having nanotube shaped surface morphology deposited by MW-CBD have been reported. Mg doped ZnO films were deposited on p-Si substrates using a MW-CBD method without any template. Zinc nitrate (ZnNt) and Magnesium nitrate (MgNt) were used as precursor materials and doping source materials, respectively. Doping precursor various amount of MgNt were 1%, 5% and 10%. The solution which in the Si substrate immersion was transferred into a CEM Mars 6 model microwave oven and irradiated at 900W for *5 min*. After MW treatment, the film was removed from the solution and rinsed with deionized water and dried under N_2 flow. To investigate the crystalline structure and the orientation of the films, XRD patterns were used. The lattice parameters and texture coefficient values of the films were determined. Field emission scanning electron microscope (FESEM) was used to analyze the surface morphology of the nanotube Mg doped ZnO (Figure 1).

Acknowledgements: This work was supported by Anadolu University Commission of Scientific Research Projects under Grant No. 1305F082 and 1402F055.

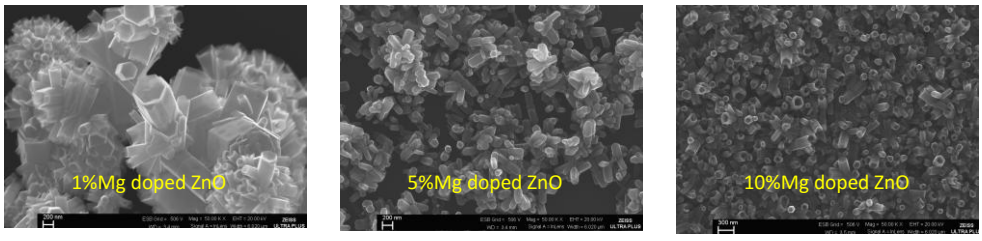

Figure 1. FESEM micrograph of the Mg doped ZnO

XPS Analysis of Electrodeposited grown F-doped ZnO rods

Saliha Ilican, Seval Aksoy, Yasemin Caglar and Mujdat Caglar
Department of Physics, Faculty of science, Eskisehir, Turkey
e-mail: silican@anadolu.edu.tr

In recent years, researchers have been investigated on electrodeposited ZnO films, but the effect of F doping in ZnO on the physical properties is less discussed. In this study, F-doped ZnO rods were grown by electrochemical deposition on p-Si and p-n heterojunctions consisting these rods were fabricated. Undoped and F doped ZnO were electrodeposited in a solution consist of $1x10^{-3}$ M of hexamethylenetetramine and zinc nitrate hexahydrate. Experiments were carried out in an environment with relatively low temperature of 90^{o}C, and deposition time and potentiostatic applied voltage were adjusted as 90min and -1,0V. p-Si substrate and Pt wire were used as working electrode and counter electrode respectively. Doping concentration was chosen to be 1 to 15%. SEM results showed that film surfaces have almost homogeneous consist of rods, and all rods exhibited flower like hexagonal shape. The X-ray photoelectron spectroscopy (XPS) results confirmed that the fluorine doping process was performed successfully into the ZnO film (Fig.1).

Acknowledgements: This work was supported by Anadolu University Commission of Scientific Research Projects under Grant No: 1207F118 and 1305F082.

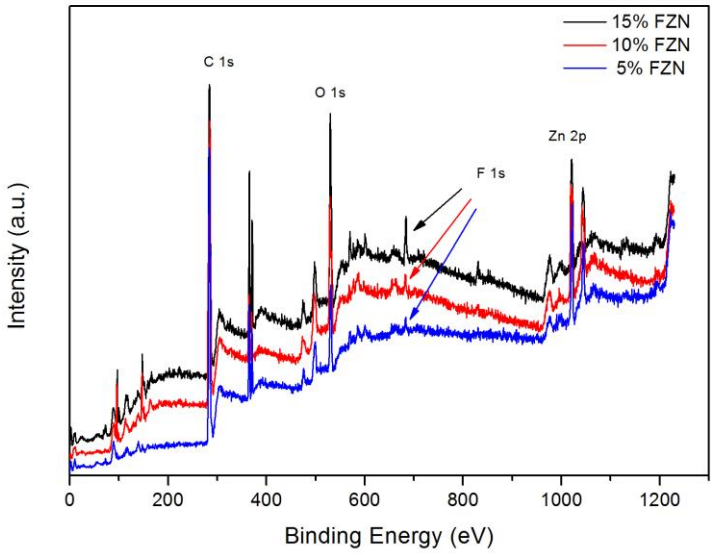

Fig.1. XPS survey scans for the films.

The Effect of Na Doping on Crystallinity and Microstructure Properties of ZnO Films by MW-CBD

S. Aksoy, Y. Caglar, S. Ilican and M. Caglar

Department of Physics, Faculty of Science, Anadolu University, Eskisehir, Turkey

e-mail: sevala@anadolu.edu.tr

Zinc oxide (ZnO) has received much attention because of its physical properties and common applications. Especially, ZnO exhibiting a wide optical band gap (3.37 eV), a large exciton binding energy (60 meV) at room temperature, a hexagonal wurtzite structure (c = 0.5207 nm, a = 0.3250 nm), high piezoelectricity and electrochemical coupling properties has received great attention.

The controlling of the structural and optical properties of the films is important to understand and improve the device applications. Various dopants are known to enhance the structural and optical properties of ZnO films. Among these doped films, Na doped ones have been prepared by means of various techniques such as sol–gel method [1], metalorganic chemical vapor deposition [2], RF sputtering method [3], thermal evaporation [4]. However, the Na doped ZnO film has not been deposited using electrochemical methods yet. Microwave synthesis is a synthesis method that is entirely different from the other method. In this method, a microwave diffuses to the material being heated volumetrically. It means that the microwave energy diffuses inside the sample. In the event of conventional heating a reverse of heat flow has occurred. The microwave synthesis offers the greatest possibility for energy saving, higher reaction rates, rapid volumetric heating, higher selectivity and higher yields of products [5, 6].

In this study, ZnO films that were doped with various Na concentrations were deposited using a microwave hydrothermal method onto p-Si substrates. In the production process of Na doped ZnO films, zinc acetate dihydrate ($Zn(CH_3COO)_2.2H_2O$) as the zinc cation precursor and, sodium nitrate ($NaNO_3$), as the sodium source were used. For the structural and morphological characterizations of the deposited films X ray diffraction (XRD) and Field Emission Scanning Electron Microscopy (FESEM) were used.

Acknowledgements: This work was supported by Anadolu University Commission of Scientific Research Projects under Grant No. 1305F082 and 1402F055.

[1] S. Ilican, Effect of Na doping on the microstructures and optical properties of ZnO nanorods, Journal of Alloys and Compounds 553, 255 (2013).

[2] M. Lei, H. He, Q. Yu, C. Chen, Y. Lu, Z. Ye, Optical properties of Na-doped ZnO nanorods grown by metalorganic chemical vapor deposition, Materials Letters160,547 (2015).

[3] W. Ko, S. Lee, G. Baek, J. P. Hong, Na mole concentration dependence on optical p-type behaviors of Na-doped ZnO nanowires, Current Applied Physics 14, 103 (2014).

[4] X. P. Yang, J. G. Lu, H. H. Zhang, Y. Chen, B. T. Kan, J. Zhang, J. Huang, B. Lu, Y. Z. Zhang, Z. Z. Ye, Preparation and XRD analyses of Na-doped ZnO nanorod arrays based on experiment and theory, Chemical Physics Letters 528, 16 (2012).

[5] Y. Caglar, K. Gorgun, S. Aksoy, Effect of deposition parameters on the structural properties of ZnO nanopowders prepared by microwave-assisted hydrothermal synthesis, Spectrochimica Acta Part A: Molecular and Biomolecular Spectroscopy 138, 617 (2015).

[6] T. Krishnakumar, R. Jayaprakash, Nicola Pinna, V.N. Singh, B.R. Mehta, A.R. Phani, Microwave-assisted synthesis and characterization of flower shaped zinc oxide nanostructures, Materials Letters 63, 242 (2009).

A Comparative Study on Undoped and Magnesium Doped ZnO Nanopowders

Yasemin Caglar[1], Kamuran Gorgun[2], Seval Aksoy[1], Mujdat Caglar [1]and Saliha Ilican[1]

[1]*Department of Physics, Faculty of science, Eskisehir, Turkey*

[2]*Department of Chemistry, Faculty of Arts and Sciences, Eskisehir Osmangazi University, Eskisehir, Turkey*

e-mail: yasemincaglar@anadolu.edu.tr

Recently, it has been widely studied Zinc oxide (ZnO) based materials due to the ZnO is a key functional oxide with unique properties. ZnO can be deposited using various techniques. Among these methods, microwave assisted hydrothermal synthesis (MW-HTS) is a simple and cost effective technique that can be produced homogeneous and high-quality powders. Compared with conventional methods, microwave irradiation requires very short reaction times, produces small inorganic particles with narrow particle size distributions, and consumes low energy. In this study, undoped, 1% and 5% Magnesium (Mg) doped ZnO nanopowders were synthesized via MW-HTS. The effect of Mg dopant on the structure and orientation of the ZnO nanopowders have been investigated by X-ray diffraction (XRD) study. For these measurements X-ray powder diffractometer was used. As seen the XRD spectra, all the samples exhibit polycrystalline nature. Field emission scanning electron microscope (FESEM) was used to analyze the surface morphology of the undoped and Mg doped ZnO nanopowders. Needle shaped rods are shown in the SEM images and depending on the doping concentration the diameters of these needles first slightly becomes larger and then the needle shape turns into hexagonal rod for 5% Mg doping ratio.

Acknowledgements: This work was supported by Anadolu University Commission of Scientific Research Projects under Grant No: 1305F082 and 1402F055.

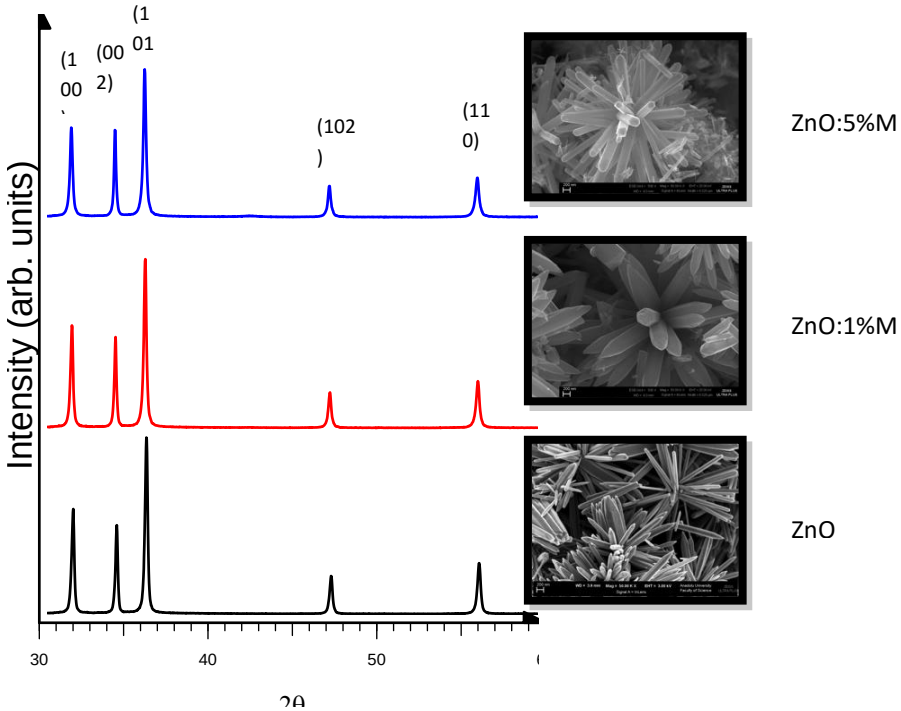

Fig. 1. XRD patterns and SEM images of nanopowders.

Ruthenium(II) complexes bearing 2,2'-pyridine-2,6-diylbis(5,6-dimethyl-1*H*-benzimidazole) ligands: Synthesis, characterization and applications on DSSC as dye

O. Dayan[1], A. Bilici[1], Z. Şerbetci[2], F. Yakuphanoğlu[3] and N. Özdemir[4]

[1]*Department of Chemistry, Faculty of Sciences and Arts, Çanakkale Onsekiz Mart University, Çanakkale, Turkey*

[2] *Department of Chemistry, Faculty of Sciences and Arts, Bingol University, Bingol, Turkey*

[3]*Firat University, Faculty of Arts and Sciences, Department of Physics, Elazig, Turkey*

[4] *Ondokuz Mayıs University, Faculty of Arts and Sciences, Department of Physics, Samsun, Turkey*

E-mail:osmandayan@comu.edu.tr

Tridentate benzimidazole ligands have attracted much attention because of their easily availability, low-toxicity and high complexation ability with transition metal ions. Because having high thermal stability, good catalytic performance and superior optical properties, their complexes are important. On the other hand, dye sensitized solar cells (DSSCs) have been under extensive research because of low-cost manufacturing process. In this work, a new ruthenium dye bearing 2,2'-pyridine-2,6-diylbis(5,6-dimethyl-1*H*-benzimidazole) ligands have been synthesized, and characterized with different techniques such as NMR, IR and UV-vis. Additionally, complexes was tested in DSSCs as dyes.

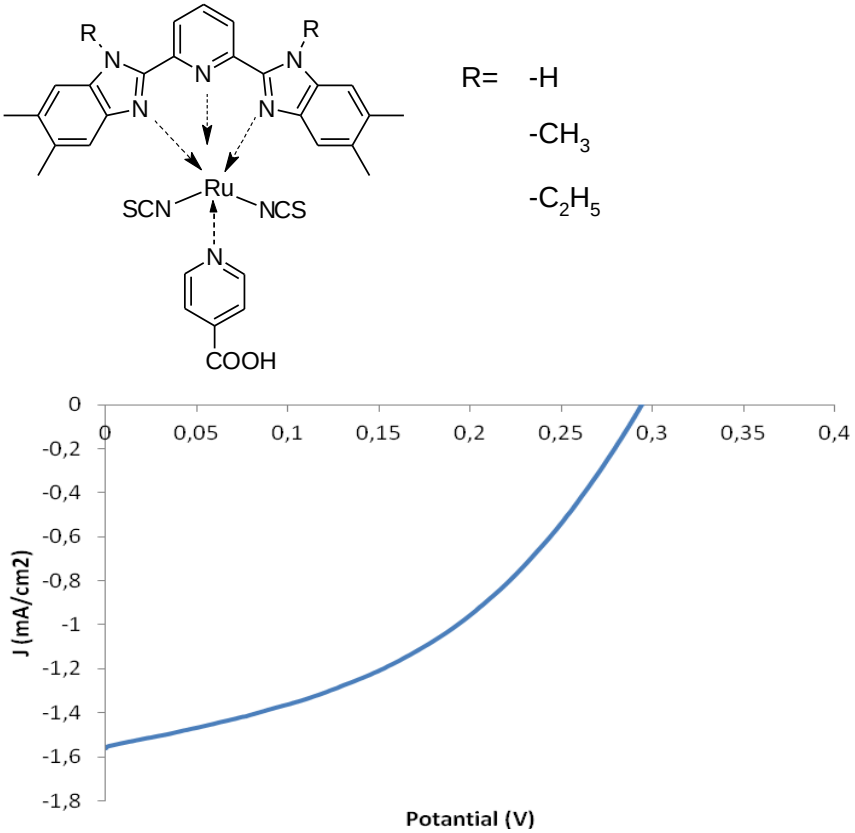

This research has been supported by The Scientific and Technical Research Council of Turkey (TUBİTAK) (Project No: 114Z439).

Preparation and Characterization of Poly (2-anilino-ethanol) Barium titanate Composites

E. Ahlatcıoğlu Özerol[1,3], B. Filiz Şenkal[1], M. Okutan[2] , A. Çelik Bozdogan[2],Y. Kaya[2]

[1]Istanbul Technical University, Department of Chemistry, Maslak, İstanbul/ TURKEY
[2]Yıldız Technical University, Department of Physics, Davutpaşa, Istanbul/ TURKEY
[3]Yıldız Technical University, Bioengineering Department, Maslak, Istanbul/ TURKEY

Conducting polymers are finding increasing number of applications in various semiconducting devices such as in chemical sensors, optical devices, etc. Among conducting polymers, polyaniline (PANI) has been investigated most extensively in the recent years since it can be synthesized easily, relatively cheaper, good chemical stability and sensitivity [1].

The electromagnetic properties of PANI can be modified by addition of inorganic fillers. Addition of magnetic particles may improve magnetic and dielectric properties of host materials. Therefore, PANI combined with magnetic particles provides materials exhibiting new properties [2]. Barium titanate ($BaTiO_3$) is a lead-free ferroelectric and piezoelectric material with a perovskite structure [3]. It exhibits various electrical and magnetic properties, of which the complex permeability and the complex permittivity, in particular, are important in determining their high frequency characteristics [4].

In this study, Poly (2-anilino-ethanol) (PANI-OH) has been synthesized in the presence of boric acid as a dopant and different weight percentage (1%, 2%, 5%, 10%) of Barium titanate ($BaTiO_3$). The obtained materials have been characterized by FT-IR, SEM, electrical and magnetical measurements. Dielectric properties of the composites have been investigated.

[1] Preparation and microwave adsorption properties of core–shell structured barium titanate/polyaniline composite, Jing Hongxia, Li Qiaoling, Ye Yun, Guo Zhiwu, Yang Xiaofeng, Journal of Magnetism and Magnetic Materials,332, (2013),10-14.

[2] N.Gandhi, K.Singh, A.Ohlan, D.P. Singh, S.K. Dhawan, Composites Science and Technology 71 (2011) 1754–1760

[3] M.H. Frey, D.A. Payne Physical Review B, 54 (1996), 3158

[4] Q.L. Li, C.R. Zhang, J.Q. Li Chinese Journal of Chemical Physics, 23 (2010), 603–607

Europium Based Composite Material as a Negative Dielectric Constant Medium

Z. Güven Özdemir[1], Ö. Aslan Çataltepe[2], N. Yilmaz Canli[1],, M. Kılıç[1], Y. Karabul[1], M. Okutan[1], Ü. Onbaşlı[3]

[1] Department of Physics, Yıldız Technical University,34210 Esenler, Istanbul, Turkey.
[2] Faculty of Engineering, Gedik University, 34876, Istanbul, Turkey.
[3] Department of Physics, Marmara University, Rıdvan Paşa Cad., Gülhane Sok. 4/12, 34730, Göztepe, İstanbul, Turkey.
E-mail : zguvenozdemir@yahoo.com , zguven@yildiz.edu.tr

In recent years, there have been an increasing number of researches in developing novel negative dielectric constant (NDC) materials [1,2]. A NDC material is considered as the fundamental step for producing metamaterial and artificial negative refractive index materials. NDC materials have been used in wide variety of technological applications such as electromagnetic shielding, optical power limiting, electromagnetic cloaking devices, perfect absorbers, non-destructive sensors etc. In this respect, we have focused on searching NDC property for Europium based copper oxide layered composites. In the present study, the room temperature dielectric properties of $EuBa_2Cu_3O_{7+x}$ (Eu-123) have been investigated by HP-4194A Impedance Analyzer. It has been determined that the Eu-123 has NDC in low frequency radio wave band. Moreover, it has been observed that the loss tangent decreases in the same frequency region. We have also investigated the Nyquist plot in complex impedance plane and ac conductivity mechanism of the sample. The impact of magnetic field varying from 0-4kG on dielectric properties has also been investigated.

[1] S. Anantha Ramakrishna,Tomasz M. Grzegorczyk, Physics and Applications of Negative Refractive Index Materials, CRC Press, Taylor & Francis Group, Bellingham, Washington,USA (2008).

[2] Q. Hou, K. Sun, P. Xie, K. Yan, R. Fan, Y. Liu, Ultrahigh dielectric loss of epsilon-negative copper granular composites, Mater. Lett, 169, 86 (2016).

This research has been supported by Yıldız Technical University Scientific Research Projects Coordination Department with the Project Number 2014-01-01-GEP04.

The Influence of Poly(3,4-ethylenedioxythiophene)-poly(styrenesulfonate) doping on the Impedance Spectra of NiPc Thin Films

B.Süngü Mısırlıoğlu, Z. Güven Özdemir, and A. Altındal
Department of Physics, Yildiz Technical University, Istanbul, Turkey
E-mail : banu@yildiz.edu.tr

In recent years, electronic device applications have been mainly focused on semiconducting thin film organic materials. Especially, metal-centered Phthalocyanine (MPc) thin films have a promising potential for new generation electronic device implements due to their great processability, chemical stability and very sensitive electrical properties to temperature, dopant material and gas environments. From this point of view, this work has been devoted to investigate the effect of doping concentrations of Poly(3,4-ethylenedioxythiophene)-poly(styrenesulfonate) on the impedance spectra of pure NiPc thin films. The impedance spectra of thin film of NiPcs have been investigated within the frequency interval of 5 Hz- 13 MHz for the temperatures increasing from 25^{o}C to 140^{o}C. It has been observed that while impedance, resistance and capacitive reactance values remarkably decrease, conductivity exhibits an increasing behavior with both increasing temperature and doping concentration. Furthermore, the complex plane representation of impedance i.e. Nyquist curves, show semi-circles with decreasing diameters as the temperature increases. It has been also pointed out that the time constants for all compositions decrease with increasing temperatures. Ultimately, all these results suggest that doping Poly(3,4-ethylenedioxythiophene)-poly(styrenesulfonate) to NiPc improves the electrical properties of the material especially at high temperature region.

Preparation and Polymerization of 2-hydroxy aniline and Investigation of Electro-optical Properties

Fatma Tuba Çoğalmış[1], Burak Korkmaz[1], Mustafa Okutan[2], Bahire Filiz Senkal[1], Esma Ahlatcıoglu[1]

[1]Istanbul Technical University, Department of Chemistry, Maslak, İstanbul/TURKEY

[2]Yildiz Technical University, Department of physics, Davutpasa, İstanbul/TURKEY

The semiconducting and conducting polymers, which have conjugated structure such as polyaniline, polypyrrole and polythiophene, have been used in an increasing number of applications [1].

PANI is one of the most promising conducting polymers because of its remarkable chemical stability, facile synthetic route and relatively high electrical conductivity [2].

In this study, 2-hydroxy aniline was polymerized oxidatively by using $NH_4S_2O_8$ as an oxidant in the presence of HBr and HCl as dopant agents. derivative. Polymerization of the chalcon based monomer was carried out HBr as dopant and as oxidant.

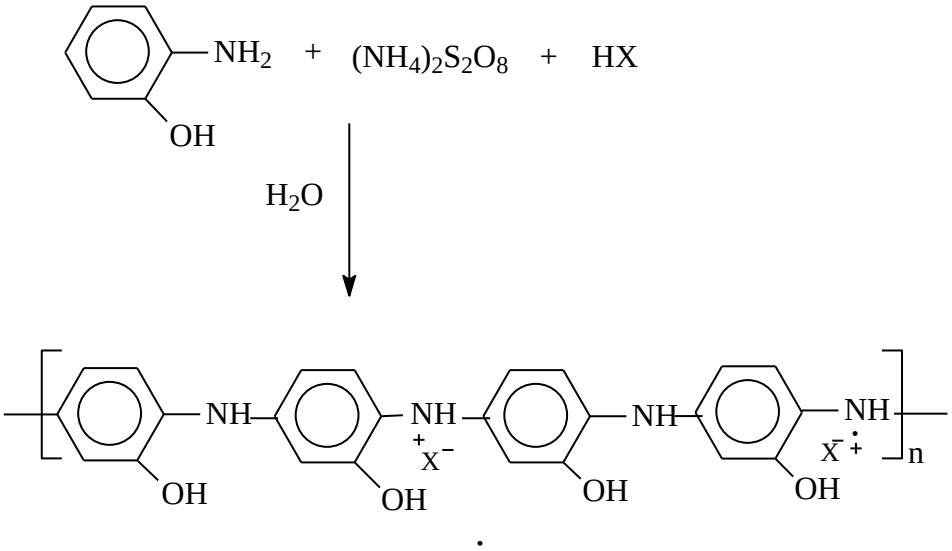

Scheme 1. Preparation of poly (2-hydroxy aniline)

Electro-optical properties of the polymer were investigated. The enhancement of the optical and electrical properties of the system was studied by impedance spectroscopy and four point probe technique.

[1] R.S. Sethi, M.T. Goosey, In:J.A. Chilton, M.S. Goosey, Editors, Special polymer for electronic and optoelectronic, London, Chapman and Hall, 1995.

[2] A.G. MacDiarmid, Curr. Appl. Phys. 1 (4–5) (2001) 269.

Electrochemical investigation of 5,5'-(pyrimidine-4,5-diyl)bis(1,3,4-thiadiazole-2-amine) films on mild steel in acidic media

Ramazan Solmaz, Ahmet Çetin
Bingöl University, Science and Letters Faculty, Chemistry Department, 12000, Bingöl, Turkey
E-mails: rsolmaz@bingol.edu.tr, acetin74@hotmail.com

Abstract

In this study, a mild steel specimen was exposed to 1 M HCl solution in the absence and presence of 1.0 mM 5,5'-(pyrimidine-4,5-diyl)bis(1,3,4-thiadiazole-2-amine) (PBTA) for 1 hour and corrosion protective properties of a film of the organic compound formed on the mild steel surface was electrochemically investigated. For this aim, the change of open circuit potential as a function of exposure time (E_{ocp}-t), potentiodynamic polarization, electrochemical impedance spectroscopy (EIS) and linear polarization resistance (LPR) techniques were used. It was found that PBTA forms a very protective organic film on the steel surface. The inhibition efficiency of the inhibitor was higher than 95%. This inhibitor acts by reducing the rates of both anodic metal dissolution and cathodic hydrogen evolution reactions.
Keywords: 5,5'-(pyrimidine-4,5-diyl)bis(1,3,4-thiadiazole-2-amine), mild steel, electrochemical impedance spectroscopy, corrosion inhibition.

1. Introduction

The adsorption of organic molecules, which have heteroatoms such as sulfur, nitrogen or oxygen as well as double and triple bonds, the metal/solution interface is of great interest in surface science. The investigation of adsorbed species on metal surfaces is very important in developing and understanding of electrochemical studies such as double layer, electroorganic synthesis, electrokinetics and electrocatalysis [1, 2]. The adsorption of organic compounds on metal surface can significantly change the corrosion resisting properties of metals. Therefore, investigation of the relation between the adsorption and corrosion inhibition is of great importance. The existing data show that organic compounds having heteroatoms with high electron density are effective corrosion inhibitors [3-8].

Organic inhibitors act generally by adsorption and a film formation on surface of metals. Their adsorption on metal surface takes place generally via physical of chemical adsorption mechanism. Electrochemical technics, especially EIS is a very sensitive technique to determine behavior of adsorbed films at the metal/solution interface.

In this study, corrosion protective property of PBTA film formed at the metal/solution interface was investigated by electrochemical techniques.

2. Experimental

The working electrode was a mild steel specimen, which was cut from a cylindrical mild steel disc to a length of about 5 cm. The mild steel electrode was covered with a polyester block except its only bottom surface, which has 0.785 cm^2 surface area. The surface of the steel was mechanically abraded using different grades of sand papers, which ended with the 1200 grade. Then, the electrodes were washed with distilled water and ethanol, immersed into the ultrasonic bath to remove possible corrosion products or metal particles from the surface, washed once again with ethanol and water. After drying with a filter paper, they were immersed into the test solutions as quickly as.

The electrochemical tests were performed in 1 M HCl solution in the absence and presence of 1.0 mM PBTA. The molecular structure of PBTA is given in Fig. 1. The corrosive solutions were opened to

atmosphere, and the temperature was controlled thermostatically at 298 K during the electrochemical measurements.

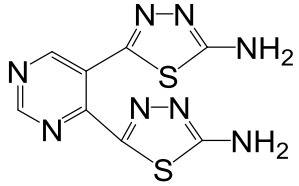

Fig. 1. Chemical structure of PBTA

The potentiodynamic polarization curves, EIS and LPR measurements were carried out using a CHI 660D A.C. Electrochemical Analyzer under computer control. An electrochemical cell with a three-electrode configuration was used. The auxiliary and reference electrodes were a platinum sheet with 2 cm^2 surface area and an Ag/AgCl (3 M KCl), respectively. All potential values in this study were given versus to this electrode. The working electrode was immersed in test solution for 1 h to establish steady state open circuit potential (E_{ocp}). After reaching a steady-state E_{ocp}, the electrochemical measurements were performed. The potentiodynamic polarization curves were obtained by scanning potential from cathodic potentials to the anodic domain. Scan rate was 1 mV s^{-1}. The EIS experiments were conducted in the frequency range from 100 kHz to 0.01 Hz at open circuit potential. The amplitude was 5 mV. LPR measurements were carried out by recording the electrode potential ±0.010 V around open circuit potential with 1 mV s^{-1} scan rate. The polarization resistance (R_p) was determined from the slope of the obtained current-potential curves.

3. Results and discussion

In Fig. 2, potentiodynamic polarization curves of mild steel in 1 M HCl solution without and with the addition of 1.0 mM inhibitor are shown. As it is seen from these lines, the addition of PBTA to 1 M HCl solution reduces current density. This results show that this compounds could protect the steel corrosion in this media most probably by forming a protective film over the surface. This film inhibits both hydrogen evolution reaction and metal dissolution. However, the reduction in cathodic cthodic currents is more pronounced. Corrosion potential of the steel in the absence and presence of PBTA slightly shifted to a cathodic potential. Therefore, it can be concluded that this compound is a as mixed type corrosion inhibitor with predominantly cathodic one.

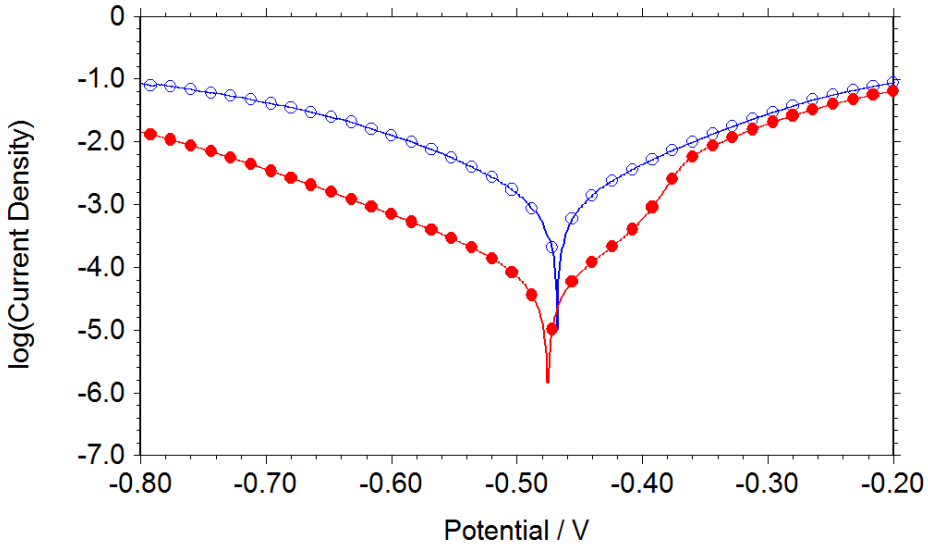

Fig. 2. Potentiodynamic polarization plots of mild steel in 1 M HCl solution in the absence (○) and presence of 1 mM PBTA (●)

Corrosion current densities (i_{corr}) were determined by the extrapolation of the linear portions of the current-potential curves to the corresponding corrosion potentials. The i_{corr} values in the absence and presence of the inhibitor are 0.762 and 0.028 mA cm^{-2}, respectively. The inhibition efficiency (I %) was calculated from the corresponding current densities according to following equation;

$$I\% = \left(\frac{i_{corr} - i'_{corr}}{i_{corr}} \right) x100 \qquad (1)$$

where, i_{corr} and i'_{corr} are corrosion current densities in the absence and presence of the inhibitor, respectively. It was found that this compound has 96.3% inhibition efficiency. The great inhibition efficiency was explained by formation of a protective organic film on the metal surface.

According to Fig. 2, the cathodic current-potential curves are almost parallel which suggests that the reaction is activation controlled and the addition of PBTA to the corrosive solution does not modify the hydrogen evolution mechanism, and the reduction of H^+ ions at the mild steel surface take place mainly through a charge transfer mechanism [9, 10]. However, the anodic reaction in the presence of the inhibitor is potential-dependent. In the low anodic overpotentials, PBTA inhibits metal dissolution reaction remarkably. However, anodic current density starts to increase after -0.40 V most probably due to the excess dissolution of iron, which leads to removing the film from the metal. The similar results have also been reported in literature for the corrosion inhibition of the metals with the formation of a protective layer of adsorbed inhibitor molecules at the metal surface [11].

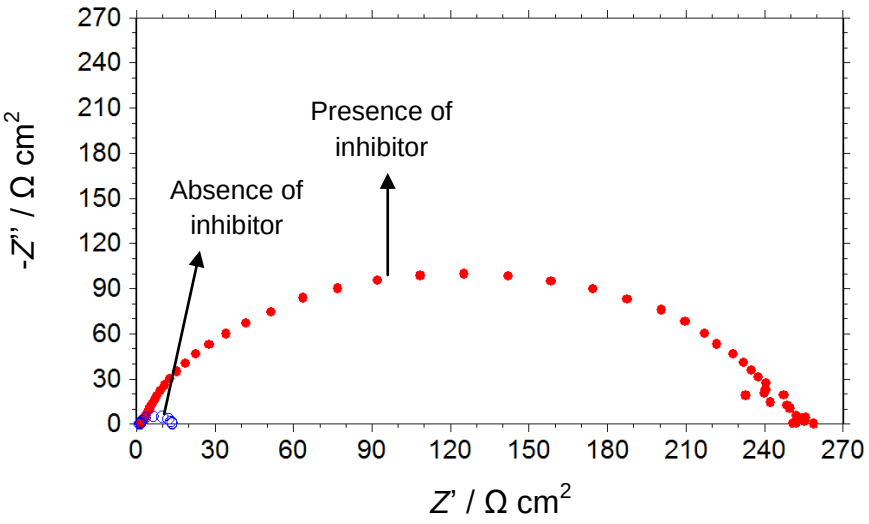

Fig. 3. Nyquist plots of mild steel in 1 M HCl solution in the absence (○) and presence of 1 mM PBTA (●)

Nyquist plots of mild steel are given in Fig. 3. Nyquist plot of the steel in the absence of the inhibitor shows a capacitive loop at high and low frequencies and followed an inductive loop at low frequencies. The high and medium frequency behaviors suggest that corrosion reaction is charge transfer controlled [12]. It is clearly seen from the plots that the diameter of Nyquist plot considerably increases after the addition of the inhibitor. This observation is an indicative of formation of an inhibitor film at the metal/solution interface. The diameter of Nyquist plots is generally assigned to the polarization resistance (R_p). The polarization resistance of the mild steel greatly increases after the addition of the inhibitor.

The polarization resistance of the steel in the absence and presence of the inhibitor was calculated using LPR technique. In this technique, the R_p was calculated from the slope of the current-potential curves according to following equation:

$$R_p = \frac{S\mathrm{d}E}{\mathrm{d}i} \quad (2)$$

where, S is the surface area of the electrode which was exposed to the electrolytes, E is the difference in applied potential and di is the difference in the current. The R_p values are 11.5 and 255 Ω cm^{-2}, respectively. The I % was calculated from R_p using the following equation;

$$I\% = \left(\frac{R_p^{'} - R_p}{R_p^{'}} \right) x100 \quad (3)$$

In this equation, R_p and $R_p^{'}$ are polarization resistance of the steel in the absence and presence of PBTA, respectively. The inhibition efficiency of PBTA was found to be 95.5%. The high inhibition efficiency of PBTA could be explained by formation of a protective film formation on the metal surface and blocking the surface against the corrosive attack.

E_{ocp} of working electrode was conducted with exposure time and plotted in Fig. 4. As it is seen from Fig. 4 that the addition of PBTA to 1 M HCl solution shifts the E_{ocp} of the steel to more positive potentials, which is indicative of a protective film formation on the metal surface. E_{ocp} values of the steel in both inhibited and un-inhibited solutions nearly remained constant after 1 h exposure. An initial increase in the absence of the inhibitor could be assigned to the dissolution of active metal from the surface.

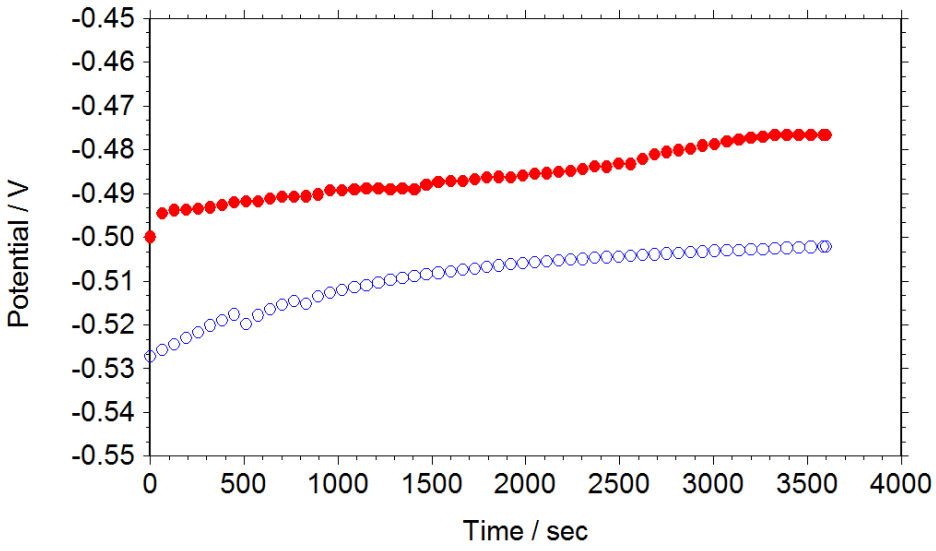

Fig. 4. Chang of open circuit potentials of mild steel in 1 M HCl solution in the absence (○) and presence of 1.0 mM PBTA (●) as a function of time.

4. Conclusions

Mild steel was exposed to 1 M HCl solution in the absence and presence of 1 mM 5,5'-(pyrimidine-4,5-diyl)bis(1,3,4-thiadiazole-2-amine) (PBTA) for 1 hour and corrosion protective properties of a film of the organic compound formed on the mild steel surface was electrochemically investigated. Following conclusions could be highlighted from the obtained data;

1. The PBTA is a good corrosion inhibitor for mild steel corrosion in HCl solution.
2. PBTA inhibits both anodic and cathodic reactions with predominantly first one.

3. The high inhibition efficiency of PBTA was explained by its adsorption on the metal surface and a protective film formation.

Acknowledgements

The authors are greatly thankful to Bingöl University Scientific Research Projects (BÜBAP) Coordination Unit and Bingöl University Central Laboratory.

References

[1] M. Özcan, R. Solmaz, G. Kardaş, I. Dehri, Adsorption properties of barbiturates as green corrosion inhibitors on mild steel in phosphoric acid, Colloid Surface A 325, 57 (2008).
[2] O. K. Abiola, Adsorption of 3-(4-amino-2-methyl-5-pyrimidyl methyl)-4-methyl thiazolium chloride on mild steel, Corros. Sci. 3078, 48 (2006).
[3] I.B. Obot, N.O. Obi-Egbedi, S.A. Umoren, Antifungal drugs as corrosion inhibitors for aluminium in 0.1 M HCl, Corros. Sci. 51, 1868 (2009).
[4] R. Solmaz, E. Altunbaş, G. Kardaş, Investigation of adsorption and corrosion inhibition effect of 1,1'-Thiocarbonyldiimidazole on Mild Steel in Hydrochloric Acid Solution, Prot. Met. Phys. Met. 47, 262 (2011).
[5] A. Chetouani, A. Aouniti, B. Hammouti, N. Benchat, T. Benhadda, S. Kertit, Corrosion inhibitors for iron in hydrochloric acid solution by newly synthesized pyridazine derivatives, Corros. Sci. 45, 1675 (2003).
[6] S.A. Abd El Maksoud, Studies on the effect of pyranocoumarin derivatives on the corrosion of iron in 0.5 M HCl, Corros. Sci. 44, 803 (2002).
[7] G. Kardas, R. Solmaz, Electrochemical investigation of barbiturates as green corrosion inhibitors for mild steel protection, Corros. Rev. 24, 151 (2006).
[8] A. Doner, E.A. Sahin, G. Kardaş, O. Serindağ, Investigation of corrosion inhibition effect of 3-[(2-hydroxy-benzylidene)-amino]-2-thioxo-thiazolidin-4-one on corrosion of mild steel in the acidic medium, Corros. Sci. 66, 278 (2013).
[9] L. Li, X. Zhang, J. Lei, J. He, S. Zhang, F. Pan, Adsorption and corrosion inhibition of Osmanthus fragran leaves extract on carbon steel, Corros. Sci. 63, 82 (2012).
[10] M. Lebrini, M. Lagrenee, H. Vezin, L. Gengembre, F. Bentiss, Electrochemical and quantum chemical studies of new thiadiazole derivatives adsorption on mild steel in normal hydrochloric acid medium, Corros. Sci. 47, 485 (2005).
[11] F. Bentiss, M. Traisnel, H. Vezin, H.F. Hildebrand, M. Lagrenee, 2,5-Bis(4-dimethylaminophenyı)-1,3,4-oxadiazole and 2,5-bis(4-dimethylaminophenyl)-1,3,4-thiadiazole as corrosion inhibitors for mild steel in acidic media, Corros. Sci. 46, 2781 (2004).
[12] Q.B. Zhang, Y.X. Hua, Corrosion inhibition of mild steel by alkylimidazolium ionic liquids in hydrochloric acid, Electrochim. Acta 54, 1881 (2009).

Kinetics Analysis for Isothermal and Nonisothermal Decomposition of 5 Aminoquinoline Oligomers

Fatih DOĞAN[a], Ali BİLİCİ[b], , İsmet KAYA[b]

[a]*Çanakkale Onsekiz Mart University, Faculty of Education, Secondary Science and Mathematics Education 17100, Çanakkale,*
[b]*Çanakkale Onsekiz Mart University, Faculty of Sciences and Arts, Department of Chemistry, Polymer Synthesis and Analysis Lab. 17020 Çanakkale, Turkey*
e-*mail:alibilici@hotmail.com ; fatihdogan_tr@hotmail.com*

ABSTRACT

In our last work, we reported the enzyme catalyzed oxidation of 5 amino quinoline compound. The some physical and chemical properties of obtained oligomers (OAQ) were also presented in that study. In here we aimed to investigate the thermal decomposition kinetics of 5-aminoquinolone oligomers under both isothermal and nonisothermal conditions using TG-DTG and DTA data. The data obtained were analyzed using various solid state reaction models. For this, a PC program designed by Dogan and Yürekli was used to determine the kinetic parameters. The activation energy values determined from these methods were very close with each other. The nonisothermal decomposition kinetics of OAQ was conducted in nitrogen atmosphere in various heating rates: 5, 10, 15 and 20 ºC/min. The activation energies determined by Kissinger ve Kim-Park methods were 191.4 and 201.5 kJ/mol, respectively. Isothermal decomposition kinetics of OAQ was also studied at 325, 330 ve 335 ºC using Flynn method and the activation energy was found to be 211,44 kJ/mol.

Keywords: 5-aminoquinoline, thermal analysis, nonisothermal decomposition, oxidation

To whom all correspondence should be addressed.

Phone: +90 286 218 00 18 Fax: +90 286 218 05 33 e-mail: fatihdogan_tr@hotmail.com, alibilici66@hotmail.com.

1. Introduction

Polyquinolines were studied since 1970 due to their excellent optical, electrical, thermal and mechanical properties[1] The polyquinolines were obtained different strategies including Suzuki coupling, Sonogashira reaction, oxidative coupling and Friedlander synthesis[2]. Among them, Friedlander protocol was effectively used to obtained the polyquinolines having interesting physical properties[3]. However, these methods need multiple-step monomer synthesis. In addition, the solubilities of products were low. The rigid polymer structures don't allow structural modifications[4]. Due to these limitations, alternative routes are highly demanded to synthesize polyquinoline-type materials.

Enzymatic polymerization is green chemical process. The polymers can be synthesized in gram scale in one step and reactions proceed under mild reaction temperatures and atmosphere. Therefore this method is accepted as one of the alternative routes [5].

In our last work, we report the enzyme (Horse Radish Peroxidase) catalyzed oxidation of 5-amino quinoline for the first time [6]. The structure of obtained oxidation product was determined by different spectroscopic techniques.

In this work, we studied the thermal decomposition kinetics of 5-aminoquinoline oligomers (5AQPH) under both isothermal and nonisothermal conditions using TG-DTG and DTA data.

2. Materials and Methods

2.1. Measurements

Thermal data were obtained by using Perkin Elmer Diamond thermal analysis. The TG-DTA measurements were made within 25–1000 ºC range, operating in dynamic mode, with the following conditions: sample weight of 5mg, heating rates of 5, 10, 15, and 20 0C/ min, atmosphere of nitrogen, and sealed platinum pan. All the experiments were performed twice for repeatability and the results showed good reproducibility with small variations in the kinetic parameters. a PC program designed by Dogan and Yürekli was used to determine the kinetic parameters [7]

2.2.Kinetic triplets

The rate of a general homogeneous reaction of the form A→B+C is conventionally measured by following the decrease in concentration of reactant A or the increase in concentration of either product B or C at constant temperature. The rate coefficient, *k*, is a function of temperature:

$$\mathbf{k} = \mathbf{A}\mathbf{T}^{m}\ e^{-E/RT} \qquad (1)$$

and by carrying out a series of experiments over a range of different but constant temperatures, the Arrhenius parameters, *E* the activation energies and *A* the pre-exponential or frequency factor, can be determined. In thermal analysis the reactions studied are almost invariable heterogeneous reactions and the reaction temperatures is usually being continuously increased or decreased according to some set (usually linear) program. In spite of these differences, much effort has been directed at obtained kinetic information from the results of thermal analysis experiments. Numerous have appeared and are still appearing on this topic and it is a field of considerable controversy. What follows is only an introductory and fairly selective account of some of the problems and the approaches suggested for their solution. Several researchers such as Flynn-Wall-Ozawa (FWO), Tang, Kissinger-Akahira-Sunose (KAS), Kissinger and Friedman put forward some mathematical relations for ensuring of kinetic information in solid-state non-isothermal decomposition reactions. Their expression are generally given as below

Flynn-Wall-Ozawa method[8]

In order to determine the kinetic parameter (*E* and *A*), Ozawa suggested the following procedure.

$$\log \beta = \log (AE/R) - \log g(\alpha) - 2.315 - 0.4567\ E/RT \qquad (2)$$

The activation energy *E* can be obtained from the slope of the regression line by the plotting of log *β* versus 1/*T*.
Tang method [9]
The following equation using an approximation formula can be expressed:

$$\ln\left(\frac{\beta}{T^{1.894661}}\right)=\ln\left(\frac{AE}{Rg(\alpha)}\right)+3.635041-1.894661\ln E-\frac{1.001450E}{RT} \quad (3)$$

The plots of versus 1/*T* give a group of straight lines. The activation energy *E* can be obtained from the slope -1.001450 *E/R* of the regression line.
Kissinger-Akahira-Sunose method[10]
The Kissinger-Akahira-Sunose (KAS) method employs the Coats-Redfern approximations and are given as below

$$\ln\left[\frac{\beta}{T^2}\right]=\ln\left[\frac{AR}{E\,g(\alpha)}\right]-\frac{E}{RT} \quad (4)$$

The value of E can be evaluated by plotting the left side of the equation versus 1/RT

Kissinger method[11]
Kissinger method uses below equation without know the solid state decomposition reaction mechanism for thermal degradation kinetic.

$$\ln(\frac{\beta}{T_{\max}^2})=\left\{\ln\frac{AR}{E}+\ln[n(1-\alpha_{\max})^{n-1}]\right\}-\frac{E}{RT_{\max}} \quad (5)$$

The activation energy *E* can be obtained from the plots of the left side versus $1/T_{max}$

Friedman method[12]

This method is a differential isoconversional method derived for thermal degradation kinetic based on Arrhenius expression.

$$\ln(\frac{d\alpha}{dt})=\ln(A)+n\ln(1-n)-\frac{E}{RT} \quad (6)$$

The dependence of the left side of equation on 1/*T*, calculated for the same *α* values at the different heating rates *β* can be used to calculate the activation energy.
In the equations *β, T_{max},* α, *g(α), β, Tm, E, A,* and *R* are, respectively, heating rate, temperature related to maximum reaction rate, degradation fraction, integral function of degradation, heating rate, pre-exponential factor and gas constant

3. Results and Discussion

3.1. Thermal decomposition process

The solid state thermal decomposition of OAQ was selected for the kinetic study. The activation energy of the thermal decomposition process was calculated by multiple heating rate kinetics. The typical TG/DTG thermograms obtained for OAQ in N_2 atmosphere are shown in Figure 1**.** The plots of conversion degree versus temperature by thermograms were drawn. All TG curves of OAQ displayed that the thermal decomposition occurred mainly in one stage over the temperature range 105.6-519.6 ^{0}C with a mass loss of 48.4 %. .From the DTG curves, the temperatures related to the maximum decomposition rates for decomposition stages of OAQ was found to be 330.2, 340.4, 346.9 and 351.8 ^{0}C, respectively.

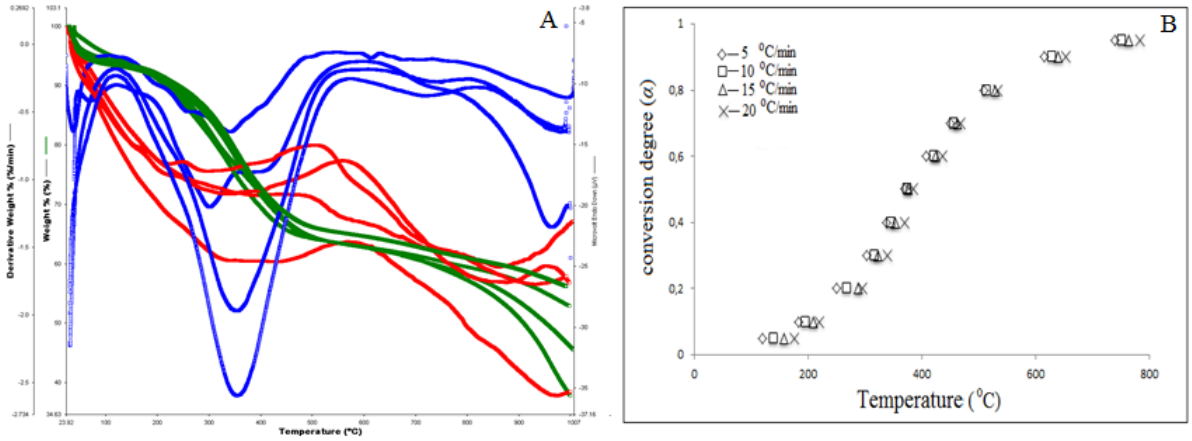

Figure 1. Corresponding TG/DTG and DTA curves at heating rates of 5, 10, 15, and 20 ^{0}C/ min (a) and α-T curves for OAQ (b).

3.2. Determination of activation energy, E

In order to the solid state decomposition kinetics of OAQ in this work the five different methods was used. These were those of FWO, KAS, Tang, FR and CR methods based on multiple heating rates. In here, isoconversional methods being independent of any thermo-degradation mechanisms have been initially used to investigate the decomposition kinetics of OAQ. From this point, Kissinger and Kim-Park methods didn't require any mechanism information. Here from, activation energies for thermal decomposition stage were determined to be 191.4 and 201.5 kJ/mol, respectively, by Kissinger and Kim-Park methods. Arrhenius curves obtained for Kissinger and Kim-Park methods are given in Figure 2.

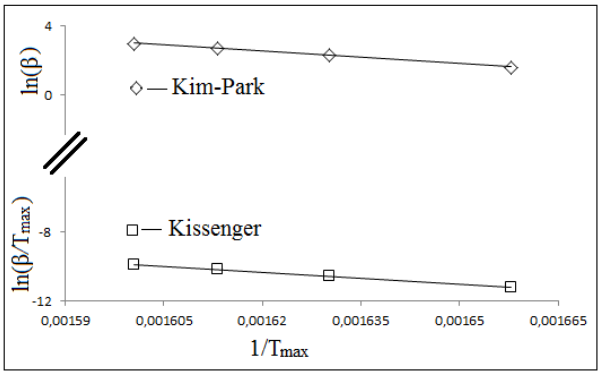

Figure 2. Kissinger and Kim-Park curves for different heating rates.

According to eqs. 2-6 activation energy may individually be calculated from the plotting of the left side of each equation versus 1000/*T*. The mean activation energy values related to the thermal decomposition stage of OAQ in N_2 were eventually calculated to be 194.3 kJ/mol by Tang method, 197.0kJ/mol by KAS method, 199.6 kJ/mol by FWO method and 199.6 kJ/mol by FR method, over a wide range of conversation. The results was given in the Table 1.

Table 1 Activation energies obtained by different methods

Conversion degree	Decomposition stage							
	Tang	lnA	FWO	lnA	KAS	lnA	Friedman	lnA
0.05	65.6	19.2	67.4	19.4	66.6	19.9	70.2	20.5
0.1	154.6	31.2	158.5	31.5	156.2	32.7	161.3	33.9
0.2	190.3	40.6	192.7	40.7	191.1	41.2	195.4	43.6
0.3	186.2	38.1	188.8	38.4	187.4	39.8	191.5	41.5
0.4	187.1	38.4	190.6	39.1	189.2	40.3	191.8	40.7
0.5	185.4	37.3	187.2	37.5	186.1	38.2	189.9	40.2
0.6	190.3	40.6	192.1	40.9	191.4	41.4	194.8	42.3
0.7	196.2	41.7	198.7	42.1	197.6	42.8	201.6	44.2
0.8	205.3	42.8	208.8	43.5	207.7	43.9	211.7	46.1
0.9	244.4	45.6	247.6	46.3	246.2	47.4	249.4	48.7
0.95	332.5	54.2	335.3	55.7	334.4	56.3	338.6	58.6
Mean	194.3	39.0	197.0	39.5	199.6	40.3	199.6	41.8

E values of OAQ were estimated in the ranging of α = 0.05-0.95. The values of logarithmic pre-exponential factor LnA of OAQ was also found to be 39.0 s^{-1} by Tang method, 40.3 s^{-1} by KAS method, 39.5 s^{-1} by FWO method and 41.8 s^{-1} by FR method, over a wide range of conversation. As can be seen in Table 1, the results obtained agrees better with each other, over the range of α given. Constant mass loss lines were also determined by measuring the temperature at a given mass % for each heating rate. The Arrhenius type plots related to the thermal decomposition process are depicted in Figure 3, for masses ranging from 0.05 to 0.95 in N_2.

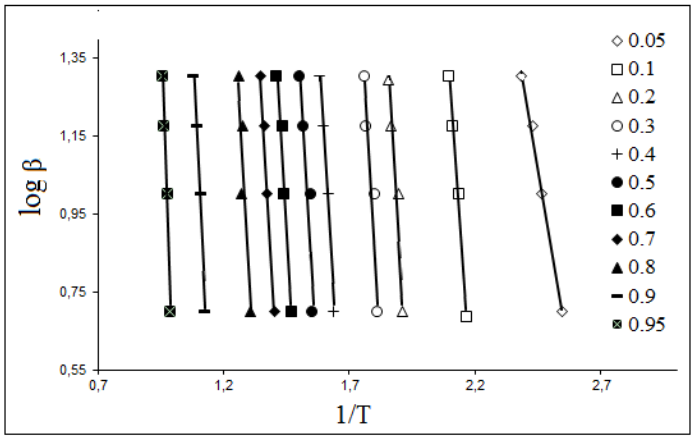

Figure 3 Constant mass loss lines drawn by FWO method in the region of 0.2< α <0.8.

The thermal decomposition of OAQ in N_2 represents a same behavior for Friedman, Tang, KAS, and FWO method. The initial activation energy required to initial decomposition stages was about 65.6 kJ/mol. In order to find out the mechanism of the thermal decomposition of OAQ, master plots was used to. The experimental master plots *P(u)/P(u0.5)* against *α* constructed from experimental data of the thermal decomposition of OAQ under different heating rates and the theoretical master plots of various kinetic functions are all shown in Figure 4.

The comparisons of the experimental master plots with theoretical ones (Figure 4) show that the kinetic processes of the thermal decomposition of OAQ agree with the $\boldsymbol{D_6}$ master curve for dehydration and decomposition stages very well.

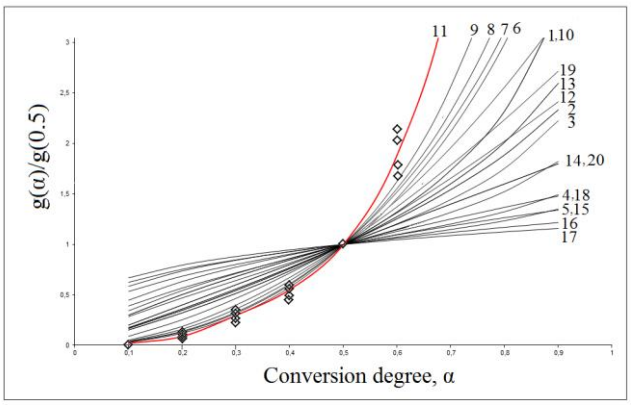

Figure 4. Curves of ln[*βR/E*]-ln[*P(u)*] against differential form

Isothermal decomposition kinetics of OAQ is also studied by isothermal thermogravimetry at temperatures 325, 330 and 335 °C. Isothermal weight-time curves obtained in this way are shown in Figure 5.

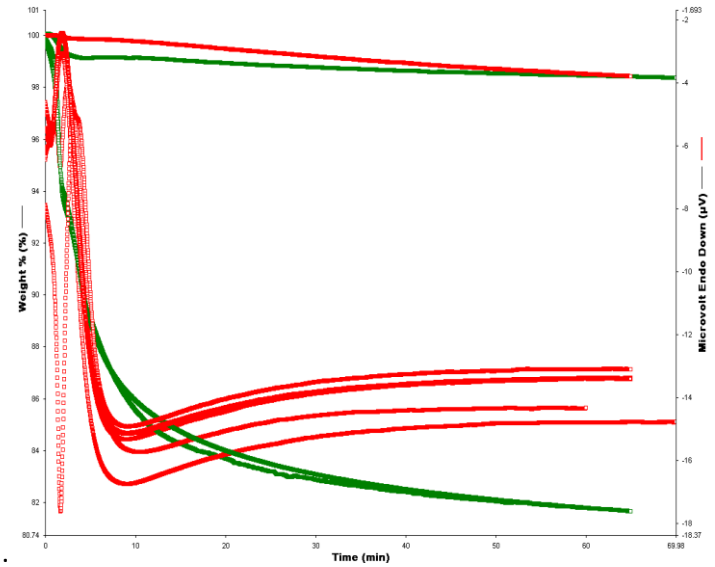

Figure 5. Isothermal weight loss vs. time for OAQ.

In isothermal thermogravimety, Flynn method was chosen for kinetic method. The relationship are given as below.

$$lnt=[g(\alpha)-lnA]+EaT \qquad (7)$$

Then the activation energy was calculated from the Arrhenius plot of ln t vs. 1/T (Figure 6). The obtained values of the kinetic parameter are: *Ea* = 204.22 kJ/mol.

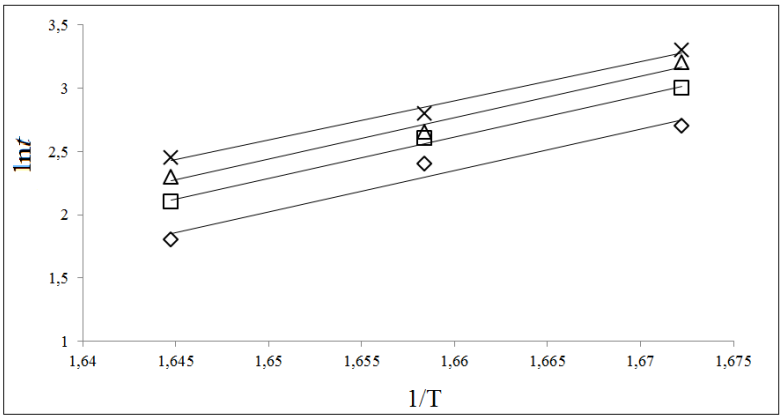

Figure 6. The Arrhenius plot by Flynn method in isothermal thermogravimety.

4. Conclusion

The thermal stability, thermal decomposition process, and kinetic parameters, such as activation energy, pre-exponential factor of OAQ were investigated. The activation energies of the thermal decomposition obtained by the Kissinger, Kim-Park, Tang, KAS, FWO, and FR methods in N_2 were found to be 191.4, 201.5, 194.3, 197.0, 199.6 and 199.6 kJ/mol, respectively, over a wide range of conversation. The resulting logarithmic values of the pre-exponential factor ln A were 39.0 s^{-1} by Tang method, 40.3 s^{-1} by KAS method, 39.5 s^{-1} by FWO method and 41.8 s^{-1} by FR method. From the results obtained by the master plots method the most possible decomposition mechanisms was chosen D_n mechanism for the decomposition stage.

Acknowledgments: This research has been supported by The Scientific and Technical Research Council of Turkey (TUBİTAK) (Project No: 113Z265).

References

1. Stille, J. K. Macromolecules 1981, 14, 870.
2. Dibble, David J.; Umerani, Mehran J.; Mazaheripour, Amir; Park, Young S.; Ziller, Joseph W, Gorodetsky, Alon A. Macromolecules, 2015, 48 (3), 557..
3. Zhang, X.; Shetty, A. S.; Jenekhe, S. A. Macromolecules 1999, 32, 7422.
4. Tonzola, C. J.; Alam, M. M.; Jenekhe, S. A. Adv. Mater. 2002, 14, 1086.
5. S Shoda, H Uyama, J Kadokawa, S Kimura, S. Kobayashi. *Chem. Rev.*, 2016, 116 (4), pp 2307.
6. A. Bilici, İ.H. Geçibesler, İ. Kaya, Enzymatic Synthesis of 5-Amino Quinoline Oligomers and Evaluation of Their Free Radical Scavenging Activity, Submitted, 2016
7. Dogan, F. Ph.D. Thesis, Ege University, Izmir, Turkey, 2006
8. Ozawa ,T., 1965, Bulletin of Chemical Society of Japan, 38, 881
9. W. Tang, Y. Liu, X. Yang, C. Wang, Ind. Eng. Chem. Res. 2004, 43, 2054.
10. H. F. Kissinger, Anal. Chem. 1957, 29, 1702.
11. Akahira, T., Sunose, T. Chiba Institute of Technology Sci. Technol. 1971. (16), 22.
12.Friedman, H. L., 1965, *J. Polymer Sci*., C6, 183.

Synthesis and Characterization of Mn-doped ZnS Thin Films

A. A. Kaya[1], N. Kucuk[1], I. Kucuk[1], K. Erturk[2], Y. E. Firat[1], A. Peksoz[1] and M. I. Sengunes[1]

[1]Department of Physics, Faculty of Art and Science, Bursa, Gorukle, Turkey
[2]Department of Physics, Faculty of Art and Science, Tekirdag, Turkey
E-mail :aslitay@uludag.edu.tr

In the present work, un-doped and Mn-doped ZnS thin films (ZnS:Mn) were growth by the spin coated method at room temperature. The concentration of the Mn ions was changed from 2 to 6%. Different analytical techniques including UV-Visible Spectroscopy (UV-Vis.), Scanning Electron Microscope (SEM) and Atomic-Force Microscopy (AFM) were used to investigate the influence of Mn concentration on surface morphology, magnetic and optical properties of produced thin films. In order to determine the electrical characterization, the resistivity measurements of the films were performed by four-probe technique. In summary, ZnS:Mn thin films were growth onto glass substrates by spin coater method and the influence of Mn doping on the magnetic and optical properties of un-doped ZnS thin films was reported. These results were also compared to the ZnS:Mn thin films produced by different techniques. In UV-Vis. measurements, the band gap energy corresponding to the absorption edge estimated were found to be 3.5–3.8 eV depending on the Mn doping ratio.

Magnetic and Optic Properties of Fe/Ni:ZnO Diluted Magnetic Semiconductor Nanoparticles

M. I. Sengunes[1], A. Adam[1], A. A. Kaya[1], I. Kucuk[1], N. Kucuk[1] and K. Erturk[2]

[1]*Department of Physics, Faculty of Art and Science, Bursa, Gorukle, Turkey*

[2]*Department of Physics, Faculty of Art and Science, Tekirdag, Turkey*

E-mail :aslitay@uludag.edu.tr

In the present study, Fe/Ni-doped ZnO nanoparticles (i.e. $Zn_{0.9}Fe_{0.1}O$, $Zn_{0.95}Fe_{0.05}O$; $Zn_{0.90}Ni_{0.05}Fe_{0.05}O$ and $Zn_{0.85}Ni_{0.05}Fe_{0.1}O$) were successfully synthesized by the sol-gel technique. Structural, optical and magnetic properties of these Fe/Ni-doped ZnO nanoparticles were examined as a function of Fe, Ni concentrations. The surface morphological study was made with the help of Scanning Electron Microscope (SEM), the optical study was studied with the help of UV-Visible Spectroscopy (UV-Vis.) and magnetic study was with the help of Vibrating Sample Magnetometer (VSM). Room temperature magnetic measurements of the nanoparticles were carried out in the field range of (-2 T)–(2 T). Hysteresis loop showed the clear room temperature ferromagnetism in all the samples. The optical band gap, E_g, of the diluted magnetic semiconductors was determined from the absorption spectra. The measured values of the band gap energy were found to be 2.5–3.1 eV.

Organic photodetector for Solar Tracking Systems

A. Dere

Physics Department, Faculty of Science, Firat University, Elazig, TURKEY

Nanoscience and Nanotechnology Laboratory, Firat University, Elazig, TURKEY

Organic photodetectors are interesting for solar track applications due to low cost and easy preparation. Here, we fabricated coumarin doped fullerite films based organic photodetectors. The electronic parameters of the diode are improved with various coumarin doping. The transient photocurrent of the photodetectors suggests that the coumarin doped fullerite photodiode is sensitive to light intensity. It is evaluated that coumarin doped fullerite films/p-Si devices can be used as a photodetectors in optoelectronic applications.

Keywords: Organic photodetector, Organic Semiconductor

Pentacene organic thin film phototransistors for optoelectronic applications

A. Dere, F. Yakuphanoglu
Physics Department, Faculty of Science, Firat University, Elazig, TURKEY
Nanoscience and Nanotechnology Laboratory, Firat University, Elazig, TURKEY

Organic thin-film transistors (OTFTs) are emerging as attractive candidates for low-cost, large-area, and flexible circuit applications. In this paper we review fabrication processes and photosensing applications of the pentacene organic thin-film transistors (OTFTs) with an emphasis on papers published. We describe the state of the art in organic electronics, focusing on pentacene organic semiconductor being studied to realize devices with enhanced performance, including soluble inorganic dielectrics and channel electrodes. We focus on the photoresponse characteristics of the pentacene organic thin film transistors. The correlation between the channel widths of the pentacene transistors and the photoresponse charge transport mechanism is discussed.

Keywords: Organic Semiconductor, Organic Thin film Transistor

Synthesis and optoelectronic device properties of 2,2,4,4-Bis[spiro(7,8-Dioxy-3-(3-methylphenyl)-*2H*-chromen-2-one]-4,4,6,6,-bis[spiro(2′,2′′-dioxy-1′,1′′-biphenylyl)] cyclotriphosphazene compound

Furkan Özen[1], A. Dere[2], Kenan Koran[1], F. Yakuphanoglu[2], Ahmet Orhan Görgülü[1]

[1]*Department of Chemistry, Faculty of Science, Firat University, Elazığ, Turkey*
[2]*Department of Physics, Faculty of Science, Firat University, Elazığ, Turkey*
E-mail : a.dere@firat.edu.tr

Phosphorous-nitrogen double bond containing compounds is called as phosphazene. Hexachlorocyclotriphosphazene and poly(dichlorophosphazene) are well known and most studying types of cyclophosphazene and polyphosphazes [1]. Phosphazene derivatives possess different physical properties such as fluorescence [2], flame retardants [3], and dielectric and proton conductivity [4,5].

2,2,4,4-Bis[spiro(7,8-dioxy-3-(3-methylphenyl)-*2H*-chromen-2-one]-6,6-bis[spiro(2′,2′′-dioxy-1′,1′′-biphenylyl)cyclotriphosphazene **(2)** was synthesized from the reaction of cyclotriphosphazene **(1)** containing dioxybiphenyl [6] with 7,8-dihydroxy-3-(3-methylphenyl)-*2H*-chromen-2-one in the presence of xylene/Cs_2CO_3 system. The structure of **2** was characterized by using spectroscopic techniques. A hybrid optoelectronic device was fabricated on p-type silicon wafer by drop casting method. The diode exhibited both a photoconductive and photovoltaic behavior. The diode has a high photoresponsivity and it can be used as photosensor in optoelectronic applications.

Acknowledgement:
The authors are grateful to the Research Fund of the TUBITAK for their support (for the synthesis of compound) with the TBAG-110T652.

[1] Allcock, H.R. Phosphorus-Nitrogen Compounds. Cyclic, Linear, and High Polymeric Systems. New York: Academic Press Inc. (1972).
[2] Çoşut, B., Dyes and Pigments, 100, 11-16, (2014).
[3] Jiang, P., Gu, X., Zhanga, S., Sun, J., Wua, S., Zhao, Q. Phosphorus Sulfur and Silicon, 189, 1811–1822, (2014).
[4] Alidağı, H. A., Gırgıç, Ö. M., Zorlu, Y., Hacıvelioğlu, F., Çelik, S. Ü., Bozkurt, A., Kılıç, A., Yeşilot, S. Polymer, 54, 2250-2256, (2013).

Synthesis and Photodiode Applications of Cyclotriphosphazene Compound Bearing 7,8-Dihydroxy-3-(3-methylphenyl)coumarin Groups

Furkan Özen[1], A. Dere[2], Kenan Koran[1], F. Yakuphanoglu[2], Ahmet Orhan Görgülü[1]

[1]*Department of Chemistry, Faculty of Science, Firat University, Elazığ, Turkey*

[2]*Department of Physics, Faculty of Science, Firat University, Elazığ, Turkey*

E-mail : a.dere@firat.edu.tr

Phospazenes are a kind of phosphorus-nitrogen compounds that contain –P=N-. Linear, cyclic and polyphosphazenes are the three major types. Cyclic and polyphosphazes are the most known and studying types. The phosphazene compounds have many potential applications [1,2].

2-(2,3,4-trimethoxyphenyl)-1-(3-methylphenyl)acrylonitrile **(2)** was synthesized from the reaction of 2,3,4-trimethoxybenzaldehyde **(1)** with 3-methylphenylacetonitrile [3,4]. 7,8-dihydroxy-1-(3-methylphenyl)coumarin **(3)** was synthesized from the reaction of (**2)** with pyridinium hydrochloride by using microwave. 2,2-Bis[spiro(7,8-dioxy-4-methylcoumarin)]-4,4,6,6,-bis[spiro(2′,2′′-dioxy-1′,1′′-biphenylyl)]cyclotriphosphazene **(5)** compound was synthesized from the reaction of 2,2-dichloro-4,4,6,6-bis[spiro(2′,2′′-dioxy-1′,1′′-biphenylyl)cyclotriphosphazene **(4)** [5] with 7,8-dihydroxy-1-(3-methylphenyl)coumarin **(3)** in xylene/Na_2CO_3 system. The structures of the compounds were defined by IR, ^{1}H, ^{13}C, ^{13}C-APT and HETCOR spectroscopy. A photodiode was prepared using a p-type silicon and cyclotriphosphazene compound bearing 7,8-dihydroxy-3-(3-methylphenyl)coumarin groups. The photoresponse properties of the diode are due to the optical absorption properties. The obtained electronic parameters of the diode suggest that the photodiode with cyclotriphosphazene compound bearing 7,8-dihydroxy-3-(3-methylphenyl)coumarin groups thin film could be used in various optoelectronic devices and applications.

Acknowledgement:

The authors are grateful to the Research Fund of the TUBITAK for their support (for the synthesis of compound) with the TBAG-110T652.

[5] Allcock, H.R. Phosphorus-Nitrogen Compounds. Cyclic, Linear, and High Polymeric Systems. New York: Academic Press Inc. (1972).

[6] Koran, K., Ozen, F., Torğut, G., Pıhtılı, G., Cil, E., Arslan, M., Görgülü, A.O. Polyhedron, 79, 213-220 (2014).

[7] Buu-Hoi, N.P., Saint-Ruf, G., and Lobert, B., J. Chem. Soc.(C), 16, 2069, (1969).

[8] Basaran, I., Sinan, S., Cakir, U., Bulut, M., Arslan, O., Ozensoy, O., Journal of Enzyme Inhibition and Medicinal Chemistry, 23, 32-36, (2008).

[9] Carriedo, G.A., Catuxo, L.F., Alonso, F.J.G., Elipe, P.G., González, P.A. Macromolecules, 29, 5320-5325 (2009).

The Observation on Physical Properties of New Generation High Temperature Shape Memory Alloys

[1]Canan AKSU CANBAY,[2]Zuhal KARAGOZ GENÇ, [3]Memet SEKERCI,

[1]Department of Physics, Faculty of Science, University of Firat, 23119, Elazig, Turkey

[2]Department of Metallurgy and Materials Engineering, Facultyof Engineering, Adiyaman University, 02040 Adiyaman, Turkey

[3]Department of Chemistry, Faculty of Science, University of Firat, 23119, Elazig, Turkey

Shape memory (SM) is the term used to describe the property of shape memory alloys (SMAs), which undergo a reversible thermoelastic martensitic transformation between a high temperature phase and low temperature phase. The technical importance of these materials is based on their mechanical properties such as pseudoelasticity (PE) and shape memory effect (SME). Shape memory effect is related to the thermoelastic martensitic transformation exhibited by a diffusionless reconfiguration of the crystalline lattice of the material under applied temperature or stress changes. . Generally Cu-based SMAs are good candidates because of their easy production and lower manufacturing cost. Besides this, the properties of Cu-based SMAs can be improved by modifying the elements and the compositions of the elements. CuZnAl and CuAlNi SMAs have large grain size and high degree of ordering which cause bad ductility in these alloys.

Thermal and structural investigations of new generation quaternary shape memory alloy was made. Differential scanning calorimetry (DSC), differential thermal analysis (DTA) and X-ray measurements were detected to analysis the physical properties of the produced SMA.

The Synthesis of New Phase Change Materials as Potential Building Materials

Zuhal KARAGOZ GENC[a], Yılmaz KARATUT[a], Seyfettin YILMAZ[a], Murat GENC[b], Canan AKSU CANBAY[c]

[a]Department of Metallurgy and Materials Engineering, Engineering Faculty, Adiyaman University,02040, Adiyaman, Turkey

[b]Department of Chemistry, Faculty of Science and Arts, Adiyaman University, 02040, Adiyaman, Turkey.

[c]Department of Physics, Faculty of Science, Firat University, 23119, Elazig, Turkey

Phase change materials (PCMs) are known as a good candidate with high energy utilization efficiency, because they can store and release enormous amounts of latent heat energy through changing their state in a narrow temperature range [1-2]. In recent years, PCMs have exhibited a good potent in applications for intelligent fibers, buildings and textiles, transportation packaging, commercial refrigeration of temperature-sensitive products, etc [3].In this study a series of myristic-stearic acid/TiO_2 as form-stable phase change materials (PCMs) were synthesized in a sol-gel process using n-butyl titanate precursor. The chemical compositions and structures of the synthesized composites were characterized by Fourier transform infrared spectroscopy. Their morphological properties, crystalloid phase and latent heat storage capacities were studied by scanning electron microscope (SEM), X-Ray diffractometer (XRD) and differential scanning calorimetry (DSC).

References

[1] Jiang, F. Wang, X. Wu, D Applied Energy 2014;134 :456–468.

[2] Sharma A, Tyagi VV, Chen CR, Buddhi D Renew Sustain Energy Rev. 2009;13:318–45.

[3] Khudhair AM, Farid MM Energy Convers Manage 2004;2:263–75.

Thermal Performance of Stearic-Decanoic Acid /TiO2 Phase Change Materials Fabricated by N-Butyl Titanate Precursor

Murat GENC[a], Canan AKSU CANBAY[b], Zuhal KARAGOZ GENC[c], Memet ŞEKERCİ[d]

[a]Department of Chemistry, Faculty of Science and Arts, Adiyaman University, 02040, Adiyaman, Turkey.

[b]Department of Physics, Faculty of Science, Firat University, 23119, Elazig, Turkey

[c]Department of Metallurgy and Materials Engineering, Engineering Faculty, Adiyaman University,02040, Adiyaman, Turkey

[d]Department of Chemistry, Faculty of Science, Firat University, 23119, Elazig, Turkey

PCMs (phase change materials) are attractive materials for thermal energy storage due to their characteristic of constant temperature and their large latent heat in the course of absorbing or releasing energy [1-2]. They can be used as energy storage material in TES applications like industrial waste heat recovery and solar energy collectors [3]. Based on the principle of sol–gel method and the mechanism of silane coupling agent can be used to adjust the gel structure, four different kinds of composite phase change materials (PCMs) were prepared by using stearic-decanoic acid mixture as phase change material (PCM), tetraethoxysilane ($SiC_8H_{20}O_4$) adsorbed PCM, fly ash adsorbed PCM and barite adsorbed PCM as raw materials via sol–gel process. Fourier transformation infrared spectroscopy (FT-IR), scanning electron microscope (SEM) and X-Ray diffractometer (XRD) were used to determine the chemical structure, morphological properties, and crystalloid phase of the microencapsulated PCMs.

References

[1] Latibari ST, Mehrali M, Mehrali M, Mahlia TMI, Metselaar HSC, Energy 61 (2013) 664-672.

[2] Mehrali M, Latibari ST, Mehrali M, Indra Mahlia TM, Cornelis Metselaar HS.
Energy 2013;58(0):628e34.

[3] Calvet N, Py X, Olivès R, Bédécarrats J-P, Dumas J-P, Jay F Energy 2013;55(0):956e-64.

New soluble esterified metallo and metal-free porphyrazine complexes with eight (4-thiobutyl 1,4-benzodioxane-2-carboxylate)] groups

E. Gonca

Faculty of Engineering, Department of Chemical Engineering, Çanakkale Onsekiz Mart University, Terzioglu Campus, TR 17020 Çanakkale, Turkey

E-mail :egonca@comu.edu.tr

A range of different substituents provides porphyrazine ligands with interesting new features such as greatly enhanced organic solubility compared to their phthalocyanine counterparts, or additional donor sites to create multinuclear complexes [1]. Unsubstituted metallo and metal-free porphyrazine structures are less or insoluble in common organic solvents. Compared to unsubstituted metal porphyrazines, ester-containing porphyrazines are highly soluble in chlorinated hydrocarbons such as dichloromethane, chloroform. A further step for porphyrazine esters is the possibility to design supramolecular structures with donor groups on the ester moiety [2].

The new soluble esterified metallo and metal-free porphyrazine complexes with eight (4-thiobutyl 1,4-benzodioxane-2-carboxylate)] substituents on the periphery were reported. The functionality of the hydroxybutyl groups was demonstrated by esterification of porphyrazine derivatives with 1,4-benzodioxane-2-carboxylic acid in the presence of dicyclohexylcarbodiimide and *p*-toluenesulfonic acid. Unlike the parent porphyrazines, the symmetrically functionalized porphyrazines with eight ester units were soluble in common organic solvents such as chloroform, dichloromethane, tetrahydrofuran, acetone, and toluene and insoluble in water and *n*-hexane. The newly synthesized compounds were characterized by elemental analysis, FT-IR, UV-Vis, mass, ^{1}H, and ^{13}C NMR spectroscopy.

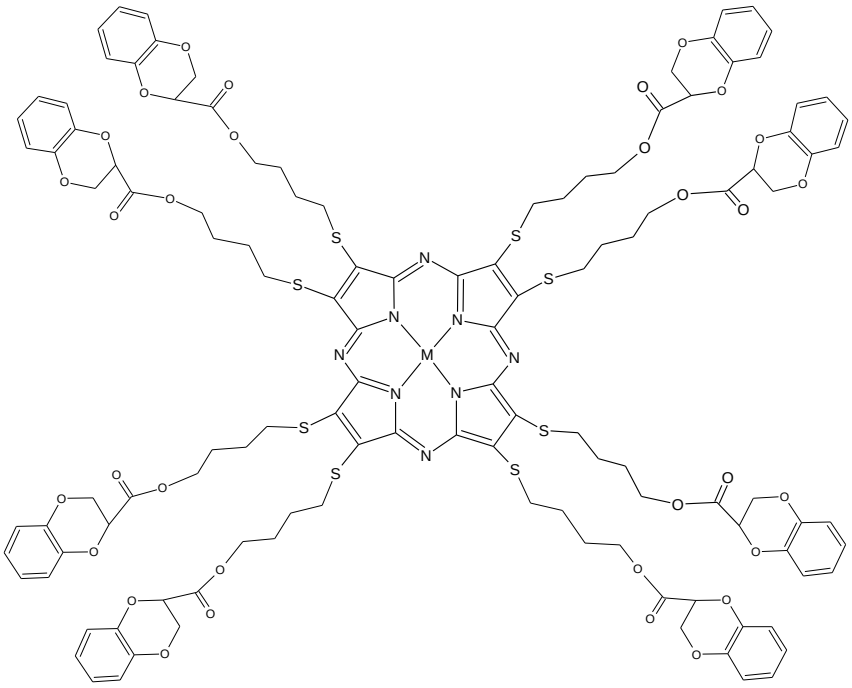

[1] H. Eichhorn, M. Rutloh, D. Wöhrle, J. Stumpe, J. Chem. Soc., Perkin Trans. 2, 1801 (1996).

[2] B. Akkurt and E. Hamuryudan, Dyes Pigments 79, 153 (2008).

Light Controller Solar Simulator System for Solar Cells

Fahrettin Yakuphanoglu

Physics Department, Faculty of Science, Firat University, Elazig, TURKEY

Nanoscience and Nanotechnology Laboratory, Firat University, Elazig, TURKEY

Here, we manufactured a light controller solar simulator system to analyze organic solar cells, dye sensitized solar cells, silicon solar cell, quantum dots solar cells. This system can be used to determine photovoltaic mechanism, photovoltaic parameters, and recombination mechanism of the solar cells.

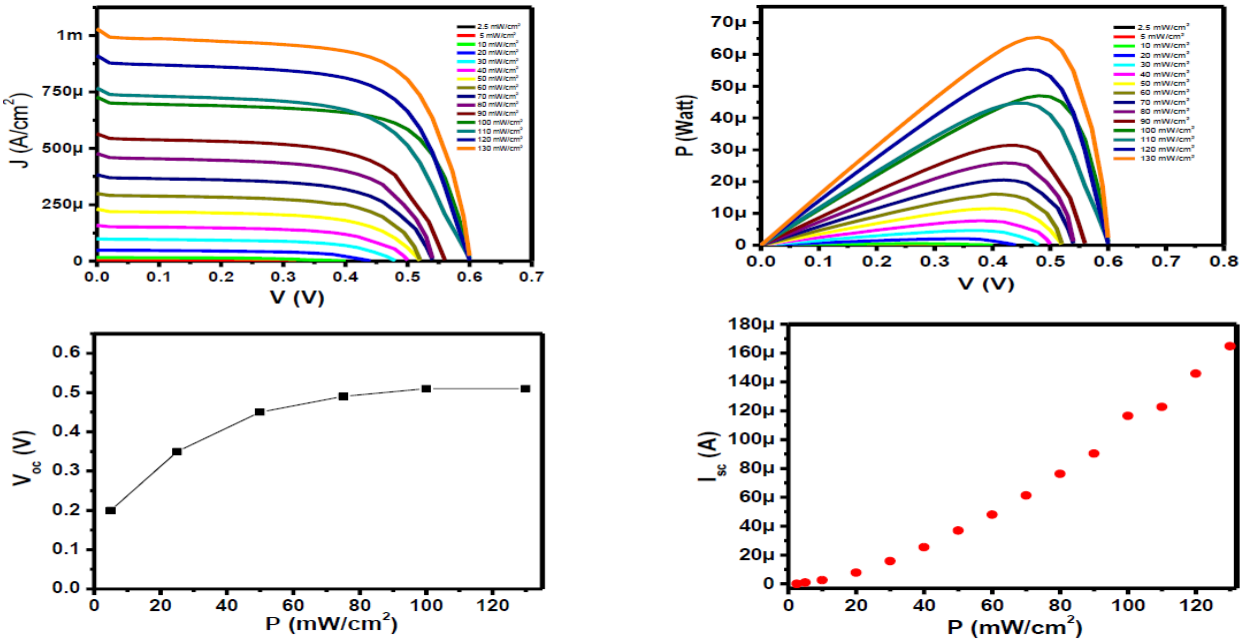

Keywords: Solar Cells, Solar Simulator

Cross-linked PTMA polymers as Cathode Material in Li-Ion Batteries

Muhammet Aydin[1, 2], Mesut Gorur[3]*, Faruk Yilmaz[1]*

[1]Department of Chemistry, Gebze Technical University, Kocaeli, 41400, Turkey
[2]Central Research Laboratory, Namık Kemal University, Tekirdag, 59030, Turkey
[3]Department of Chemistry, Istanbul Medeniyet University, Istanbul, 34700, Turkey
email: fyilmaz@gtu.edu.tr

In the age of mobile communication, scientists have focused their attention to develop energy storage devices with high energy density and power capacity as well as long cycle life. Organic radical batteries (ORB) have attracted great deal of attention for their fast redox kinetics, high power capacity and energy density. Besides, they do not contain toxic heavy metals and thus they are regarded as environmentally friendly [1]. In this respect, polymers with redox-active 2,2,6,6-tetramethylpiperidine-1-oxyl (TEMPO) side-groups have been employed as cathode material in Li-ion rechargeable batteries [2].

In this work, crosslinked poly(2,2,6,6-tetramethyl-1-piperidin-4-yl methacrylate) (PTMPM) polymers (**P1a-c**) were first prepared using ethylene glycol dimethacrylate (EGDM) and two different telechelic poly(ethylene glycol) dimethacrylate (PEGDM) polymers (Mn= 550 and 1000), respectively, as crosslinking agents. The obtained crosslinked polymers (**P1a-c**) were oxidized with 3-chloroperbenzoic acid (*m*-CPBA) to obtain crosslinked poly(2,2,6,6-tetramethylpiperidinyloxy-4-yl methacrylate) (PTMA) polymers (**P2a-c**) with redox-active TEMPO side units (Scheme 1). Subsequently, these polymers were employed as the cathode material in the preparation of rechargeable Li-ion button cell. The produced batteries were then characterized for their charge-discharge cycle performances.

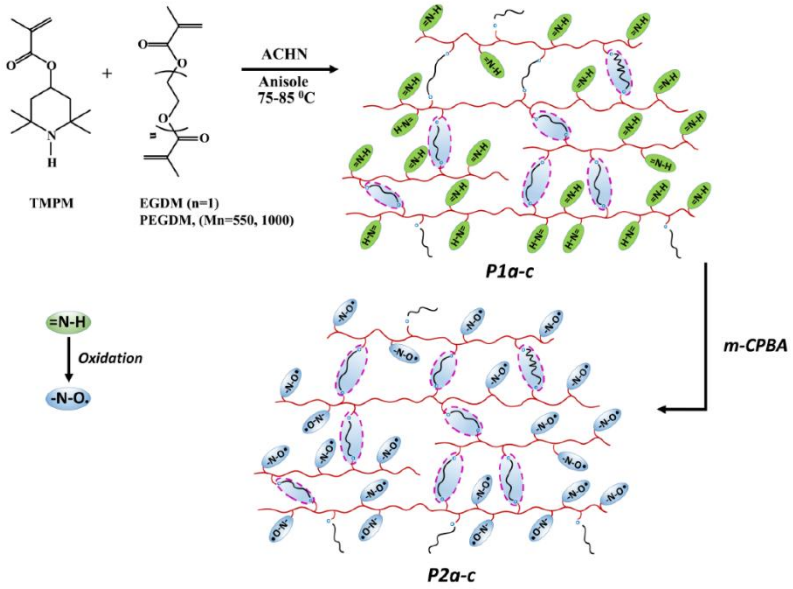

Scheme 1. Synthesis of crosslinked PTMA polymers (**P2a-c**).

*The authors acknowledge TUBITAK for the financial support (Project No: 114Z302).

References:

1. M. Aydin, B. Esat, C. Kilic, M. E. Kose, A. Ata, F. Yılmaz, Eur. Polym. J., 47 (2011), 2283-2294.
2. M. Aydin, M. Gorur, and F. Yilmaz, React. Funct. Mater. 102 (2016), 11-19.

The Investigation with Quantum Chemical Methods of Imidazole Molecule As Oled Material

M. Tursun[1], İ. Kavlak[1], G.S. Kürkçüoğlu[2]

[1]*Department of Physics, Graduate School of Natural and Applied Sciences, Eskişehir Osmangazi University, Eskişehir, Türkiye*

[2]*Department of Physics, Faculty of Arts and Sciences, Eskişehir Osmangazi University, Eskişehir, Türkiye*

E-mail: tursun.mahir@gmail.com

In this study; the optimized geometric parameters, normal mode frequencies, intensities and corresponding vibration assignments of imidazole have been investigated by density functional theory (DFT) with B3LYP and MP2 levels with the 6-311++G(d,p) basis set in the gas phase and in benzene, toluene, ethanol, methanol and dichloromethane solvents. Furthermore, reliable vibration assignments have been made on the basis of potential energy distribution (PED). The vibration frequencies of the imidazole molecule in different solvents were examined. In this way, solvent effects were investigated on the molecule. Additionally, electronic transition energies have been calculated with TD-B3LYP method in polarizable continium model (PCM) in gas phase and in the solvents, respectively. The result obtained calculations, HOMO-LUMO energy levels are determined, and then solvent effects of absorption spectra of imidazole molecule are discussed experimentally and theoretically. HOMO-LUMO energy levels of imidazole molecule in some solvents were given in Figure 1. An excellent correlation is seen between theoretical and experimental results.

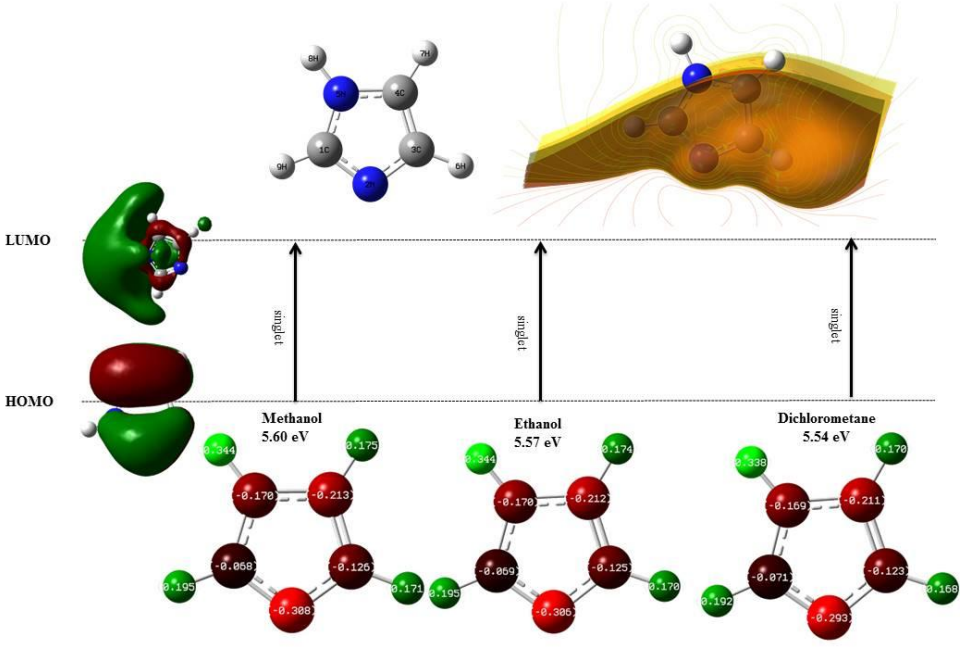

Figure 1. The HOMO-LUMO energy levels of imidazole molecule in some solvents.

This work was supported by the Research Fund of Eskisehir Osmangazi University. Project no: 201519047.

Pt(II) complexes as potential antitumor reagents

Iftikhar Ahmad[1], Mehmet Karakus[1], Alp Akman[2], Gülçin Abban[3], Ahmet Fahir Demirkan[2]

[1]Department of Chemistry, Faculty of Arts&Science, Denizli, Turkey

[2]Department of Orthopaedics and Traumatology, Faculty of Medicine, Denizli, Turkey

[3]Department of Histology and Embryology , Faculty of Medicine, Denizli, Turkey

mkarakus@pau.edu.tr

The application of metal complexes in the field of medicinal, bioinorganic and bioorganic chemistry [1] has become more and more important in the people life. Recently, *DNA binding studies and cytotoxicity of a dinuclear* Pt(II) complexes were studied [2]. Our main focus is to synthesize new Pt(II) complexes with diimine ligands. The structure (Scheme 1) and properties of the complexes are investigated.

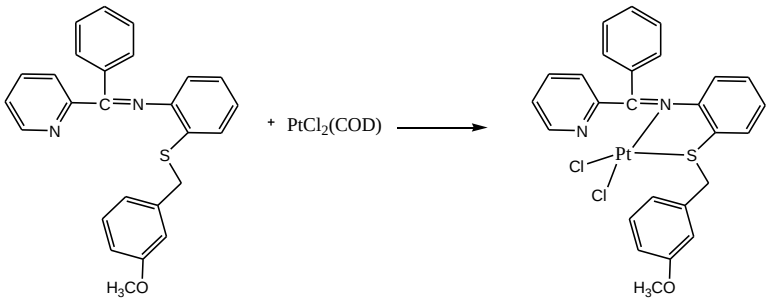

Scheme 1: Synthesis of Pt(II) complexes.

References

1. Zhang C. X. and Lippard S.J., *Current Opinion in Chem. Bio.* 2003, *7*, 481.

2. Terenzi, A., Ducani, C., Blanco, V., Zerzankova, L., Westendorf, A.F., Peinador, C., Quintela, J.M., Bednarski, P.J., Barone, G., Hannon, M.J. *Chemistry. A European Journal,* 2012, 18: 10983-10990.

Synthesis and Properties of Ru(II)-Complexes with Aminophosphine Ligands

Ozlem Sarı, Mehmet Karakuş*
Department of Chemistry, Faculty of Arts&Science, Denizli, Turkey
mkarakus@pau.edu.tr

Organophosphines are ligands commonly used in organometallic chemistry due to their ability to stabilise low metal oxidation states and influence both steric and/or electronic properties of catalytic species [1-3]. The application of metal-containing compounds in the field of catalysis, medicinal, bioinorganic and bioorganic chemistry has become more and more important. We now report the synthesis the Ru(II)-(p-cymene) complexes with new aminophosphines. The structure of Ru(II)-(p-cymene) complexes are given figure 1.

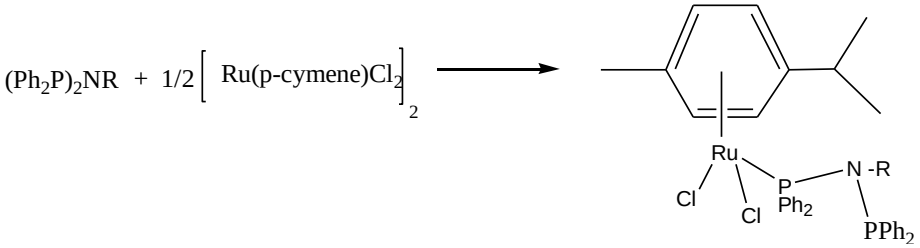

R: aril or alkyl groups

Figure 1: Synthesis of Ru(II) complexes.

This study was supported by Pamukkale University (Grant no: 2015FBE050)

References

1. A. D. Phillips, L. Gonsalvi, A. Romerosa, F. Vizza and M. Peruzzini, *Coord. Chem. Rev.*, 2004, **248**, 955.
2. Keles, M.; Altan, O.; Serindag, O. *Heteroatom Chem.*, 2008, *19(2)*, 113-118.
3. M. B. Smith, S. H. Dale, S. J. Coles, T. Gelbrich, M. B. Hursthouse, M. E. Light and P. N. Horton, *CrystEngComm*, 2007, **9**, 165.

Determination of Radiation Shielding and Dielectric Properties on Sodium Silicate/Tungsten Glass Structure

M. Kılıç[1], Y. Karabul[1], Ü. Alkan[2], M. Okutan[1], S. Bakırdere[3], O. İçelli[1]

[1]*Department of Physics, Yıldız Technical University, İstanbul, Turkey*

[2]*Department of Computer Engineering, Istanbul Gelişim University, İstanbul, Turkey*

[3]*Department of Chemistry, Yıldız Technical University, İstanbul, Turkey*

e-mail: mekilic@yildiz.edu.tr

Glasses materials can be transparent to the visible light and the fact that their attributes may be improved to a large level by altering the adopting variations and composition in the preparation techniques, these materials can be one of the best possible alternatives to concrete and can be used as radiation shielding materials [1]. Silicate melts, their structure and properties are usual objects of geochemistry, glasses and metallurgical productions. Natural silicate melts often contain alkali, alkaline earth, aluminum and transition metal oxides, e.g. iron oxides, as the main components. In the glass technology iron gets into melt as impurity in trace amounts or specially been added in small quantities to the batch. Transition metals can influence the optical properties of the final glass and viscosity of the melt due to structural changes of matter [2]. Tungsten has wide application in industry such as X-ray technology, chemical industry, high temperature technology, machine construction owing to its good electrical conductivities, good X-ray performance, high-elastic modulus, low vapor pressure, high melting point and thermal conductivities [3].

In this study, Tungsten were doped with different weight (0.5, 1.0, and 1.5) of sodium silicate. In this way, Sodium Silicate/Tungsten glass were prepared. To obtain radiation shielding properties of this glasses, the experimental gamma-ray lineer attenuation coefficients were determined by using NaI(Tl) scintillation detector. Also the dielectric properties of the glasses were investigated using dielectric spectroscopy. A detailed analysis of this investigation will be presented.

[1] S.A.M. Issa, Effective atomic number and mass attenuation coefficient of $PbO–BaO–B_2O_3$ glass system, Radiat. Phys. Chem. 120 (2016) 33–37. doi:10.1016/j.radphyschem.2015.11.025.

[2] E.V. Belova, Y.A. Kolyagin, I.A. Uspenskaya, Structure and glass transition temperature of sodium-silicate glasses doped with iron, J. Non. Cryst. Solids. 423-424 (2015) 50–57. doi:10.1016/j.jnoncrysol.2015.04.039.

[3] F. Bo, L. Xianping, W. Jinqing, W. Pengcheng, The flotation separation of scheelite from calcite using acidified sodium silicate as depressant, Miner. Eng. 80 (2015) 45–49. doi:10.1016/j.mineng.2015.06.017.

Synthesis and characterization of PEDOT/PFHP electrochromic bilayer surfaces

M. Yıldırım[1], U. Cengiz[2], İ. Kaya[3], A. Caglar[4]

[1]*Department of Materials Science & Eng., Faculty of Engineering, Canakkale Onsekiz Mart University(COMU), Turkey*

[2]*Department of Chemical Engineering, Faculty of Engineering, COMU, Turkey*

[3]*Department of Chemistry, Faculty of Science and Arts, COMU, Turkey*

[4]*Department of Bioengineering & Materials Science Engineering, COMU, Turkey*

E-mail:mehmetyildirim@comu.edu.tr

Polymeric electrochromics (ECs) have been good candidates for production of electrochromic devices (ECDs). They are preferred due to various colour options, low response time, high optical contrast and easy and flexible formation. Some recent studies have been focused on their surface characteristics like morphology and wettability [1]. Superhydrophobic ECs could be supplied by low surface energy as well as high roughness. Hydrophilic surfaces are contaminated by water based pollutants and moisture. Thus, it is important to make them hydrophobic-superhydrophobic for high durability.

In this study, PEDOT/PFHP bilayer surfaces were prepared. PEDOT sublayer increased the roughness of the surface. Perfluorohexyl substituted polypyrrole (PFHP) as the top layer supplied low surface energy. PEDOT sublayers were prepared by electropolymerization using bulk electrolysis technique. PFHP was synthesized chemically and coated onto PEDOT surface by spin and dip coating. Experimental conditions were varied to compare their effects. SEM-EDX analyses were carried out to determine the surface characteristics. Wettability properties were characterized by static contact angle measurements. EC properties were measured by spectroelectrochemical analysis.

PEDOT monolayer is hydrophilic and becomes superhydrophilic over particular thikness. PFHP monolayer deposited onto ITO-glass by dip or spin coating has also low water contact angle (WCA) as about 70-95˚ due to the flat surface formation. However, PFHP coated PEDOT films (PEDOT/PFHP bilayers) have relatively higher WCAs changing from 100 to 170˚ depending on the experimental conditions. This indicates that PEDOT as rough polymeric layer increases the roughness of top layer and PFHP supplies low surface energy due to the perfluorohexyl substitutions. Thus, PEDOT/PFHP bilayer film occurs superhydrophobic in particular experimental conditions. Spectroelectrochemical analyses showed EC properties of bilayer films. SEM-EDX analyses showed that solvent kinds used significantly effected the surface morphology.

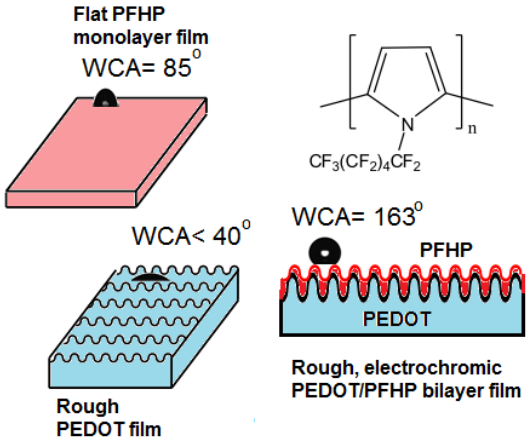

As a result, PEDOT/PFHP bilayer surfaces produced in particular conditions could be used in superhydrophobic EC surface production.

Acknowledgment: This work was financially supported by the Scientific and Technological Research Council of Turkey (TUBITAK, Project 113Z246).

[1] A. Caglar, U. Cengiz, M. Yıldırım and İ. Kaya, J. Appl. Polym. Sci. 331, 262 (2015)

Synthesis and characterization of superhydrophobic, electrochromic PEDOT/PFCE bilayer surfaces

M. Yıldırım[1], U. Cengiz[2], İ. Kaya[3], G. E. Demir[4], A. Caglar[4]

[1]*Department of Materials Science & Eng., Faculty of Engineering, Canakkale Onsekiz Mart University(COMU), Turkey*

[2]*Department of Chemical Engineering, Faculty of Engineering, COMU, Turkey*

[3]*Department of Chemistry, Faculty of Science and Arts, COMU, Turkey*

[4]*Department of Bioengineering & Materials Science Engineering, COMU, Turkey*

E-mail:mehmetyildirim@comu.edu.tr

Conducting polymer based electrochromic devices (ECDs) are highly interesting topic in recent years. Colour changes between redox states are their main characteristics. These optical changes generally characterized by spectroelectrochemical analysis. Nowadays, their surface wettability as well as electrochromic characteristics have attracted more attention [1]. Superhydrophobic/superoleophobic electrochromic polymer surface production have been main goal of these studies.

At the first part of this study, a perfluoroalkyl substituted carbazole ester compound (FCE) was synthesized and then chemically polymerized using $FeCl_3$ catalyst. The obtained polymer (PFCE) was spin and dip coated onto ITO/glass surfaces to obtain monolayer PFCE surfaces. Moreover, PEDOT/PFCE bilayer surfaces have been prepared in various experimental conditions to increase the water contact angle (WCA) indicating the hydrophobicity of the surfaces. PEDOT was coated as the first layer electrochemically. WCA measurements of the films were characterized by static contact angle measurements and EC behaviors by spectroelectrochemical analysis. SEM-EDX measurements were carried out to determine the relationship between morphology and molar content of fluorine on the surfaces with the WCA values measured. PEDOT sublayer increased the roughness of the surface. PFCE as the top layer supplied low surface energy.

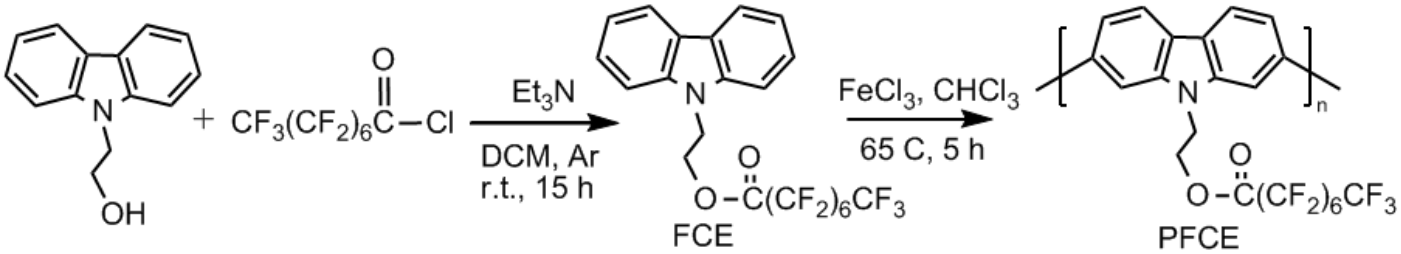

PEDOT monolayer is hydrophilic and becomes superhydrophilic over particular thikness. PFCE monolayers by dip and spin coating have 104 and 133˚ of WCA. On the other hand PEDOT/PFCE bilayer surfaces become superhydrophobic (WCA>170˚) in particular conditions. Spectroelectrochemical analyses showed EC properties of bilayer films. SEM-EDX analyses showed low fluorine content on film surfaces.

Resultantly, PEDOT/PFCE bilayer surfaces could be used in superhydrophobic EC surface production in particular experimental conditions.

Acknowledgment: This work was financially supported by the Scientific and Technological Research Council of Turkey (TUBITAK, Project 113Z246).

[1] A. Caglar, U. Cengiz, M. Yıldırım and İ. Kaya, J. Appl. Polym. Sci. 331, 262 (2015)

Theoretical investigation of the electronic structure, elastic, dynamic properties of intermetallic compound NiBe under pressure

M. Evecen[1], Y. Ö. Çiftci[2], and E. Aldirmaz[1]

[1] Department of Physics, Faculty of Arts and Sciences, Amasya University, 05100 Amasya, Turkey

[2]Department of Physics, Faculty of Sciences, Gazi University Teknikokullar, 06500, Ankara, TURKEY

meryem.evecen@amasya.edu.tr

Future aerospace systems depend strongly on the availability of high temperature structural materials which are both strong and lightweight. Unfortunately, the mechanical strengths of almost all structural materials decrease as the temperature increases; an exception to this general rule is found in intermetallic compounds. A disadvantage of intermetallic compounds is that they are either intrinsically brittle because of their complex crystallographic structures, or they are too dense for aerospace applications. Amongst all these compounds, in the beryllide group probably have the lowest densities and has demonstrated some transition beryllides exhibit attractive specific strengths at elevated temperatures, and these are of considerable interest for structural applications. From the beryllide group, NiBe is of particular interest because it has a relatively simple ordered B2 crystal structure and exhibits a wide range of stoichiometry. In this study, we investigated the structural, electronic, elastic and dynamic properties of NiBe intermetallic compound under pressure, by performing *ab initio* density functional theory using the Cambridge Serial Total Energy Package (CASTEP). The calculated structural parameters, such as the lattice constant (a_0), bulk modulus (B) and its pressure derivative (B_0) and elastic constants, are calculated using the CsCl-(B2 phase) structure. The band structure and corresponding density of states (DOS) are quantitatively analyzed. The mechanical properties and ductile behaviors of this compound are also predicted based on the calculated elastic constants. It is found that the substituted structure are stable for NiBe compound between 0 and 50 GPa pressure

Keywords: Intermetallics, Elastic properties, Electronic structure, Ab-initio calculations.

[1] T. G. Nieh, J. Wadsworth and, & C. T. Liu, Hardening behavior of nickel beryllides, Scripta metallurgica, *22*(9), 1409-1413. (1988).

Structural, mechanical, electronic, dynamic, and optical properties of semiconductor half- Heusler compound LiScSi under pressure from first – principle study

Yasemin Ö. Çiftci[1], Meryem Evecen[2]
[1]*Department Of Physics, Gazi University, Faculty of Sciences , Ankara, TURKEY*
[2]*Physics Department, Amasya University, Faculty of Arts and Sciences, Amasya, TURKEY*
yasemin@gazi.edu.tr; meryem.evecen@amasya.edu.tr

Compounds formed in the half-Heusler structure have proven to be an important class of materials in recent years. Due to their potential applications in cooling and power generation, high-performance thermoelectric materials have attracted a lot of attention from the science community. Half-Heuslers (HH) are ternary compounds with MgAgAs structure[1]. The structural, mechanical, electronic, dynamic, and optical properties of MgAgAs- based LiScSi compound were investigated by the ab initio calculations based on the density functional theory. The lattice constant, bulk modulus, first derivative of bulk modulus were obtained by fitting the calculated total energy-atomic volume results to the Murnaghan equation of state. These results were compared with the previous data. The band structure and corresponding density of states (DOS) were also calculated and discussed(Fig.1). The elastic properties were calculated by using stress-strain method which shows that MgAgAs phase of this compound is mechanically stable. The presented phonon dispersion curves and one-phonon DOS is also confirms that this compound is dynamically stable. In addition, the heat capacity and entropy of LiScSi were calculated by using the phonon frequencies. Finally, the optical properties such as dielectric function, absorption coefficient, reflectivity function, extinction coefficient, refractive index, energy loss spectrum were obtained under different pressures.

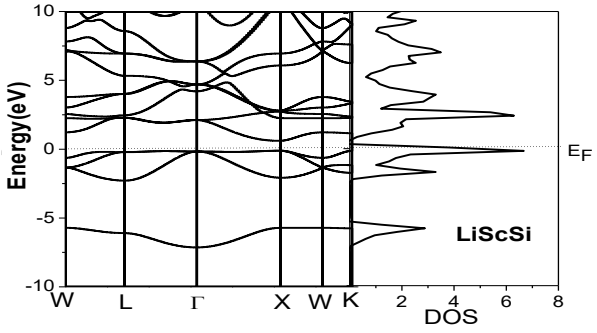

Fig.1 Band structure and DOS for LiScSi

References

[1] C. Uher, J. Yang, S. Hu, D. T. Morelli, G. P. Meisner, Phys. Rev. B 59(1999) 8615.

Ab Initio calcuations on Graphene Nanocarbon Material

M.T. Bilkan[1]

[1]*Department of Physics, Faculty of Science, Çankırı Karatekin University, Çankırı, Turkey*

E-mail:mtbilkan@gmail.com.tr

The physical and chemical some properties such as optimized structure, electronic, vibrational and thermochemical properties of Graphene Nanocarbon Materials were examined by using Density Functional Theory (DFT) with a hybrid functional Becke's Three Parameter Hybrid Functional Using the Lee-Yang-Parr Correlation Functional (B3LYP). The calculations have been conducted with 6-31G(d) and 6-311++G(d,p) basis sets by Gaussian09 program. The optimized structures were determined and were compared with experimental. In the optimization process, located at the edge of graphene layer, open-ended carbon atoms is covered with hydrogen atoms and "Ghost Atoms". The Ghost Atoms are an atom with mechanics type *Bq* is set up as a ghost of the corresponding atom, with its normal basis functions and numerical integration grid points but no nuclear charge or electrons. The wave numbers and intensities of the vibrational frequencies of optimized geometric structures were also computed. The results show that the calculated structural, vibrational and electronic parameters of graphene layer are very suitable with the experimental ones.

Structural and vibrational properties of polypyrrole organic polymer

M.T. Bilkan[1] and Ç. Bilkan[2]

[1]*Department of Physics, Faculty of Science, Çankırı Karatekin University, Çankırı, Turkey*

[2]*Department of Physics, Faculty of Science, Gazi University, Ankara, Turkey*

E-mail:mtbilkan@gmail.com.tr

Polypyrrole (PPy) is a type of organic polymer formed by polymerization of pyrrole. In this study, the structural and electronic properties of PPy were examined by using Density Functional Theory (DFT) with a hybrid functional Becke's Three Parameter Hybrid Functional Using the Lee-Yang-Parr Correlation Functional (B3LYP). The calculations have been conducted with 6-31G(d) and 6-311++G(d,p) basis sets by Gaussian09 program. The optimized structures were obtained. In the optimization process, located at the edge of PPy, open-ended carbon atoms is covered with hydrogen atoms and "Ghost Atoms". The Ghost Atoms are an atom with mechanics type *Bq* is set up as a ghost of the corresponding atom, with its normal basis functions and numerical integration grid points but no nuclear charge or electrons. The wave numbers and intensities of the vibrational frequencies of optimized geometric structures were also computed. In this study, we also investigated the effects of PPy interfacial layer the electrical characteristics in Cr/p-Si (MS) SBDs with and without PPy interfacial layer. In order to see the effect of PPy interfacial layer on electrical characteristics, both the Cr/p-Si (MS) and Cr/PPy/p-Si (MPS) type SBDs were fabricated and the obtained these electrical parameters from the forward and reverse I-V, C-V and G/□-V measurements. The results show that the calculated structural and vibrational properties of PPy are very suitable with the experimental ones. All of experimental results also confirmed that the use of PPy interlayer between metal and semiconductor can be used an alternative material to replace the conventional SiO_2 interlayer.

Viscosity Properties of Biocompatible Gelatinous Solutions with Glucose and Sodium Chloride

N. Koyuncu[1], İ. Ulusaraç [1], B. Demirbay[2] and F.G. Acar[1,*]

[1]*Department of Physics Engineering, Faculty of Science and Letters, İstanbul Technical University, 34469 Maslak, İstanbul, Turkey*

[2]*Physics Engineering Program, Institute of Science and Technology, İstanbul Technical University, 34469 Maslak, İstanbul, Turkey*

[*] E-mail :acarg@itu.edu.tr

Nowadays, the key element called biocompatibility takes a significant role for the revolution of the biomaterial science. Biocompatible materials are synthetic or a natural material which is used in various medical treatments and it can be replaced in any part of a biological systems, particularly tissues. The application fields of biomaterials are not only limited by medicine. Those materials have a wide aspect in science such that physics, material science, chemistry, and so on [1]. Biocompatible materials generally divide into three categories; metals such as stainless steel which is used as implants to provide stability and to restore the initial bone mechanics since it speeds up the healing process, ceramics such as aluminum oxide that is used as a dental restorative material. Also, some polymers such as silicones can be used as pacemakers or hydrocephalic shunts. The use of natural polymers such like a gelatin can be evaluated in ocular tissue engineering.

The biocompability of materials can be examined in consideration of some special parameters such as viscosity. The term of viscosity is one of the measure of the internal friction of a moving fluid. If the fluid has large viscosity, its molecular form has a huge internal friction opposite and the fluid which has a low viscosity, easily moves since it has a less friction. In this study, for the investigation of fluid types, sodium chloride (NaCl), glucose solutions which have various percentages, were mixed with pure gelatin solutions to prepare gelatin based solutions. Therefore, 2% of pure gelatin solution with 1%, 2%, 3%, 4% and 5% of NaCl and glucose solutions were obtained separately. Each gelatin based solutions consists of 80% of pure gelatin content and 20% of NaCl or glucose content. Depending on the viscosity of each prepared solution was analyzed respectively. All the experimental procedure were done in optimum conditions at the room temperature. As a result of the measurements, pure gelatin content and gelatin based solutions were compared each other considering shear stress, shear rate and viscosity values. The measurements of prepared solutions which have low viscosity, were performed by using the Fungilab Rotational Viscometer.

By taking into consideration of our laboratory work, fluid type, viscosity behavior and corresponding mathematical models of all prepared gelatin based substances will be presented.

[1] www.fy.chalmers.se/projects/biocompatiblematerials/publications/Biocomp

Transport Mechanisms of InAs/InP Quantum Dashes and InAs/GaAs Quantum Dots Based p-i-n Laser Heterostructure

N. Ayarcı, O.Özdemir[1], and K. Bozkurt[1]

[1] *Department of Physics, Faculty of Science and Letter, İstanbul, State, Turkey*

E-mail :nayarci@yildiz.edu.tr

In this work, carrier transport mechanisms of InAs/GaAs Quantum Dots and InAs/InP Quantum Dashes based p-i-n laser heterostructure were studied through temperature dependent current density voltage measurements. This structures were designed to emit a laser light at 1300 and 1550 nm, respectively. In both structures, first, carriers were tunneled from quantum well into QDots in InAs/GaAs and QDashes in InAs/InP and then recombine within Qdots and QDashes to emit a long wavelength laser light at 1300nm and 1550 nm, respectively. The transport of carrier was manifested as tunneling and recombination as the carrier conduction mechanisms.

Keywords: Long wavelength laser diode, Quantum Dots, Quantum Dashes

Synthesis and Characterization of Polymers Containing Phenothiazine Unit

Ruhiye Nilay Tezel, İsmet Kaya

Çanakkale Onsekiz Mart University, Faculty of Sciences and Arts, Department of Chemistry, Polymer Analysis Laboratory, 17020 Çanakkale.

E-mail: *nilaytezel@gmail.com*

Phenothiazine is a kind of heterocyclic compounds which possess simultaneously a nitrogen atom with lone-pair electrons and an electron-giving sulfur atom in the same six-member ring. Meanwhile, the skeleton structure of phenothiazine shows a butterfly conformation in the ground state which can efficiently impede the intermolecular aggregation. The additional electron-rich sulfur atom endows phenothiazine a stronger electron-donating ability than common amine-type dyes, resulting in a wide application of phenothiazine in DSSCs as donor segments [1]. In addition, due to hole conductivity of the phenothiazines and its ability reversibly form a stable radical cation, polymer molecules containing phenothiazine units are also of great interest for electronic application. Polymers with phenothiazine redox functionality are promising candidates as cathode active materials due to their electron donating properties.

In this study aliphatic and aromatic bridging monomers containing phenothiazine unit were synthesized and convert into corresponding polymers via oxidative polymerization. The structures of monomers and polymers were confirmed FT-IR, ^{1}H-NMR, ^{13}C-NMR, UV-Vis spectral techniques. The characterization was undertaken by GPC, TGA, DSC, SEC, CV and fluorescence analyses. In addition, morphological properties of these compounds were determined with SEM analyses.

Keywords: Phenothiazine, oxidative polymerization, characterization of polymers

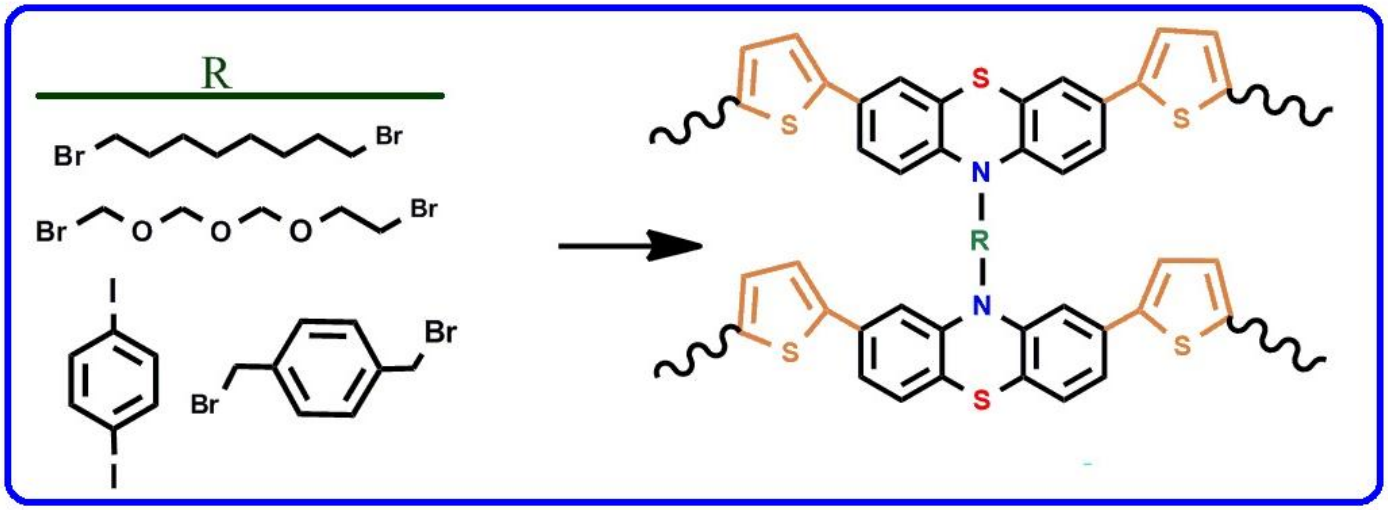

References:

[1] H.-H. Gao, X. Qian, W.-Y. Chang, S.-S. Wang, Y.-Z. Zhu, J.-Y. Zheng, Oligothiophene-linked D-π-A type phenothiazine dyes for dye-sensitized solar cells, 307, (2016), 866-874.

Conductivity Mechanism of SmA Liquid Crystal 4-((S)-3,7-Dimethyloctyloxy)-2-[[[4-(S)-2-methylbutoxyphenyl]imino]methyl]phenol in Different Temperatures

Nimet Yilmaz Canli [1], Alptekin Yildiz[2], Pınar Çağlar[3], Hale Ocak[4], M. Okutan[1], Belkız Bilgin Eran[4]

[1]*Yildiz Technical University, Department of Physics, 34220 Istanbul, Turkey*

[2]*Istanbul Technical University, Department of Physics Engineering, 34469 Maslak, Istanbul, Turkey*

[3]*Yildiz Technical University, Department of Molecular Biology and Genetics, 34220 Istanbul,Turkey*

[4]*Yildiz Technical University, Department of Chemistry, 34220 Istanbul, Turkey*

E-mail:niyilmaz@yahoo.com

Determination of liquid crystals' conductivity mechanisms depending on different temperatures becomes important because of the technological device applications. In this study, ac conductivity and electronic properties of the 4-((S)-3,7-Dimethyloctyloxy)-2-[[[4-(S)-2-methylbutoxyphenyl]imino]methyl]phenol have been analyzed by means of impedance spectroscopy measurements. The mesophase behaviour has been studied by differential scanning calorimetry and polarizing microscopy. It has been found that this liquid crystal (LC) exhibits enantiotropic Smectic A (SmA) mesophase at very low temperatures. The real and imaginary parts of dielectric constant have been calculated by capacitance method. It has been determined that the conductivity mechanism of the LC alters with the temperature interval 25-80 ^{o}C. The frequency dependence of ac conductivity (σ_{ac}) of the LC has been analyzed by means of frequency exponent parameter, s.

This research has been supported by Yildiz Technical University Scientific Research Projects Coordination Department with the Project Number **2013-01-02-KAP06**.

Keywords: Liquid crystal, Ac conductivity, Dielectric strength, Impedance Spectroscopy.

The Temperature Effect on Dielectric Behaviour of Ethyl-4-(7,7,8,8,9,9,10,10,10-nonafluorodecyloxy)biphenyl-4'- carboxylate (ENBC) Liquid Crystal

Nimet Yilmaz Canli [1], ***Gürkan Karanlık*** [2], ***Alptekin Yildiz*** [3], ***Hale Ocak*** [2], ***M. Okutan*** [1], ***Belkız Bilgin Eran*** [2]

[1]*Yildiz Technical University, Department of Physics, 34220 Istanbul, Turkey*

[2]*Yildiz Technical University, Department of Chemistry, 34220 Istanbul, Turkey*

[3]*Istanbul Technical University, Department of Physics Engineering, 34469 Maslak, Istanbul, Turkey*

E-mail:niyilmaz@yahoo.com

Dielectric spectroscopy (DS) is a very powerful and important tool for better understanding of the molecular dynamics and relaxation phenomena in LCs. In this study, phase transition temperatures and electronic properties of Ethyl-4-(7,7,8,8,9,9,10,10,10-nonafluorodecyloxy)biphenyl-4'-carboxylate (**ENBC**) liquid crystal [1] which exhibits enantiotropic SmA mesophase have been analyzed by means of dielectric and impedance spectroscopy measurements. In order to analyze phase transition temperatures of the **ENBC**, the temperature dependences of the real and imaginary parts of the dielectric constant of LC have been calculated. In this way, the influence of temperatures on the dielectric properties of LC and how the dielectric properties change depending on the LC phase within the temperature interval of 25-180 ^{o}C have been revealed. By these dielectric measurements, phase transition temperatures T (°C) of the liquid crystal, which were characterized by Differential Scanning Calorimetry (DSC), have also been verified. These results show that dielectric investigation would be an alternative method to DSC, which have great importance in liquid crystal studies for determining transition temperature.

This research has been supported by Yildiz Technical University Scientific Research Projects Coordination Department with the Project Number: **2015-01-02-DOP08**.

[1] Yilmaz Canli N., Yildiz A., Karanlık G., Bilgin Eran, B., Okutan M. **Conductivity Mechanism of Ethyl-4-(7,7,8,8,9,9,10,10,10-nonafluorodecyloxy)biphenyl-4'- carboxylate (ENBC)** Journal of Nanoelectronics and Optoelectronics. Volume 11, number 1, 36-40, (**2016**).

Investigation of photoconductive properties of single-layered organic photoreceptors

N. Can, B. Can Ömür, and A. Altındal

Yildiz Technical University, Department of Physics, Esenler, İstanbul, Turkey

E-mail : can@yildiz.edu.tr

Photoconductive material is a new type of high technology information material which can generate electron-hole pairs upon illumination. Recent research has focused on the organic photoconductors since they have many remarkable advantages such as non-poisonous, low cost and mechanical and architectural flexibility. Organic photoconductive materials have been widely used in xerography, plate-making printings, laser printers and photovoltaic devices. Those industrialized organic photoreceptors fabricated in dual-layered function-separated structure, consisting of charge generation layer and charge transport layer, lead to some shortcomings such as relative complicated architectural techniques. From this point of view, the single-layered organic photoreceptor is a new attractive subject in the research of photoreceptors.

In the present work, the fabrication of single-layered configuration photoreceptors is described. Samples of small molecule organic compound, bulk fullerene (C_{60}) and their blends in different weight percents were prepared in the form of thin films. The photoconducting properties of the sample films were analyzed on a home made photocurrent measuring instrument, where a monochromator was used to obtain the monochromatic light from a 250 W Xe lamp. The photoconductivity study shows that photosensitivity of the films strongly depends on the blend ratios. The photoconductivity experiment also shows that small molecule based single-layered photoreceptors provide an opportunity to fabricate cheap and practical devices.

Keywords: photoconductivity, small molecule, organic semiconductors, fullerene

Dielectric Characterization of Conducting Polymers/ Borax Composites

M. Kılıç[1], Y. Karabul[1], S. Erdönmez[1], A. E. Bulgurcuoğlu[1], Ö. Yağcı[1], Ü. Alkan[2], M. Okutan[1] and O. İçelli[1]

[1]*Department of Physics, Yıldız Technical University, İstanbul, Turkey*

[2]*Department of Computer Engineering, Istanbul Gelişim University, İstanbul, Turkey*

e-mail: oicelli@yildiz.edu.tr

Conducting polymers, such as polythiophene, polypyrrole and polyaniline have become issue of increased research concern because of facile synthesis, good environmental and thermal stabilities, high electrical properties [1]. Conducting polymer composites have receive remarkable interest from researches due to wide application areas such as solar cells, electrochromic devices, sensors, rechargeable batteries[2],[3].

The aim of this study is to investigate dielectric properties of borax doped conducting polymers. For this purpose, we prepared polythiophene/borax, polypyrrole/borax and polyaniline/borax composites. Dielectric properties of conducting polymers doped %10, %25, %50 borax were analyzed by dielectric spectroscopy. Dielectric constant, dielectric loss and AC conductivity of conducting polymer/ borax composites were investigated as a function of frequency.

References

[1] RuoChen L., ZhengPing L., Polythiophene: Synthesis in aqueous medium and controllable morphology, Chinese Science Bulletin, 54, 2008-2032 (2009).

[2] Balllav N., Biswas M., Conducting composites of polythiophene and polyfuran with acetylene black, Polymer International, 52, 179-184 (2005)

[3] Shown I., Ganguly A., Chen L., Chen K., Conducting polymer-based flexible supercapacitor, Polymer International, 3, 2-26 (2015).

Synthesis, characterization, and photovoltaic properties of free-base, Co^{II}, Mg^{II}, Ni^{II}, and Zn^{II} containing porphyrazines as electron-transporting materials for dye-sensitized solar cells

Osman Gürbüz[1,*], İbrahim Erden[2], and Mustafa Okutan[1]

[1]Department of Physics, Yıldız Technical University, Esenler, 34210, Istanbul-Turkey

[2]Department of Chemistry, Yıldız Technical University, Esenler, 34210, Istanbul-Turkey

**Corresponding author. Tel: +90 212 3837070 Ex: 7268; Fax: +90 212 3834011*

E-mail address: osgurbuz@yildiz.edu.tr (O. Gürbüz).

In order to analyze the interests between chemical structures of new organic dyes based on octakis (pyranosulfanyl) porphyrazines complexes and their properties as compared with photovoltaic applications, along with -spacers have been designed, synthesized and characterized. The experiments were performed on five compounds, four of them were metallated at the core with Co (II), Mg (II), Ni (II) or Zn (II) ions, and the fifth one was metal-free porphyrazines (H_2-Pz). The photovoltaic and electrochemical properties of these dyes were investigated, and their performances as photosensitizers in dye-sensitized solar cells (DSSCs) were examined. The new compounds have been characterized by elemental analysis, UV-Vis, FT-IR, ^{1}H-NMR and mass spectra. The spectral properties such as electronic spectra, aggregation and fluorescence of compounds were studied in chloroform. Complexes showed similar fluorescence behavior. The photovoltaic cell efficiencies (PCE) of the devices were in the range of 2.19–5.52% under simulated AM 1.5 solar irradiation of 100 mW/cm^2, and the highest Voc reached 1.27V. Compared with the H_2-Pz, Mg-Pz, Co-Pz, Ni-Pz and Zn-Pz based on DSSCs, the Zn-Pz based DSSCs exhibited significantly excellent photovoltaic activities under their radiation of visible light. Furthermore, the results of the studies show that the PCE values of metallated porphyrazines based DSSCs were bigger than that of metal-free porphyrazines (H_2-Pz) ligand under visible light irradiation.

Effect of Fullerenon Diode Parameters of Co-dopped PVC/p-Si

İbrahim Hüdai Taşdemir[1], Özkan Vural[2]

[1]*Amasya University, Faculty of Arts and Science, Department of Chemistry, Amasya, Turkey*

[2]*Amasya University, Faculty of Arts and Science, Department of Physics, Amasya, Turkey*

e-mail:ozkan.vural@amasya.edu.tr

Sandwich structures based on metal-semiconductor and metal-insulator-semiconductor are generally named as Schottky barrier diodes [1-3].Electrical circuits involve Schottky barrier diodes in prospective electronics are of great importance because of numerous advantages such as their low forward voltage drop and high switching speeds and these superiorities make them ideal for output devices in switching power supplies, and applications with high frequency [1-3].In this study Al/PVC-Co/p-Si (D1) and Al/PVC-Co-C_{60}/p-Si (D2) Schottky barrier diodes were fabricated (Fig. 1) and their electrical parameters were comparatively analyzed from the *I–V* characteristics and effect of C_{60} as a dopant in PVC-Co was investigated. Diodes parameters such as ideality factor, barrier height, series resistance and shunt resistance were calculated at ambient conditions. In the presence of C_{60} as a dopant in PVC-Co structure, improvement in investigated parameters were noticed such as ideality factor was decreased from 2.63 to 1.55, barrier height was decreased from 0.82 eV to 0.80 eV, serial resistance was lowered from 1868 Ω to 723Ω.

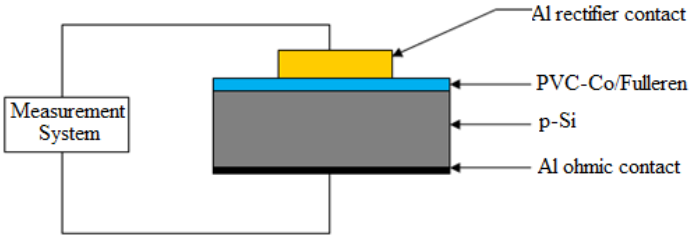

Fig. 1 Schematic cross-section of the Al/PVC-Co-C_{60}/p-Si Schottky structure

References

[1] *H.C. Card* and *E.H. Rhoderick*, Studies of tunnel MOS diodes I. Interface effects in silicon Schottky diodes. *J. Phys. D.* (*Appl. Phys.*)*4, 1589* (*1971*)

[2] A. Singh, K. C. Reinhardtand W. A. Anderson, Temperature dependence of the electrical characteristics of Yb/p-InPtunnel metal-insulator-semiconductor junctions. J. Appl. Phys. 68, 3475 (1990)

[3] S. Chand and J. Kumar, Current-voltage characteristics and barrier parameters of Pd2Si/p-Si(111) Schottky diodes in a wide temperature range, Semicond. Sci. Technol. 10, 1680 (1995)

Acknowledgement

This work was supported financially by Scientific Research Unit of Amasya University with the grant numbers of “FMB-BAP 13-058“and “FMB-BAP 14-069” and Central Research Laboratory of Amasya University

Effect of TiO2 Layer Thickness on Diode Parameters

İbrahim Hüdai Taşdemir[1], Mehmet Okan Erdal[2], Özkan Vural[3]

[1]*Amasya University,Faculty of Arts and Science, Department of Chemistry, Amasya, Turkey*

[2]*Necmettin Erbakan University,Seydişehir Vocational High School, Konya, Turkey*

[3]*Amasya University,Faculty of Arts and Science, Department of Physics, Amasya, Turkey*

e-mail:ozkan.vural@amasya.edu.tr

Electrical devices involve different type of diode in prospective electronics is of great importance. In this study, effect of thickness of TiO_2 layer on diode parameters of Schottky structures based on p-type Si was investigated. Si wafer surface (100) was covered with thin film of TiO_2 dispersion in H_2O having various TiO_2 concentration to construct p-Si/TiO_2/Al barrier diode with different thickness of TiO_2 and electrical characteristics such as current–voltage (*I–V*) and capacity-voltage (*C–V*) of these devices were measured at ambient conditions. Some parameters including ideality factor (*n*), barrier height (ϕ_{B0}) and series resistance (R_s) were calculated. As TiO_2 thickness (as a function of concentration in dispersion) was increased, diodes were deviated from ideality as could be inferred from the increase of ideality factor from 1.52 to 2.11 when TiO_2 thickness was increased from 0.13µm to 0.78 µm.

Acknowledgement

This work was supported financially by Scientific Research Unit of Amasya University with the grant numbers of “FMB-BAP 13-058“and “FMB-BAP 14-069” and Central Research Laboratory of Amasya University

Enhancement of photovoltaic performance of PCPDTTBTT solar cells with inclusion of Gold (Au) nanorods

Pelin Kavak[1], Nimet İlkem Evcimen[2], Emren Nalbant Esentürk[2], Elif Altürk Parlak[3], Kubilay Kutlu[1]

[1]Yildiz Technical University, Department of Physics, Faculty of Arts and Science, Istanbul,Turkey
[2]Middle East Technical University, Department of Chemistry, Ankara,Turkey
[3]Scientific and Technological Research Council of Turkey (TÜBİTAK) Marmara Research Centre (MAM), Chemistry Institute, Kocaeli, Turkey
E-mail: pelinay84@gmail.com

Polymer-fullerene bulk heterojunction solar cells (PSCs) are currently attracting a great deal of attention having already shown great promise as renewable, lightweight, and low cost energy sources[1-2]. The poly [N-9,7di-2-thienyl-2,1, 3-hepta-decanyl-2,7-carbazole-alt-5,5-benzothiadiazole) is one of the new generation of polymers that have been designed for organic photovoltaic applications. Metal Nanoparticles are usually made of aluminum (Al), Ag, Au or copper (Cu) because these metals strongly interact with the sunlight. Specifically, aluminum and silver lead to surface plasmons resonance in the ultraviolet spectrum while Au and Cu lead to surface plasmons resonance in the visible spectrum. In this letter, the effect of Gold (Au) nanorods (NRs) on PCPDTTBTT performance of solar cells has been investigated. Power conversion efficiency of PCPDTTBTT solar cells improved to 0.92% from 0.74% with inclusion of Au nanorods (about 24% improvement).

[1] S.H. Park, A. Roy, S. Beaupre, S. Cho, N. Coates, J.S. Moon, D. Moses, M. Leclerc, K. Lee, A.J. Heeger, Bulk heterojunction solar cells with internal quantum efficiency approaching 100%, Nat Phot., 3 (2009), pp. 297–302.
[2] H.Y. Chen, J. Hou, S. Zhang, Y. Liang, G. Yang, Y. Yang, L. Yu, Y. Wu, G. Li, Polymer solar cells with enhanced open-circuit voltage and efficiency, Nat Phot., 3 (2009), pp. 649–653

The Investigation of Frequency Dependence of Electrical Parametres of $Al/Bi_4Ti_3O_{12}/n$-Si (MIS) with 540 ^oA Structures

Perihan DURMUŞ

[1]*Physics Department, Faculty of Arts and Sciences, Gazi University, 06500, Teknikokullar, Ankara, TURKEY*

E-mail :pdurmus@gazi.edu.tr

In this study, the frequency and voltage dependence of capacitance-voltage (C- V) and conductance-voltage (G/w-V) characteristics of the $Al/Bi_4Ti_3O_{12}/n$-Si (MIS) structures were investigated by considering series resistance (R_S) and interface state (N_{SS}) effects in the wide frequency range of 100 Hz-1 MHz respectively. Experimental results confirmed that the main electrical parameters are a strong function of frequency and voltage. The voltage dependent profile of N_{SS} and R_S were obtained using low-high frequency and Nicolian and Brews methods. Both the values of Rs and Nss decrease with increasing frequency almost as exponentially. Also, the measured capacitance (C_m) and conductance (G_m/w) values at high frequency were corrected to eliminate of the Rs effect or obtain the real values of them. Experimental results show that the existence of an interfacial layer and Nss at metal/semiconductor interface and Rs play an important role on the electrical characteristics of MIS structure. The high values of C and G/w at low frequencies can be attributed to the charges at traps, surface and dipole polarizations. Because at low frequencies; both these charges can be easily follow the ac signal and polarization processes will be occurs due to their relaxation time.

Influence of frequency on dielectric properties, electric conductivity and electrical modulus of Al/Bi4Ti3O12/n-Si (MIS) structures

Perihan DURMUŞ

[1]*Physics Department, Faculty of Arts and Sciences, Gazi University, 06500, Teknikokullar, Ankara, TURKEY*

E-mail :pdurmus@gazi.edu.tr

The frequency dependence of dielectric constant (ε'), dielectric loss (ε''), loss tangent (tan δ) and the ac electrical conductivity (σ_{ac}) of Al/$Bi_4Ti_3O_{12}$/n-Si Schottky barrier diodes were studied in the wide range of frequency (1kHz-5MHz) at room temperature. All these parameters were calculated from the forward and reverse bias capacitance/conductance-voltage (C/G-V) measurements in the wide applied bias voltage by using HP 4192A LF impedance analyzer. Experimental results show that both dielectric properties and ac conductivity were quite sensitive to frequency at relatively at low frequencies in depletion and accumulation regions. While the values of ε' and ε'' decrease with increasing frequency, σ_{ac} increase. In addition, the value of σ_{ac} at high frequencies (f≥50 kHz) starts as almost exponentially, but this change in σ_{ac} is considerably low. Such behavior of σ_{ac} at low and intermediate frequencies was corresponding to the dc conductivity and at high frequency range corresponding to ac conductivity. In order to good interpret of conduction and polarization processes, the real (M') and imaginary (M '') components of the electrical modulus were also calculated from the ε' and ε'' data for two different frequencies. It was found that the values of M' and M'' were quite sensitive to frequency and applied bias voltage. As a result, High-dielectric $Bi_4Ti_3O_{12}$ are more effective on the dielectric properties and conductivity.

Effect of spacer group on optoelectronic properties of napthaleneimide containing poly(2,5-dithienylpyrrole)s

Pınar Çamurlu, Neşe Güven

[1]*Akdeniz University, Department of Chemistry, 07058, Antalya, Turkey*

E-mail :pcamurlu@akdeniz.edu.tr

Here in were disclose synthesis and characterization of a napthaleneimide containing poly(2,5-dithienylpyrrole) having shorter spacer group than its preceding derivative [1]. For this purpose, 2,5-dithienylpyrrole derivative (SNS-Napth2) was synthesized through a click reaction between SNS-N_3 and 2-(prop-2-yn-1-yl)-1H-benzo[de]isoquinoline-1,3(2H)-dione (Figure 1). The monomer was electrochemically polymerized in $LiClO_4$/AN both potentiodynamically and potentiostatically. The polymer revealed ambipolar redox behavior, where reversible, stable n- type doping ($E_{1/2,p}$= -1.31 V) and p-type doping ($E_{1/2,p}$= 0.53 V) was achieved in cathodic and anodic regime, respectively. The optical band gap of P(SNS-Napth2) was calculated as 3.33 eV. Spectroelectrochemistry analysis of PPyNI reflected electronic transitions at 334 nm and 480-900 nm due to π– π * transition and charge carrier band formations, respectively. Our studies have shown that lowering the spacer group lowers the reversibility of n- type doping and increases the band gap.

We are grateful to TUBITAK (Project No: 110T640) for the support of this study.

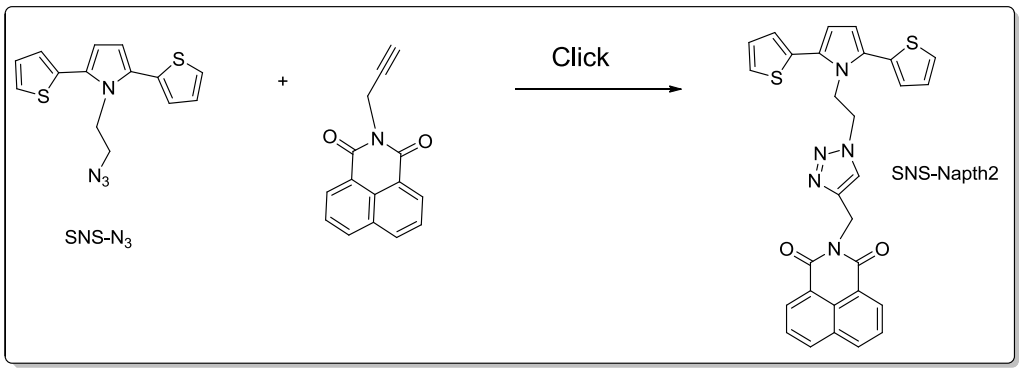

Figure 1. The synthetic route of SNS-Napth2

References

[1] Camurlu P., Karagoren N. Both p and n-Dopable, Multichromic, Napthalineimide Clicked Poly(2,5-dithienylpyrrole) Derivatives J. Electrochem. Soc. 160, H560 (2013).

A Comphensive Study on Dielectric Mechanism of Conducting Polymers/ Sodium Silicate Composites

S. Erdönmez, A. E. Bulgurcuoğlu, Y. Karabul, M. Kılıç, Z. G. Özdemir, M. Okutan, A. Altındal
Department of Physics, Yıldız Technical University, İstanbul, Turkey
e-mail: erdonmez@yildiz.edu.tr

Conducting polymers have attracted tremendous attention due to their unique electrical, optical and magnetic properties [1]. Among the conducting polymers, polyaniline, polythiophene and polypyrrole have incomparable properties because of their environmental and thermal stability, ease of synthesis and high electrical properties [2]. Conducting polymer composites generated by integrating some organic or inorganic materials into conductive polymer, have extensive application scope, such as solar cells, electrochromic device, sensors, light emitting diodes [3].

In this study, several conducting polymers were doped with different weight percentage of sodium silicate. In this way, Polythiophene/Sodium Silicate, Polypyrrole/Sodium Silicate and Polyaniline/ Sodium Silicate composites are prepared. Dielectric properties of Conducting Polymers/ Sodium Silicate composites were investigated using dielectric spectroscopy. The real (ε') and the imaginary parts (ε") of the complex dielectric constant were measured by impedance analyzer. ε', ε", dielectric loss (tanδ) and AC conductivity were expressed in detail.

References

[1] E. Ahlatcıoğlu Özerol, B.F. Şenkal, M. Okutan, Preparation and characterization of graphite composites of polyaniline, Microelectronic Engineering, 2015, 76-80.

[2] Erdonmez S., Ozkacanc E. Power-law conductivity in polythiophene/copper(II) acetylacetonate composites, Polymer International, 2012, 31-36

[3] Majid K, Tabassum R, Shah AF, Ahmad S and Singla ML, Dielectric Properties of Polythiophene- CoO Composites, J Mater Sci: Mater Electron 20.958-966 (2009).

Synthesis of Mono and Di-Nuclear Ruthenium(II) Complexes

S.B.Kavukcu , S.Denizaltı, H.Türkmen
Department of Chemistry, Ege University, 35100 Bornova-Izmir, Turkey
E-mail:sbkavukcu@gmail.com

Platinum-based drugs are clinically used on a daily basis to treat cancers[1]. The limitations of platinum-based drugs, dose dependent side effects and development of drug resistance mechanisms, have boosted the research for finding other metal-based drugs. Among metals, ruthenium is probably the one showing the greatest promises. Ruthenium appears to be less toxic than platinum and several biological studies have indicated that ruthenium complexes possess diverse modes of action[2]. The redox chemistry of ruthenium is rich and compatible with biological media, and the overall toxicity of ruthenium is lower than platinum, thus allowing higher doses of treatment. Recently, studies has been shown that between the metals in the bimetallic system affected electronic interaction, anticancer properties and catalytic activity. Electron conduction between the two metals is provided by the π-conjugated bonds and thereby change the metal's oxidation. In this work, we prepared a series of ruthenium complexes (**I**, **II**) to investigate their anticancer and antimicrobial activities. These complexes were characterized by ^{1}H, ^{13}C NMR and elemental analyses.

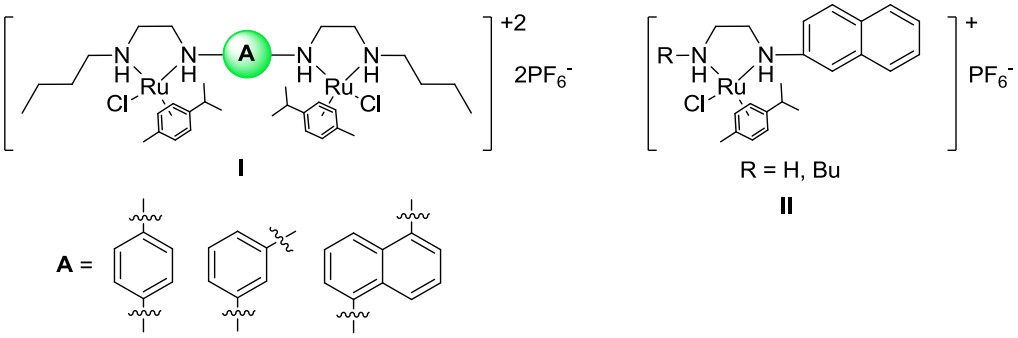

References

[1] Wong B., Vancamp L., Trosko J. E. and Mansour V. H., 1969, "Platinum Compounds: a new class of potent antitumour agents", Nature, 222, 385-386.

[2] Kostova J., 2006, "Ruthenium complexes as anticancer agents", Curr. Med. Chem., 13, 1085-1107.

Acknowledgments

This project is supported by TUBITAK(214Z098)

High Performance BenzimidazoliumIodides Bearing Triazole Group; As Solid Electrolyte in Dye-Sensitized Solar Cells

S. Dayan[1], M. O. Karataş[2],N. Kalaycıoğlu Özpozan[1], B. Alıcı[2]

[1]*Department of Chemistry, Faculty of Science, Kayseri, Erciyes University, Turkey*

[2]*Department of Chemistry, Faculty of Arts and Sciences, Malatya, İnönü University, Turkey*

E-mail: serkandayan_@hotmail.com

Dye-sensitized solar cells (DSSC) have attracted much attention as cost-effective devices that can convert sunlight into electrical energy. The technical development and scientific investigation of DSSCs in recent years have realized high power conversion efficiencies. In typical high-efficiency

DSSCs, organic liquid electrolytes containing the I^-/I_3^- redox couple have been routinely used because of the demands for sufficient mass transport and fast dye regeneration. However, the use of liquid electrolytes limits the practical development of DSSCs, retarding their commercialization. Replacing the liquid electrolytes with solid-state electrolytes (SSE) has been considered as one of the crucial issues in order to fully capitalize on the merits of DSSCs, through improving their mechanical stability and simplifying fabrication processes, including the elimination of the need for hermetic sealing [1,2].

In this study, we chose to prepare three new benzimidazole iodides were synthesized and characterized by H-NMR, C-NMR, UV-vis spectrophotometer, ionic conductivity and elemental analysis methods. The synthesized benzimidazole iodides was used as solid electrolyte in DSSC.

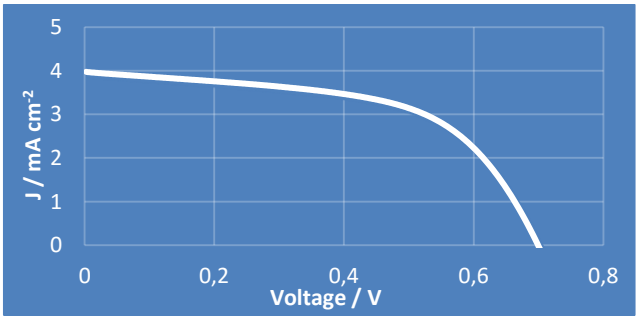

Figure-1 Photocurrent density–voltage characteristics for DSSC based benzimidazolium iodide

References

[1] P.Wang, S. M.Zakeeruddin, J. E. Moser,M. K.Nazeeruddin, T.Sekiguchi, M.Gratzel, A stable quasi-solid-state dye-sensitized solar cell with an amphiphilic ruthenium sensitizer and polymer gel electrolyte, Nat. Mater. 2, 402 (2003).

[2] P.Wang, S. M. Zakeeruddin, P.Comte, I. Exnar, M. Gratzel, Gelation of Ionic Liquid-BasedElectrolyteswithSilicaNanoparticlesforQuasi-Solid-StateDye-Sensitized Solar Cells, J. Am. Chem. Soc., 125, 1166 (2003).

Acknowledgments

We acknowledge the financial support granted by Erciyes University (ERUBAP), (FDK-2015-6013).

Potential usage of a new structurally characterised porphyrin derivative in organic light emitting diodes

Seyit Ali Güngör, Solgül Şahin, Ferhan Tümer
Department of Chemistry, Faculty of Science and Arts, Kahramanmaraş, Turkey
E-mail: gungorseyitali@gmail.com

The porphyrins are naturally occurring macrocyclic compounds, which have a crucial role in living organisms. The porphyrin ring structure is aromatic, with a total of 26 electrons in the conjugated system. Porphyrin based compounds have found several applications including photodynamic therapy, Biomimetic catalysis, dye-sensitized solar cells and so on due to their versatile physical and chemical properties [1]. Porphyrin materials have potential usage for organic electronics, specifically for organic light emitting diodes using luminescent emission [2]. Porphyrin derivatives and their metal complexes are sensitive chromogenic reagent and usually exhibit characteristic sharp and intensive absorption bands in the visible region. Porphyrin compounds exhibits an intensive absorption called the Soret band in the region of 400-500 nm range. This band is widely used for spectrophotometric determination of metalloporphyrins. Porphyrin compounds have received considerable attention due to their saturated red chromaticity and the narrow emission width in the range of 635–660 nm [3,4]. In this work, a novel α,α-5,10-bis-(*o*-aminofenil)-15,20-difenilporfirin derivative was prepared and characterised by the spectroscopic and analytical methods. Molecular structure of the compound was determined by single crystal X-ray diffraction study. Photophysical properties of the structurally characterized porphyrin derivative was studied by photoluminescence and UV-Vis. absorption studies both in the solid state and solutions. Crystal structure of the compound is shown in Figure.

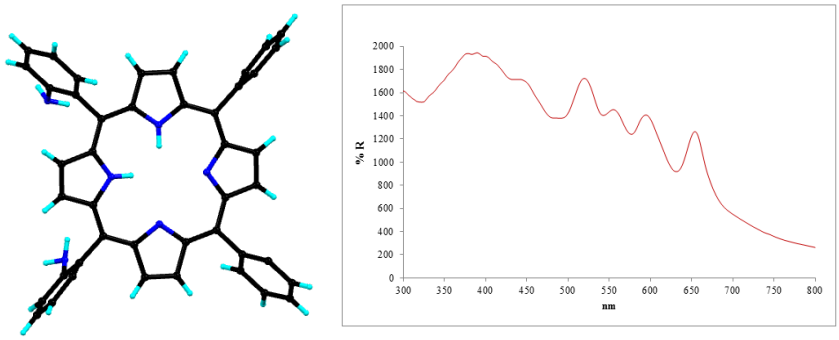

Figure: Molecular structure of α,α-5,10-bis-(*o*-aminofenil)-15,20-difenilporfirin and its solid state UV-Vis spectrum.

Acknowledgments: We are grateful to Research Council of Turkey (Tubitak Grant number: 113Z907 cost project) for financial support.

References

[1] M. Biesaga, K. Pyrzynska, M. Trojanowicz,Talanta 51, 209 (2000).
[2] M. G. Walter, A. B. Rudine, C. C. Wamser, Journal of Porphyrins and Phthalocyanines 14(9), 759 (2010).
[2] C. T. Chen, Chem. Mater. 16, 4389 (2004).
[3] M. A. Baldo, D. F. O'Brien, Y. You, A. Shoustikov, S. Sibley, M. E. Thompson, S. R. Forrest, Nature 395, 151 (1998).

Subsituent and complexation effects on material properties of new porphyrin-imine compounds

Seyit Ali Güngör, Songül Şahin, Mehmet Tümer
Department of Chemistry, Faculty of Science and Arts, Kahramanmaraş, Turkey
E-mail: gungorseyitali@gmail.com

One of the most important molecules typically found in the biological compounds is the porphyrins. These molecules have intensely colored red or purple. The porphyrin ligands have the exigible molecular and material properties, consisting of very large dipole moments, polarizabilities and hyperpolarizabilities [1]. The non-linear optical properties of these materials are of particular interest, in some sense energy transfer with molecular control, and in some sense potential applications in optical communications, data storage and electrooptical signal processing [2]. Material properties of porphyrin derivatives can be adjusted by attaching electron donor-acceptor groups or by complexation with metal ions [3]. In this work, mono-para-amino tetraphenylporpyrin and some salicylaldeyhde derivatives was used to obtain novel asymmetric iminoporphyrin compounds. In further work, we prepared Cu(II), Zn(II), Mn(III) and Fe(III) dinuclear complexes of these compounds. Photophysical material properties of the new popyrin compounds and their metal complexes were investigated both in the solution and solid state. The effect of substitute groups and complexation on photophysical properties was examined in detail.

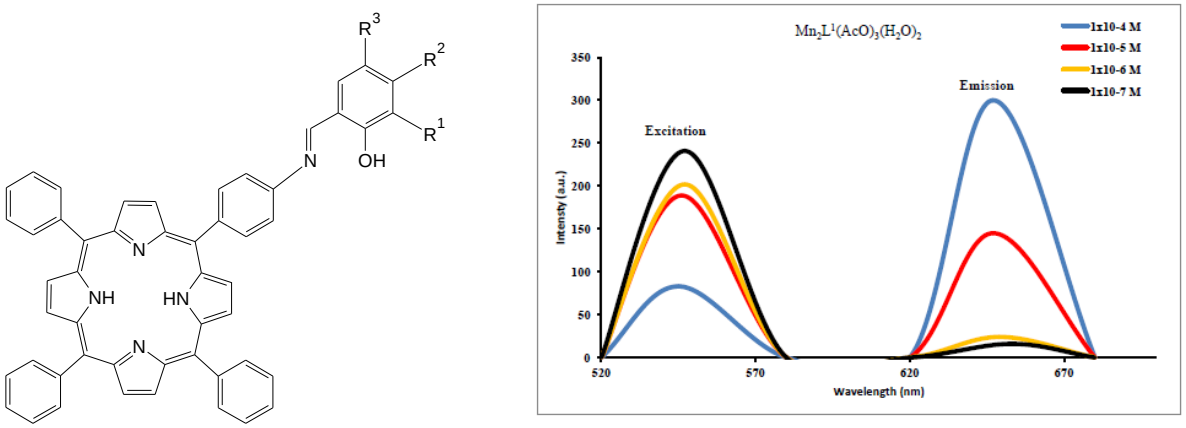

Fig. The proposed structure of new porpyrin imine compounds (HL^1: R^1=R^3= H, R^2: CH_3; HL^2: R^1=R^3= I, R^2: H; HL^3: R^1=R^3= Cl, R^2: H) and excitation and emission spectra of Mn(III) complex of HL^1)

Acknowledgments: We are grateful to Research Council of Turkey (Tubitak Grant number: 113Z907 cost project) for financial support.

References

[1] L.K. Yan, A. Pomogaeva, F . L . Gu, Y. Aoki, Theor. Chem. Acc., 125, 511 (2015).
[2] C. Li, J. Ly, B. Lei, W. Fan, D. Zhang, J. Han, M. Meyyappan, M. Thompson, C. Zhou, J. Phys. Chem. B 108, 9646, (2004).
[3] S. Purtas¸ M. Kose, F. Tümer, M. Tümer, A. Golcü, G. Ceyhan, Journal of Molecular Structure 1105, 293, (2016).

The reactions of the 4,7-dihydroindole with ketones: Initial Scope and Mechanistic Insights

Sinan Bayindir[1,2], Nurullah Saracoglu[1]

[1] *Department of Chemistry, Faculty of Sciences, Atatürk University, Erzurum, Turkey*

[2] *Department of Chemistry, Faculty of Sciences and Arts, Bingöl University, Bingöl, Turkey*

*E-mail: snanbay@atauni.edu.tr

Indoles and bis(indolyl)alkanes are important members of heterocyclic compounds due to their biological activities and synthetic applications [1]. As a result of these synthetic applications and biological activities, the synthesis of the substituted indoles and 2,2'-bis(indolyl) methanes make it very intriguing among the organic and medicinal chemist [2]. Although the C3-alkylation of indole can be achieved by various catalytic methods, a general protocol for the direct regioselective C2-alkylation of indoles does not exist [3]. Given the limited availability of synthetic routes toward 2-alkylindoles, straight forward approaches are always needed. In this study, we aim to an efficient synthesis of 2-alkylindole (**4**) and 2,2'-bis(indolyl)methane (**6**) derivatives, which are not readily available by present synthetic methods. Our synthetic approach is based on a dipole change of indole ring toward electrophilic substitution. During this study, we examined the reactions of the various ketones that have different electronic nature and one or two equivalent 4,7-dihydroindole (**1**).

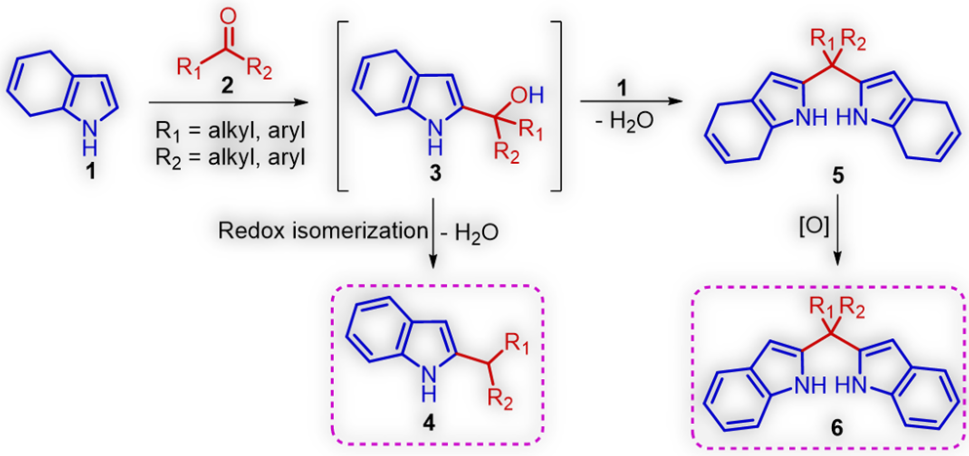

Figure. Synthesis approach of the 2-alkylindole and 2,2'-bis(indolyl)methane derivatives

References

[1] Ruiz, C., Valderrama, K., Zea, S. and Castellanos, L., (2013). Mariculture and natural production of the antitumoural (+)-Discodermolide by the caribbean marine sponge discodermia dissoluta. *Marine Biotechnology*, 15(5), 571-583.

[2] Carbone, A., Parrino, B., Di Vita, G., Attanzio, A., Spano, V., Montalbano, A. and Cirrincione, G., (2015). Synthesis and antiproliferative activity of thiazolyl-bispyrrolo[2,3-b]pyridines and indolyl-thiazolyl-pyrrolo[2,3-c]pyridines, Nortopsentin analogues. *Marine Drugs*, 13(1), 460-492.

[3] Kilic, H., Bayindir, S. and Saracoglu, N., (2014). 4,7-Dihydroindole: A synthon for the preparations of 2-substituted indoles. *Current Organic Synthesis*, 11(2), 167-181.

Synthesis of 4,5,6,7-Tetrahydro-1H-indole Based Amphiphile and Self-Assembly Studies

Sinan Bayindir[1], Kwang So-Lee[2], Jon R. Parquette[2], and Nurullah Saracoglu[3]

[1] Department of Chemistry, Faculty of Sciences and Arts, Bingöl University, Bingöl, , Turkey

[2]Department of Chemistry, The Ohio State University, Columbus, USA

[3] Department of Chemistry, Faculty of Sciences, Atatürk University, Erzurum, , Turkey

[*]E-mail: snanbay@atauni.edu.tr

Organic nanostructures based on π-conjugated systems have attracted increasing interest in the last years due to unmatched properties encouraging applications in the fields of optoelectronics, photonics and chemosensors as well as in nanoscale devices. [1-3]. Herein, we demonstrated a simple strategy to prepare nanostructures from indole based structures appended NDI-peptide. The indole based amphiphile**s 3** were prepared by sequential imidation of naphthalene dianhydride (NDI) with NH_2-lysine, and 4,5,6,7-tetrahydro-1*H*-indole (**2**). Amphiphilic building blocks were obtained via four synthesis steps. Consequently, the self-assembly of prepared amphiphilic molecule was obtained some irregular nanostructures, such as nanospheres, nanoring and nano-plate formations.

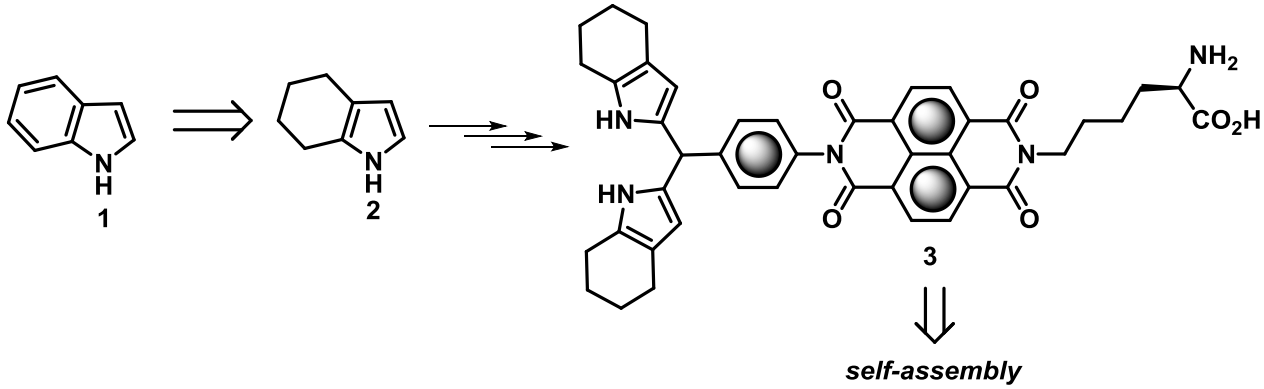

Figure. Synthesis of the indole-based amphiphile and nanostructures formed by self-assembly of amphiphile

References

Wu, M.; Ye, Z. Y.; Liu, Y. F.; Liu, B.; Zhao, X. J. (2011). Release of hydrophobic anticancer drug from a newly designed self-assembling peptide. *Mol Biosyst, 7* (6), 2040-2047.

Sun, Y.; Li, Z. B.; Wang, Z. H. (2012). Self-assembled monolayer and multilayer films based on *L*-lysine functionalized perylene bisimide. *Journal of Materials Chemistry*, 22(10), 4312-4318.

Martin, A. D.; Robinson, A. B.; Mason, A. F.; Wojciechowski, J. P.; Thordarson, P. (2014). Exceptionally strong hydrogels through self-assembly of an indole-capped dipeptide. *Chem. Comm.,* 50(98), 15541-15544.

Bioactive material design for the biological studies

S. Akar and M. Tümer

Chemistry Department, K.Maras Sütcü Imam University, K.Maras, Turkey

E-mail :sultanakarr@gmail.com

The azoimine compounds have the both -N=N- and –CH=N- groups. In these groups, the nitrogen atoms give the electrons to the metal ions and form the stable transition metal complexes. Properties of the azoimine ligands and their transition metal complexes were extensively investigated. Some researchers investigated the biological, tautomerism, electrochemical, photophysical, sensor and dye properties of the azoimine compounds[1]. We obtained a novel compound from the reaction of the 3-methoxy salicylaldehyde and azo amine compound in the methanol solution. The compound has orange color and suitable for synthesis the hybrid compound. The compound was characterized by the analytical and spectroscopic methods. The groups such as methoxy, hydroxy, imine and azo are important for biological studies. The synthesized compound has $–OCH_3$, -OH, -CH=N and N=N groups. The electrochemical properties of the compound was investigated in DMF solution and at different scan rates. The compound showed reversible redox potentials in the positive regions. The solution / solid state electronic and photoluminescence spectra of the compound were investigated and different bands determined in their spectra.

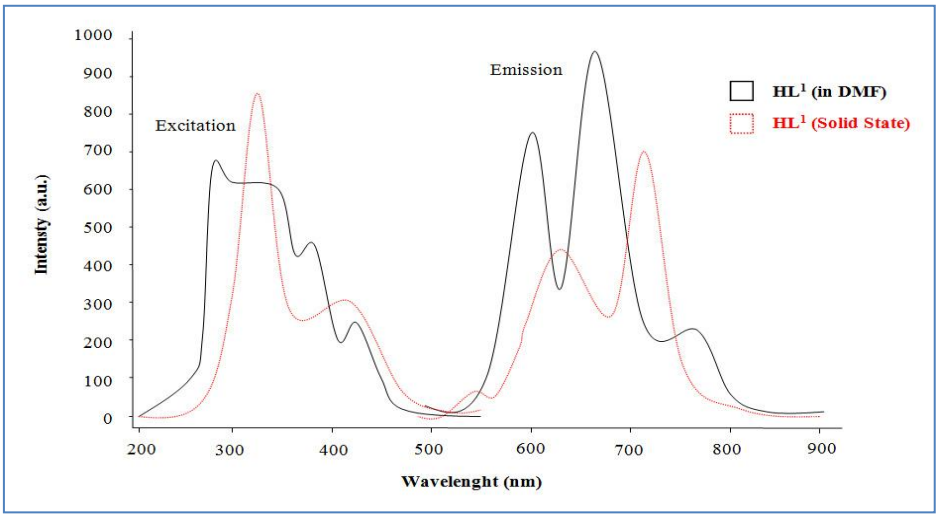

Figure. The photoluminescence spectra of the organic compound.

Acknowledgments

We are grateful to The Scientific & Technological Research Council of Turkey (TUBITAK) (Project number: 115Z065) for the support of this research.

Reference

[1] H. Karaer, İ. E. Gümrükçüoğlu, Synthesis and Spectral Characterisation of Novel Azo-Azomethine Dyes. Turk. J. Chem., 23, 67 (1999).

Bifonctionnal imine compounds for hybrid material preparing

S. Akar and F. Tümer
Chemistry Department, K.Maras Sütcü Imam University, K.Maras, Turkey
E-mail :sultanakarr@gmail.com

Azo dyes are an important class of the organic photoactive materials, due to their excellent optical switching properties. In addition, the azo dyes and their metal complexes are involved in many biological reactions such as inhibition of DNA, RNA and biological activity against bacteria and fungi. They are increasingly used in textile, leather and plastic industries. These compounds have a great ability to coordinate with many metal ions and form stable complexes. The coordination compounds of azo–azomethine ligands are also widely used in medicine, for corrosion prevention, metal recovery as well as to treat nuclear wastes [1]. We synthesized a novel bifunctional imine compound and characterized it by the analytical and spectroscopic methods. We obtained the single crystals of the compound from the ethanol solution and we characterized its molecular structure by the X-ray diffraction method. The electrochemical properties of the compound was investigated in DMF solution and at different scan rates. The compound showed reversible redox potentials in the positive regions. The solution / solid state electronic and photoluminescence spectra of the compound were investigated and different bands determined in its spectra.

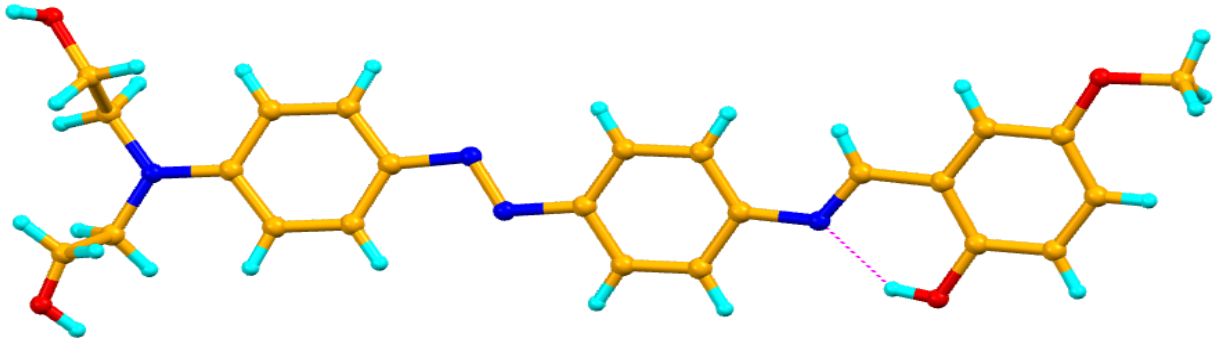

Figure. The X-ray ORTEP diagram of the organic compound.

Acknowledgments
We are grateful to The Scientific & Technological Research Council of Turkey (TUBITAK) (Project number: 115Z065) for the support of this research.

Reference

[1] E. İspir. The synthesis, characterization, electrochemical character, catalytic and antimicrobial activity of novel, azo-containing Schiff bases and their metal complexes. Dyes and Pig., 82, 13 (2009).

Low Voltage Pentacene Based Organic Thin Film Transistors With High Dielectric Constant Gate Insulator

S. Rüzgar*, M. Caglar, S. Ilican, Y. Caglar

Department of Physics, Anadolu University, Eskisehir, Turkey

*E-mail: serifruzgar@anadolu.edu.tr

The organic based field effect transistors (OFETs) have been intensively researched because of their unique properties such as their potential for application in low cost, large-area fabrication and flexible electronics [1]. Ordinary OFETs operation works at large bias (larger than 20 V). This condition leads to excessive power consumption and limits their real-world applications. Therefore, the reducing OFET operating voltages and high-mobility organic semiconductors are important for real applications. The low voltage transistor can be provided with high capacitance of insulator layer [2-3].

In this study, Pentacene based OFET with top contacts bottom gate configurations were fabricated. Titanium dioxide (TiO_2) with high dielectric constant was prepared for gate insulator with sol gel spin coating method on ITO substrate. As an active layer Pentacene thin-film with 50 nm thicknesses was evaporated dielectric layer by using thermal evaporation method (Vaksis PVD Handy-MT/101T, Turkey). After the deposition of the Pentacene film, finally the source and drain electrodes were prepared by evaporating a 100 nm Au layer through a shadow mask. The channel width and length of the transistor are 1000 µm and 50 µm, respectively.

The electrical measurements of Pentacene based-OFET were performed using a KEITHLEY 4200 SCS/CVU semiconductor characterization system with connected SIGNATONE Semi-Automatic Probe Station at room temperature under dark condition. The Pentacene based-OFET exhibited a p-channel behavior (Fig. 1). The mobility, I_{on}/I_{off} ratio and threshold voltage for this device were found to be 5.87 $cm^2 V^{-1} s^{-1}$, ~ 10^3 and -0.08 V, respectively.

References

[1] C. D. Dimitrakopoulos and P. R. L. Malenfant, Organic Thin Film Transistors for Large Area Electronics, Adv. Mater. (Weinheim, Ger.) 14 99 (2002)

[2] F. C. Chen, C. W. Chu, J. He, and Y. Yang, Organic thin-film transistors with nanocomposite dielectric gate insulator, Appl. Phys. Lett. 85, 3295 (2004)

[3] Y. D. Park, D. H. Kim, Y. Jang, M. Hwang, J. A. Lim, and K. Cho, Low-voltage polymer thin-film transistors with a self-assembled monolayer as the gate dielectric, Appl.Phys. Lett. 87, 243509 (2005)

Acknowledgements

This work was supported by Anadolu University Commission of Scientific Research Projects under Grant No. 1101F009 and 1501F030

Determination of hydration level by using nanostructured CdO films

B.Şahin[1] and T. Kaya[2]

[1]*Department of Physics, Faculty of Arts and Sciences, Mustafa Kemal University, Hatay, 31034, Turkey*

[2]*School of Engineering and Technology, Central Michigan University, Mt. Pleasant, 48859, USA*

E-mail :sahin38@gmail.com

Metal oxide based biosensors have shown great potential for health care and environmental monitoring. The efficiency of sensing materials depends on their structure and components which effects their stability, reusability and sensitivity. Highly transparent conducting semiconducting materials such as tin oxide (SnO_2), zinc oxide (ZnO) and cadmium oxide (CdO) are widely used for many sensor applications [1]. Among these, CdO is a promising material for electronic applications. This research reports a new technique for hydration level detection by using nanostructured CdO-based films. CdO films were grown on glass substrates via SILAR (Successive Ionic Layer Adsorption and Reaction) method. CdO films were also annealed at 300 ^{o}C, 350 ^{o}C and 400 ^{o}C in air ambient. The observation hydration level is very important for monitoring human body condition [2, 3]. This research describes the hydration level detection properties of nanostructured CdO films. The structure, morphology and sensing properties of the CdO films were investigated by powder x-ray diffraction (XRD), scanning electron microscopy (SEM) and I-V measurements. To the best of our knowledge this is the first ever research of the hydration detection properties of nanostructured CdO films.

References

[1] K. Sankarasubramanian, P. Soundarrajan, K. Sethuraman, K. Ramamurthi, Chemical spray pyrolysis deposition of transparent and conducting Fe doped CdO thin films for ethanol sensor, Materials Science in Semiconductor Processing 40 (2015) 879–884

[2] B. Sahin, M.Alomari, T.Kaya. Hydration Detection through use of artificial sweat in doped- and partially-doped nanostructured CuO films, Ceramics International 41 (2015) 8002–8007 .

[3] B. Sahin, T.Kaya, Highly improved hydration level sensing properties of Copper Oxide films with Sodium and Potassium doping, Applied Surface Science 362 (2016) 532-537.

Peripheral tetra substituted metallophthalocyanines carrying redox active cobalt(II), manganese (III), titanium(IV) center and their electropolymerization properties

T. Keleş[1], Ü.E. Özen[2], Z. Bıyıklıoğlu[1], A. Koca[2]

[1]*Department of Chemistry, Karadeniz Technical University, Trabzon, 61080, Turkey*

[2]*Department of Chemical Engineering, Marmara University, İstanbul, 34722, Turkey*

E-mail :turgutkls5055@gmail.com

Phthalocyanines are well-known 18 π-electron aromatic molecules [1]. Phthalocyanines are very important compounds owing to their blue-green color and electronic properties. Electropolymerization is a desired property for preparation of composite electrode, which has potentials for the usage in different electrochemical technologies such as, electrocatalytic, electrochromic and electrosensing applications [2]. For these reasons, in this study, we designed and synthesized a novel series of peripherally tetra-substituted metallophthalocyanines carrying redox active cobalt(II), manganese (III), titanium(IV) center for the first time. Electrochemical properties of peripherally tetra-substituted metallophthalocyanines were established by cyclic (CV) and square wave (SWV) voltammetry. This study was supported by The Scientific & Technological Research Council of Turkey (TÜBİTAK, project no: 114Z914).

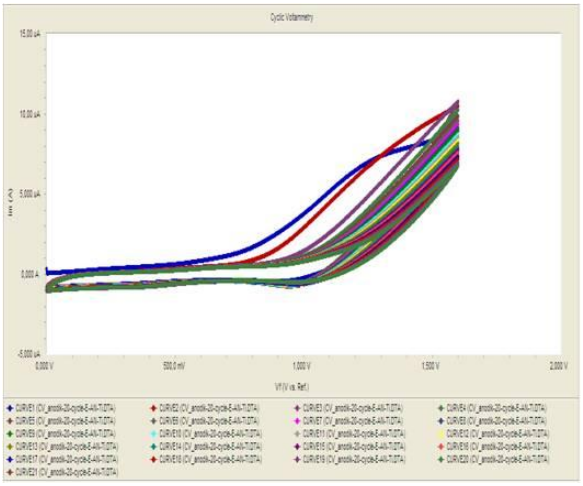

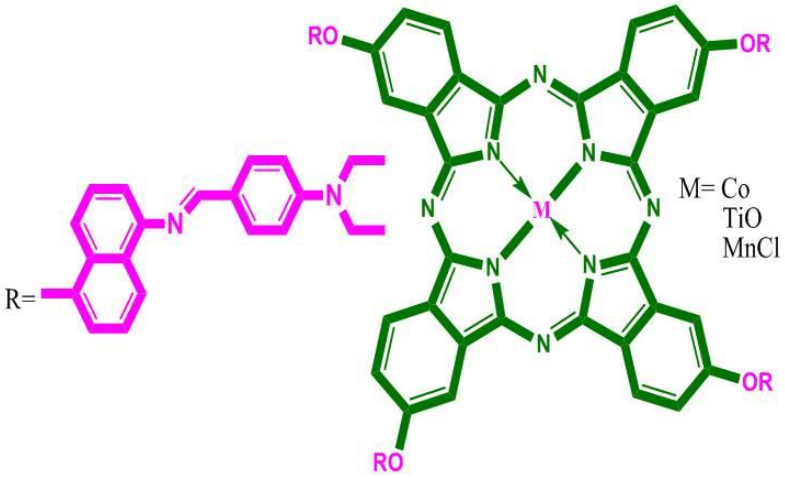

References

[1] Z. Bıyıklıoğlu, H. Baş, H. Alp, Non-aggregated axially disubstituted silicon phthalocyanines bearing electropolymerizable ligands and their aggregation, electropolymerizaton and thermal properties. Dalton Trans. 44, 14054 (2015).

[2] H. Li, T.F. Guarr, Formation of electronically conductive thin films of metal phthalocyanines *via* electropolymerization, Chem. Commun. 13, 832 (1989).

Synthesis and electrochemical properties of electropolymerizable metallophthalocyanines bearing [2-(4-{[(1E)-(4-morpholin-4-ylphenyl)methylene]amino}phenyl)ethoxy] groups

T. Keleş[1], Ü.E. Özen[2], A. Koca[2], Z. Bıyıklıoğlu[1]

[1]*Department of Chemistry, Karadeniz Technical University, Trabzon, 61080, Turkey*

[2]*Department of Chemical Engineering, Marmara University, İstanbul, 34722, Turkey*

E-mail :turgutkls5055@gmail.com

Metallophthalocyanines (Pcs) are one of the important types of tetrapyrole compounds. In addition to multifunctional dye, phthalocyanine has received great attention for applications in different areas [1]. In the last few years, we have focused our research on the electrochemistry of phthalocyanines bearing polymerizable substituents [2]. Modifications of phthalocyanines with functional polymerizable substituents extend the versatility of their electrochemical applications. For these reasons, in this study, we designed and synthesized a novel series of peripherally tetra-substituted metallophthalocyanines carrying redox active cobalt(II), manganese (III), titanium(IV) center for the first time. Electrochemical properties of peripherally tetra-substituted metallophthalocyanines were established by cyclic (CV) and square wave (SWV) voltammetry. This study was supported by The Scientific & Technological Research Council of Turkey (TÜBİTAK, project no: 114Z914).

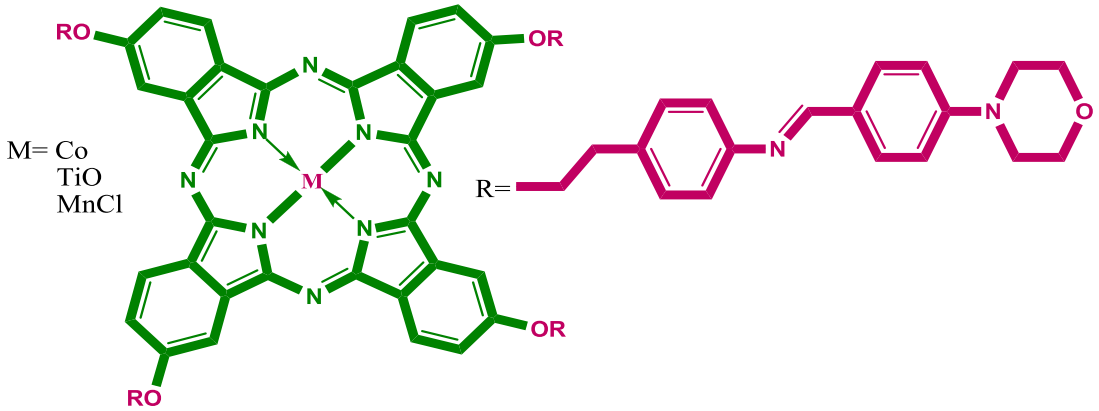

References

[1] D.D. Erbahar, G. Gümüş, Ö. Pamir, E. Musluoğlu, V. Ahsen, I. Gürol, M. Harbeck, Polyalkoxy substituted phthalocyanines sensitive to phenolic compounds in water. Sens. Actuators B 227, 227 (2016).

[2] D. Çakır, T. Arslan, Z. Bıyıklıoğlu, An effect of the substituent position and metal type on the electropolymerization properties of chalcone substituted metallophthalocyanines. Dalton Trans. 44, 20859 (2015).

Magnetic Field Effect on Electrical Properties of Conducting PANI/Cu Composites

Y. Karabul[1], M. Kılıç[1], M. Okutan[1], S. Bakırdere[2], O. İçelli[1]
[1]*Department of Physics, Yıldız Technical University, İstanbul, Turkey*
[2]*Department of Chemistry, Yıldız Technical University, İstanbul, Turkey*
e-mail: karabul@yildiz.edu.tr

Composites of the conducting polymer have numerous interesting physical attributes and significant application possibilities. Appropriate mixtures of metallic micro particles with conductive polymers may cause composite materials possessing unique chemical and physical properties that can have large application potential in different technology [1]. Polyaniline (PANI) is one of the most technologically essential conducting products. It indicates uncommon optical, electrical and chemical phenomenon, both in insulating and conducting forms, that offers a potential for utilization in different applications such as, in sensors, photovoltaic devices, electronics, displays, and energy storage [2]. Various dopants have been used in order to enhance the conductivity, resistance and of PANI. Copper is used widely in the electronic packaging industry due to their excellent thermal conductivity, which can dissipate the heat generated by electronic components quickly [3]. In this study, PANI/Cu composites in different concentration (10%, 25%, 50%) were measured by impedance spectroscopy under the magnetic field. The dielectric parameters (dielectric constants, loss and strength) were investigated in the frequency range of 10^2 Hz-10^6 Hz at room temperature.

References

[1] A. Liu, L.H. Bac, J.-S. Kim, B.-K. Kim, J.-C. Kim, Synthesis and characterization of conducting polyaniline-copper composites., J. Nanosci. Nanotechnol. 13 (2013) 7728–7733.

[2] U.S. Akhtar, M.S. Miran, M.A.B.H. Susan, M.Y.A. Mollah, M.M. Rahman, Preparation and characterization of polyaniline-silica composite material, Bangladesh J. Sci. Ind. Res. 47 (2012) 249–256.

[3] H. Hao, W. Mo, Y. Lv, S. Ye, R. Gu, P. Yu, The effect of trace amount of Ti and W on the powder metallurgy process of Cu, J. Alloys Compd. 660 (2016) 204–207. doi:10.1016/j.jallcom.2015.11.140.

Synthesis and Dielectric Property of Novel Conducting Polymeric Hydrogel

Y. Firat[1], O. Gurbuz[1], G. Ali[2], M. Okutan[1]

[1]*Yildiz Technical University, Department of Physics, 34220 Istanbul, Turkey*

[2]*İstanbul Technical University, Departman of Physics Engineering, 34469, Istanbul, Turkey*

yldryfrt@yildiz.edu.tr

In present study, a novel conducting polymeric hydrogel (CPH) was synthesized, characterized and it was embedded by an electrolyte solution. Initially, polymeric hydrogels were synthesized as free radical cross-linking co-polymerization of acrylamide (AAm) and methylenebisacrylamide (BIS) as crosslink agent in slab forms with the same thickness. The AAm and BIS concentrations were kept fix as 1 M and 7.3 mM, respectively. The polymer host is characterized by scanning electron microscopy (SEM). Dielectric properties of CPH was studied Impedance spectroscopy from 5Hz to 13MHz at room temperature. The reel part (ε') and imaginary part (ε'') of complex dielectric constant were evaluated and alfa parameter (α) and Debye relaxation time (τ) were calculated. The energy loss tangent ($\tan\delta$), impedance (Z), reactance (X) and resistance (R) were measured. Critical frequency determined from values of energy loss tangent ($\tan\delta$). The dielectric constants decreases whereas the loss tangents increased with increasing electrolyte content. As frequency increase from 5Hz to 13MHz, reduction of resistance of Conducting Polymeric Hydrogel demonstrate that they are conductive materials.

Keywords: Conducting Polymeric Hydrogel; Dielectric Constant; Dielectric Loss; SEM.

References

[1] Okutan, M., Coskun, R., Ozturk, M., & Yalcin, O. (2015). Dielectric properties of Rhodamine-B and metal doped hydrogels. PHYSICA B-CONDENSED MATTER, 457, 5-11.

[2] Yalcin, O., Coskun, R., Okutan, M., & Ozturk, M. (2013). Comparison Effects and Dielectric Properties of Different Dose Methylene-Blue-Doped Hydrogels. JOURNAL OF PHYSICAL CHEMISTRY B, 117(30), 8931-8938.

Nonlinear Optical Properties of Some Amides

Y. Kaya[1], A. A. Kaya[2]

[1]*Department of Chemistry, Faculty of Art and Science, Bursa, Gorukle, Turkey*

[2]*Department of Physics, Faculty of Art and Science, Bursa, Gorukle, Turkey*

E-mail :ykaya@uludag.edu.tr

Since the invention of the laser in 1960, there have been significant developments in the field of nonlinear optical materials. Nonlinear optical (NLO) materials, defined as materials in which light waves can interact with each other, are key materials for the fast processing of information and optical storage applications. The important development in nonlinear optical materials occurred in 1970, when Davydov et al. reported a strong second harmonic generation (SHG) in organic materials [1].

In this study, four different amides, naphthalene-2-carboxylic acid (2-hydroxy-2-phenyl-ethyl)-amide (**I**), naphthalene-2-carboxylic acid (2-hydroxy-ethyl)-amide (**II**), n-(2-Hydroxy-2-phenyl-ethyl)-4-nitro-benzamide (**III**), n-(2-Hydroxy-ethyl)-4-nitro-benzamide (**IV**) were optimized using the density functional theory (DFT) with the B3LYP method combined with the 6-311++G(d,p) basis set as seen in Figure 1.

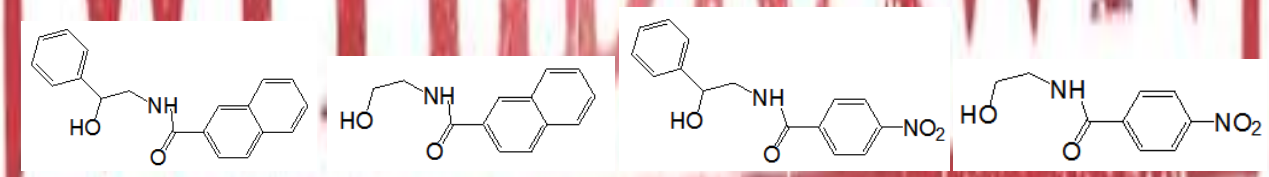

I **II** **III** **IV**

Figure 1. Four different amides using in this study

The dipole moment (□), the linear polarizability (□) and the first hyperpolarizability (□) were calculated at the same level for all amides (**I**-**IV**). Urea is one of the reference materials and frequently used for comparative purpose in the study of the NLO properties. The calculated values of □□□□□and □ for the selected compounds are greater than those of urea. These results indicate that the selected compounds possess good non-linear optical properties.

References

[1].B. L.Davydov, L.D. Derkacheva, V. V. Dunina, M. K. Zhabotinski, V. K. Zolin, L. G. Kreneva, M. A. Samokhina, Connection Between Charge Transfer and Laser Second Harmonic Generation. JEPT Lett. 12, 9, 1970.

Purificationand Characterizationof GlutationReductaseFromJapaneseQuail (CoturnixCoturnixJaponica) Erythrocytes

Taner Bozkuş[1],Yusuf Karagözoğlu[1],Mehmet Çiftci[1], Yusuf Temel[2]

1) Department of Chemistry, Faculty of Science and Arts, Bingol University, Bingol, Turkey
2) Department of Medical Services and Techniques, Solhan Vocational School of Health Services, BingolUniversity, Bingol,Turkey

E-mail: y-karagoz@hotmail.com

Glutathione reductase (glutathione:NADP+ oxidoreductase; EC1.8.1.7) is essential for the maintenance of cellular glutathione in its reduced form, which is necessary for the normal functioning of the cell. During the catalyzing reduction of glutathione disulfide (GSSG) to reduced glutathione(GSH), this is a tripeptide consisting of L-γ-glutamyl-L-cysteinylglycine,theenzymeuses NADPH or NADH as a reducingagent. GSH has an important role in the synthesis and degradation of proteins, regulation of enzymes, formation of thedeoxyribonucleotideprecursors of DNA, and protection of the cells against free radicals and reactive oxygen species [1].

In this study, glutation reductase (GR) was purified from Japanese quail (Coturnixcoturnixjaponica) erythrocytes and some characteristics of the enzyme were investigated. The purification procedure was composed of two-steps: homogenate preparation and 2,5-ADP Sepharose 4B affinity gel chromatography. Thanks to the two consecutive procedures, the enzyme, having the specific activity of 33,75 EU/mg proteins, was purified with a yield of 46.2% and 1028-fold. The enzymatic activity was measured by Beutler's method [2]. One enzyme unit was defined as the enzyme amount reducing 1 µmol $NADP^+$ per min at 25 °C. The control of enzyme purity, using Laemmli's procedure[3], the molecular weight of the enzyme was found to be 78.690 k Daby sodium dodecyl sulfate polyacrylamide gel electrophoresis(SDS-PAGE). Optimal pH, stable pH, optimal ionic strength, optimal temperature and using Lineweaver–Burkcurves [4], for the K_M and V_{max} values of NADPH and GSSG were also determined for the enzyme.

References

[1] Gül M., Kutay FZ., Temocin S., and Hanninen O., 2000.Cellular and clinicalimplications of glutathione.Indian J. Exp. Biol.38,625–634.

[2] Beutler E., 1971. Red cell metabolism manual of biochemical methods. AcademicPress, London. pp.68-71.

[3] Laemmli DK., 1970. Clevage of structural proteins during in assembly of the head of bacteriophage T. Nature 227, 680-683.

[4] LineweaverH., Burk D.,1934. The determination of enzyme dissocation constants, J. Am. Chem. Soc. 57, 685.

Purification and Some Properties of Glucose 6-Phosphate Dehydrogenase From Chicken Liver

Yusuf Karagözoğlu[1], Mehmet Çiftci[1], Ebru Akkemik[2]

1) Department of Chemistry, Faculty of Science and Arts, Bingol University, Bingol, Turkey
2) Department of Food Engineering, Faculty of Engineering and Architecture, Siirt, Turkey
E-mail: y-karagoz@hotmail.com

Abstract

Glucose 6-phosphate dehydrogenase (G6PD) was purified from chicken liver and some properties of the enzyme were investigated. The purification procedure was composed of two steps: homogenate preparation and 2',5'-ADP Sepharose 4B affinity gel chromatography. With the aid of the these two steps, the enzyme, having the specific activity of 5.070 EU/mg proteins, was purified with a yield of 33.028 % and 589.534- fold. The purified enzyme appeared a single band on sodium dodecyl sulfate polyacrylamide gel electrophoresis (SDS-PAGE). The molecular weight of the enzyme was found to be 82.640 kDa by SDS-PAGE. Substrates of G6PD that K_M and V_{max} values for $NADP^+$ and G6-P were also determined for the enzyme.

Introduction

Glucose 6-phosphate dehydrogenase (E.C.1.1.49; G6PD) is the key and first enzyme of the pentose phosphate metabolic pathway, catalyzing the conversion of glucose 6- phosphate to 6-phosphogluconate in the presence of $NADP^+$. This reaction yields NADPH, protecting the cell against the oxidant agents by producing reduced glutathione. NADPH is also a synthetic coenzyme used in several biomolecules, such as fatty acids, steroids, and some amino acids. In the case of NADPH deficiency, the concentration of reduced glutathione in living systems decreases, resulting in cell death. [1, 2, 3]. Firstly Yoshida isolated G6PD from human erythrocytes [4]. In next years, was used purified the natural substrates, G6-P and $NADP^+$ from ion-exchange materials for the purificate to this enzyme. Fist time which was used the affinity chromatography (2',5'-ADP Sepharose 4B) De Flora and co-workers[5] is the common technique.

Material and Methods

Preparation of the homogenate

After fresh chicken liver (10g) samples washing with 0.9% potassium chloride solution stored at 80°C. Initially they were cut into small pieces, were homogenized using ultra-turrax homogeniser with 30 mM KH_2PO_4 (mono potassium phosphate) (pH 7.5) buffer that contained 1 mM PMSF, 1 mM EDTA and 1 mM DTT. And then the suspension was centrifuged at 4 °C, 13,500 rpm for 60 min, the precipitate was thrown. Supernatant was centrifuged at 4 °C, 13,500 rpm 15 min again, supernatant on the upper part was taken with a dropper, and the precipitated part was removed.

Activity determination

Beutler's method was used for measurement of the enzymatic activity [6]. One enzyme unit was defined as the enzyme amount reducing 1mmol $NADP^+$ per 1 min.

2′,5′-ADP sepharose 4B affinity chromatography

Two grams of dried 2,5-ADP Sepharose-4B was used for a column (1x 10 cm) of 10 mL bed volume. The gel was washed with 300 mL of distilled water to eliminated dirtinesses matters and air then suspended in 0.1 M K-acetate/0.1 M K phosphate buffer (pH 6.0), and packed in the column. After settling of the gel, the column was equilibrated with 50 mM K-phosphate buffer including 1 mM EDTA, and 1 mM DTT, pH 7.85, with the aid of a peristaltic pump. The flow rates for washing and equilibration were calibrated to 20 mL/h. A 25 mL of supernatants were loaded onto the column and the column was washed with 30 mL of 50 mM K-phosphate buffer including 1 mM EDTA, 1 mM DTT, and 80 mM KCl pH 7.85. Washing was continued until the final absorbance became zero at 280 nm. Finally, the enzyme of G6PD was eluted with 20 mL of 80 mM K-phosphate+ 80 mM KCl + 0.5 mM $NADP^+$ + 1 mM EDTA, pH 7.85 [7].

Protein determination

Measurements of protein amounts were made using spectrophotometer at 595 nm throughout with the Bradford method [8] using bovine serum albumin as a standard.

Sodium dodecyl sulfate–polyacrylamide gel electrophoresis and molecular weight determination

Stacking gels and separating gels were prepared at 3 and 10% acrylamide concentrations using the Laemmli procedure[9]. 1% Sodium dodecyl sulfate (SDS) was added to the gel solution and was began to run. Staining of the gel took for 2 hours in a solution of 0.1% Coommassie Brilliant Blue R-250 containing 50% methanol and 10% acetic acid and 40% distilled water. Finally, washing the gel process was in a same solvent not putting dye until the protein bands were cleared. To the determine the molecular mass of the enzyme was used walking distances of standard proteins and purified enzyme within the photographed gel.

Kinetic studies

Activity measurements were carried through in five different concentrations of glucose 6-phosphate (G6P; 0.003, 0.0075, 0.015, 0.030 and 0.060 mM) at constant (0.2 mM) $NADP^+$ concentrations with a view to determine K_M and V_{max} values for G6P substrate of chicken liver G6PD enzyme Lineweaver–Burk plot [10] was drawn using the obtained values. K_M and V_{max} values were determined for G6P with the help of this plot (Figure 4). Similarly, activity measurements were carried through in five different concentrations of $NADP^+$ (0.0025, 0.005, 0.01, 0.02 and 0.045 mM) at constant concentration of G6P (0.6 mM), Lineweaver–Burk plot was drawn and K_M and V_{max} values were calculated for $NADP^+$ (Figure 5).

Results

Chicken liver glucose 6-phosphate dehydrogenase was purified 578.534-fold with a yield of 33.028%. The specific activity at the second step was 5.070 EU/mg of protein (Table 1). The purity molecular weight of the enzyme determined with SDS-PAGE method(Figure 2). For the chicken liver glucose 6-phosphate dehydrogenase and standard proteins, *Rf* values were estimated and *Rf*–log MW graph was drawn according to the Laemmli procedure, showing a molecular weight of 82.640 kDa for the enzyme (Figure 3). A K_M of 0.136 mM and a V_{max} of 0.009 EU/mL were obtained for $NADP^+$ and 0.082 mM and 0.011EU/mL for G-6P calculated from the Lineweaver-Burk graphs (Figures 4 and 5).

Table 1. Purification scheme of glucose 6- phosphate dehydrogenase from chicken liver

Purification step	Total volume (mL)	Activity (EU/mL)	Total Activity (EU)	Protein (mg/mL)	Total Protein (mg)	Specific Activity (EU/mg)	Yield %	Purification (fold)
Homogenate	20	0.175	3.500	20.37	407.4	0.0086	100	1
2',5'-ADP Sepharose 4B affinity chromatography	4	0.289	1.156	0.057	0.228	5.070	33.028	589.534

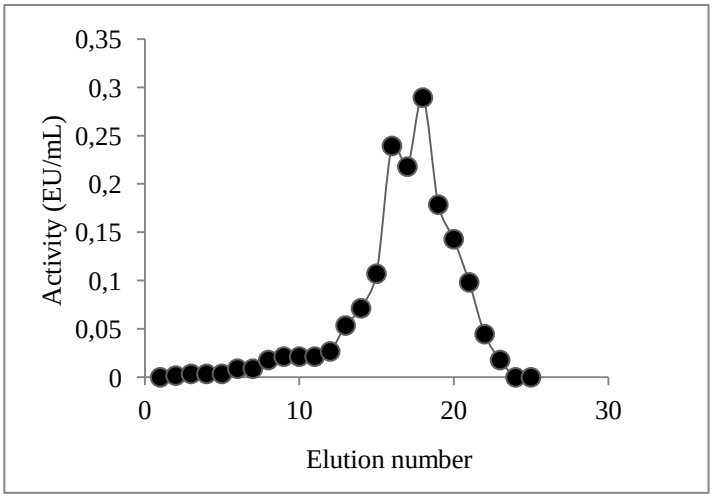

Figure 1. Purification of glucose 6- phosphate dehydrogenase on 2',5'-ADP Sepharose 4B affinity column

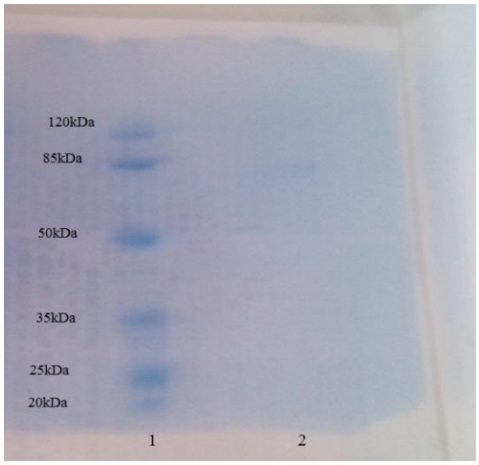

Figure 2. SDS-PAGE: lanes 2, standard proteins; lane 1, purified of glucose 6- phosphate dehydrogenase from 2',5'-ADP Sepharose 4B affinity column

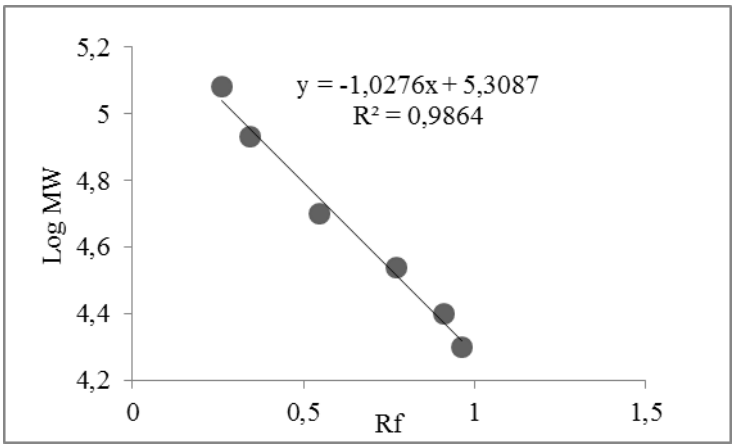

Figure 3. Standard *Rf*–log MW graph of glucose 6- phosphate dehydrogenase (G6PD) using SDS-PAGE. Standards: *E. Coli* β-galactosidase (120 kDa), bovine serum albumin (85 kDa), chicken egg white ovalbumin (50 kDa), bovine erythrocytes carbonic anhydrase (35 kDa), bovine milk β-lactoglobulin (25 kDa), chicken egg white lysozyme (20 kDa).

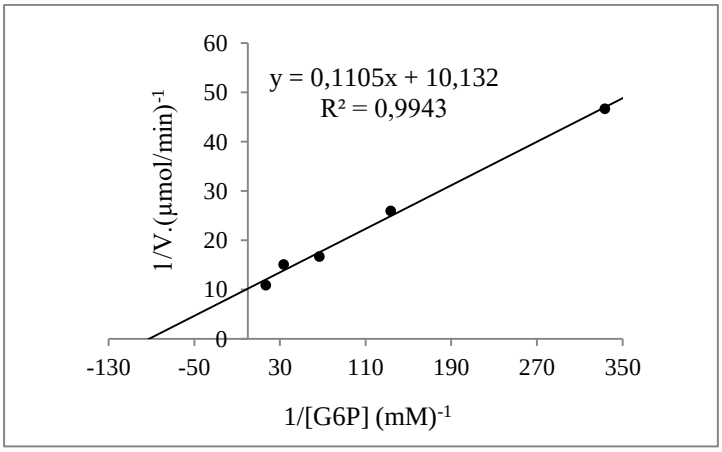

Figure 4. Lineweaver–Burk graph with five different G6-P concentrations and with constant $NADP^+$ concentration

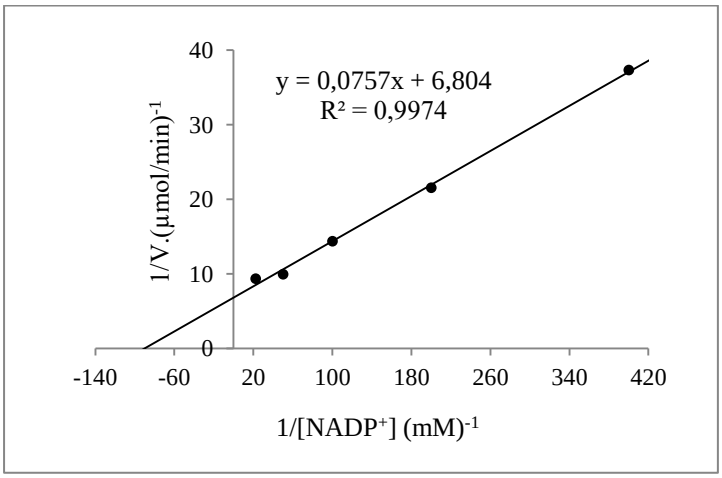

Figure 5. Lineweaver–Burk graph with five different $NADP^+$ concentrations and with constant G6-P concentration

Discussion

In the present study, G6PD enzyme was purified from 10 grams of chicken liver and we were able to obtain 578.534-fold purification with a yield of 33.028%. The specific activity and purification degree were similar to those of previous studies [11, 12, 13, 14]. Our yield is higher than those obtained respectively in mouse liver with 8.7% yield [15], in bovine lens with 13.7% yield [16], in sheep kidney cortex with 16.96% yield [17], in dog liver with 18% yield [18] and is lower than those obtained respectively in human erythrocytes with 41% yield [19], in chicken erythrocytes with 54.68% yield [20], in rabbit erythrocytes with 56% yield [5], in human placenta with 62% yield [21]. Determined monomer molecular mass of G6PD shows similarity with sheep liver (85 kDa) [22]. These K_M values are similar to those obtained in rat adipose tissue [23], in goose erythrocytes[11], buffalo erythrocytes [12], and in rainbow trout liver[14]. The K_M for G6-P is higher than that for $NADP^+$, suggesting the higher affinity of G6PD to G6-P when compared with $NADP^+$.

Acknowledgements

This work was supported by the Scientific Research Projects Unit of Bingol University, Grant BAP-718-182-2014.

References

[1] Lehninger A.L., Nelson D.L., Cox M.M., 2000. in: Principles of Biochemistry, second ed., Worth Publishers Inc, New York, pp. 558–560.

[2] Beutler E., 1995. Glucose 6-phosphate dehydrogenase deficiency and other enzyme abnormalities, in: E. Beutler, M.A. Lichtman, B.S. Coller, T.J. Kipps (Eds.), Williams Hematology, fifth ed., Mc Graw-Hill Company, New York, pp. 564–581.

[3] Morelli A., Benatti U., Gaetani GF., De Flora, A., 1978. Biochemical mechanisms of glucose-6-phosphate dehydrogenase deficiency, Proc. Natl. Acad. Sci. USA 75, 1979–1983.

[4] Yoshida A., Huang, I.Y., 1986. Structure of Human G6PD; Academic Press Inc. Ltd.: London,

[5] Ninfali P., Orsenigo T., Barociani L., Rapa S., 1990. Rapid purification of glucose-6-phosphate dehydrogenase from mammal's erythrocyte. Prep. Biochem., 20: 297-309.

[6] Beutler E., 1971. Red cell metabolism manual of biochemical methods. Academic Press, London. pp.68-71.

[7] Adem S., Ciftci M., 2012. Purification of rat kidney glucose 6-phosphate dehydrogenase, 6-phosphogluconate dehydrogenase, and glutathione reductase enzymes using 2',5'-ADP Sepharose 4B affinity in a single chromatography step. Protein Expression and Purification. 81(1):1–4. doi: 10.1016/j.pep.2011.08.031.

[8] Bradford M.M., 1976. A rapid and sensitive method for quantitation of microgram quantities of protein utilizing the principle of protein-dye-binding. Anal. Biochem. 72, 2487251.

[9] Laemmli DK., 1970. Clevage of structural proteins during in assembly of the head of bacteriophage T. Nature 227, 680-683.

[10] Lineweaver H., Burk D., 1934. The determination of enzyme dissocation constants, J. Am. Chem. Soc. 57, 685.

[11] Beydemir S., Yilmaz H., Ciftci M., Bakan E., and Kufrevioglu OI., 2003b. Purification of glucose 6-phosphate dehydrogenase from goose erythrocytes and kinetic properties. Turkish Journal of Veterinary and Animal Sciences 27: 1179–1185.

[12] Ciftci M., Beydemir S., Yilmaz H., and Altikat S., 2003. Purification of glucose 6-phosphate dehydrogenase from buffalo (Bubalus bubalis) erythrocytes and investigation of some kinetic properties. Protein Expression and Purification 29: 304–310.

[13] Ciftci M, Ciltas A, and Erdogan O., 2004. Purification and characterization of glucose 6-phosphate dehydrogenase from rainbow trout (Oncorhynchus mykiss) erythrocytes. Veterinary Medicine-Czech 49(9): 327–333.

[14] Comakli V., Akkemik E., Ciftci M and, Kufrevioglu OI., 2015. Purification and characterization of glucose 6-phosphate dehydrogenase enzyme from rainbow trout (Oncorhynchus mykiss) liver and investigation of the effects of some metal ions on enzyme activity toxicology and Industrial Health Vol. 31(5) 403–411.

[15] Velasco P., Barcia R., Ibarguren I., Sieiro AM and Ramos-Martinez JI., 1994. Purification, characterization and kinetic mechanism of glucose-6- phosphate dehydrogenase frommouse liver, International Journal of Biochemistry, vol. 26,no. 2, pp. 195–200.

[16] Ulusu NN., Kus MS., Acan NL and Tezcan EF., 1999. A rapid method for the purification of glucose-6-phosphate dehydrogenase from bovine lens, International Journal of Biochemistry and Cell Biology, vol. 31, no. 7, pp. 787–796.

[17] Ulusu NN and Tandogan B., 2006. Purification and kinetics of sheep kidney cortex glucose-6-phosphate dehydrogenase, Comparative Biochemistry and Physiology—B Biochemistry and Molecular Biology, vol. 143, no. 2, pp. 249–255.

[18] Özer N., Bilgi C and Ögüs IH., 2002. Dog liver glucose-6-phosphate dehydrogenase: purification and kinetic properties, The International Journal of Biochemistry&Cell Biology, vol. 34, no. 3, pp. 253–262.

[19] Erat M., 2004. Purification of human erythrocyte glucose 6-phosphate dehydrogenase and glutathione reductase enzymes using 2′,5′-ADP Sepharose 4B affinity column material in single chromatographic step, Protein Expression and Purification, vol. 34, no. 2, pp. 257–260.

[20] Yılmaz H., Çiftci M., Beydemir Ş., Bakan E., 2002. Purification of glucose 6-phosphate dehydrogenase from chicken erythrocytes and investigation of some kinetic properties. Prep. Biochem., 32: 287-301.

[21] Aksoy Y., Ögüs IH and Özer N., 2001. Purification and some properties of human placental glucose-6-phosphate dehydrogenase," Protein Expression and Purification, vol. 21, no. 2, pp. 286–292.

[22] Turkoglu V., Aldemir S., and Ciftci M., 2003. Purification and characterization of glucose 6-phosphate dehydrogenase from sheep liver. Turkish Journal of Chemistry 27: 395–402.

[23] Levy HR., 1979. Glucose-6-phosphate dehydrogenases, in: A. Meister (Ed.), Adv. Enzymol., vol. 48, John Wiley and Sons, New York, p. 97.

Novel D-π-D 4,5-Diazafluorenone and derivate dyes for use in Dye-Sensitized Solar Cell

Z. Orman[1], İ. Erden[1], F. Aytan Kılıçarslan[1], Osman Gürbüz[2]

[1]*Yildiz Technical University, Chemistry Department, 34220 İstanbul, TURKEY*

[2]*Yildiz Technical University, Physical Department, 34220 İstanbul, TURKEY*

zeorman@gmail.com

Dye-sensitized solar cells (DSSCs) have attracted considerable attention due to the advantages of low-cost, simple fabrication procedure and relatively high efficiency [1]. Photosensitizers such as ruthenium complexes [2] and metal-free organic dyes [3] have been developed to serve as efficient light harvesters for DSSCs. A series of novel ruthenium 4,5-Diazafluorenone and their derivatives dyes which are featured with a D-π-A structure have been designed and synthesized for use in dye-sensitized solar cells (DSSCs). 4,5- Diazafluorenone and their derivatives are generally regarded as one of the most promising candidates for photonic and optoelectronic devices due to their high thermal stability ease of preparation and good electron-transporting property[4]. They are also widely used in the preparation and investigation of charge-transfer complexes, activation of photoconductivity of organic semiconductors and as electron transport materials [5]. As a continuation of our efforts to develop functional materials suitable for DSSCs. New fluorenone-functionalized organic photosensitizers of the type D-π-A were designed and synthesized here with isophthaldialdehyd as the one electron donor 4,5- diazafluorenone unit [6].

In present study, D-π-A feature novel 4,5-diazafluorenone and ruthenium complex was synthesized. The chemical diagrams of D-π-A feature novel 4,5-diazafluorenone was reported in Figure 1. This material enables the movement of electrons in the π-conjugation are the imine group.

The structure of all synthesized complexes, elemental analysis, FTIR, UV-Vis, H-NMR and MS were illuminated with fluorescence. Current density–voltage (J–V) characteristics of the DSSCs were measured on solar simulator under AM 1.5 illumination with an incident light intensity of 100 mW/cm^2.

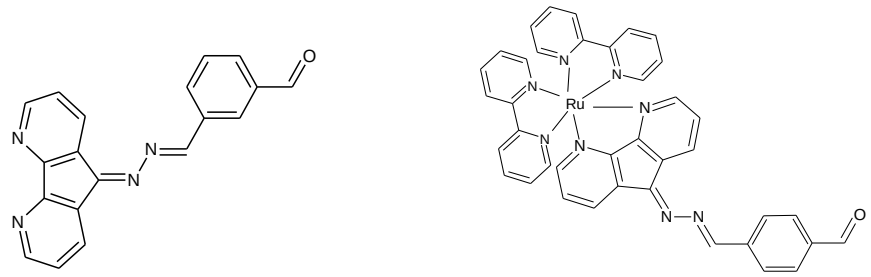

Figure1. Molecular structures of D-π-A feature novel 4,5-diazafluorenone ligand and ruthenium complex

[1] M.K. Nazeeruddin, A. Kay, I. Rodicio, R. Humpbry-Baker, E. Miiller, P. Liska, et al. "Conversion of light to electricity by cis-scnis(2,2′-bipyridyl-4,4′-dicarboxylate)ruthenium(Ⅱ) charge-transfer sensitizers (X = C1-, Br-, I-, CN-, and SCN-) on nanocrystalline TiO_2 electrodes", J Am Chem Soc, 115, 6382-6390, (1993).

[2] M.K. Nazeeruddin, F. De Angelis, S. Fantacci, A. Selloni, G. Viscardi, P. Liska, et al. "Combined experimental and DFT-TDDFT computational study of photoelectrochemical cell ruthenium sensitizers", J Am Chem Soc, 127, 16835-16847, (2005).

[3] Ping S., Yuhua T., Shenghui J, Huajie C., Xiaoyan Z., Xueye W.,Bin Z., Songting T., "Efficient triphenylamine-based dyes featuring dual-role carbazole, fluorene and spirobifluorene moieties", Organic Electronics, 12,125-135, (2011).

[4] Duryodhan S., Harihara P., Dhananjaya P., Jen-Fu Y., Ying-Chan H., Jiann-T'Suen L., Kuang-Lieh L., Kung-Hwa W., Hong-Cheu Lin., "Synthesis and applications of novel acceptor-donor-acceptor organic dyes with dithienopyrrole and fluorene-cores for dye-sensitized solar cells", Tetrahedron, 67, 303-311, (2011).

[5] M. Gratzel, Journal of Photochemistry and Photobiology, Photochemistry Reviews, 4:145, (2003).

This research has been supported by the Scientific and Technological Research Council of Turkey (TUBITAK), Project Number: 113Z910 project.

Synthesis of New N-coordinate Ruthenium Dye For Dye-Sensitized Solar Cells (DSSCs)

S. Dayan, N. Kalaycıoğlu Özpozan and Y. Yıldız,
Department of Chemistry, Faculty of Science, Kayseri, Erciyes University, Turkey
E-mail: yesimyildiz736@gmail.com

The replacement of fossil fuels by renewable energy sources is a big challenge to scientists [1]. Grätzel's type dye-sensitized TiO_2 solar cells (DSSC) can be considered a promising technology for solar energy conversion in the near future [2]. Many different photosensitizers have been tested, such as transition metal complexes [3], organic dyes [4] and, more recently, perovskites [5].

Summarize, a new series of *N*-coordinate ruthenium complexes bearing sulfonamide fragments and 2,2′-Bipyridine-4,4′-dicarboxylic acid ligand were designed and synthesized. The structural elucidations of the materials were characterized by different methods such as IR, ^{1}H-NMR, ^{13}C-NMR, Elemental Analysis and UV-vis. The synthesized ruthenium complexes were tested as dye in dye-sensitized solar cell (DSSC).

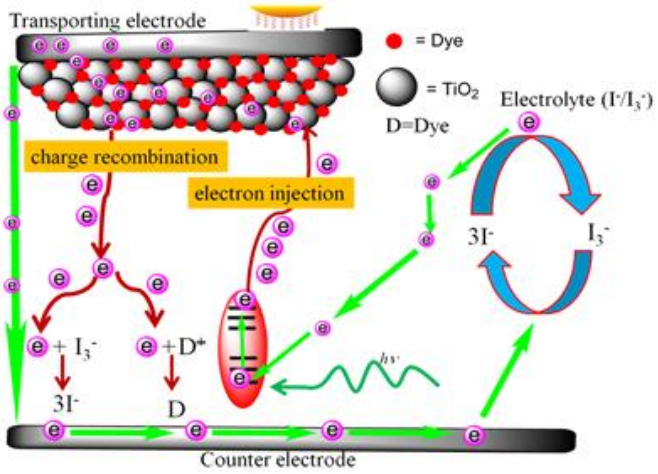

Figure-1 Dye-Sensitized Solar Cells (DSSCs)

References

[1] B. C. O'Regan and M. Grätzel, A low-cost, high-efficiency solar cell based on dye-sensitized colloidal TiO_2 films Nature 353, 737 (1991).

[2] Q. B. Meng, K. Takahashi, X. T. Zhang, I. Sutanto, T. N. Rao, O. Sato, A. Fujishima, Fabrication of an Efficient Solid-State Dye-Sensitized Solar Cell, Langmuir 19, 3572 (2003).

[3] H. Wang, J. Li, F. Gong, G. Zhou, and Z. Wang Ionic Conductor with High Conductivity as Single-Component Electrolyte for Efficient Solid-State Dye-Sensitized Solar Cells J. Am. Chem. Soc. 135, 12627 (2013).

Acknowledgments

We acknowledge the financial support granted by Erciyes University (ERUBAP), (FYL-2016-6572).

Pd^{II} Impregnated MWCNT, SiO_2, Fe_3O_4 Materials and Its Application in the Hydrogenation of Nitroarene

S. Dayan[1], N. Kalaycıoğlu Özpozan[1], N. Kayacı[1], O. Dayan[2], N. Özdemir[3]

[1]*Department of Chemistry, Faculty of Science, Kayseri, Erciyes University, Turkey*

[2]*Laboratory of Inorganic Synthesis and Molecular Catalysis, Çanakkale Onsekiz Mart University, Çanakkale, Turkey*

[3]*Department of Physics, Faculty of Art and Sciences, Ondokuz Mayıs University, Samsun, Turkey*

E-mail: serkandayan_@hotmail.com

The hydrogenation reactions of various organic molecules are necessary, typically using a hydrogen donor together with a strong base and catalyst, and are preferred for large-scale industrial applications, energy and lowering toxicity. Furthermore, the transfer hydrogenation (TH) reaction of ketones is a pivotal reaction for secondary alcohols that has recently attracted much attention. In addition, palladium compounds have attracted considerable interest in the reduction of ketones as catalysts [1-3].

Herein, a new series of MWCNT, Al_2O_3, SiO_2 and Fe_3O_4-$[PdCl_2(L)_2]$ materials were synthesized by an impregnation method using and were solid-supported. The structural elucidations of the materials were characterized by different methods such as FT-IR, TG-DTA, Nitrogen Adsorption-Desorption (BET), SEM-EDX, TEM and XRD. In addition, the synthesized MWCNT, Al_2O_3, SiO_2 and Fe_3O_4-$[PdCl_2(L)_2]$ materials were used as catalysts in the hydrogenation of nitroarenes in aqueous media at ambient temperature in the presence of $NaBH_4$ by UV–vis spectrophotometer (Figure 1).

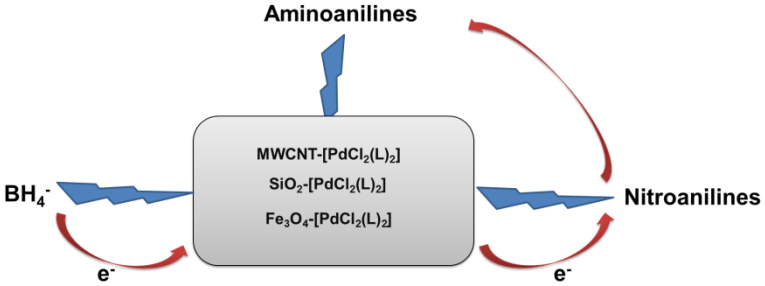

Figure 1. Schematic representation of the reaction model of the catalytic reduction of nitroanilines (NA) to aminoanilines (phenylendiamines) (AA)

References

[1] R. Noyori, S. Hashiguchi, Asymmetric Transfer Hydrogenation Catalyzed by Chiral Ruthenium Complexes, Accounts Chem. Res. 30, 97–102 (1997).

[2] M. J. Palmer, M. Wills, Asymmetric transfer hydrogenation of C=O and C=N bonds, Tetrahedron-Asymm. 10, 2045 (1999).

[3] D.E.J.E. Robinson, S.D. Bull, Kinetic resolution strategies using non-enzymatic catalysts Tetrahedron-Asymm. 14, 1407 (2003).

Sulfonamide Functionalized Ru^{II} *N*-Coordinate Complexes For Reductive Amination Reaction

S. Dayan, N. Kalaycıoğlu Özpozan and N. Kayacı

Department of Chemistry, Faculty of Science, Erciyes University, Kayseri, Turkey

E-mail: nlgnkyc@hotmail.com

Reductive amination (RA), the coupling of ketones or aldehydes with amines in the presence of a reducing agent, is one of the most powerful methods for one-step synthesis of substituted amines. This method is extremely valuable from a synthetic point of view, since it avoids the isolation of in situ generated imine products, which is not easy due to the limited stability of imines. In most of the RA procedures developed, stoichiometric boron hydride reduction and heterogeneous hydrogenation dominate the scene [1-2].

Herein, a new series of functionalized [$RuCl_2$(*p*-cymene)(L)] (L=aromatic sulfonamide compounds) complexes has been prepared by reaction of aromatic sulfonamide compounds and [$RuCl_2$(*p*-cymene)]$_2$. The Ru^{II} complexes were stable toward air and moisture and were detailed characterized by ^1H, ^{13}C NMR, FT-IR and EA methods. The new complexes were found be an active catalyst for transfer hydrogenative reductive amination under aqueous conditions with sodium formate as hydrogen source. Various carbonyl compounds such as aromatic aldehydes were successfully reacted with amines to gives new amines. All the [$RuCl_2$(*p*-cymene)(L)] type complexes were found as good catalyst in the reductive amination reaction (Figure-1).

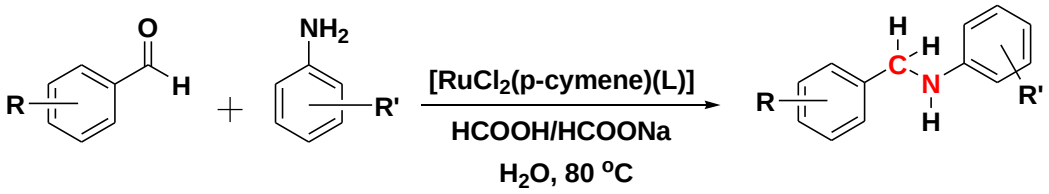

Figure-1 Reductive amination reaction with [$RuCl_2$(*p*-cymene)(L)] complexes

References

[1] S. Gomez, J. A.Peters, T. Maschmeyer, The Reductive Amination of Aldehydes and Ketones and the Hydrogenation of Nitriles: Mechanistic Aspects and Selectivity Control, Adv. Synth. Catal. 344, 1037 (2002).

[2] D. Gulcemal, S. Gulcemal, M. C. Robertson, J. Xiao, A New Phenoxide Chelated Ir^{III} N-Heterocyclic Carbene Complex and Its Application in Reductive Amination Reactions, Organometallics 34, 4394-4400 (2015).

Acknowledgments

We acknowledge the financial support granted by Erciyes University (ERUBAP), (FDK-2015-6143).

Flower-Like Hibrit Turkish Black Radish Peroxidase-Cu^{2+} Nanobiocatalyst

N.Özdemir[1], I. Ocsoy[2,3], C. Altınkaynak[2,3], S. Tavlasoglu[1], R. Kalın[4,5], N. Sadegihan[5], H. Özdemir[5]

[1]Department of Chemistry, Faculty of Science, Erciyes, University, Kayseri, Turkey

[2] Department of Analytical Chemistry, Faculty of Pharmacy, Erciyes University, Kayseri, Turkey

[3]Nanotechnology Research Center, Erciyes University, Kayseri, Turkey

[4]Department of Basic Sciences, Faculty of Science, Erzurum Technical University, Erzurum, Turkey

[5]Department of Chemistry, Faculty of Science, Ataturk University, Erzurum, 25030 Turkey

E-mail :ozdemirn@erciyes.edu.tr

The dye based colors are the indication of the water pollution and are first contaminants identified in the wastewater. It is well known that the dyes can threaten aquatic life and have also toxic, mutagenic and carcinogenic effects towards living organisms [1]. Several methods, such as physical, chemical, physical and/or biological, have been in used for dye decolorization [1]. The biological methods, especially using enzyme, have potential to decolor large volume of wastewater in an effective and economical way [2].

Peroxidases (EC 1.11.1.x; donor: hydrogen-peroxide oxidoreductase) catalyze the oxidation of a large variety of substrates in the presence of H_2O_2. Peroxidases have been extensively used for the dye decolorization.

In this study, Turkish blackradish peroxidase enzyme-copper ions (Cu^{2+}) based flower-like shaped hybrid nanoflowers (TBNFs) were prepared with highly enhanced enzymatic activity and stability. The synthesis of TBNFs was accomplished using a described method before [3,4]. The structure of the synthesized TBNFs was confirmed by EDX and XRD. To best of our knowledge, the TBNFs are produced and used, for the first time, for decolorization of a representative victoria blue dye (VB). Dye decolorization capability of TBNFs was employed at different time and pH values to determine the optimal conditions for efficient decolorization. The reusability of TBNFs was also tested.

[1] T. Robinson, G. McMullan, R. Marchant, P. Nigam, Bioresource Technology 77, 247-255 (2001).

[2] H. S. Rai, M. S. Bhattacharyya, J. Singh, T. K. Bansal, P. Vats, U. C. Banerjee, Critical. Rev. Environ. Sci. Technol., 35: 219-238 (2005).

[3] B. Somtürk, M. Hancer, I. Ocsoy, N. Özdemir, Dalton Transactions, 44(31), 13845-13852 (2015).

[4] C. Altınkaynak, İ. Yılmaz, Z. Köksal, H. Özdemir, I. Ocsoy, N. Özdemir, International Journal of Biological Macromolecules, 84, 402-409 (2016).

Synthesis of N-(2-Aminophenyl)-Aromaticsulfonamides Hydrochloride: As Inhibitory of Peroxidase EnzymeActivity

N. Özdemir, S. Dayan, B. Somtürk Yılmaz, N. Kalaycıoğlu Özpozan and Y. Yıldız
Department of Chemistry, Faculty of Science, Kayseri, Erciyes University, Turkey
E-mail: ozdemirn@erciyes.edu.tr

The structures containing sulfonamide fragment are generally obtained from R-sulfonyl chloride with primary or secondary amines in basic media. Recently, there has been an increase in studies regarding compounds bearing sulfonamide moiety because of their potential applications such as in the metal complexes of sulfonamide, medicinal chemistry, as catalysts, in chemical luminescence and in material chemistry. Additionally, sulfonamide derivatives are known to contain inherent pharmacological properties such as antimicrobial, anti-inflammatory, antiviral, anti-proliferative, angiogenesis [11] and enzyme inhibitory (α, β, δ-carbonic anhydrase, human carbonic anhydrase, adenine nucleotide translocator etc.) activities [1-2].

Herein, [*N*-(2-aminophenyl)-arylsulfonamides] hydrochloride derivatives have been successfully synthesized by the reaction of aromatic sulfonylchloride, 1,2-diaminobenzene and hydrochloric acid. All the synthesized sulfonamides were characterized by different methods such as NMR, FT-IR, UV-vis, elemental analysis. Their inhibitory effects on the activity of horseradish peroxidase (HRP) enzyme were evaluated by UV-vis spectrophotometers. The half maximal inhibitory concentration (IC50) values and Ki values for sulfonamide inhibitors were calculated to be 0.636±0.001 mM, 0.24±0.003 mM, 0.23±0.002 Mm, 0.34±0.002 mM and 0.26±0.004 mM for SD-1604, SD-1510, SD-1603, SD-1605 and SD-1536, respectively. The inhibition results show that all the compounds inhibited horseradish peroxidase enzyme activity. Particular, SD- 1603 was found as the most active compound for horseradish peroxidase in comparison with others and all of the compounds showed noncompetitive inhibition. Additionally, the Km and Vmax values for guaiacol substrate were found as 0.051 mM mM and 1.01 EU/mL/min, respectively.

Inhibitors	IC50 value (mM)	Ki constant (mM)	Inhibition type
SD-1604	0.636±0.001	0.939±0.16	Non-competitive
SD-1510	0.24±0.003	0.525±0.15	Non-competitive
SD-1603	0.23±0.002	0.719±0.133	Non-competitive
SD-1605	0.34±0.002	0.556±0.03	Non-competitive
SD-1536	0.26±0.004	0.312±0.076	Non-competitive

Figure-1IC50 value, Ki constant and inhibition type of sulfonamide analogues for horseradish peroxidase

References

[1] S. Dayan, N. Ozpozan Kalaycıoğlu, J-C. Daran, A. Labande, R. Poli, Synthesis and characterization of half-sandwich ruthenium complexes containing aromatic sulfonamides bearing pyridinyl rings: Catalysts for transfer hydrogenation of acetophenone derivatives. Eur. J. Inorg Chem.18, 3224 (2013).

[2] Z.H.Chohan, H.A.Shad, C.T. Supuran, Synthesis; characterization and biological studies of sulfonamide Schiff's bases and some of their metal derivatives. J Enzyme Inhib. Med. Chem., 1, 58 (2012).

Synthesis of Lactoperoxidase Incorporated Hybrid Nanoflower and Its Excellent Activity and Stability

N.Özdemir[1], I. Ocsoy[2], Z. Koksal[3], H. Özdemir[3], and C. Altinkaynak[2]

[1]Department of Chemistry, Faculty of Science, Erciyes University, Kayseri, Turkey

[2] Department of Analytical Chemistry, Faculty of Pharmacy, Erciyes University, Kayseri, Turkey

[3]Department of Chemistry, Faculty of Science, Ataturk University, Erzurum, Turkey

E-mail:ozdemirn@erciyes.edu.tr

Enzymes which catalyze reactions with high specificity and very high rapidity are biocatalysts. There is a new developed method a simple and an efficient approach in order to prepare the enzymes which have enhanced enzymatic activity. Recently, Zare and co-workers reported an elegant approach for the synthesis of immobilized enzymes in the form of nanoflower with highly enhanced catalytic activity and stability [1].

In this study, lactoperoxidase (LPO) enzyme and metal ions hybrid nanoflowers (HNFs) were synthesized using a described method [2] and tested different experimental parameters. And the synthesized HNFs were also used for the detection of dopamine and epinephrine. The HNFs formed of LPO enzyme purified from bovine milk and copper metal ions (Cu2+) were synthesized at two different temperatures (+4°C and 20°C) in PBS (pH:7.4) The effects of experimental conditions, pH values and storage temperatures, on the activity and stability of LPO-copper phosphate HNFs were evaluated using guaiacol as a substrate in the presence of hydrogen peroxide (H_2O_2). Optimum pHs were determined as pH 8 and pH 6 for LPO-copper phosphate HNF and free LPO, respectively and LPO-copper phosphate HNF has higher activity than free LPO at the each pHs. Enzymatic activities of LPO-copper phosphate HNF at pH 6 and pH 8 were calculated as 70.48 EU/mg, 107. 23 EU/mg, respectively while free LPO shows 45.78 EU/mg and 30.12 EU/mg, respectively. Compared with free LPO, LPO-copper phosphate HNFs exhibited ~160% and ~360% increase in activities at pH 6 and pH 8, respectively. Additionally, LPO-copper phosphate HNFs displayed perfect reusability after six cycles. Finally, we demonstrated that the LPO-copper phosphate HNFs can be utilized as a nanosensor.

References

[1] Ge, J. Lei, J. Zare R.N. Protein–inorganic hybrid nanoflowers. Nature Nanotechnology, 2012, 7, 428–432.

[2] B. Somturk, M. Hancer, I. Ocsoy, N. Özdemir, Dalton Transactions, 44(31), 13845-13852 (2015).

[3] [2] H. S. Rai, M. S. Bhattacharyya, J. Singh, T. K. Bansal, P. Vats, U. C. Banerjee, Critical. Rev. Environ. Sci. Technol., 35: 219-238 (2005).

[4] C. Altınkaynak, İ. Yılmaz, Z. Köksal, H. Özdemir, I. Ocsoy, N. Özdemir, International Journal of Biological Macromolecules, 84, 402-409 (2016).

Organic Photocapacitors

A. Dere
Physics Department, Faculty of Science, Firat University, Elazig, TURKEY
Nanoscience and Nanotechnology Laboratory, Firat University, Elazig, TURKEY

Graphene oxide doped methylene blue/p-type silicon based photocapacitors were prepared by drop casting method. The photocapacitor behavior of the GO doped MB devices were determined using capacitance-voltage and capacitance-time measurements. The transient photocapacitance behavior of the device is controlled by solar light intensity. The photocapacitance properties of GO doped MB/p-Si devices are changed with GO dopant. The obtained results indicate that GO doped MB /p-Si devices can be used as a photocapacitorin optoelectronic applications.
.

Keywords: Photocapacitor**,** Organic Semiconductor

Organic photodetector applications of 2,2-Bis[spiro(7,8-dioxy-4-methylcoumarin)]-4,4,6,6,-bis[spiro(2′,2′′-dioxy-1′,1′′-biphenylyl)] cyclotriphosphazene compound

Furkan Özen[1], A. Dere[2], Kenan Koran[1], F. Yakuphanoglu[2], Ahmet Orhan Görgülü[1]

[1]*Department of Chemistry, Faculty of Science, Firat University, Elazığ, Turkey*

[2]*Department of Physics, Faculty of Science, Firat University, Elazığ, Turkey*

E-mail : a.dere@firat.edu.tr

Phosphazenes, which consist of repeating units of –P=N– in their structure, are compounds having linear or cyclic structure connected to the two organic or inorganic side groups (R) in each phosphorus atom. Due to the reactivity of -Cl atom in their structure, the type of organic or inorganic group bonded as side groups to the phosphazene compounds changes physical and chemical properties of these compounds [1,2].

2,2-Bis[spiro(7,8-dioxy-4-methylcoumarin)]-4,4,6,6,-bis[spiro(2′,2′′-dioxy-1′,1′′-biphenylyl)] cyclotriphosphazene **(2)** compound was synthesized from the reaction of 2,2-dichloro-4,4,6,6-bis[spiro(2′,2′′-dioxy-1′,1′′-biphenylyl)cyclotriphosphazene **(1)** [3] with 7,8-dihydroxy-4-methyl coumarin in the presence of xylene/Cs_2CO_3 system. The structure of **2** was characterized by using spectroscopic techniques. 2,2-Bis[spiro(7,8-dioxy-4-methylcoumarin)]-4,4,6,6,-bis[spiro(2′,2′′-dioxy-1′,1′′-biphenylyl)] cyclotriphosphazene **(2)** compound thin film was coated on p-Si substrate having ohmic contact by drop casting method. The photo electronic properties of the diode were analyzed by transient photocurrent and I-V characteristics under various illumination intensities. The photocurrent of the diode in the reverse bias increases with solar light illumination. This indicates that the diode exhibited a photodiode behavior. The I_{on}/I_{off} ratio for the diode was found to be $8.87x10^3$ under 1 SUN.

Acknowledgement:

The authors are grateful to the Research Fund of the TUBITAK for their support (for the synthesis of compound) with the TBAG-110T652.

References

[1] Allcock, H.R. Phosphorus-Nitrogen Compounds. Cyclic, Linear, and High Polymeric Systems. New York: Academic Press Inc. (1972).

[2] Koran, K., Ozen, F., Biryan, F., Görgülü, A.O. "Synthesis, Structural Characterization and Dielectric Behavior of New Oxime-Cyclotriphosphazene Derivatives", Journal of Molecular Structure, 1105, 135-141 (2016).

[3] Carriedo, G.A., Catuxo, L.F., Alonso, F.J.G., Elipe, P.G., González, P.A. "Preparation of a New Type of Phosphazene High Polymers Containing 2,2'-Dioxybiphenyl Groups", Macromolecules, 29, 5320-5325 (2009).

Effect of substrate temperature on the physical properties of PbS thin films deposited by ultrasonic spray pyrolysis

E. Sarica[1], V.Bilgin[1] and S. Elmas[2]

[1]Department of Physics, Faculty of Arts and Sciences, Canakkale Onsekiz Mart University, Canakkale, Turkey

[2]Department of Ceramics, Faculty of Fine Arts, Canakkale Onsekiz Mart University, Canakkale, Turkey

E-mail:saricaemrah@gmail.com

Lead sulphide (PbS) has some superior physical properties such as having high absorption coefficient (~10^5 cm^{-1}), narrow and direct band gap (~0.4 eV for bulk PbS) at room temperature, and further, band gap tuning via crystallite size which is known as quantum size effects because of its relatively large exciton Bohr radius (~18 nm)[1-2]. These properties make the PbS is one of the attractive material in terms of using in opto-electronic devices, such as photodetectors[3], solar cells[4].

In this work PbS thin films were deposited onto glass substrate by using ultrasonic spray pyrolysis technique at different substrate temperature (200°C, 250°C, 300°C and 350°C) in order to investigate the effect of substrate temperature on physical properties of deposited films. Structural, morphological and optical properties of deposited films have been investigated by using X-ray diffractometry, Atomic Force Microscopy and UV-Vis Spectrophotometry, respectively. From the XRD patterns, lattice parameters, crystalline size, texture coefficient have been calculated. It was seen that the films deposited at low substrate temperature (at 200°C, 250°C) have cubic structure but the higher temperatures caused to change in crystal structure. AFM images show that all deposited films have almost homogenous surface without any crack formation with the low roughness (~4 nm-10 nm). In order to investigate optical properties of deposited films transmittance and absorbance spectra were taken at room temperature and optical parameters such as optical absorption coefficient, optical band gap, Urbach parameters have been calculated.

These investigations revealed that substrate temperature has an important effect on structural, morphological and optical properties of PbS films.

References

[1] S.I. Sadovnikov and A.I. Gusev, Structure and properties of PbS films, Journal of Alloys and Compounds, 573, 65-75 (2013).

[2] S. Thangavel, S. Ganesan, S. Chandramohan, P. Sudhagar, Y.S. Kang, C.H. Hong, Band gap engineering in PbS nanostructured thin films from near-infrared down to visible range by in situ Cd-doping, Journal of Alloys and Compounds, 495, 234-237 (2010).

[3] R. Saran and R.J. Curry, Lead sulphide nanocrystal photodetector technologies, Nature Photonics. 10, 81-92 (2016).

[4] J. Hernandez-Borja, Y.V. Vorobiev, R. Ramirez-Bon, Thin film solar cells of CdS/PbS chemically deposited by ammonia-free process, Solar Energy Materials & Solar cells. 95,1882-1888 (2011).

The Synthesis of D-π-D Derivated 4,5-Diazafluorenone for Dye-Sensitized Solar Cell, Investigation of Spectroscopic and Electrical Properties

F. Aytan Kılıçarslan[1], Osman Gürbüz[2], M. Okutan[2], İ. Erden[1]

[1]*Yildiz Technical University, Department of Chemistry, 34220 Istanbul, Turkey*

[2]*Yildiz Technical University, Department of Physics, 34220 Istanbul, Turkey*

faytank@hotmail.com

4,5- Diazafluorenone and their derivatives are generally regarded as one of the most promising candidates for photonic and optoelectronic devices due to their high thermal stability ease of preparation and good electron-transporting property [1]. They are also widely used in the preparation and investigation of charge-transfer complexes, activation of photoconductivity of organic semiconductors and as electron transport materials [2]. As a continuation of our efforts to develop functional materials suitable for DSSCs. New 4,5-diazafluorenone-functionalized organic photosensitizers of the type D-π-A were designed and synthesized here with isophthaldialdehyd as the two electron donor 4,5- Diazafluorenone unit [3].

In present study, D-π-A feature novel 4,5-diazafluorenone and ruthenium complex was synthesized. The chemical diagrams of D-π-A feature novel 4,5-diazafluorenone was reported in Figure 1. This material enables the movement of electrons in the π-conjugation are the imine group. The structure of all synthesized complexes, elemental analysis, FTIR, UV-vis, H-NMR and MS were illuminated with fluorescence. Current density–voltage (J–V) characteristics of the DSSCs were measured on solar simulator under AM 1.5 illumination with an incident light intensity of 100 mW/cm^2.

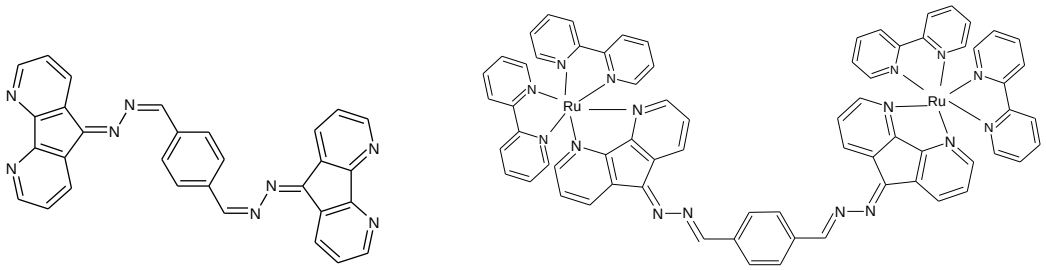

Figure1. Molecular structures of D-π-A feature novel 4,5-diazafluorenone ligand and ruthenium complex

This research has been supported by the Scientific and Technological Research Council of Turkey (TUBITAK), Project Number: 113Z910 project.

References

[1] S. Ping, T. Yuhua, J. Shenghui, C. Huajie, Z. Xiaoyan, W. Xueye, Z.Bin, T. Songting, "Efficient triphenylamine-based dyes featuring dual-role carbazole, fluorene and spirobifluorene moieties", Organic Electronics, 12,125–135, (2011).

[2] S. Duryodhan, P. Harihara, P. Dhananjaya, Y. Jen-Fu, H. Ying-Chan, L. Jiann-T'Suen, L. Kuang-Lieh, W. Kung-Hwa, Lin. Hong-Cheu, "Synthesis and applications of novel acceptor-donor-acceptor organic dyes with dithienopyrrole and fluorene-cores for dye-sensitized solar cells", Tetrahedron, 67, 303-311, (2011).

[3] M. Gratzel, Journal of Photochemistry and Photobiology, Photochemistry Reviews, 4:145, (2003).

Structural, Electronic and Thermodynamic Properties of AlmZn2Xn (X=Pb,Tl; m+n = 3) ternary alloy using DFT Calculations

Meryem Evecen[*1], Hasan Tanak[1] and Emine Aldırmaz[1]

[1] *Department of Physics, Faculty of Arts and Sciences, Amasya University, 05100 Amasya, Turkey*

meryem.evecen@amasya.edu.tr

The structural, electronic and thermodynamic properties of isolated neutral $Al_m Zn_2 X_n$ clusters for X=Pb, Tl; $m+n$ = 3 have been investigated by performing density functional theory calculations at B3LYP/CEP-121G level. In here, we calculated more stable structure of $Al_mZn_2X_n$ (X=Pb,Tl; $m+n$ = 3) cluster in proportion to others. In all cases, the energies are given relative to the lowest energy structures found for the singlet and doublet state except for Zn_2Pb_3(triblet). When analyzing the results for all clusters are found to be energetically favorable, with higher multiplicities generally being less favorable two dimension structure. In order to investigate the chemical stability and reactivity behavior of clusters, chemical hardness (η) and softness (S) were also performed. Considering the chemical hardness, small HOMO–LUMO gap means a soft molecule and large gap means a hard molecule. One can also relate that the molecule with less gap_{H-L} means it is more reactive and less stable. The η and S can be calculated as follow: $\eta = (E_{LUMO} - E_{HOMO})/2$ and $S = 1/2\eta$. The calculated values of E_{LUMO}, E_{HOMO}, gap_{H-L}, η, S and μ analyzed and we saw the ternary alloys are more hard than bimetallic alloys. The chemical hardness and softness were also analyzed with increasing number of Pb and Tl atoms in the cluster. In summary, ternary alloy is more hard than bimetallic alloy and also Pb dope is make it more soft than Tl.

Keywords: Cluster, Ternary, Electronic structure, Ab-initio calculations.

References

1. El-Khair, M. A., Daoud, A., Ismail, A."Effect of different Al contents on the microstructure, tensile and wear properties of Zn-based alloy." *Mater. Lett.,* Vol. 58, No. 11, 1754-1760, 2004.
2. Skoko, Ž., Popović, S., Štefanić, G., "Microstructure of Al-Zn and Zn-Al alloys." *Croatica chemica acta* Vol. 82, No. 2, 405-420, 2009.

Acknowledgements, this study was supported financially by the Research Centre of Amasya University (Project No: FMB-BAP 15-092).

Analysis on molecular structure and vibrational spectra of (E)-4-Bromo-N-(2,3,4-trimethoxybenzylidene)aniline using theoretical approaches

Meryem Evecen[*1] **and Hasan Tanak**[1]

[1]Department of Physics, Faculty of Arts and Sciences, Amasya University, 05100 Amasya, TURKEY

[*]corresponding author: meryem.evecen@amasya.edu.tr

The chemistry of Schiff-bases is very important because of use as anion sensors [1], antimicrobial activity [2], photochromism and thermochromism [3] and nonlinear optical properties[4]. In this work, (E)-4-Bromo-N-(2,3,4-trimethoxybenzylidene)aniline has been investigated theoretically. The molecular structural parameters and vibrational frequencies performed by density functional theory (DFT) technique with the 6-311++G(d,p) basis set. In addition, molecular electrostatic potential (MEP) and frontier molecular orbital energies are performed.

References

[1] Y. M. Hijji, B. Barare, A. P. Kennedy, R. Butcher, Sens. Actuators B, 136, 297 (2009).

[2] M. Yildiz, H. Unver, B. Dulger, D. Erdener, N. Ocak, A. Erdonmez, T. N. Durlu, J. Mol. Struct. 738, 253 (2008).

[3] E. Hadjoudis, A. Rontoyianni, K. Ambroziak, T. Aziembowska, I. M. Mavridis, J. Photochem. Photobiol. A, 162, 521 (2004).

[4] A. Karakas, H. Unver, A. Elmali, J. Mol. Struct. 877, 152 (2008).

Acknowledgment, this study was supported financially by the Research Centre of Amasya University (Project No: FMB-BAP 16-092).

Structural, HOMO-LUMO and MEP analysis of Schiff base copper(II) complex $Cu(C_8H_7O_2N)_2(OH_2)$ by DFT method

Meryem Evecen[1*] and Hasan Tanak[1]

[1]Department of Physics, Faculty of Arts and Sciences, Amasya University, 05100 Amasya, TURKEY

[*]corresponding author: meryem.evecen@amasya.edu.tr

Schiff bases have often been used as chelating ligands in the field of coordination chemistry for obtaining thermotropic liquid crystalline polymers and their metal complexes have been used as radiopharmaceuticals for cancer targeting, as dioxygen carriers and as model systems for biological macromolecules [1]. Schiff base complex have been playing an important role in the development of coordination chemistry related to catalysis and enzymatic reactions, magnetism and molecular architectures [2]. Schiff base compounds display interesting photochromic and thermochromic features in the solid state and can be classified in terms of these properties.

In this study, we report a theoretical study on molecular structure, molecular electrostatic potential and frontier molecular orbital energies of the title crystal. The theoretical geometrical parameters in the ground state have been investigated by density functional method (B3LYP) with Lanl2dz basis set. The optimized geometric bond lengths and bond angles are in well agreement with the experimental data.

References

[1] H. Tanak, M. Toy, Molecular structure, vibrational spectra, NLO and MEP analysis of bis[2-hydroxy-KO-N-(2-pyridyl)-1-naphthaldiminato-KN]zinc(II), Spectrochimica Acta Part A 115, 145 (2013).

[2] H. Tanak, A. Ağar, M. Yavuz, Combined Experimental and Computational Modeling Studies on 4-[(2-Hydroxy-3-methylbenzylidene)amino]-1,5-dimethyl-2-phenyl-1,2-dihydro-3H-pyrazol-3-one. International Journal of Quantum Chemistry, 111, 2123 (2011).

Acknowledgement, this study was supported financially by the Research Centre of Amasya University (Project No: FMB-BAP 15-092 and FMB- BAP 16-0175).

Synthesis and characterization of fluorescent polyphenols containing azomethine linkages via oxidative polycondensation

İsmet KAYA[1], Feyza KOLCU[1,2] and Sabriye SATILMIŞ[1]

[1]*Çanakkale Onsekiz Mart University, Faculty of Sciences and Arts, Department of Chemistry, Polymer Synthesis and Analysis Laboratory, 17020, Çanakkale, Turkey*

[2]*Çanakkale Onsekiz Mart University, Lapseki Vocational School, Department of Chemistry and Chemical Processing Technologies, Çanakkale, Turkey*

e-mail: feyzakolcu@comu.edu.tr

Preparation of conjugated aromatic polyimines, containing phenols in the backbone and side group substitutions, has been successfully achieved by a chemical oxidative polycondensation of a series of Schiff bases in aqueous alkaline medium using NaOCl as oxidant at optimum reaction temperature of 90 °C. The molecular structures of synthesized compounds were evidenced by the FT-IR, UV-Vis, ^{1}H-NMR and ^{13}C-NMR techniques. Using thermogravimetric analysis-differential thermal analysis (TG-DTA) and size exclusion chromatography (SEC), the characterization of all compounds could be identified. The initial degradation temperatures of the polymers were found in the range of 170-221 °C. UV-Vis measurements gave information about the optical (E_g) band gaps. Fluorescence measurements were carried out to obtain the maximum PL intensities. The spectral analysis outcame signified a green light emission behavior when irradiated at different wavelengths. Cyclic Voltammetry (CV) was an effective method to explore the HOMO and LUMO energy levels and electrochemical ($E_g^{'}$) band gaps of the polymers. The HOMO energy levels of the synthesized polyimines were lower than those of the monomers indicating the more conjugated structures of the polymers. Combined with fluorescent behavior and good thermal stability, the morphologic properties of the polymers were illustrated using Scanning Electron Microscopy (SEM) images at different amplifications. The result of this study revealed that polyphenols containing imine linkages were crucial for π-conjugated polymers whose electronic composition and properties could be adjusted by side group [1].

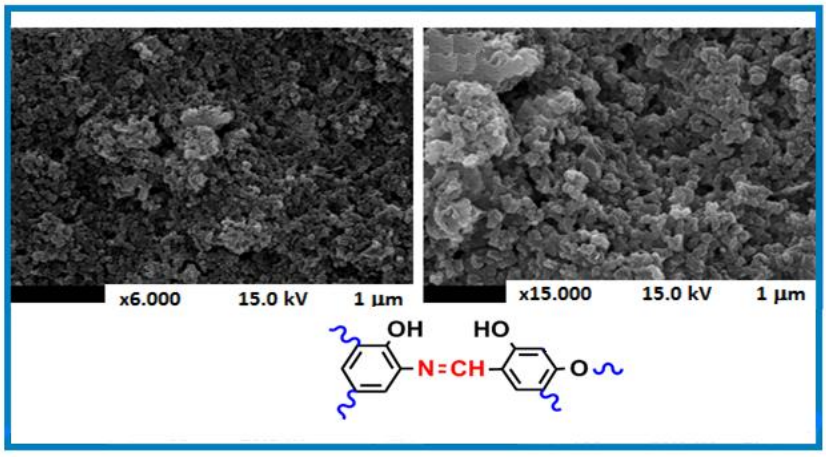

Key words: Oxidative polycondensation, imine polymers, polyphenols, fluorescent behaviour.

References

[1]. Kaya İ, Vilayetoglu AR. Synthesis and characterization of oligosalicylaldehyde-graft-oligoaniline and its beginning oligomers. J. Appl. Polym. Sci. 2002;85:218-226.

Linear PTMA copolymers as Cathode Material in Li-Ion Batteries

Mesut Gorur[1]*, Muhammet Aydin[2,3], Faruk Yilmaz[2]*
[1]Department of Chemistry, Istanbul Medeniyet University, Istanbul, 34700, Turkey
[2]Department of Chemistry, Gebze Technical University, Kocaeli, 41400, Turkey
[3]Central Research Laboratory, Namık Kemal University, Tekirdag, 59030, Turkey
email: mesut.gorur@medeniyet.edu.tr

The wide-spread use of mobile devices led scientists to develop fast-charging batteries with high capacity and long cycle life. Organic radical batteries (ORB) have attracted considerable attention for their fast redox kinetics, high power capacity and energy density. Additionally, ORBs are regarded as environmentally friendly, since they do not contain toxic heavy metals [1]. In this respect, polymers having redox-active 2,2,6,6-tetramethylpiperidine-1-oxyl (TEMPO) groups have been used as cathode material in Li-ion rechargeable batteries [2].

In this study, linear TEMPO-containing copolymers with hydrophilic (**P2**) and hydrophobic side groups (**P4**) were prepared via ATRP of 2,2,6,6-tetramethylpiperidin-4-yl methacrylate (TMPM) with polyethylene glycol methyl ether methacrylate (PEGMA, Mw:300) and lauryl methacrylate, respectively, and subsequent oxidation of the obtained polymers (**P1** and **P3**) (Scheme 1). Then, **P2** and **P4** were employed as the cathode material in the preparation of rechargeable Li-ion button cell. The produced batteries were characterized for their charge-discharge cycle performances.

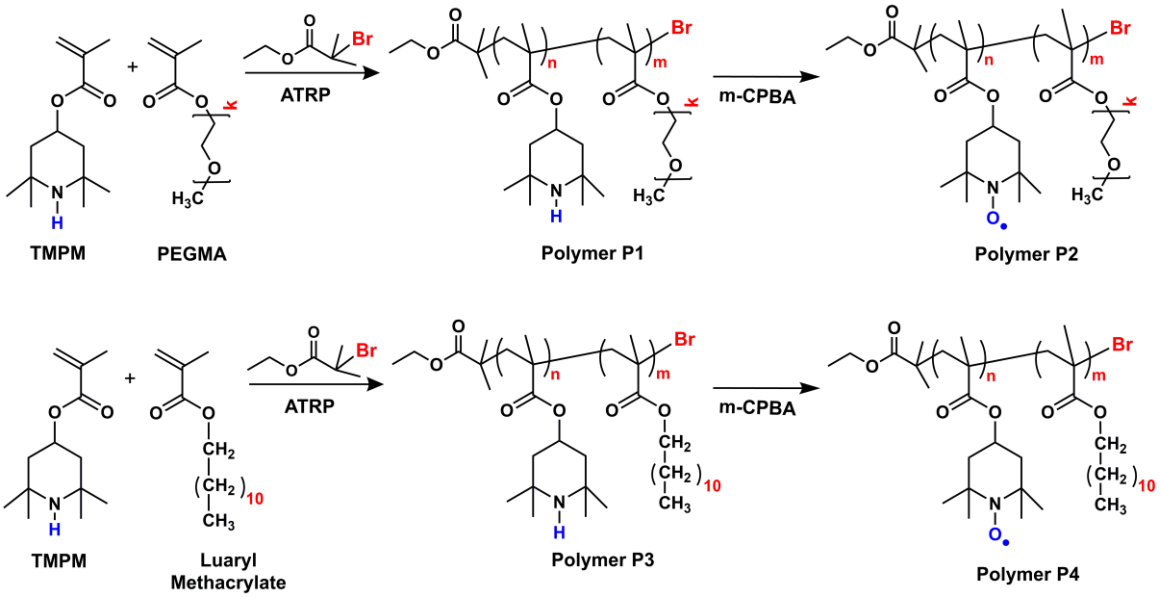

Scheme 1. Synthesis of linear PTMA copolymers (**P2** and **P4**).

*The authors acknowledge TUBITAK for the financial support (Project No: 114Z302).

References:

1. M. Aydin, B. Esat, C. Kilic, M. E. Kose, A. Ata, F. Yılmaz, Eur. Polym. J., 47 (2011), 2283-2294.
2. M. Aydin, M. Gorur, and F. Yilmaz, React. Funct. Mater. 102 (2016), 11-19.

Double-Layer Dye-Sensitized Solar Cells using as BaTiO3:Y3+ Second Layer

S. Dayan, N. Kalaycıoğlu Özpozan
Department of Chemistry, Faculty of Science, Erciyes University, Kayseri, Turkey
E-mail: serkandayan_@hotmail.com

Dye-sensitized solar cells (DSCs) have attracted much attention because of their simple fabrication processes and fashionable colourful designs [1]. The photoelectric conversion efficiency of the advanced DSCs has exceeded 10%, which is almost equal to that of amorphous Si solar cells. DSCs are composed of a dye-sensitized porous oxide electrode on a transparent conducting glass, an electrolyte and a Pt coated counter electrode. To date, TiO_2-anatase nanoparticles are typically applied to the porous oxide electrodes. TiO_2 nanoparticles with large surface area can adsorb a great amount of dye molecules, giving a large light harvesting and an efficient electron injection [2,3].
Herein, perovskite structure which $BaTiO_3:Y^{3+}$ have been successfully synthesized by hydrothermal method with Titanium(IV) *n*-butoxide ($Ti(OC_4H_9)_4$), Bariumnitrate ($Ba(NO_3)_2$) and Yttrium(III) nitrate hexahydrate. The structural elucidation of the material was characterized by different methods such as FT-IR, TG/DTA, XRD and SEM-EDX.
The synthesized $BaTiO_3:Y^{3+}$was tested as second-layer in dye-sensitized solar cells (DSSCs).

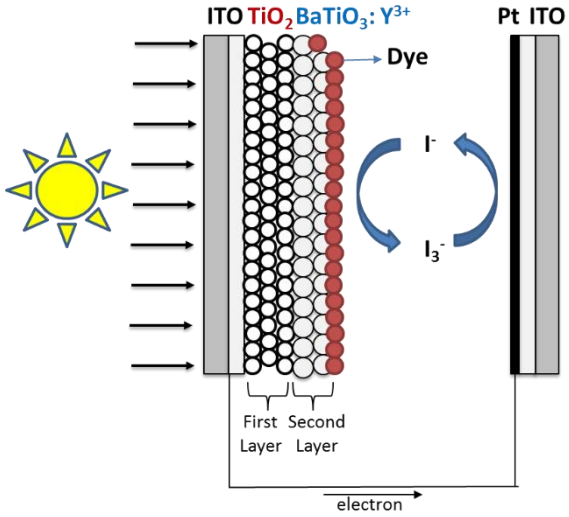

Figure-1 Second Layer Dye-Sensitized Solar Cells (DSSCs)

References

[1] B. C. O'Regan and M. Grätzel, A low-cost, high-efficiency solar cell based on dye-sensitized colloidal TiO_2 films Nature 353, 737 (1991).
[2] S. Mathew, A. Yella, P. Gao, R. Humphry-Baker, B. F. E. Curchod, N. Ashari-Astani, I. Tavernelli, U. Rothlisberger, M. K. Nazeeruddin and M. Grätzel, Dye-sensitized solar cells with 13% efficiency achieved through the molecular engineering of porphyrin sensitizers, Nat. Chem., 6, 242 (2014).
[3] K. Nakataand A. Fujishima, TiO_2photocatalysis: Design and applications, J. Photochem. Photobiol., C, 13,169-189 (2012).

Acknowledgments

We acknowledge the financial support granted by Erciyes University (ERUBAP), (FDK-2015-6013).

Esterified metal-free and metallo-porphyrazine derivatives with octa (4-thiobutyl 2-naphthyloxy acetate)] units

E. Gonca

Faculty of Engineering, Department of Chemical Engineering, Çanakkale Onsekiz Mart University, Terzioglu Campus, TR 17020 Çanakkale, Turkey

E-mail :egonca@comu.edu.tr

Porphyrins, phthalocyanines, tetrabenzoporphyrins, and porphyrazines, which can be called as tetrapyrrole derivatives, receive comprehensive consideration owing to both theoretical studies and several applications in advanced materials science. For porphyrazine structures, the solubility amount is an important feature and the most of their reactions are the best determined in soluble one. A couple of unsubstituted metal-free and metallo-porphyrazines are a little soluble in some organic solvents. Compared to unsubstituted metallo-porphyrazine structures, ester-having porphyrazines are good soluble in chlorinated hydrocarbons such as $CHCl_3$ and CH_2Cl_2 [1,2]. The applications of ester-containing tetrapyrrole compounds are very variable such as tumor growth suppressor, electro-photographic photoconductors, optical storage agent, and photosensitizer in photodynamic therapy [3,4].

Metal-free and metallo-porphyrazines with octa (4-thiobutyl 2-naphthyloxy acetate) substituents on the peripheral position through flexible butylthio-bridges have been synthesized through the esterification reaction of octakis(hydroxybutylthio)porphyrazinato magnesium with a 2-naphthyloxy acetic acid in the existence of dry pyridine, dicyclohexylcarbodiimide and *p*-toluene sulfonic acid. The symmetrical porphyrazine complexes with eight ester units are soluble in some organic solvents such as $CHCl_3$, CH_2Cl_2, THF, acetone, and toluene and insoluble in *n*-hexane. The electronic spectra exhibit an intense π-π^* transition of naphthyl identity together with characteristic Q and B bands of the porphyrazine core. The synthesized structures are characterized by using elemental analysis, FT-IR, UV-Vis, MS, ^{1}H, and ^{13}C NMR spectroscopy.

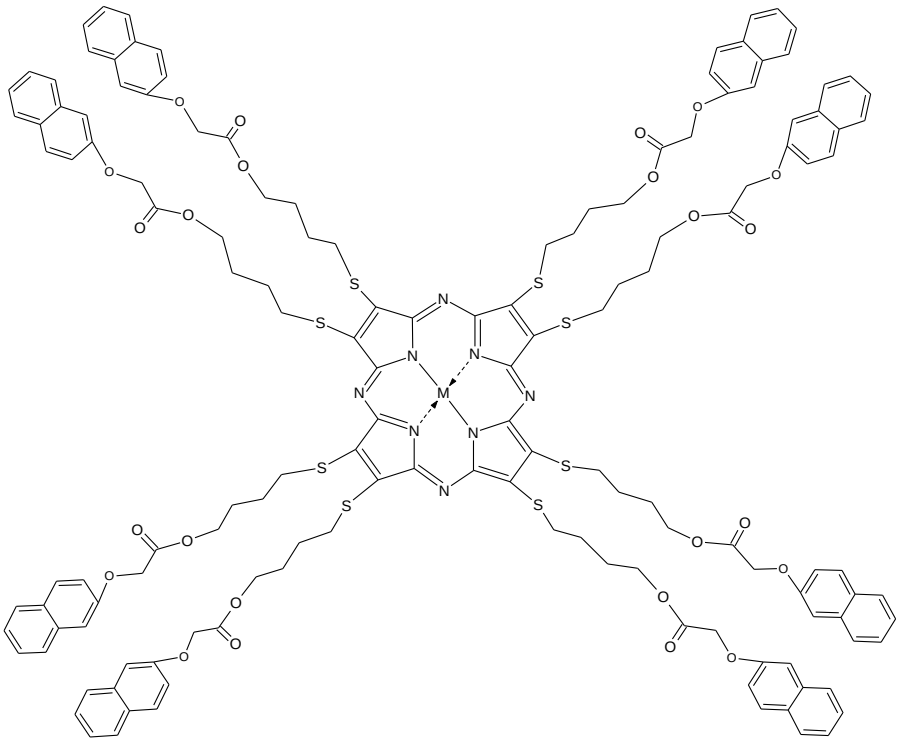

[1] H.Y. Yenilmez, İ. Özçeşmeci, A.İ. Okur, A. Gül, Polyhedron 23, 787-791 (2004).

[2] E. Gonca, J. Coord. Chem. 66, 1720-1729 (2013).

[3] V.V. Rozhkov, M. Khajehpour, S.A. Inogradov, Inorg. Chem. 42, 4253–4255 (2003).

[4] W. Liu, T.J. Jensen, F.R. Fronczek, R.P. Hammer, K.M. Smith, M.G.H. Vicente. J. Med. Chem. 48, 1033-1041 (2005).

Tetrakis-phthalocyanines bearing electron-withdrawing fluoro groups for electronic technology

A. Turgut Bilgiçli, A. Günsel, M. Nilüfer Yarasir *, M. Kandaz*
Department of Chemistry, Sakarya University, 54140 Esentepe, Sakarya, Turkey
E-mail:mkandaz@sakarya.edu.tr
E-mail:nyarasir@sakarya.edu.tr

Phthalocyanines are a class of macrocyclic compounds (a family of aromatic macrocycles) possessing a conjugated system of 18 π-electrons. The presence of a π-electron system is more important for the charge carrier transport. So, they exhibit a number of unique optical, electronic, catalytic and structural properties which make them of great interest in various scientific and technological areas ranging from nanotechnology to medicine. There has been growing interest in the use of phthalocyanines in a variety of new high technology fields including semiconductor devices, Langmuire Blodgett films, electrochromic display devices, gas sensors, liquid crystals, nonlinear optics, information storage, organic light emitting diodes (OLED), photodynamic cancer therapy (PDT) and various catalytic processes [1-3]. In this study, we reported the synthesis of novel tetrasubstituted zinc(II) ,Co (II) phthalocyanines at the peripheral position with 1,3-bis(2,3,5,6-tetrafluorophenylthio)propan-2-ol groups. The new synthesized compounds have been characterized by elemental analysis, FTIR, 1H-, 13C-NMR, UV-Vis and MS spectral data.

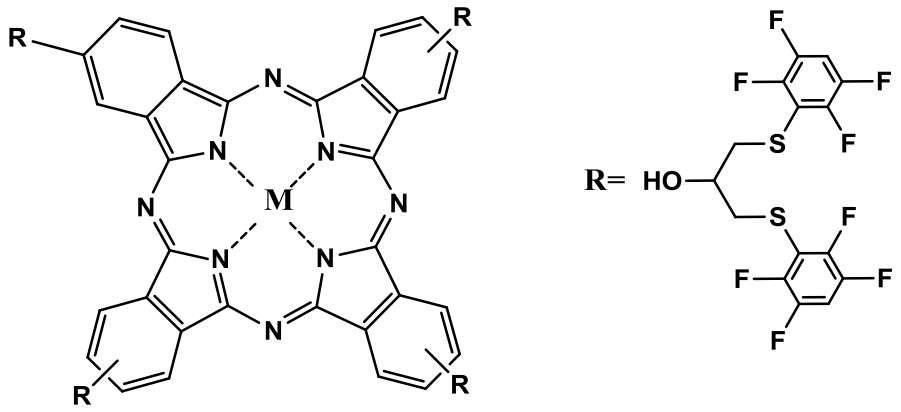

M=Zn,Co

References

[1] A.T. Bilgiçli, M. Kandaz, A.R. Özkaya, B. Salih, Heteroatom Chem. 20, (2009) 5.
[2] M. Kandaz, O. Güney, B. Filiz Senkal, Polyhedron 28, (2009), 3110-3114.
[3] G. de la Torre, C.G. Claessens, T. Torres, Chemical Communications 20, (2007), 2000.

Functional fluoro substituted tetrakis- metallophthalocyanines for organic p-n heterojunction applications

A. Günsel, A. Turgut Bilgiçli, M. Nilüfer Yarasir * ,M. Kandaz*

Department of Chemistry, Sakarya University, 54140 Esentepe, Sakarya, Turkey

E-mail:mkandaz@sakarya.edu.tr

E-mail:nyarasir@sakarya.edu.tr

Phthalocyanines derivatives show interesting chemical and physical properties. Therefore, excellent technologies have been developed around these functional materials in the last decade by facile substitution on the periphery (a, b, and g).By placing stronger electron-withdrawing fluorine atoms on the Pc ring results in both the valence and conduction band energies being further lowered. Thus, MPcFn (n: number of fluorine atoms) exhibits n-type behavior, while unsubstituted phthalocyanines possess p-type due to doping with electron accepting molecules. These unusual properties of MPcFn have led scientists to expose their chemistry to use in a number of different industrial applications [1-3 In this study, we reported the synthesis of tetrasubstituted zinc(II) ,Co (II) phthalocyanines at the peripheral position with 1,3-bis(2,3,5,6-tetrafluorophenoxy)propan-2-ol. The new synthesized compounds have been characterized by elemental analysis, FTIR, ^{1}H- , ^{13}C-NMR, UV-Vis and MS spectral data.

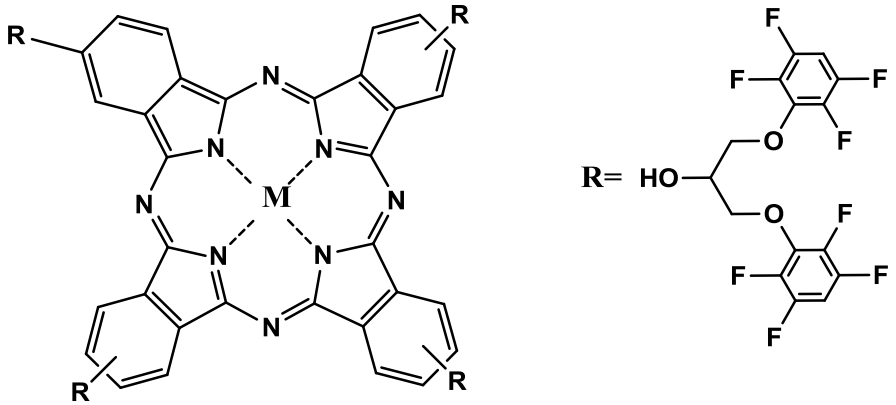

M=Zn,Co

References

[1] A. Günsel, M. Kandaz, A. Koca, B. Salih, J. Fluorine Chem.129 (2008) 662-668.

[2] Y. Liu, D. Yang, C. Wang, J. Phys. Chem. B 110 (2006) 20789-20793.

[3] T. Manaka, M. Iwamoto, Thin Solid Films 438/439 (2003) 157-161.

Highly soluble phthalocyanines containing fluoro groups for organic material technologies

M. Nilüfer Yarasir*, A. Turgut Bilgiçli, A. Günsel, M. Kandaz*
Department of Chemistry, Sakarya University, 54140 Esentepe, Sakarya, Turkey
E-mail:mkandaz@sakarya.edu.tr
E-mail:nyarasir@sakarya.edu.tr

Phthalocyanines have been known as excellent functional materials for a long time, so diverse chemical and technological applications have developed around these interesting and advanced materials. Possible technological applications of phthalocyanines, such as semi-conductivity, electrochromic displays, chemical sensors and catalysts have encouraged many researchers to synthesize various types of metal phthalocyanine [1-2]. Althoughphthalocyaninesbearing electron-donating substituents have frequently been studied, those bearing electron-withdrawing ones have not extensively studied, especially those containing fluorine atoms [3]. In this study, we reported the synthesis of novel tetrasubstituted zinc(II) ,Co (II) phthalocyanines at the peripheral and nonperipheral position with 1,3-bis(3,5-bis(trifluoromethyl)phenoxy)propan-2-ol groups. The new synthesized compounds have been characterized by elemental analysis, FTIR, ^{1}H- , ^{13}C-NMR, UV-Vis and MS spectral data.

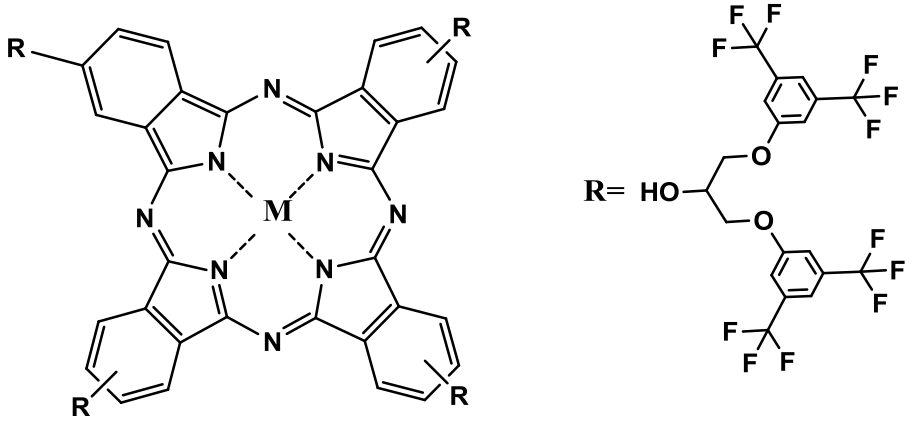

M=Zn,Co

References

1. S. Ünlü, M.N. Yarasir, M. Kandaz, A. Koca , B. Salih, Polyhedron, 27 (2008), 2810.
2. M. Kandaz, S.L.J. Michel, B.M. Hoffman, J. Porphyr. Phthalocyan. 7 (2003) 700.
3. B.A. Bench, W.W. Brennessel, H.-J. Lee, S.M. Gorun, Angew. Chem., Int. Ed. 41 (2002) 750.

Octasubstituted ionophore chiral metallophthalocyanines for sensor applications

M. Nilüfer Yarasir, A. Turgut Bilgiçli, A. Günsel, M. Kandaz*

Department of Chemistry, Sakarya University, 54140 Esentepe, Sakarya, Turkey

E-mail:mkandaz@sakarya.edu.tr

Phthalocyanines have been studied extensively over the last few decades for their applications in material science. In recent years, the applications of metallophthalocyanine complexes have extended to optical limiting devices, molecular electronics, liquid crystals, gas sensors, semiconductor materials, photovoltaic cells [1-2].Multi-functional, differently octasubstituted ionophore chiral metallophthalocyanine (MPc's where M=, Co), bearing reactive functionalities on the periphery, propane 1,2-diolsulfanyl moieties, which facilitated solubility in polar solvents and metal ion binding, were prepared from the corresponding anhydrous metal salt and substituted 4-(1,2-propanediolsulfanyl)-5-chlorobenzene- 1,2-dicarbonitrile compound. The newly synthesized ligand and MPc were characterized by elemental analysis, , FTIR, ^{1}H- ,^{13}C-NMR, UV-Vis and MS spectral data.

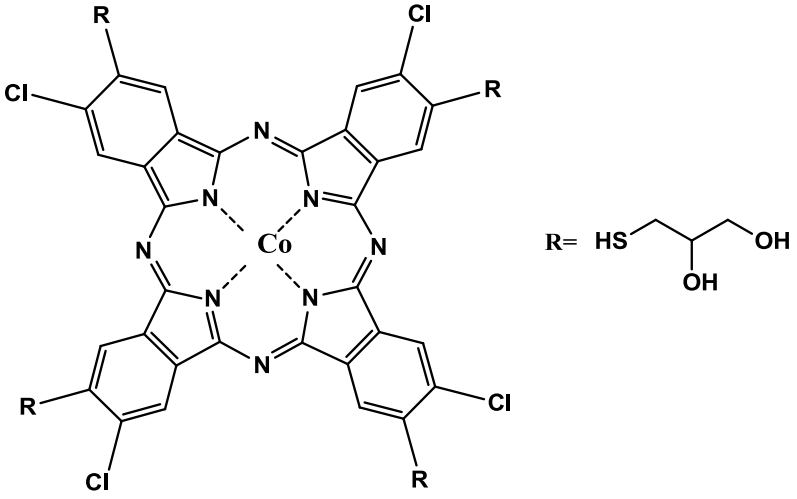

References

1. M. Kandaz, H.S.Çetin, A. Koca, A.R. Özkaya, Dyes Pigments 74 (2007) 298-305

2. M. Hanack, T. Schneider, M. Barthel, J.S. Shirk, S.R. Flom, R.G.S. Pong, Coord. Chem. Rev. 219 (2001) 235-258.

Peripheral and non-peripheral-designed multi functional gallium and indium phthalocyanines for gas sensor applications

A. Günsel, E. Güzel, A. Turgut Bilgiçli, M. Nilüfer Yarasir, M. Kandaz*
Department of Chemistry, Sakarya University, 54140 Esentepe, Sakarya, Turkey
E-mail:mkandaz@sakarya.edu.tr

Metallophthalocyanines (MPc) are known as commercially available dyes due to their chemical and thermal stability. Efforts in the development of new types of phthalocyanines and studies of their properties in recent years have been of great importance in various technological fields, such as electron transfer, selective metal sensors, liquid crystals and fibrous assemblies. One of the principal strategies for controlling MPc's properties requires ring substitution on the peripheral and/or non-peripheral positions of the phthalocyanine ring [1,2]. A novel type of ionophore ligands, 3'-(2,3-dihydroxypropylthio)-phthalonitrile and 4'-(2,3-dihydroxypropylthio)-phthalonitrile, and their α- and β-tetrasubstituted metallo phthalocyanines, (MPc), (M = Ga(III) and In(III) have been prepared and fully characterized by elemental analysis, FTIR, ^{1}H- ,^{13}C-NMR, UV-Vis and MS spectral data.

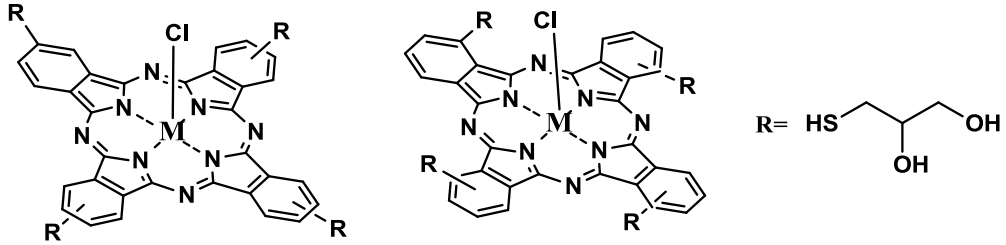

M= Ga, In

References

1. A.Günsel, M. Kandaz , A. Koca, B. Salih, Polyhedron 30 (2011) 1446-1455.
2. M. Hanack, T. Schneider, M. Barthel, J.S. Shirk, S.R. Flom, R.G.S. Pong, Coord. Chem. Rev. 219 (2001) 235-258

Synthesis and Characterization of a New Metal-Organic Hybrid Material

Seda Yatkın[1], Osman Dayan[1], Melek Tercan[1]

[1]Department of Chemistry, Faculty of Arts and Science, Çanakkale, Turkey

Inorganic-organic hybrid materials have been drawing more attention, because they can combine the physical and chemical properties of the inorganic and organic components [1]. This materials have great potential as electrical and optical functional materials and heterogenous catalysts. Metal-organic hybrid materials (MOM's) with varied structures and topologies based on supramolecular assemblies could be achieved [2,3].

In this study 1,3-dibenzyl-*1H*-benzimidazol-3-ium chloride ligand and Co hybrid material of this ligand were prepared. The ligand and the hybrid material were characterized by FT-IR and UV techniques. Particle size and morphology of nanoparticles were confirmed by SEM and TEM techniques. The obtaining material was examined as a catalyst in the hydrogenation of 2-nitroaniline to *o*-phenylenediamine and 52.93% conversion was observed.

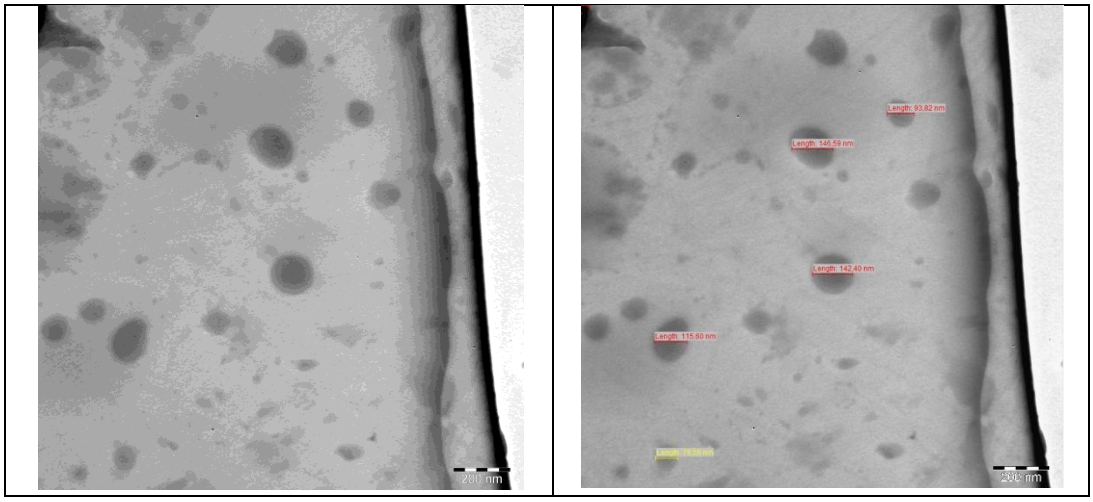

References

[1] K. Fu, C.X. Ren, C. Chen, L. X. Cai, B. Tan and J. Zhang, Auxiliary ligand-controlled photochromism and decolourization of two bipyridinium-based metal–organic hybrid materials with various water clusters, CrysEngComm. 16, 5134 (2014).

[2] Z. Xiao,X. Yang, S.Zhao, D. Wang, Y. Yang, L. Wang, Metal–organic hybrid materials built with tetrachlorophthalate acid and different N-donor coligands: Structure diversity and photoluminescence, Journal of Solid State Chemistry. 234, 36 (2016).

[3] S. Mistri, E. Zangrando, A. Figuerola,A. Adhikary, S. Konar, J. Cano and S. C. Manna, Syntheses, crystal structures, and magnetic properties of metal−organic hybrid materials of Mn(II)/Co(II): three-fold interpenetrated α‑Polonium-like network in one of them, Cryst. Growth Des. 14, 3276 (2014).

Fabrication and Electrical Characterization of Ln-based Metal–Organic Frameworks as new Class of Photovoltaic Solar Cells

M. B. Coban[1,2], and C.Kocak[3], G. Oylumluoglu[3], H. Kara[2,3]

[1]*Center of Sci and Tech App and Research, Balikesir University, Balikesir, Turkey*

[2]*Department of Physics, Faculty of Art and Science, Balikesir University, Balikesir, Turkey*

[3]*Department of Physics, Faculty of Science, Mugla Sıtkı Kocman University, Mugla, Turkey*

E-mail: hkara@balikesir.edu.tr

Recently, a great deal of attention has been paid to the development of Ln based Metal Organic Frameworks (Ln-MOFs) due to their fantastic structures and wide potential applications. The design of MOFs with excellent luminescence and photovoltaic properties has attracted increasing attention in pursuit of multifunctional materials. In particular, MOFs containing photoactive ligands or guest molecules have been designed and characterized as potential materials for photovoltaic applications. This includes their use as scaffolds or hosts for commercially available dyes for use as dye-sensitized solar cells (DSCs). In this study, we report the fabrication of multifunctional Ho-based MOFs. The photoluminescence properties were investigated in UV and NIR region and also the performance of solar cells was investigated by measuring current density–voltage (J–V) curves.

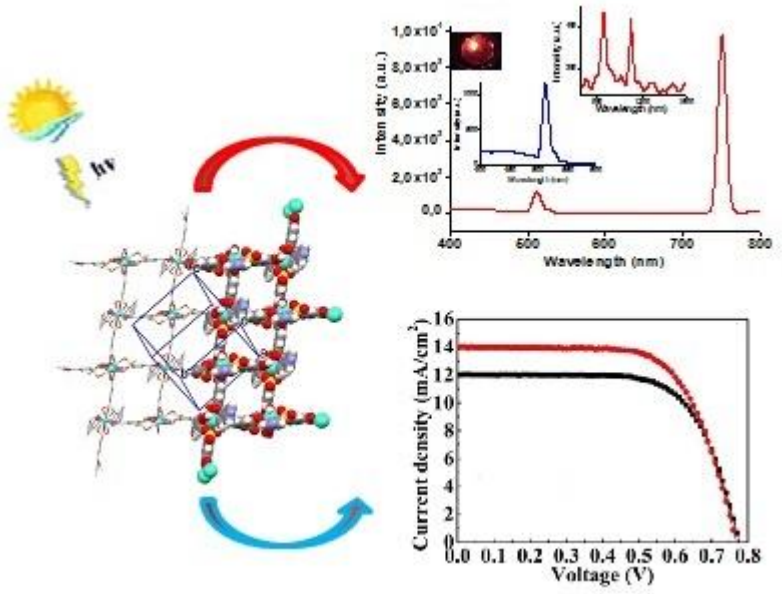

[1] M. B. Coban, U. Erkarslan, G. Oylumluoglu, M. Aygun, H. Kara, Hydrothermal Synthesis, Crystal Structure and Photoluminescent Properties; 3D Holmium (III) Coordination Polymer, Inorg. Chim. Acta 447, 87 (2016).

[2] Hui Xu, Runfeng Chen, Qiang Sun, Wenyong Lai, Qianqian Su,Wei Huang and Xiaogang Liu, Recent progress in metal–organic complexes for optoelectronic applications, Chem. Soc. Rev., 43, 3259 (2014).

Recent advances in the photovoltaic applications of coordination polymers and Electrical Characterization under irradiation and in dark

M. B. Coban[1,2], and C.Kocak[3], G. Oylumluoglu[3], H. Kara[2,3]

[1]*Center of Sci and Tech App and Research, Balikesir University, Balikesir, Turkey*

[2]*Department of Physics, Faculty of Art and Science, Balikesir University, Balikesir, Turkey*

[3]*Department of Physics, Faculty of Science, Mugla Sıtkı Kocman University, Mugla, Turkey*

E-mail: hkara@balikesir.edu.tr

Recently, coordination polymers have attracted a great deal of attention in a variety of scientific fields due to their excellent properties and photovoltaic and photoluminescence applications. Metal–organic frameworks (MOFs) represent a class of highly porous coordination polymers formed metal ions and organic linkers. Although, photovoltaics is one of the most investigated areas, investigation on MOFs as photovoltaic materials has been scarce. In this study, we report the fabrication of multifunctional Eu-based MOFs. The photoluminescence properties were investigated in the visible and NIR regions and also the performance of solar cells was investigated by measuring current density–voltage (J–V) curves under irradiation and in dark.

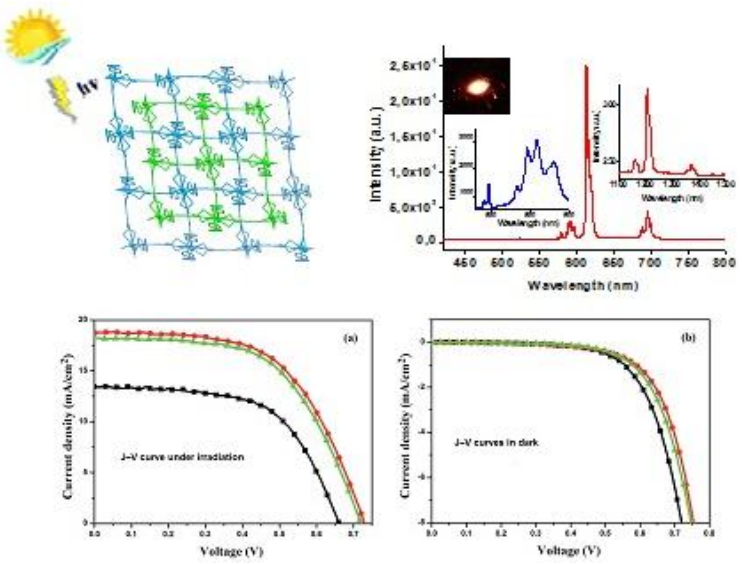

[1] M. B. Coban, U. Erkarslan, G. Oylumluoglu, M. Aygun, H. Kara, Hydrothermal Synthesis, Crystal Structure and Photoluminescent Properties; 3D Holmium (III) Coordination Polymer, Inorg. Chim. Acta 447, 87 (2016).

[2] Hui Xu, Runfeng Chen, Qiang Sun, Wenyong Lai, Qianqian Su,Wei Huang and Xiaogang Liu, Recent progress in metal–organic complexes for optoelectronic applications, Chem. Soc. Rev., 43, 3259 (2014).

2D-Network Simulation and Modelling of CdTe Modules

C.Kocak[1], M. B. Coban[2,,3], G. Oylumluoglu[1], H. Kara[1,3]
[1]*Department of Physics, Faculty of Science, Mugla Sıtkı Kocman University, Mugla, Turkey*
[2]*Center of Sci and Tech App and Research, Balikesir University, Balikesir, Turkey*
[3]*Department of Physics, Faculty of Art and Science, Balikesir University, Balikesir, Turkey*
E-mail: hkara@balikesir.edu.tr

CdTe solar cells have potential to replace main utility for producing electrical energy by reducing production cost. In thin film CdTe modules, the photovoltaic conversion efficiency, module performance, yield and resulting market penetration could be restricted by inhomogeneities and any localized defects within the cells-modules-. So, it has high importance to understand and to have knowledge how the defects are of the influence on module performance. Also some measurement techniques have to be introduced so as to identify the localized defects. Imaging techniques are well suited for identifying the defects localized on the sample-module-. However, in the production of large area modules, it is important to predict the quality of modules: 2-D network simulation aids to make interpretation. 2-D network simulation is performed to simulate the module – defect interaction in the module performance point of view.

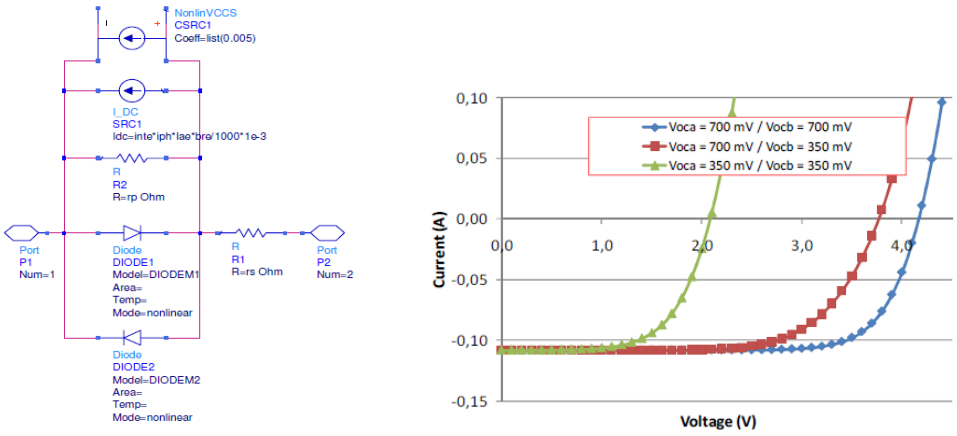

[1] Uwe Rau, Reciprocity relation between photovoltaic quantum efficiency and electroluminescent emission of solar cells, Phys.Rev.B 76, (2007).

[2] Thomas Ott, Francillina Robert Runai, Fabian Schwäble and Thomas Walter, 2D network simulation and luminescence characterization of Cu(In,Ga)Se_2 thin film modules, Progress in Photovoltaics: Research and Applications, Volume 20, Issue 5, (2012).

ANALYZING THE InGaN LED STRUCTURES FOR WHITE LED APPLICATION

İ.KARS DURUKAN[1], O.Sarıarslan[2], M.K.Öztürk[2,3], S.Özçelik[2,3],and E.Özbay[4]

[1]Life Sciences Research and Application Center, Gazi University, Ankara, Turkey
[2]Department of Physics, Faculty of Sciences, Gazi University, Ankara, Turkey
[3]Photonics Research Center, Gazi University, Ankara, Turkey
[4]Department of Physics, Bilkent University, Bilkent, Ankara
E-mail :ilknurdurukan@gazi.edu.tr

As known fact, it is impossible to make white led when we consider structures with nitrogen and arsenic. Because it is hard to obtain wide wavelength spectrum at visible area due to the alloy ratio. It is possible to cover InGaN, that gives blue spectrum, with phosphor by using MOCVD crystal growth technique [1,2]. This method is using at many areas such as telephones, tablets etc [3]. In particular, useful for saving electric power owing to lower energy consumption of LEDs [4] and [5]. Our aim is to investigate the mosaic structure of InGaN/Al_2O_3 led structure which is grown by MOCVD device. Lateral and vertical crystal size, dislocations, tilt and twist properties are investigated with HR-XRD device by Vegard and William hall semi-experimental methods. As a result, the dislocation amount decreased about 4.18 10^8 cm^2.

[1] S. Nishikawa, T. Tamura and M. Senoh, Candela-class high-brightness InGaN/AlGaN double-heterostructure blue light-emitting diodes, Appl. Phys.lett., 64, 1687 (1994).
[2] T. Tamura, T. Setomoto and T. Taguchi, Fundamental characteristics of the illuminating light source using white light emitting diodes based on InGaN semiconductors, Trans IEE of Japan, 120-A, 244 - 249 (2000).
[3] S. Nakamura and G. Fasol, The Blue Laser Diode, Springer (1997).
[4] M.G. Craford, Circuit Dev., September ,24 (1992).
[5] M.G. Craford, J. Parity (Ed.), Commercial Light Emitting Diode Technology, Kluwer Academic Publishers, Dordrecht, 323 (1996).